



**UNIVERSITY OF
KWAZULU-NATAL**

**THE CYTOTOXIC EFFECTS OF
DEOXYNIVALENOL AND FUMONISIN B₁
ON THE HT-29 HUMAN COLONIC
ADENOCARCINOMA CELL LINE**

BY

KRISHNAVENI REDDY

N.Dip.: Biotechnology (TN)

B.Med.Sci. (Hons) (UND)

Submitted in partial fulfilment of the requirements for the degree of
Masters in Medical Science in the Department of Physiology,
Faculty of Health Sciences, Nelson R, Mandela School of Medicine,
University of Kwa-Zulu Natal, Durban

2005

"Tumours destroy man in a unique and appalling way, as flesh of his own flesh which has somehow been rendered proliferative, rampant, predatory, and ungovernable . . . Yet, despite more than 70 years of experimental study, they remain the least understood. . . What can be the why for these happenings?"

—*Peyton Rous*

Winner of the Nobel Prize in Physiology or Medicine 1966

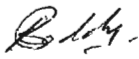
ABSTRACT

The human population can be considered as a subject of combined exposure to chemicals against which the gastrointestinal tract represents the first barrier. The most relevant are those compounds that occur in plants which are used as foods, medicines and beverages. Of special interest are the mycotoxins deoxynivalenol (DON) and fumonisin B₁ (FB₁), two of the most commonly encountered food-borne mycotoxins and curcumin, a popular spice and pigment reported to have antineoplastic properties. In this study, the HT-29 cell line was used to assess the toxicity of the mycotoxins DON and FB₁ (5µM and 50µM) as well as the possible cytoprotective effects of curcumin (50µM) on colonic cells. Mixtures of both mycotoxins were also assessed to determine any possible interaction. Cytotoxicity, DNA fragmentation, cellular morphology and cell surface alterations were evaluated using the methylthiazol tetrazolium (MTT) bioassay, the single cell gel electrophoresis (SCGE) assay, fluorescence microscopy and scanning electron microscopy respectively. Deoxynivalenol displayed cytotoxic and genotoxic effects as well as induced morphological features of apoptosis and cell surface alterations that worsened with increasing concentration. Fumonisin B₁ exhibited a proliferative effect at the high concentration however DNA damage and cell surface alterations worsened with decreasing concentration. Mixtures of DON and FB₁ displayed similar effects to those exhibited by DON in terms of cytotoxicity, DNA fragmentation, morphology and cell surface alterations indicating that DON is able to antagonise the effects of FB₁ at the concentrations tested. Curcumin appeared to exhibit a protective effect that was prominent when co-administered with the 50µM toxin concentration. Low concentrations of DON and FB₁ (5µM) were sufficient to induce apoptosis in this cell line and suggest a danger from natural contamination by these toxins. Curcumin, however, warrants further investigation with regards to its cytoprotective activities in the presence of these mycotoxins as it could present a promising candidate for a natural chemoprotective agent in the armamentarium against mycotoxin induced cancers.

AUTHOR'S DECLARATION

The experimental work presented in this manuscript represents the original work of the author and has not been submitted to any other university or tertiary institution. Where use has been made of the work of others, it has been duly acknowledged in the text.

The research described in this study was carried out under the supervision of Professor A.A. Chuturgoon in the discipline of Medical Biochemistry in the School of Medical Sciences at the Nelson R. Mandela School of Medicine, University of KwaZulu-Natal, Durban, between February 2002 and September 2004.



Miss K. Reddy

In loving memory of:

Mr Vythilingum Velen (Christie)

(14 September 1921-28 February 2002)

Mr Moganathan Reddy (Tinkey)

(17 February 1946-14 January 2005)



PUBLICATIONS

1. Reddy, K., Chuturgoon, A.A. (2004). Cytotoxicity of the trichothecene mycotoxin deoxynivalenol on the HT-29 human colon adenocarcinoma cell line. *Toxicon*. (In press).
2. Reddy, K., Chuturgoon, A.A. (2004). Cytotoxicity of the mycotoxin fumonisin B₁ on the HT-29 human colon adenocarcinoma cell line. *Mycopathologia*. (Submitted).
3. Reddy, K., Chuturgoon, A.A. (2004). Cytotoxicity of deoxynivalenol and fumonisin B₁ Mixtures on the HT-29 human colon adenocarcinoma cell line. *Toxicology and Applied Pharmacology*. (Submitted).
4. Reddy, K., Chuturgoon, A.A. (2004). The effect of dietary curcumin on the cytotoxicity induced by the mycotoxins Deoxynivalenol and Fumonisin B₁ on the HT-29 human colon adenocarcinoma cell line. *Toxicon*. (Submitted).
5. Reddy, K., Chuturgoon, A.A. (2004). Detection of DNA damage in HT-29 human colon adenocarcinoma cells exposed to the mycotoxins deoxynivalenol and fumonisin B₁ and the chemoprotective agent curcumin. *Mutation Research*. (In press).

ACKNOWLEDGEMENTS

There are many people to whom I am indebted to for their contributions toward this study and I wish to express my gratitude and sincerest thanks to all of them.

I would like to thank my supervisor, Professor A. A. Chuturgoon, for giving me the opportunity of pursuing my postgraduate studies in the Mycotoxin Research Unit as well as for his invaluable advice and guidance with respect to this study and over the last few years.

I am also extremely grateful to Mrs Rene Myburg, Miss Narisha Singh and Mrs Shamin Bux for sharing their laboratory expertise with me as well as for their assistance with the preparation of this manuscript.

My sincerest thanks go also to Dr Anita Naicker and Mr Vinogran Dorsamy of the Optics and Imaging Unit for their constant motivation as well as their assistance with fluorescence microscopy, Mr Strinivasan Naidoo of the Department of Pharmacology, Ms Chepkor Cheruiyot of the Scanning Electron Microscope Unit and Mr Logan Pillay and Ms Premie Naidoo of the Department of Medical Microbiology for their advice and assistance with techniques and methods. I would also like to thank the National Research Foundation (NRF) and the Stella and Paul Loewenstein Trust for their financial assistance.

In addition, I would like to thank Mrs Nisha Perumal and Mrs Marie Hurley for their administrative assistance and Mr Ganas Perumal, Mr Ronnie Pillay, Mr Arthur Peterson, Ms Theresa Mkhabela and Miss Hlengiwe Mbongwa for their valuable technical advice and expertise.

A special thank you goes also to Dr Thesla Palanee, Miss Kalendri Naidoo, Miss Enbavani Dorsamy, Miss Kavidha Reddy and Miss Kriebashne Nair for all their support and encouragement. In addition to Miss Donella Wright, thank you for being you!

Most importantly, to my parents Krish and Patricia and sisters Pria and Ansuri, thank you for all your support, encouragement, patience and understanding over the years. I would not have come this far were it not for you.

Finally, I would like to thank all off the staff and students, past and present, of the Department of Physiology and the Mycotoxin Research Unit. Although I have not made special mention of you, please know that all assistance received was truly appreciated.

TABLE OF CONTENTS

	PAGE
ABSTRACT	iii
AUTHOR'S DECLARATION	iv
DEDICATION	v
PUBLICATIONS	vi
ACKNOWLEDGEMENTS	vii
LIST OF FIGURES	xviii
LIST OF TABLES	xxiv
LIST OF ABBREVIATIONS	xxv
CHAPTER 1: INTRODUCTION	1
1.1 CHEMICAL CARCINOGENS	1
1.2 <i>FUSARIUM</i> TOXINS	2
1.3 CURCUMIN AND CHEMOPREVENTION	3
1.4 THE HT-29 CELL LINE	3
1.5 OBJECTIVES	3
CHAPTER 2: LITERATURE REVIEW	4
2.1 ENVIRONMENTAL CARCINOGENESIS	4
2.2 MYCOTOXINS AND MYCOTOXICOSES	5
2.2.1 Deoxynivalenol	8
2.2.1.1 Chemical and Physical Properties	8
2.2.1.2 Mechanism of action	9
2.2.1.3 Toxic Effects	12

2.2.1.3.1	Toxic Effects in Animals	12
2.2.1.3.2	Toxic effects in Man	13
2.2.2	Fumonisin B₁	13
2.2.2.1	Chemical and Physical Properties	13
2.2.2.2	Mechanism of action	15
2.2.2.2.1	Sphingolipid Metabolism	15
2.2.2.2.2	Involvement of Fumonisin B ₁	16
2.2.2.3	Toxic Effects	20
2.2.2.3.1	Toxic Effects in Animals	20
2.2.2.3.2	Toxic effects in Man	20
2.3	MYCOTOXINS AND THE GASTROINTESTINAL TRACT	21
2.4	THE COLON	23
2.4.1	Physiology of the Colon	23
2.4.2	Apoptosis	25
2.4.3	Colorectal Cancer Development	27
2.5	CHEMOPREVENTION	29
2.5.1	Mechanisms of Colorectal Cancer Chemoprevention	30
2.5.1.1	Induction of Phase 2 Enzymes	30
2.5.1.1	Suppression of Cyclooxygenases	31
2.5.2	Curcumin	33
2.5.2.1	Physical and Chemical Properties	33
2.5.2.1	Mechanism of Action	34
CHAPTER 3	CELL CULTURE	36
3.1	INTRODUCTION	36



3.2	MATERIALS AND METHODS	37
3.2.1	Materials	37
3.2.2	Methods	38
3.2.2.1	Growth and Maintenance	38
3.2.2.2	Subculturing	39
3.2.2.3	Cryopreservation	42
3.2.2.4	Thawing Cryopreserved Cells	42
3.2.2.5	Cell Counting and Cell Viability Staining	43
3.3	CONCLUSION	45
CHAPTER 4	CYTOTOXICITY OF DEOXYNIVALENOL AND FUMONISIN B₁ ON THE HT-29 CELL LINE	46
4.1	INTRODUCTION	46
4.1.1	Cytotoxicity	46
4.1.2	The Methylthiazol tetrazolium (MTT) Bioassay	47
4.2	MATERIALS AND METHODS	51
4.2.1	Materials	51
4.2.2	Methods	51
4.2.2.1	Preparation of Mycotoxin Stock Solutions	51
4.2.2.2	Preparation of Curcumin Stock Solution	51
4.2.2.3	Preparation of MTT Salt Solution	52
4.2.2.4	The MTT Bioassay	52
4.2.2.5	Statistical Analysis	55
4.3	RESULTS AND DISCUSSION	56
4.3.1	The Effect of the Ethanol Equivalents	56

4.3.2	The Effect of Deoxynivalenol	59
4.3.3	The Effect of Fumonisin B₁	62
4.3.4	The Effect of a Deoxynivalenol and Fumonisin B₁ Mixture	66
4.3.5	The Cytoprotective Effect of Curcumin in the Presence of the Selected Mycotoxins	68
4.3.5.1	Comparison of the Effects of Deoxynivalenol, Fumonisin B ₁ and the Mycotoxin Mixture	69
4.3.5.2	Comparison of the Effects of Deoxynivalenol, Fumonisin B ₁ and the Mycotoxin Mixture Following Co-treatment With Curcumin	69
4.4	CONCLUSION	73
CHAPTER 5	AN ASSESSMENT OF THE GENOTOXIC EFFECTS OF FUMONISIN B₁ AND DEOXYNIVALENOL ON THE HT-29 CELL LINE	74
5.1	INTRODUCTION	74
5.1.1	Genotoxicity	74
5.1.2	The Single Cell Gel Electrophoresis (SCGE) Assay	75
5.1.3	Detection of Apoptosis Using the SCGE assay	77
5.2	MATERIALS AND METHODS	78
5.2.1	Materials	78
5.2.2	Methods	78
5.2.2.1	Dilutions & Treatments	78
5.2.2.2	Slide Preparation	80
5.2.2.3	Cell Lysis	80
5.2.2.4	Alkali Unwinding and Electrophoresis	81

5.2.2.5	Neutralisation and Staining	81
5.2.2.6	Image Analysis	83
5.3	RESULTS AND DISCUSSION	83
5.3.1	The Effect of Ethanol	84
5.3.2	The Effect of Curcumin	84
5.3.3	The Effect of Deoxynivalenol	86
5.3.3.1	The Effect of Deoxynivalenol Only	86
5.3.3.2	The Effect of Deoxynivalenol Following Co-treatment With Curcumin	87
5.3.4	The Effect of Fumonisin B₁	88
5.3.4.1	The Effect of Fumonisin B ₁ Only	88
5.3.4.2	The Effect of Fumonisin B ₁ Following Co-treatment With Curcumin	90
5.3.5	The Effect of a Deoxynivalenol and Fumonisin B₁ Mixture	90
5.3.5.1	The Effect of a Deoxynivalenol and Fumonisin B ₁ Mixture Only	90
5.3.5.2	The Effect of a Deoxynivalenol and Fumonisin B ₁ Mixture Following Co-treatment With Curcumin	92
5.4	CONCLUSION	93
CHAPTER 6	A STRUCTURAL INVESTIGATION INTO THE EFFECTS OF DEOXYNIVALENOL AND FUMONISIN B₁ ON THE HT-29 CELL LINE	94
6.1	INTRODUCTION	94
6.1.1	Cell Morphology	94

6.1.2	Light Microscopy	95
6.1.3	Fluorescence microscopy	95
6.1.3.1	Acridine Orange and Ethidium Bromide Differential Staining	96
6.1.3.2	Hoechst 33258 Staining	98
6.2	MATERIALS AND METHODS	99
6.2.1	Materials	99
6.2.2	Methods	99
6.2.2.1	Dilutions and Treatments	99
6.2.2.2	Acridine Orange and Ethidium Bromide Differential Staining	100
6.2.2.3	Hoechst 33258 Staining	100
6.3	RESULTS AND DISCUSSION	101
6.3.1	The Effect of Ethanol	101
6.3.2	The Effect of Curcumin	102
6.3.3	The Effect of Deoxynivalenol	103
6.3.3.1	The Effect of Deoxynivalenol Only	103
6.3.3.2	The Effect of Deoxynivalenol Following Co-treatment With Curcumin	105
6.3.4	The Effect of Fumonisin B₁	107
6.3.4.1	The Effect of Fumonisin B ₁ Only	107
6.3.4.2	The Effect of Fumonisin B ₁ Following Co-treatment With Curcumin	109
6.3.5	The Effect of a Deoxynivalenol and Fumonisin B₁ Mixture	110
6.3.5.1	The Effect of a Deoxynivalenol and Fumonisin B ₁ Mixture Only	110

6.3.5.2	The Effect of a Deoxynivalenol and Fumonisin B ₁ Mixture Following Co-treatment With Curcumin	112
6.4	CONCLUSION	113
CHAPTER 7	AN ASSESSMENT OF HT-29 CELL SURFACE MORPHOLOGY FOLLOWING EXPOSURE TO FUMONISIN B ₁ AND DEOXYNIVALENOL	114
7.1	INTRODUCTION	114
7.1.1	The Cell Surface	114
7.1.2	Scanning Electron Microscopy	118
7.2	MATERIALS AND METHODS	118
7.2.1	Materials	118
7.2.2	Methods	119
7.2.2.1	Dilutions and Treatments	119
7.2.2.2	Preparation for Scanning Electron Microscopy	119
7.3	RESULTS AND DISCUSSION	121
7.3.1	The Effect of Ethanol	121
7.3.2	The Effect of Curcumin	121
7.3.3	The Effect of Deoxynivalenol	123
7.3.3.1	The Effect of Deoxynivalenol Only	123
7.3.3.2	The Effect of Deoxynivalenol Following Co-treatment With Curcumin	126
7.3.4	The Effect of Fumonisin B ₁	128
7.3.4.1	The Effect of Fumonisin B ₁ Only	128

7.3.4.2	The Effect of Fumonisin B ₁ Following Co-treatment With Curcumin	130
7.3.5	The Effect of a Mixture of Deoxynivalenol and Fumonisin B₁	132
7.3.5.1	The Effect of a Mixture of Deoxynivalenol and Fumonisin B ₁ Only	132
7.3.5.1	The Effect of a Mixture of Deoxynivalenol and Fumonisin B ₁ Following Co-treatment With Curcumin	134
7.4	CONCLUSION	136
CHAPTER 8: CONCLUSION		137
REFERENCES		139
APPENDICES		166
APPENDIX 1	REAGENTS FOR CELL CULTURE	166
1.1	COMPOSITION OF EMEM, HBSS AND PBS	166
1.2	COMPONENTS OF L-GLUTAMINE (200MM), PENICILLIN STREPTOMYCIN FUNGIZONE (PENSTREP) AND TRYPSIN VERSENE	168
1.3	PREPARATION OF COMPLETE CULTURE MEDIUM	169
1.4	PREPARATION OF CRYOPRESERVATION MEDIUM	169
1.5	PREPARATION OF TRYPAN BLUE (0.4%)	169
APPENDIX 2	REAGENTS FOR SINGLE CELL GEL ELECTROPHORESIS (SCGE)	170
2.1	PREPARATION OF 1M TRIS (PH 10)	170

2.2	PREPARATION OF TANK BUFFER, LYSING SOLUTION, TRIS (0.4M) AND LMPA (1% AND 0.5%)	170
APPENDIX 3	REAGENTS FOR FLUORESCENT MICROSCOPY	172
3.1	ACRIDINE ORANGE	172
3.2	ETHIDIUM BROMIDE	172
3.3	HOECHST 33258	172
3.4	PARAFORMALDEHYDE (10%)	172
APPENDIX 4	REAGENTS FOR SCANNING ELECTRON MICROSCOPY	173
4.1	GLUTARALDEHYDE (1%)	173
4.2	OSMIUM TETROXIDE (1%)	173
4.3	ETHANOL (70% AND 90%)	173

LIST OF FIGURES

CHAPTER 1 INTRODUCTION

Figure 1.1	Proportions of cancer deaths attributed to various factor (Chambers, 1985).	1
------------	---	---

CHAPTER 2 LITERATURE REVIEW



Figure 2.1	Factors influencing the occurrence of mycotoxins in human food or animal feed.	6
Figure 2.2	The structure of (a) the numbering system, and variable side groups of the tetracyclic trichothecene nucleus (Thrasher, 2004) and (b) deoxynivalenol (Bigwood, 2000).	9
Figure 2.3	The structure of the 80S ribosome: (a) the two subunits opened up to show the binding sites that participate in protein synthesis and (b) the formation of a peptide bond (Arms and Camp, 1995).	10
Figure 2.4	The structures of fumonisin B ₁ , sphingosine, and sphinganine (Schroeder <i>et al.</i> , 1994).	14
Figure 2.5	A schematic representation of sphingolipid biosynthesis depicting the site of action of FB ₁ in:  <i>de novo</i> sphingolipid biosynthesis as well as  in sphingolipid turnover.	17
Figure 2.6	The anatomy of the gastrointestinal tract (Raskin, 2004).	22
Figure 2.7	Schematic diagram of the colon, crypts of Lieberkuhn and associated cells (A.D.A.M. Medical Illustration Team, 2002; Schematic diagram of the colon, crypts of Lieberkuhn and associated cells, 2003).	24
Figure 2.8	An illustration of cellular biochemical and physical changes induced during apoptosis (Events in Apoptosis, 2002).	26

Figure 2.9	A stepwise model of colorectal carcinogenesis (Progression of colon cancer, 2001).	28
Figure 2.10	An illustration of (a) <i>Curcuma longa</i> (Campana, 2004), (b) turmeric powder (Turmeric powder, 2000) and (c) the chemical structure of curcumin (Zhu <i>et al.</i> , 2004).	33
CHAPTER 3 CELL CULTURE		
Figure 3.1	Cultured HT-29 colorectal adenocarcinoma cells: (a) approaching confluency and (b) following subculturing (Cell Lines, 2003).	40
Figure 3.2	An illustration depicting the process of trypsinisation.	41
Figure 3.3	A schematic diagram of a haemocytometer (adapted from Caprette, 2003).	43
Figure 3.4	Calculating cell viability using the haemocytometer (adapted from Biowhittaker cell biology products catalogue, 2002).	45
CHAPTER 4 CYTOTOXICITY OF DEOXYNIVALENOL AND FUMONISIN B₁ ON THE HT-29 CELL LINE		
Figure 4.1	An illustration of: (a) the cellular reduction of MTT salt (Rode <i>et al.</i> , 2004) and (b) formazan formation (Klipski <i>et al.</i> , 2003).	48
Figure 4.2	An illustration depicting the treatment procedure for the MTT assay	53
Figure 4.3	An illustration of the MTT bioassay.	54
Figure 4.4	The dose response graph of the equivalent EtOH controls on the HT-29 cell line over exposure periods 24 to 96 hours: [Significant difference from the untreated control: * ($p < 0.05$) and ** ($p < 0.01$)].	57

Figure 4.5	The dose response graph of varying concentrations of DON on the HT-29 cell line over exposure periods 24 to 96 hours: [Significant difference from the untreated control: * ($p<0.05$) and ** ($p<0.01$)].	59
Figure 4.6	The dose response graph of varying concentrations of FB ₁ on the HT-29 cell line over exposure periods 24 to 96 hours: [Significant difference from the untreated control: * ($p<0.05$) and ** ($p<0.01$)].	63
Figure 4.7	A dose response graph of varying concentrations of DFB ₁ on the HT-29 cell line over exposure periods 24 to 96 hours: [Significant difference from the untreated control: * ($p<0.05$) and ** ($p<0.01$)].	67
Figure 4.8	The dose response graph of the effects of DON, FB ₁ and DFB ₁ following: (a) individual treatment and (b) co-treatment with curcumin at the 48 hour exposure period: [Significant difference from the untreated control: * ($p<0.05$) and ** ($p<0.01$)].	70

CHAPTER 5 AN ASSESSMENT OF THE GENOTOXIC EFFECTS OF FUMONISIN B₁ AND DEOXYNIVALENOL ON THE HT-29 CELL LINE

Figure 5.1	An illustration of typical comets produced by (a) healthy, (b) necrotic and (c) apoptotic cells following electrophoresis (Krebsfaenger, 2001).	77
Figure 5.2	An illustration elucidating the treatment procedure for the SCGE assay.	79
Figure 5.3	The principal steps of the alkaline comet assay (Krause <i>et al.</i> , 2001).	82
Figure 5.4	Photomicrographs illustrating tail lengths observed for: (a) untreated, (b) ethanol (0.08%) treated and (c) curcumin treated cells (X100).	84
Figure 5.5	Photomicrographs illustrating tail lengths observed for cells treated with: (a) DON (5 μ M), (b) DON (50 μ M), (c) DON (5 μ M) and curcumin and (d) DON (50 μ M) and curcumin (X100).	86

Figure 5.6	Photomicrographs illustrating tail lengths observed for cells treated with: (a) FB ₁ (5μM), (b) FB ₁ (50μM), (c) FB ₁ (5μM) and curcumin and (d) FB ₁ (50μM) and curcumin (X100).	89
Figure 5.7	Photomicrographs illustrating tail lengths observed for cells following treatment with: (a) DFB ₁ (5μM), (b) DFB ₁ (50μM), (c) DFB ₁ (5μM) and curcumin and (d) DFB ₁ (50μM) and curcumin (X100).	91
Figure 5.8	Graphical representation of tail lengths observed following electrophoresis: [Significant difference between concentrations: * (p<0.01)].	92

CHAPTER 6 A STRUCTURAL INVESTIGATION INTO THE EFFECTS OF DEOXYNIVALENOL AND FUMONISIN B₁ ON THE HT-29 CELL LINE

Figure 6.1	Morphological changes of apoptosis (Rode <i>et al.</i> , 2004).	94
Figure 6.2	An illustration depicting the principle of acridine orange and ethidium bromide differential staining.	97
Figure 6.3	An illustration depicting the principle of Hoechst 33258 staining.	98
Figure 6.4	Photomicrographs illustrating AcOr/EtBr (AE) and Hoechst (H) stained (a) untreated and (b) ethanol (0.08%) treated cells showing intact cell membranes and normal nuclei (NN) (X400).	101
Figure 6.5	Photomicrographs illustrating AE and H stained curcumin (50μM) treated cells displaying normal (NN), condensed (CN) and fragmented (FN) nuclei as well as blebbing (B) (X400).	102
Figure 6.6	Photomicrographs illustrating AE and H stained (a) DON (5μM) and (b) DON (50μM) treated cells depicting condensed (CN) and fragmented (FN) nuclei (X400).	104

Figure 6.7	Photomicrographs illustrating AE and H stained (a) DON (5 μ M) and curcumin and (b) DON (50 μ M) and curcumin treated cells depicting condensed nuclei (CN) and blebbing (B) (X400).	106
Figure 6.8	Photomicrographs illustrating AE and H stained (a) FB ₁ (5 μ M) and (b) FB ₁ (50 μ M) treated cells depicting normal (NN), condensed (CN) and fragmented (FN) nuclei as well as blebbing (B) (X 400).	108
Figure 6.9	Photomicrographs illustrating AE and H stained (a) FB ₁ (5 μ M) and curcumin and (b) FB ₁ (50 μ M) and curcumin treated cells depicting condensed (CN) and fragmented (FN) nuclei as well as blebbing (B) (X400).	109
Figure 6.10	Photomicrographs illustrating AE and H stained (a) DFB ₁ (5 μ M) and (b) DFB ₁ (50 μ M) treated cells depicting condensed (CN) and fragmented (FN) nuclei as well as blebbing (B) (X400).	111
Figure 6.11	Photomicrographs illustrating AE and H stained (a) DFB ₁ (5 μ M) and curcumin and (b) DFB ₁ (50 μ M) and curcumin treated cells condensed nuclei (CN) and blebbing (B) (X400).	112

CHAPTER 7 AN ASSESSMENT OF HT-29 CELL SURFACE MORPHOLOGY FOLLOWING EXPOSURE TO FUMONISIN B₁ AND DEOXYNIVALENOL

Figure 7.1	Illustration depicting: (a) absorptive cell exterior and interior (Med Note, 1998), (b) microvillus structure (Mallery, 2004).	114
Figure 7.2	Depiction of the development of changes in the actin cytoskeleton during apoptotic cell death (stages 1-5) (Veselská <i>et al.</i> , 2003).	117
Figure 7.3	Schematic diagram illustrating specimen preparation for SEM (adapted from: Allan, 2003).	120
Figure 7.4	Scanning electron micrographs of (a) untreated control, (b) EtOH control and (c) curcumin control cells exhibiting blebbing (B) (X1000) and enlarged X4 to observe microvilli.	122

Figure 7.5	Scanning electron micrographs of the (a) 5 μ M and (b) 50 μ M DON treated cells (X1000) displaying blebbing (B) and clumping of microvilli (CM) and enlarged X4 to observe microvilli.	124
Figure 7.6	Scanning electron micrographs of (a) 5 μ M and (b) 50 μ M DON and curcumin co-treated cells displaying clumping of microvilli (CM) (X1000) and enlarged X4 to observe microvilli.	127
Figure 7.7	Scanning electron micrographs of (a) 5 μ M and (b) 50 μ M FB ₁ treated cells (X1000) and enlarged X4 to observe microvilli.	129
Figure 7.8	Scanning electron micrographs of (a) 5 μ M and (b) 50 μ M FB ₁ and curcumin co-treated cells displaying blebbing (B) and cytoplasmic leakage (L) (X1000) and enlarged X4 to observe microvilli.	131
Figure 7.9	Scanning electron micrographs of the (a) 5 μ M and (b) 50 μ M DFB ₁ treated cells displaying blebbing (B) and clumping (CM) (X1000) and enlarged X4 to observe microvilli.	133
Figure 7.10	Scanning electron micrographs of (a) 5 μ M and (b) 50 μ M DFB ₁ and curcumin treated cells displaying blebbing (B) and clumping (CM) (X1000) and enlarged X4 to observe microvilli.	135

LIST OF TABLES

CHAPTER 5 CYTOTOXICITY OF DEOXYNIVALENOL AND FUMONISIN B₁ ON THE HT-29 CELL LINE

Table 4.1	Comparison of cell viabilities following treatment with the toxins individually and in combination with curcumin: [Significant difference from individual toxin treatment: * (p<0.05) and ** (p<0.01)].	72
------------------	---	----

LIST OF ABBREVIATIONS

AA	arachidonic acid
ACF	aberrant crypt focus
AcOr	acridine orange
AE	acridine orange and ethidium bromide stained
ALS	alkali-labile sites
ANOVA	analysis of variance
APC	adenomatous polyposis coli
A-T	adenine–thymine
B	blebbing
°C	degrees Celsius
C	clumping
C3/4/8/15	carbon 3/4/8/15
Ca ²⁺	calcium ion
CCM	complete culture medium
CM	clumping of microvilli
cm	centimeter
cm ²	square centimeter
cm ³	cubic centimetre
CN	condensed nuclei
CoA	coenzyme A
COX-1	cyclooxygenase-1
COX-2	cyclooxygenase-2
Cu	copper

3-D	three dimensional
DAPI	4',6-diamidino-2-phenylindole
DAS	diacetoxyscirpenol
DCC	deleted in colorectal cancer
DFB ₁	deoxynivalenol and fumonisin B ₁ mixture
DMSO	dimethylsulphoxide
DNA	deoxyribonucleic acid
DON	deoxynivalenol
DSB	double-stranded breaks
e.g.	for example
EDTA	ethylenediaminetetracetic acid
EMEM	eagle's minimum essential medium
<i>et al.</i>	<i>et alii</i> (and others)
EtBr	ethidium bromide
EtOH	ethanol
Fas	fatty acid synthase
FB ₁	fumonisin B ₁
FCS	foetal calf serum
FN	fragmented nuclei
GI	gastrointestinal tract
GSL	glycosphingolipid
H	hoechst 33258 stained
H ₂ O	water
H ₂ O ₂	hydrogen peroxide
HBSS	hank's balanced salt solution
HCl	hydrochloric acid

HEPA	high efficiency particulate air
HEPES	<i>N</i> -2-Hydroxyethylpiperazine- <i>N'</i> -2-ethane-sulfonic acid
hr	hour
hrs	hours
IgA	immunoglobulin A
K-ras	retrovirus-associated DNA sequence
L	leakage (cytoplasmic)
LMPA	low melting point agarose
M	molar
mA	milliampere
MeOH	methanol
mg	milligram
Mg ²⁺	magnesium ion
min	minutes
ml	milliliter
mm	millimetre
μg	micrograms
μg/ml	micrograms per millilitre
μl	microlitre
μm	micrometre
μM	micromolar
MTT	3-[4,5-dimethylthiazol-2-yl]-2,5-diphenyltetrazolium bromide
NAD ⁺	oxidised nicotinamide adenine dinucleotide
NADH	reduced nicotinamide adenine dinucleotide
NADPH	reduced nicotinamide adenine dinucleotide phosphate
NIV	nivalenol

nm	nanometer
NN	normal nuclei
NSAIDS	non-steroidal anti-inflammatory drugs
O_2^-	superoxide anion
OH^\cdot	hydroxyl radical
%	percent
p	probability value
p53	phosphoprotein 53
PBS	phosphate buffered saline
PCD	programmed cell death
PFA	paraformaldehyde
PG	prostaglandin
pH	hydrogen-ion concentration
RNA	ribonucleic acid
ROS	reactive oxygen species
Sa	sphinganine
SCGE	single cell gel electrophoresis
SEM	scanning electron microscopy
So	sphingosine
SSB	single-stranded breaks
TNF	tumour necrosis factor
Tris	tris(hydroxymethyl)aminomethane
UDS	unscheduled DNA synthesis
UV	ultraviolet
V	volts

CHAPTER 1

INTRODUCTION

1.1 CHEMICAL CARCINOGENS

It has been estimated that 80% of all cancer deaths are caused by chemicals in our environment and it has been suggested that, to decrease the incidence of this disease, these compounds need to be identified and controlled. Many of these compounds, however, are products of industrialised society and are difficult to eliminate. The epidemiological data shown in Figure 1.1 indicates that the chemicals found in alcoholic beverages, pollutants, food additives and medicines represent important aetiological agents and that tobacco and diet represent the two largest sources of carcinogens.

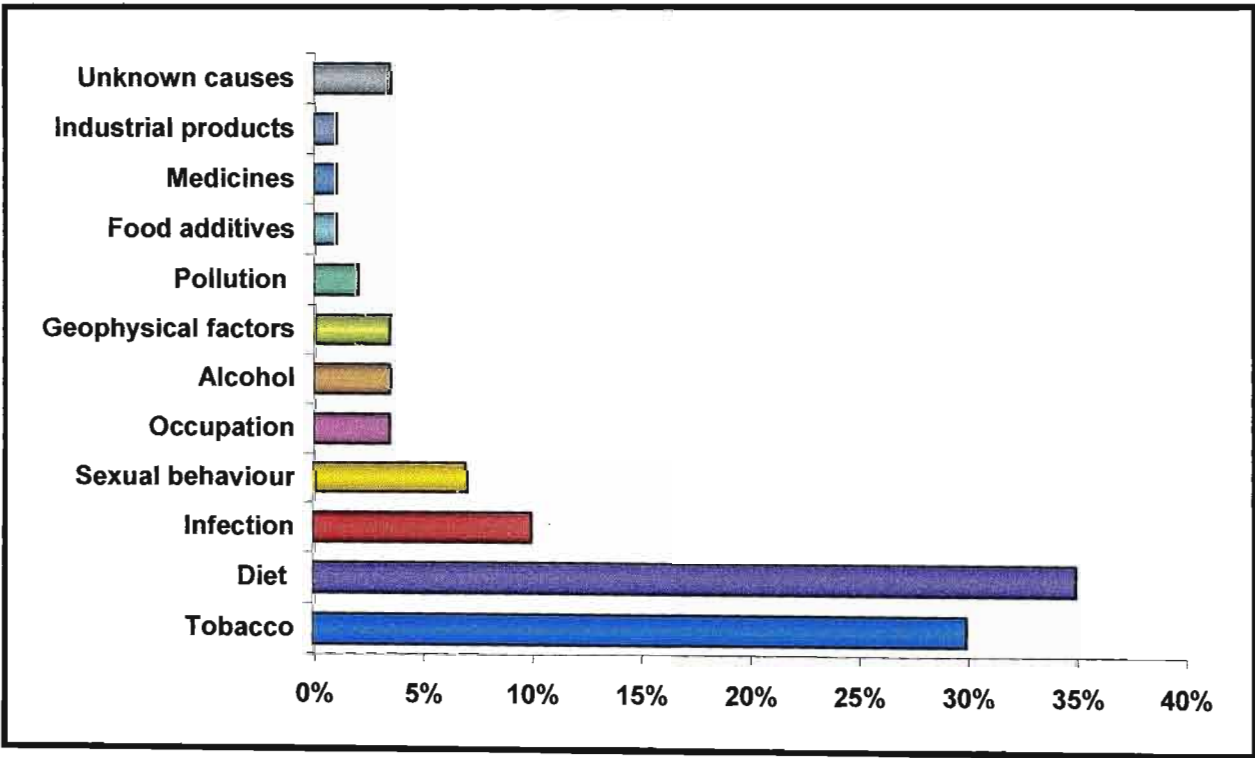


Figure 1.1: Proportions of cancer deaths attributed to various factors (Chambers, 1985).

It is possible to stop tobacco use however food borne carcinogens are naturally present in food or produced during preparation and are extremely difficult to eradicate. Diet may therefore play an important role in carcinogenesis (Chambers, 1985).

1.2 *FUSARIUM* TOXINS

Studies conducted in China (Chu and Li, 1994; Yoshizawa *et al.*, 1994; Wang *et al.*, 2000) as well as the Transkei region of South Africa (Rheeder *et al.*, 1992), have indicated that the consumption of fumonisin B₁ contaminated staple foods is aetiologically related to oesophageal cancer in humans. It is therefore possible that the ingestion of this and other *Fusarium* mycotoxins may be related to cancers in other parts of the gastrointestinal tract.

Animal studies (Lake *et al.*, 1987; Shephard *et al.*, 1994) showed that a large percentage of ingested mycotoxins are excreted in faeces therefore it can be postulated that there is a high potential of exposure in the colon region and this exposure may play a role in colon carcinogenesis. Deoxynivalenol is of particular interest, as it is known to exert toxic effects in the stomach and intestines (Kasuga *et al.*, 1998).

These mycotoxins can occur concurrently and result in multi-mycotoxin exposure among populations where these foods comprise the majority of the staple diet. Research to date has, however, focused on how single toxins affect biological systems but there is now growing concern over the effects of a combination of mycotoxins as the interactive effect of combinations of mycotoxins is poorly understood (Boeira *et al.*, 2000). The determination of their biological action has since become the focus of much research (Gorst-Allman *et al.*, 1985).

1.3 CURCUMIN AND CHEMOPREVENTION

Curcumin (diferuloylmethane) is a yellow pigment isolated from the ground rhizome of *Curcuma longa* Linn and is commonly referred to as turmeric. Widely used as a spice, colouring agent and ingredient in cosmetics and medicinal preparations, it is a phenolic compound that has been demonstrated to exhibit potent antioxidant, free radical scavenger and anti-inflammatory properties. Several epidemiology and animal model studies have demonstrated that compounds that possess such properties can inhibit carcinogenesis (Kawamori *et al.*, 1999; Chauhan, 2002; Garcea *et al.*, 2003).

1.4. THE HT-29 CELL LINE

The HT-29 cell line is widely used for experimental studies because it retains many biochemical and physiologic features of normal colorectal epithelial cells. In addition, this colorectal cell line contains no intact APC protein or functional p53 protein. The APC and p53 tumour-suppressor genes are both involved in growth inhibition and their loss leads to unregulated cellular growth (Morin *et al.*, 1996). The HT-29 cell line therefore provides a suitable system in which to determine the cytotoxic effects of various test agents.

1.5 OBJECTIVES

The objectives of this investigation were to:

- test the effects of the mycotoxins deoxynivalenol and fumonisin B₁ individually and in combination on the HT-29 human colonic adenocarcinoma cell line.
- investigate the cytoprotective effects of curcumin on the HT-29 cell line when co-administered with the selected mycotoxins.

CHAPTER 2

LITERATURE REVIEW

2.1 ENVIRONMENTAL CARCINOGENESIS

Environmental carcinogenesis is a matter of great concern and a field of extensive research. This is mainly due to the realisation that the aetiologies of most human cancers reside in environmental factors and that certain chemicals can induce cancer. The likelihood of being afflicted with cancer may therefore be a function of one's lifestyle as a consequence of exposure to carcinogenic chemicals through diet, occupation or habits. Today, the burgeoning increase of dietary related disease accompanied by the ever expanding repertoire of toxic agents brings up the concept that diet or dietary components may influence carcinogenesis

Dietary carcinogens can be divided into two categories namely microcomponents, which incorporate genotoxic agents that cause genetic alterations related to carcinogenesis and macrocomponents, which include tumour promotion-associated constituents (Sugimura, 2000). Genotoxic agents are defined as causing DNA damage which result in gene point mutations, deletions and insertions, recombinations, rearrangements and amplifications as well as chromosomal aberrations, while tumour promoters are known to cause cell proliferation with or without accompanying chronic cell damage (Sugimura, 2000). Due to historical reasons, most early research concerning carcinogenic chemicals focussed on the properties of synthetic compounds, however, in addition to recognised environmental toxic agents, in this rapidly changing world, the array of novel toxins that make their way into the gastrointestinal (GI) tract poses significant threats and needs to be better understood (Sreedharan and Mehta, 2004).

A substantial amount of evidence, accumulated over the last four decades, points to the importance of naturally occurring carcinogens as health hazards. Most of these carcinogens are secondary metabolites of microorganisms and plants and the most relevant to man are those compounds occurring in plants which are used as foods, medicines and beverages. Of special interest are the mycotoxins, a versatile family of ubiquitous fungal metabolites eliciting toxicity or mycotoxicoses in man and animals (Kasuga *et al.*, 1998).

2.2 MYCOTOXINS AND MYCOTOXICOSES

Mycotoxins are a very diverse group of secondary metabolites produced by a taxonomically wide range of filamentous fungi (Blunden *et al.*, 1991) that serve as a chemical defence system (Etzel, 2002), evoking a toxic response when introduced in low concentration to higher vertebrates and other animals by natural routes such as ingestion, inhalation or skin contact. Initially discovered when epidemics of illness were traced to the ingestion of mouldy food approximately 400 known mycotoxins are in existence today with the predominant fungal producers belonging to the *Aspergillus*, *Fusarium*, *Penicillium* and *Alternaria* genera (Szkudelska *et al.*, 2002).

These toxins are intimately associated with most foods or feeds and can be produced and accumulated at every stage of harvesting, production and storage of food under conditions favourable for the growth of the toxin-producing fungus (Szkudelska *et al.*, 2002). They therefore have the ability to contaminate animal and human feeds at all stages of the food chain (Figure 2.1). The global occurrence of mycotoxins is considered to be a major risk factor affecting human and animal health as it has been estimated that 25% of the world's crop productions is contaminated with mycotoxins (Bouhet *et al.*, 2004). It is now well established that, among other effects, several mycotoxins induce cancer in experimental animals.

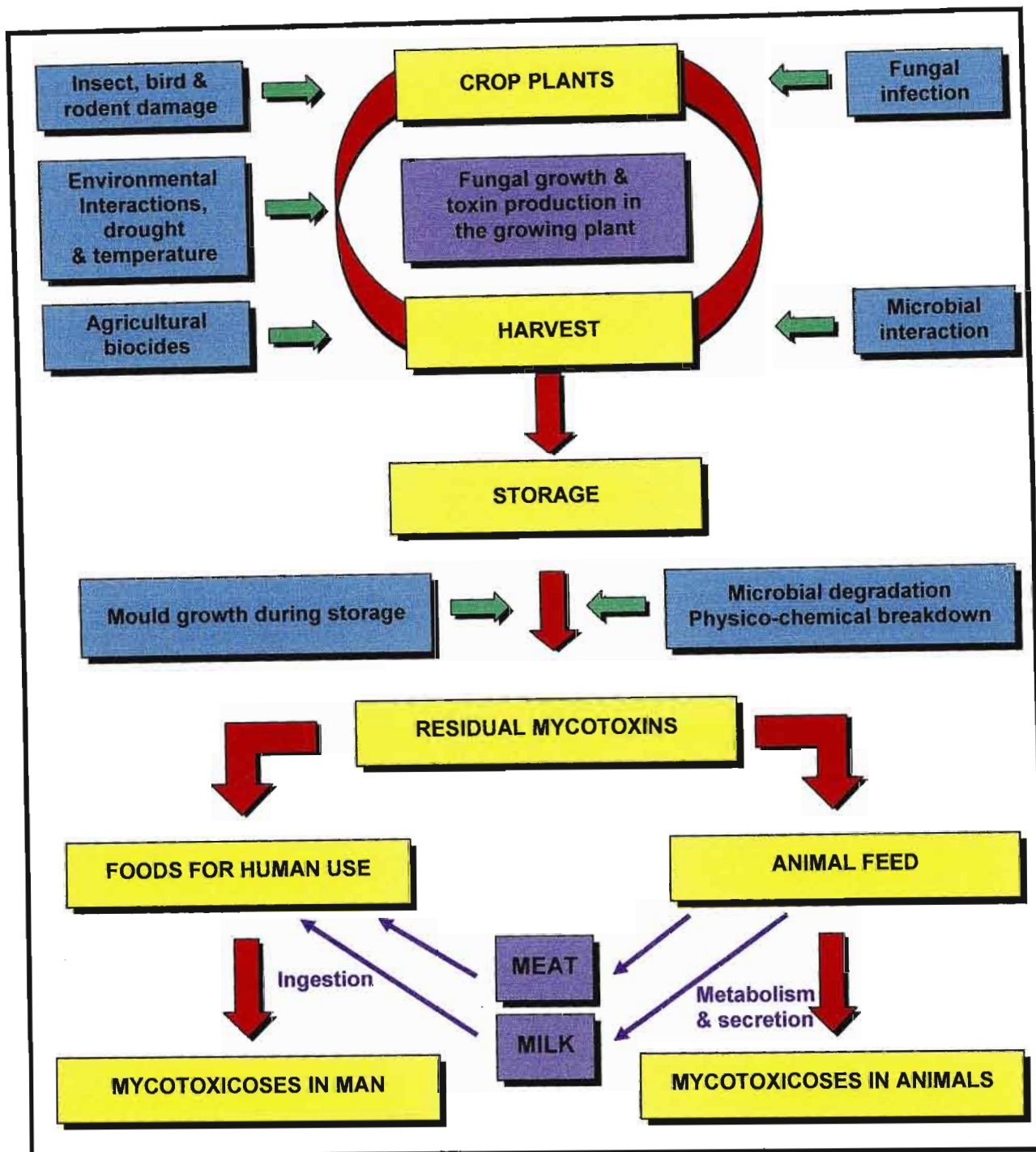


Figure 2.1: Factors influencing the occurrence of mycotoxins in human food or animal feed.

Certain mycotoxins may be of a beneficial nature and can be used as antibiotics (penicillins), immunosuppressants (cyclosporine) and in the control of post partum haemorrhages and migraine headaches (ergot alkaloids) (Etzel, 2002) while others, upon ingestion, can lead to a wide range of disease states or mycotoxicoses in humans and animals (Blunden *et al.*, 1991).

The toxic effects of mycotoxins on animal health and productivity have long been recognised in intensively farmed animals such as poultry, swine and dairy cattle as a consequence of consuming mycotoxin contaminated feedstuffs (Charoenpornsook *et al.*, 1998). These effects may be acute or long term (chronic or cumulative effect) and may include the induction of cancers and immune deficiency (Coulombe, 1993). Massive mycotoxin contamination of food resulting in outbreaks of illness, however, occurs rarely today in developing countries. The primary concern is actually the long term effects of ingesting food contaminated with low levels of mycotoxins.

One of the most prevalent fungal genera globally is *Fusarium* (Scientific Committee on Food, 2002). This genus contains a number of species that are capable of producing a variety of mycotoxins including the trichothecenes deoxynivalenol (DON), nivalenol (NIV), T-2 toxin and diacetoxyscirpenol (DAS) as well as fumonisins and zearalenone (ZEA) (Boeira *et al.*, 2000). As these fungi can naturally co-occur on foods and feeds, there is a strong likelihood of the simultaneous occurrence of two or more toxins in naturally contaminated cereals. This has been frequently documented e.g. barley, maize and wheat contaminated with DON, NIV and ZEA and maize contaminated with fumonisin B₁ (FB₁), ZEA, DON and T-2 toxin (Fazekas *et al.*, 1996) and raises the possibility of mycotoxin interaction.

The most commonly encountered food-borne mycotoxins currently include FB₁ and DON (vomitoxin) (Etzel, 2002). Although not the most toxic of all types of *Fusarium* mycotoxins, these compounds may pose a major threat to public and animal health as well as economy due to the frequency of their occurrence and implications in disease. This hazard may be compounded by the possibility of mycotoxin interaction due to their co-occurrence in grains.

2.2.1 DEOXYNIVALENOL

2.2.1.1 Chemical and Physical Properties

Deoxynivalenol, produced by the *Fusarium* species *F. graminearum* and *F. culmorum*, has been found to be one of the most frequent contaminants of agricultural crops worldwide that has great stability during storage/milling and in the processing and cooking of food as it does not degrade at high temperatures (Rotter *et al.*, 1996; Gimeno, 2000). Biosynthetically, this toxin has a 12,13-epoxy-3, 4,15- trihydroxytrichotec-9-en-8-one (Figure 2.2b) chemical structure and is derived from trichodiene which is the biochemical precursor for all trichothecenes (Desjardins *et al.*, 1993).

The trichothecenes are a group of naturally occurring, chemically related tetracyclic sesquiterpenoid compounds produced by numerous species of *Cephalosporium*, *Myrothecium*, *Stachybotrys*, *Trichoderma* and *Fusarium* that have been demonstrated to have cytotoxic, phytotoxic, antifungal and insecticidal activity (Olsson, 2000) and are regarded as one of the most diverse and important families of mycotoxins (Gorst-Allman *et al.*, 1985).

These compounds, characterised by a 12,13-epoxy-trichothec-9-ene (Figure 2.2a) skeleton (trichothecene nucleus), are colourless, mostly crystalline, optically active solids that are generally soluble in moderately polar organic solvents but only slightly soluble in water (Tamm, 1977) and contain an olefinic bond at position C-9,10, an epoxy ring at C-12,13 as well as a number of hydroxyl and acetoxy groups (Figure 2.2) (Canady *et al.*, 2001). Structural diversity amongst the trichothecenes arises from the position, number, and type of functional groups attached to the 12,13-epoxy-trichothec-9-ene skeleton (Kimura *et al.*, 2003).

These compounds do not require metabolic activation to exert their toxic effects. They are lipophilic and are easily absorbed through the skin, respiratory and intestinal tracts (Thrasher, 2001).

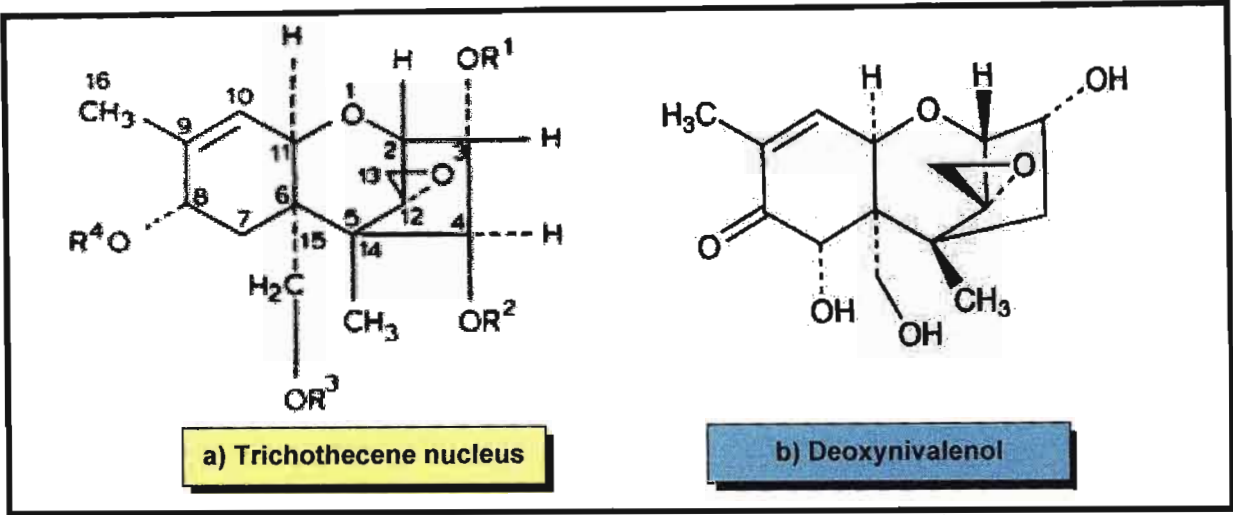


Figure 2.2: The structure of (a) the numbering system, and variable side groups of the tetracyclic trichothecene nucleus (Thrasher, 2001) and (b) deoxynivalenol (Bigwood, 2000).

Trichothecenes produced by *Fusarium* species belong to two categories according to their functional groups. Group A is characterised by an oxygen functional group other than a carbonyl group at C-8 and includes T-2 toxin and HT-2 toxin while group B is characterised with a carbonyl group at C-8 and includes DON and nivalenol (Scientific Committee on Food, 2002). Deoxynivalenol, which lacks a substituent at C-4, is considered to be the least toxic of this group of compounds (Rotter *et al.*, 1996).

2.2.1.2 Mechanism of Action

The most prominent mechanism of the trichothecenes, including DON, at the biochemical and cellular level is the inhibition of protein synthesis (Ueno, 1977).

Their potency depends on structural substituents and requires an unsaturated bond at the C9–C10 position and integrity of the 12,13-epoxy ring (Canady *et al.*, 2001). Studies with radiolabeled trichothecene mycotoxins suggest that the toxin interaction with cells is best viewed as a free, bidirectional movement of these low-molecular-weight chemicals across the plasma membrane and specific, high-affinity binding to the 60S ribosome, where they interfere with the activity of peptidyl transferase (Hernández and Cannon, 1981; Wannemacher and Wiener, 2002).

Peptidyl transferase is an integral ribosomal enzyme of the large ribosomal subunit, which catalyses the transfer of the peptide attached to the tRNA occupying the P site to the amino acid of the tRNA occupying the A site with the formation of a peptide bond (a covalent bond) between the two adjacent residues in a growing protein molecule (Moore and Steitz, 2003). Depending on the degree of substitution, trichothecenes can bind to either selected peptidyltransferase centres (highly substituted) or to most or all centres (small trichothecenes) thereby affecting peptide bond formation and the resultant polypeptide chain.

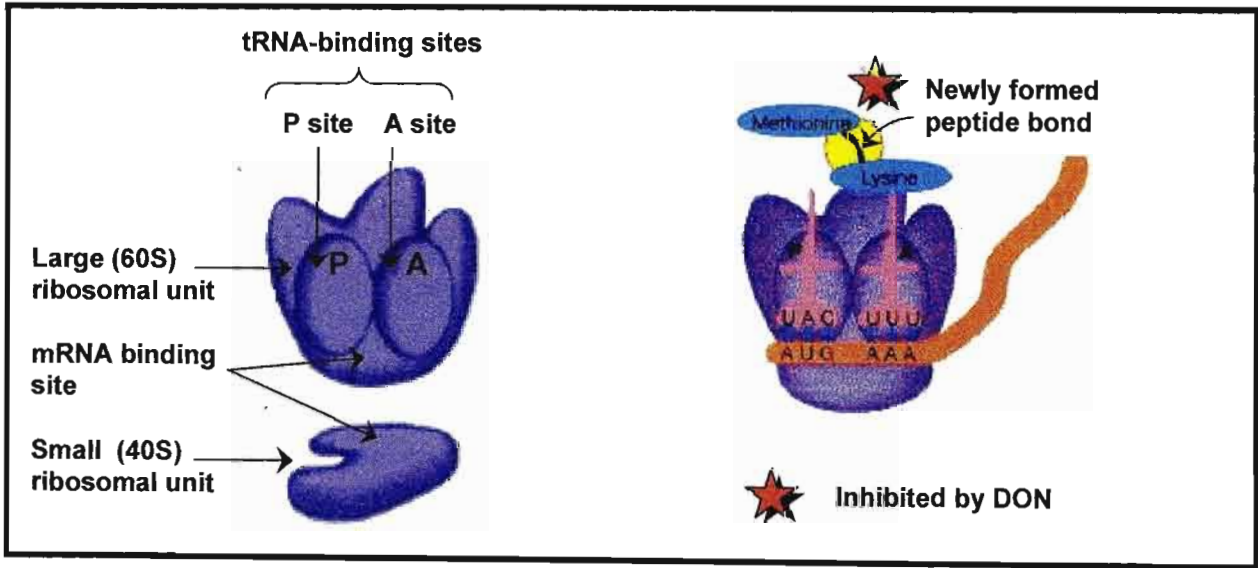


Figure 2.3: The structure of the 80S ribosome: (a) the two subunits opened up to show the binding sites that participate in protein synthesis and (b) the formation of a peptide bond (Arms and Camp, 1995).

Trichothecenes with substituents at both C-3 and C-4 predominantly inhibit polypeptide chain initiation whereas those lacking one substituent at either side, like DON are inhibitors of chain elongation (Figure 2.3) (Rotter *et al.*, 1996).

Deoxynivalenol has also been demonstrated to inhibit both DNA and RNA synthesis. Scheduled DNA synthesis is inhibited in various types of cells as well as in mice and rats, although to a lesser degree than protein synthesis (Wannemacher and Wiener, 2002). The mechanism of inhibition is not clear but is believed to be related indirectly to the cessation of protein synthesis as the pattern by which DNA synthesis is inhibited is consistent with the primary effect of these toxins on protein synthesis (Wannemacher and Wiener, 2002). The inhibition of RNA synthesis is thought to be a secondary effect of the inhibition of protein synthesis (Rotter *et al.*, 1996).

In addition, Moon and Pestka (2002) demonstrated that DON induces cyclooxygenase-2 (COX-2) expression in macrophages. This rate-limiting enzyme is known to be superinduced by protein synthesis inhibitors and catalyses the oxygenation of arachidonic acid to prostaglandin endoperoxides. The resulting metabolites are converted enzymatically into prostaglandins and thromboxane A₂, which play both physiologic and pathologic roles in a diverse range of inflammatory sequelae.

Deoxynivalenol has also been reported to exert a haemolytic effect on erythrocytes as well as toxic effects on cell membranes. In addition, DON was shown to induce apoptosis in lymphatic and haematopoietic tissue (Scientific Committee on Food, 2002).

2.2.1.3 Toxic Effects

Deoxynivalenol is known to cause both acute and chronic adverse health effects in man and animals and involves the characteristic induction of vomiting. Amongst the animals, swine appear to be most susceptible to DON in comparison to cattle and poultry (Beasley, 1999). As the gastrointestinal tract and digestive physiology of the pig are very similar to that of humans, they provide a good model of extrapolation to man (Bouhet *et al.*, 2004). This may be of significance when considering the effects of this toxin in man.

2.2.1.3.1 Toxic Effects in Animals

The main overt effects at low dietary concentrations (subchronic exposure) in various animal species has been demonstrated to result in reduced feed intake (anorexia), reduced weight gain, and changed levels in some blood parameters including serum immunoglobulins. Several studies have demonstrated effects on immunoglobulin A (IgA) which indicates the possibility of suppression of humoral and cellular immunity, resulting in an increased susceptibility for infectious diseases. Postnatal mortality, embryotoxic effects have also been observed in mice at maternally toxic doses (Scientific Committee on Food, 1999). The main effects at higher dietary concentrations (acute/subacute exposure) include vomiting (in pigs), delayed gastric emptying (in rats and mice), feed refusal, weight loss and diarrhoea. Necrosis in various tissues such as the GI tract, bone marrow and lymphoid tissues has also been observed following acute intoxication (Scientific Committee on Food, 1999).

The reducing feed intake or anorexic effect of DON is thought to be brought about by the increased synthesis of the hormone neurotransmitter serotonin following the increased uptake of tryptophan by the brain as a consequence of protein synthesis inhibition although irritation of the GI tract may also play a role (Cunningham, 2004).

The emetic effect is thought to be mediated by affecting serotonergic activity in the central nervous system or via peripheral actions on serotonin receptors (Scientific Committee on Food, 2002).

2.2.1.3.2 Toxic Effects in Man

In man, acute toxicity has been found causing vomiting and irritation to the respiratory tract. Outbreaks of toxicosis associated with consumption of mould contaminated wheat and corn and related to the presence of *F. graminearum* have been reported in Japan (red mould disease), India (DON toxicosis) and China (fusariotoxycosis) (Bhat *et al.*, 1989; Li *et al.*, 1999; Wijnands and van Leusden, 2000).

Although increased COX-2 expression *in vitro* has been associated with increased cellular proliferation and decreased apoptosis (Kovvali *et al.*, 2003), evidence for carcinogenicity and/or mutagenic properties of DON in humans or animals is inadequate (Scientific Committee on Food, 1999). It has been reported that the immunotoxicity and the general toxicity of DON are the critical effects to be considered (Gimeno, 2000).

2.2.2 FUMONISIN B₁

2.2.2.1 Chemical and Physical Properties

Fumonisin B₁ is a polar 1,2,3-propanetricarboxylic acid, 1,1'-[1-(12-amino-4,9,11-trihydroxy-2-methyl-tridecyl)-2-(1-methylpentyl)-1,2-ethane-diyl]ester (Figure 2.4) and the predominant member of a group of structurally related compounds known as fumonisins. This mycotoxin is produced by *Fusarium verticillioides* (*moniliforme*), *F. proliferatum* and *Aspergillus ochraceus*, some of the most prevalent moulds in agricultural products worldwide (Rumora *et al.*, 2002).

Fumonisin B₁ has, thus far, been established as non-mutagenic and non-genotoxic using the salmonella mutagenicity and DNA repair assays respectively. It has been demonstrated to be carcinogenic in an established bioassay for tumour-promoters via the induction of γ-glutamyl transpeptidase-positive foci in the livers of both noninitiated and diethylnitrosamine-initiated rats (Schroeder *et al.*, 1994). This mycotoxin has also been characterised as a mitogenic as well as an anti-proliferative agent (Rumora *et al.*, 2002).

Structurally, FB₁ has a polyhydric alcohol backbone (Abado-Becognee *et al.*, 1998) that is very similar to sphingosine (So) and sphinganine (Sa) (Figure 2.4), the long-chain sphingoid base backbones of complex sphingolipids. This class of membrane lipids encompasses ceramides and more complex phosphosphingolipids and glycosphingolipids (GSL) that occur primarily in cellular membranes, lipoproteins and other lipid-rich structures of all eukaryotic cells (Wang *et al.*, 1991; Merrill *et al.*, 2001; Merrill, 2002).

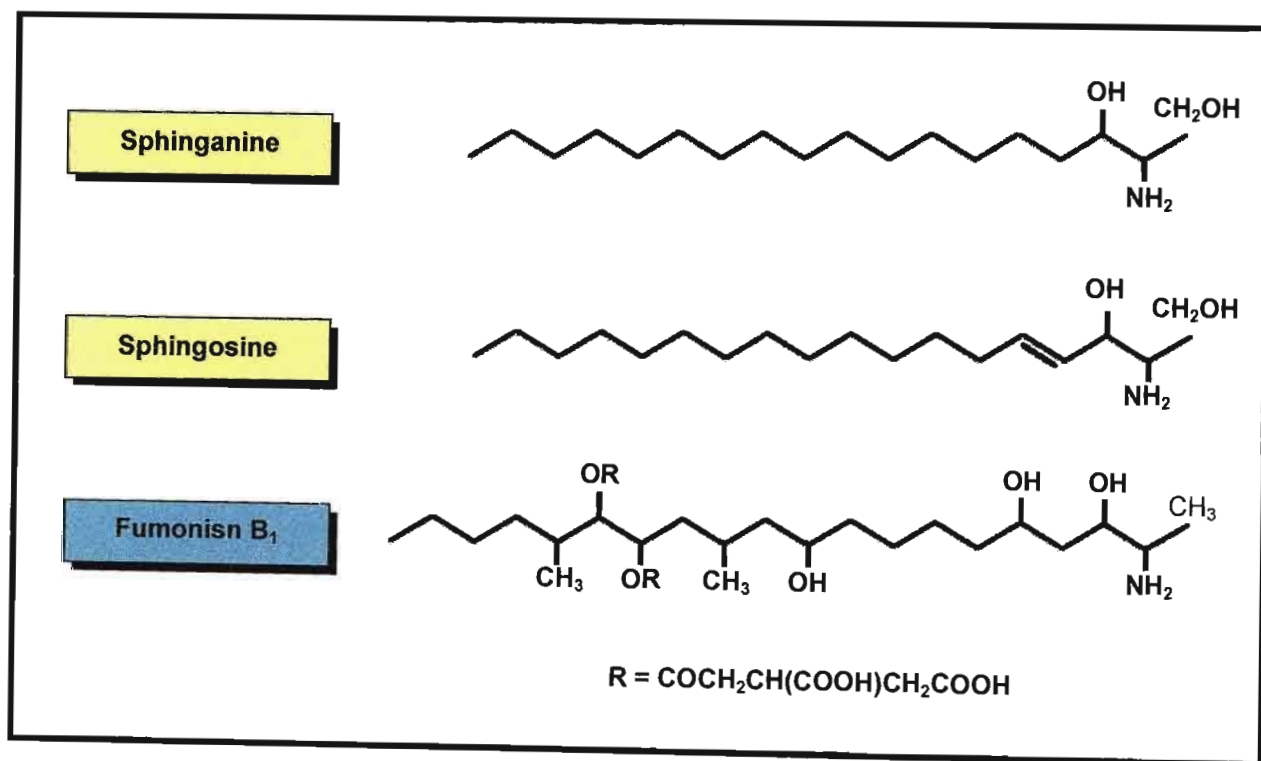


Figure 2.4: The structures of fumonisin B₁, sphingosine, and sphinganine (Schroeder *et al.*, 1994).

In addition to forming specialised structures in cells, these sphingolipids mediate cell-cell and cell-substratum interactions, modulate the behaviour of cellular proteins and receptors and participate in signal transduction (Merrill, 2002). They are consequently believed to play critical roles in cell growth, differentiation, transformation and death (Wang *et al.*, 1991).

The similarity between FB₁ and the sphingoid bases has led to the hypothesis that the mechanism of action of FB₁ may involve interference with sphingolipid metabolism.

2.2.2.2 Mechanism of Action

2.2.2.2.1 Sphingolipid Metabolism

Bioactive sphingolipids are formed both as intermediates of sphingolipid biosynthesis and by the turnover of complex sphingolipids. Briefly, the pathway of *de novo* sphingolipid biosynthesis occurs at the cytosolic face of the endoplasmic reticulum (Malagarie-Cazenave *et al.*, 2002) and begins with the condensation of L-serine and palmitoyl-CoA, a reaction catalysed by the pyridoxal phosphate-dependent serine palmitoyltransferase.

Its product, 3-ketosphingosine (3-dehydrosphinganine), is immediately reduced by the NADPH-dependent 3-dehydrosphinganine reductase to yield Sa (D-erythrosphinganine, dihydrosphingosine). The Sa is then acylated by ceramide synthase (*N*-acyltransferase) to form dihydroceramide and the subsequent introduction of the 4,5-double bond by the dihydroceramide desaturase enzyme leads to the formation of ceramide, an inducer of apoptosis and a precursor for the more complex sphingolipids such as sphingomyelin and glycosphingolipids (Michel *et al.*, 1997; Hannun and Obeid, 2002).

Turnover of these more complex sphingolipids occurs in the acidic organelles as well as in several other subcellular compartments and involves the production of ceramide by the breakdown of sphingolipids by glycosidases (for glycolipid degradation) and sphingomyelinases (for sphingomyelin degradation). The ceramide is then deacylated by ceramidase to release So which may then be reacylated to ceramide via ceramide synthase or phosphorylated by sphingosine kinase to form the mitogenic and anti-apoptotic sphingosine 1-phosphate (Malagarie-Cazenave *et al.*, 2002). The sphingoid base 1-phosphates may then be cleaved by sphingoid lyases to form fatty aldehydes and ethanolamine phosphates which can be redirected into other biosynthetic pathways (Riley *et al.*, 2001). In this way, the sphingolipid signaling pathways maintain the balance between cell death and regeneration, a critical factor in carcinogenesis.

2.2.2.2.2 Involvement of Fumonisin B₁

This ability of FB₁ to obstruct or disrupt sphingolipid biosynthesis was confirmed by Wang *et al* (1991) who demonstrated, using rat hepatocytes, that fumonisins block sphingolipid biosynthesis by competitively inhibiting the enzyme ceramide synthase (sphingosine [sphinganine] *N*-acyltransferase). This key component, as mentioned previously, catalyses both the acylation of Sa in the *de novo* biosynthesis of sphingolipids as well as the reacylation of So derived from sphingolipid turnover or dietary sources/growth medium (Wang *et al.*, 1991; Riley *et al.*, 2001). Ceramide synthase recognises the amino group (sphingoid-binding domain) and the tricarballic acid side chains (fatty acyl CoA domain) of FB₁ and allows the binding of the mycotoxin to the catalytic site of this enzyme. This is the first event in the process referred to as "disruption of sphingolipid metabolism" which encompasses all the changes that occur in biosynthetic rates and intracellular concentrations of the intermediates and end products within both the *de novo* sphingolipid pathway and branch pathways.

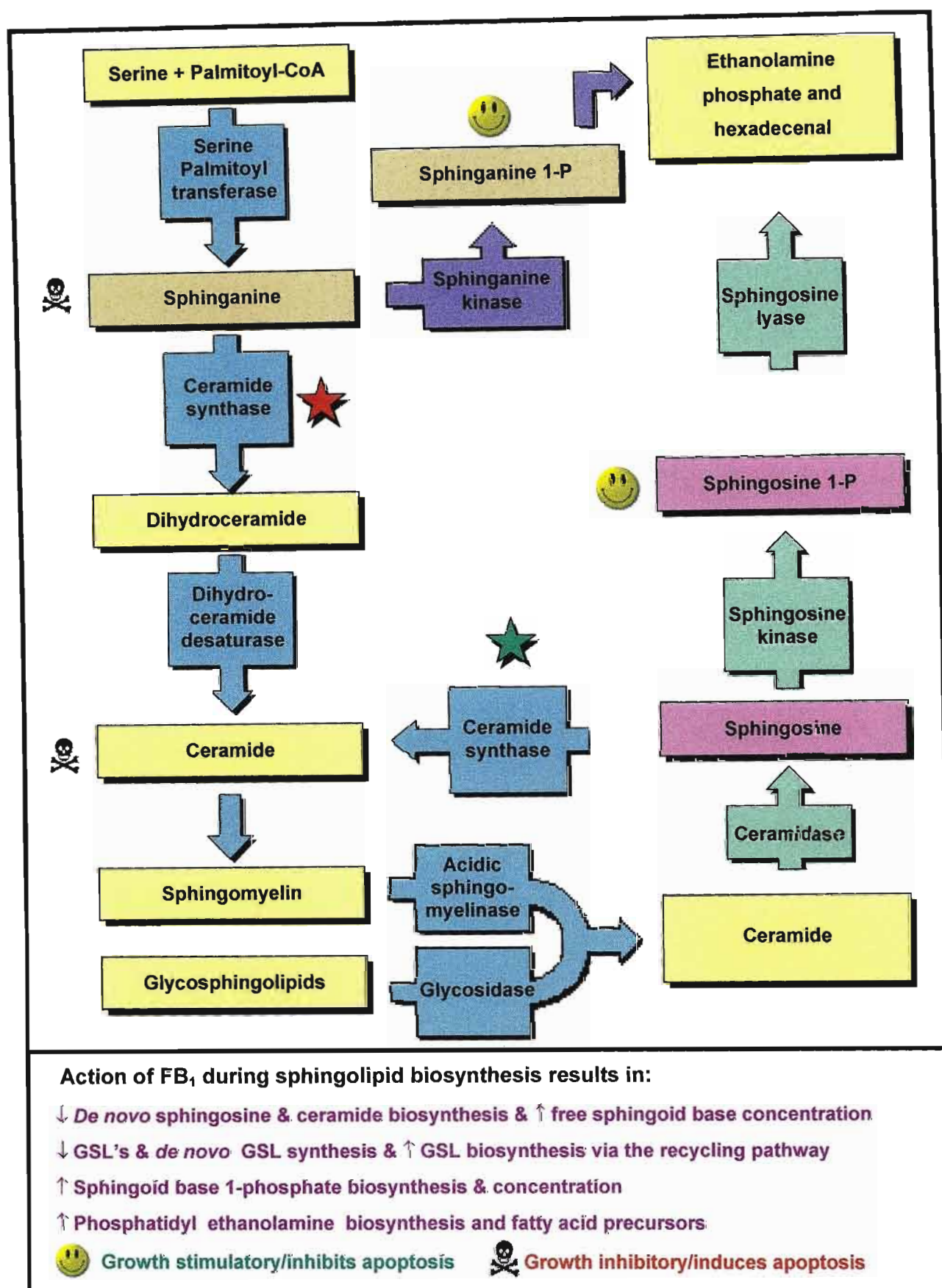


Figure 2.5: A schematic representation of sphingolipid biosynthesis depicting the site of action of FB₁ in: ★ *de novo* sphingolipid biosynthesis as well as in ★ sphingolipid turnover.

The biochemical consequences of this disruption includes decreased ceramide synthesis, alterations in the cellular concentration of specific glycosphingolipids and increased intracellular concentrations of free sphingoid bases and their 1-phosphates (Wang *et al.*, 1999; Riley *et al.*, 2001).

As ceramide is a precursor of complex sphingolipids (Hannun and Obeid, 2002), the inhibition of its synthesis leads to a concentration-dependent reduction in complex sphingolipids such as sphingomyelin and glycosphingolipid. The depletion of these complex sphingolipids impairs the function of certain membrane proteins resulting in membrane damage and therefore plays a role in the abnormal behaviour and altered morphology of FB₁ treated cells. Decreased ceramide synthesis also results in reduced ceramide induced cell death as ceramide is a pro-apoptotic sphingolipid (Riley *et al.*, 2001).

Continued inhibition of ceramide synthase in *de novo* sphingolipid biosynthesis and sphingolipid turnover results in the accumulation of the free sphingoid long-chain bases Sa and, to some extent, So. These sphingoid bases are then broken down to form their respective 1-phosphates by a reaction catalysed by the rate limiting enzymes sphinganine kinase and sphingosine kinase. The sphingoid base 1-phosphates are then cleaved by sphingoid lyases to form fatty aldehydes and ethanolamine phosphates which can lead to imbalances in phosphoglycerolipids and fatty acids *in vitro* (Riley *et al.*, 2001).

Once the reducing capacity of the kinases is exceeded, the sphingoid bases accumulate to toxic concentrations and result in cell death. The sphingoid bases then leave the cell and appear in tissues, serum and urine, an event that is widely used as a biomarker of FB₁ exposure (Merrill, 2002). This is generally a consequence of complete inhibition of ceramide synthase by FB₁ (Riley *et al.*, 2001).

Partial inhibition, however, is also a possibility. In such a case cell death induced by increased ceramide concentration would be reduced and the rate of sphingoid base 1-phosphate biosynthesis could increase without any apparent increase in the free sphingoid base concentration resulting in cell proliferation (Merrill, 2002). Consequently, alterations in sphingolipid signalling pathways induced by FB₁ can lead to altered rates of cell death and regeneration.

The exact mechanism by which this toxin stimulates DNA synthesis is not clear however several mechanisms have been postulated. The first possible mechanism is related to the accumulation of sphingoid bases or their metabolites. Zhang *et al.* (1990) demonstrated that the exogenous addition of sphingosine-1-phosphate as well as sphingosine stimulated DNA synthesis in Swiss 3T3 cells, a model system often used to study the regulation of cell growth.

However in 1994, Schroeder *et al.*, demonstrated that the *de novo* accumulation of Sa, albeit to a lesser extent than So, also stimulated mitogenesis in Swiss 3T3 fibroblasts and that mitogenic concentrations of FB₁ had no effect on cellular levels of sphingoid base 1-phosphate. This suggested that mitogenesis may be due rather to a direct action of sphingoid bases perhaps via one of the systems they are known to affect than via conversion of the sphingoid bases to a metabolite.

A second possible mechanism is that FB₁ might prevent or block the formation of a growth inhibitory sphingolipid such as ganglioside G_{M3}. Studies have shown that bacterial neuraminidase lowers the concentration of ganglioside G_{M3} and stimulates DNA synthesis and that the exogenous addition of gangliosides G_{M1} and G_{M2} inhibits platelet-derived growth factor and epidermal growth factor-stimulated mitogenesis. It is therefore possible that FB₁ might stimulate DNA synthesis by preventing the formation of one of these complex sphingolipids (Schroeder *et al.*, 1994).

Research thus far, however, has indicated that it is the accumulation of Sa and So, which appear to be responsible for most of the deleterious cellular effects of this mycotoxin (Merrill, 2002). This accumulation as well as the inhibition of complex lipid synthesis is of extreme concern in human as well as animal health as disruption of lipid metabolism has been established as either the initial or key event in the cascade of molecular changes leading to the diseases associated with exposure to toxic concentrations of fumonisins (Riley *et al.*, 2001).

2.2.2.3 Toxic Effects

2.2.2.3.1 Toxic Effects in Animals

Fumonisin B₁ has been demonstrated to exert diverse effects on animals. It is carcinogenic in the liver and kidney of male rats and liver of female rats (Gelderblom *et al.*, 1991), hepatotoxic in all animals where it has been tested and nephrotoxic, neurotoxic, immunosuppressive, immunostimulatory, teratogenic and hepatocarcinogenic in rats (Gelderblom *et al.*, 1992; Schroeder *et al.*, 1994; He *et al.*, 2002a). In addition FB₁ is of major agricultural concern as it has been implicated as an etiologic agent in the development of equine leukoencephalomalacia and porcine pulmonary oedema (Dugyala *et al.*, 1998).

2.2.2.3.2 Toxic Effects in Man

The role of fumonisins in human health is unclear, however the consumption of *F. moniliforme* contaminated maize has been correlated to the high incidence of human oesophageal cancer in the Transkei region of southern Africa and primary liver cancer in China and other countries (Ueno *et al.*, 1997; Wang *et al.*, 2000) which indicates that this mould is also carcinogenic to humans.

The potential carcinogenicity of FB₁ may be related to its ability to stimulate cell division (Riley *et al.*, 2001) since many non-genotoxic carcinogens are believed to increase the risk of various types of genetic errors and cell transformation by stimulating cell proliferation. Cell division is necessary for conversion of adducts or other single stranded DNA damage to gaps or mutation and allows for mitotic recombinations that result in changes that are more profound than those from a single mutation. Consequently the stimulation of cell proliferation may provide a plausible molecular mechanism to explain the role of FB₁ in initiation and promotion during tumour formation (Schroeder *et al.*, 1994).

The disruption of sphingolipid metabolism and the resultant accumulation of sphingoid bases by FB₁ may consequently be partially accountable for the toxic and carcinogenic activity of this mycotoxin (Schroeder *et al.*, 1994; Dugyala *et al.*, 1998).

2.3 MYCOTOXINS AND THE GASTROINTESTINAL TRACT

The gastrointestinal (GI) or digestive system consists of the gastrointestinal tract (a long tube running from the mouth to the anus) as well as several accessory organs that connect to and participate in the functioning of the system. This complex organ system is ultimately responsible for the fate of swallowed food, which it carries from the mouth down the oesophagus to the stomach and then through the small and large intestine to be excreted out through the rectum and anus. It represents the first barrier against exogenous compounds as it is in constant direct interaction with the environment (Jacobson and Sernka, 1983; Bouhet *et al.*, 2004).

Processes occurring in the GI tract include transport of ingested food, digestion of nutrients, absorption of hydrolysed products, excretion of undigested residues and metabolic waste and protection against microbial infiltration (Jacobson and Sernka, 1983). There is, therefore, great potential for exposure to ingested chemicals, food contaminants and natural toxins.

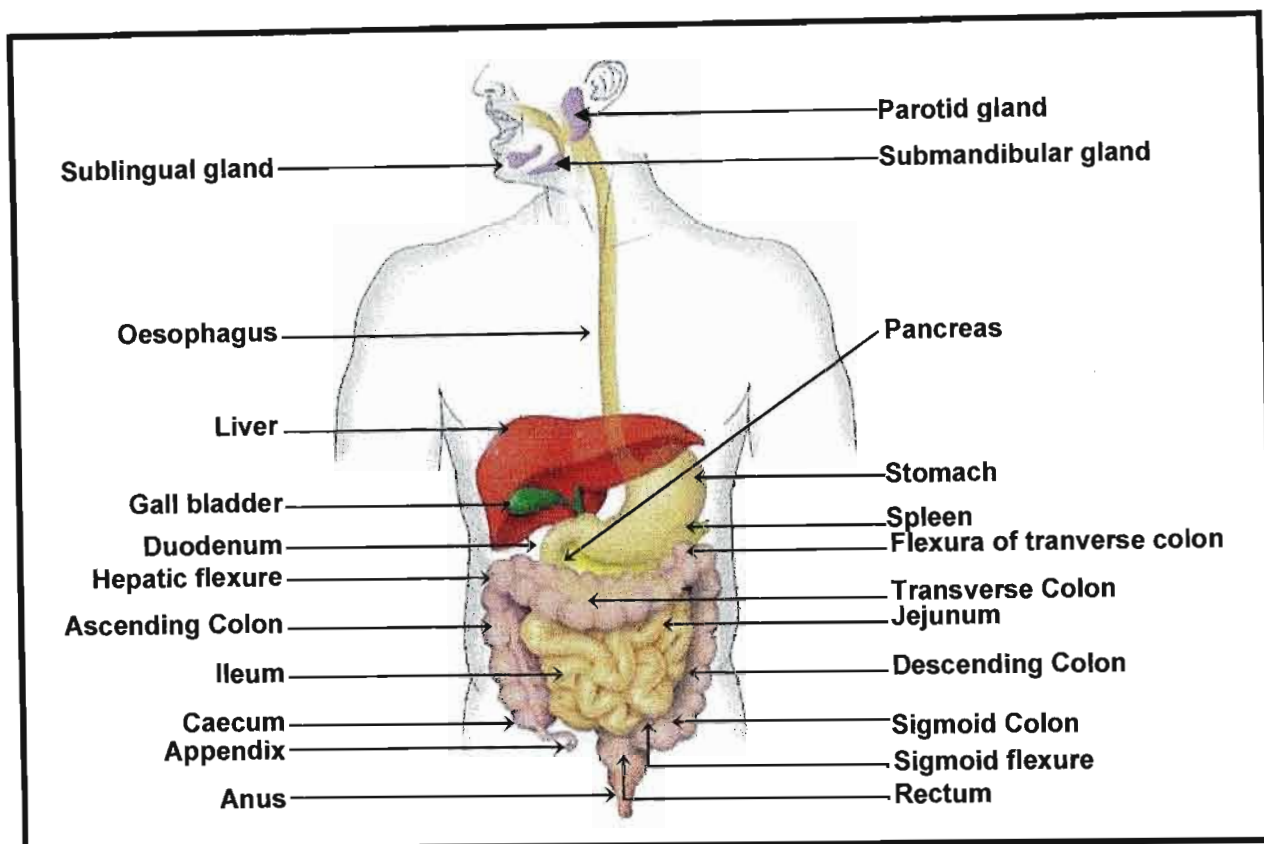


Figure 2.6: The anatomy of the gastrointestinal tract (Raskin, 2004).

The large surface area and prolonged exposure time can increase the risk of toxin-mediated damage and bioaccumulation of ingested chemicals can lead to a variety of metabolic and systemic dysfunctions, and in some cases outright disease states. A major consequence of this is the development of cancer.

Fumonisin B₁ has been demonstrated to be poorly absorbed. Norred *et al.* (1993) showed that 80% of the radiolabeled FB₁ administered to rats was excreted in faeces within 48 hours. Similarly, 96 hours after administration of a single dose of radioactive-labeled DON to rats, 64% of the radioactivity was recovered in the faeces and 25% in the urine (Lake *et al.*, 1987). The colon or large intestine contributes to concentration of faecal effluent through water and electrolyte absorption, storage and controlled evacuation of faecal material and digestion and absorption of undigested food (Jacobson and Sernka, 1983). It can therefore be postulated that there is a high potential of exposure in the colon region and this exposure may play a role in colon carcinogenesis.

2.4 THE COLON

2.4.1 PHYSIOLOGY OF THE COLON

The human colon is a muscular organ measuring approximately 125cm in length *in vivo* and colon can be functionally divided through the transverse colon into two parts, the right and left colon. The right colon (caecum and ascending colon) plays a major role in water and electrolyte absorption and fermentation of undigested sugars, and the left colon (descending colon, sigmoid colon and rectum) is predominantly involved in storage and evacuation of stool (Thomson and Shaffer, 1997).

The colon wall consists of the four basic layers namely the mucosa, submucosa, circular muscle and longitudinal muscle (Figure 2.7). The mucosa lacks the villous projections found in the small intestine and presents a relatively smooth surface, but numerous crypts (analogous to the crypts of Lieberkuhn) extend from its surface, an arrangement that enhances the functional surface area. Cell types lining the surface and the crypts include several different types of cells (Figure 2.7), including columnar absorptive cells and the characteristic mucous secreting goblet cells, which are named for their shape that incorporates a narrow cytoplasm base and mucous resembling the bell of a wine goblet (Wheater *et al.*, 1987).

Goblet cells predominate in the base of the glands and as faeces pass along the large intestine and become progressively dehydrated, the mucous secreted becomes increasingly important in protecting the mucosa from trauma (Thomson and Shaffer, 1997). The luminal surface, however, is almost entirely lined by the absorptive cells. The absorptive cells have a striated border formed by microvilli, which greatly increases the surface area exposed to the lumen. The middle part of the glands represents the transition between the two (Wheater *et al.*, 1987).

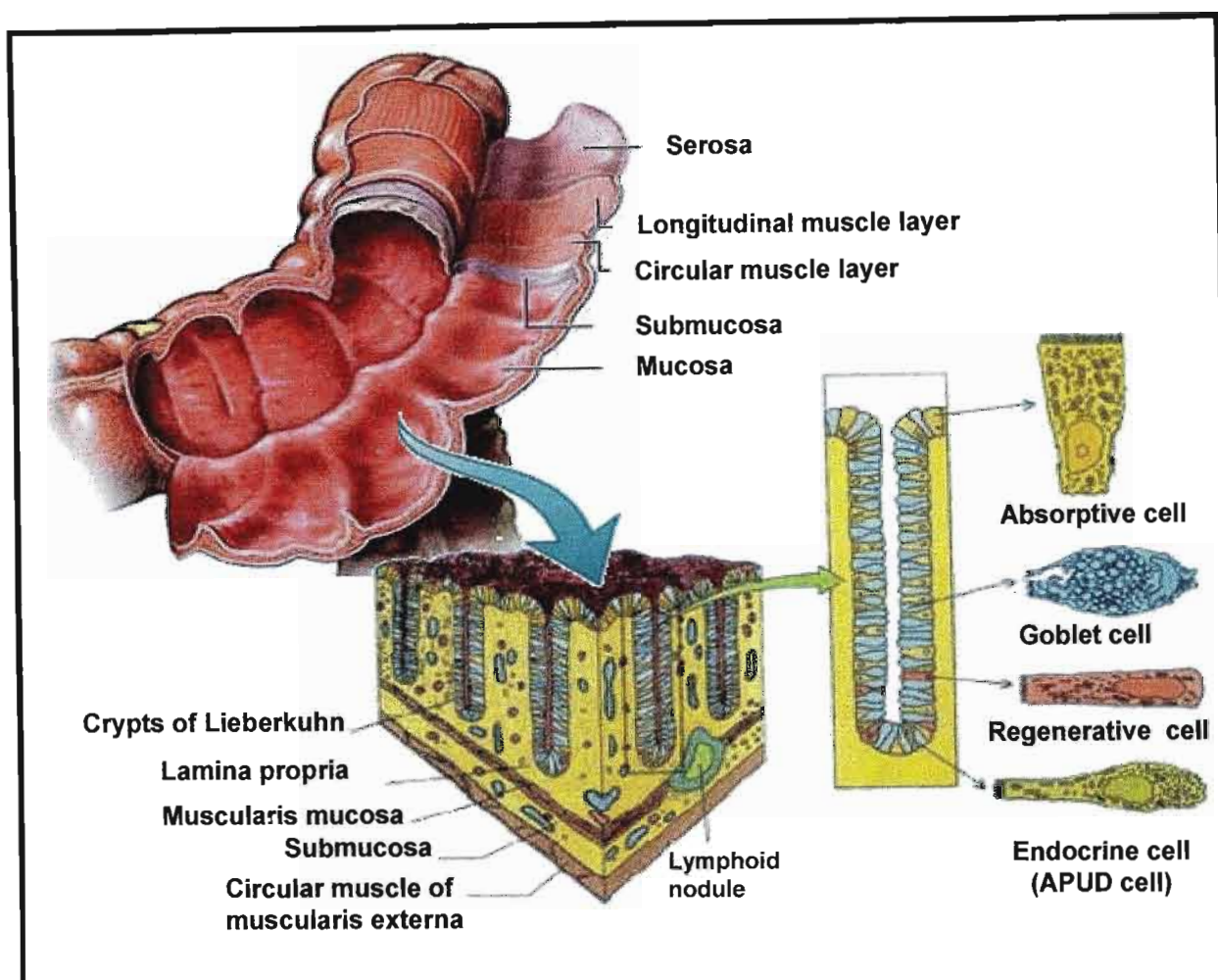


Figure 2.7: Schematic diagram of the colon, crypts of Lieberkuhn and associated cells (A.D.A.M. Medical Illustration Team, 2002; Schematic diagram of the colon, crypts of Lieberkuhn and associated cells, 2003).

The normal colon epithelium is characterised by rapid, continual cell turnover at the level of the colonic crypt with the surface epithelium being replaced approximately every six days. Cell death is therefore essential for preservation of normal cell balance, morphology and function (Ramachandran *et al.*, 2000).

The highly proliferative compartment is located in the lower third of the crypt and as the cells migrate up the crypt, they mature, differentiate, lose their dividing ability and eventually die (Wheater *et al.*, 1987). This cell death is a tightly controlled, finely orchestrated event known as apoptosis (Vermes *et al.*, 1997).

Apoptosis or programmed cell death (PCD), requires the cell to be metabolically active (Sun *et al.*, 1994) and is an energy dependent, asynchronous, genetically controlled cell elimination mechanism by which senescent, damaged, redundant and deleterious cells are abolished and their contents with precious caloric value are reutilised by phagocytosing adjacent cells or macrophages (Vermes *et al.*, 1997; Ramachandran *et al.*, 2000). This form of 'cell suicide' occurs in a regulated and sequential manner resulting in a cascade of biochemical events which leads to the death of the cell (Figure 2.8). It may be induced by a wide range of intracellular as well as extracellular signals such as death receptors (Fas, tumour necrosis factor), withdrawal of growth factors (interleukin-3, insulin-like growth factor-1), cytotoxic T cells or injury via radiation, toxins or free radicals (Renehan *et al.*, 2001).

There are three distinct phases of apoptosis following induction. During the first phase, the cell detaches from its substratum and adjacent cells with a loss of junctional complexes or desmosomes as well as specialised membrane structures such as microvilli. The integrity of the cell membrane and of the mitochondria remains initially intact. The DNA is then digested by specific endonucleases into fragments and ultimately packed into vesicles. The changes in DNA include strand breakage (karyorhexis) and condensation of nuclear chromatin (pyknosis). The endoplasmic reticulum swells and exocytoses its contents and the cell becomes denser as the cytoplasm shrinks and involutes (Kam and Ferch, 2000).

In the second phase, the cell produces pseudopodia (budding) which contain organelles or nuclear fragments, and these break off into membrane bound vesicles. The remaining cell becomes a round, smooth, membrane bound remnant or apoptotic body (Kam and Ferch, 2000).

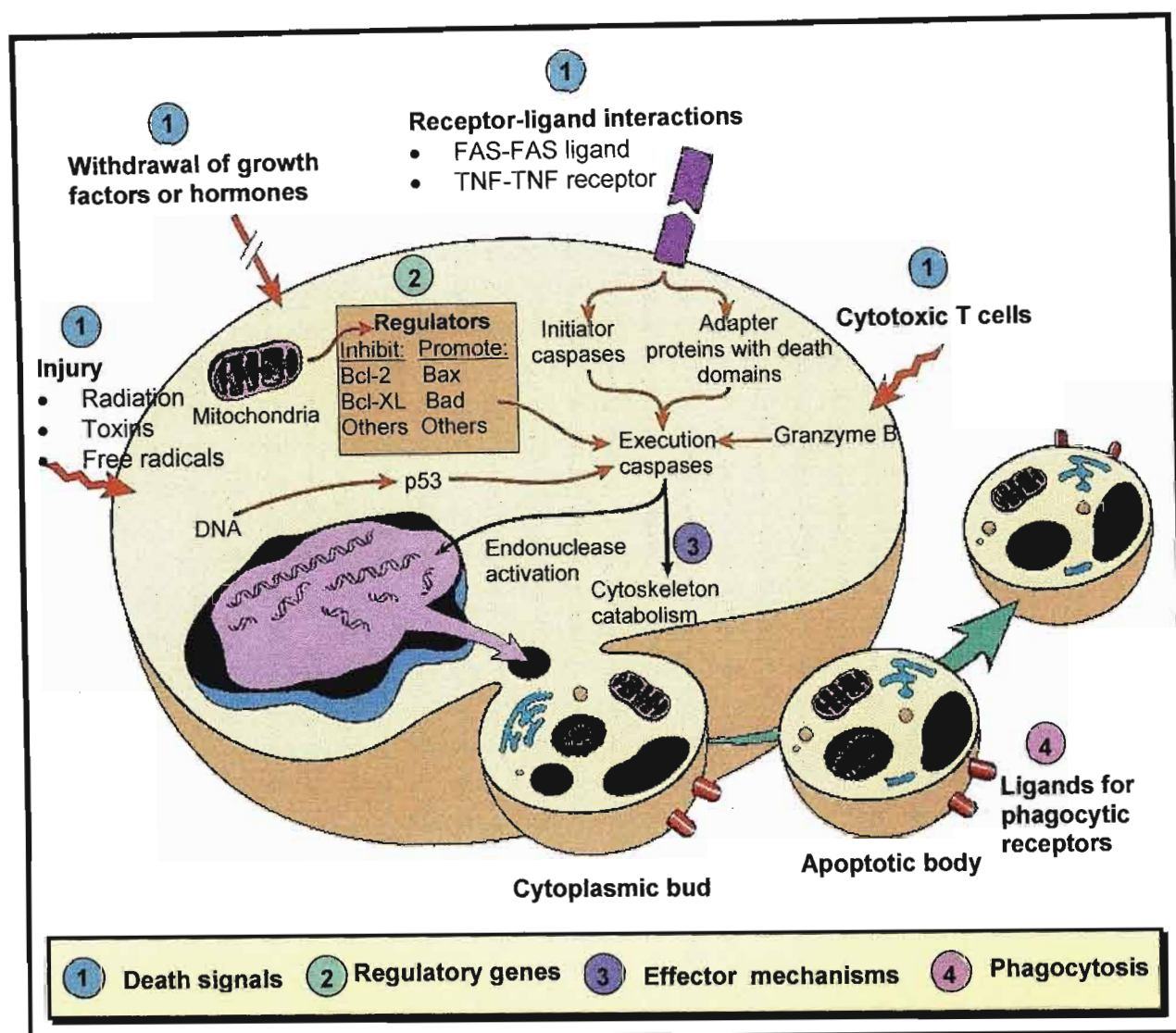


Figure 2.8: An illustration of cellular biochemical and physical changes induced during apoptosis (Events in Apoptosis, 2002).

In the third phase, the cell membrane becomes permeable to membrane impermeable dyes. The apoptotic body and membrane bound buds may then be phagocytosed by macrophages, adjacent epithelial cells, vascular endothelium or tumour cells (Kam and Ferch, 2000). Apoptosis occurs only in dispersed cells and the entire process occurs quickly therefore the cell remnants do not elicit any inflammatory reaction (Vermes *et al.*, 1997).

Another form of cell death that may occur is necrosis (accidental cell death). Necrosis is a passive process that proceeds independently of the metabolic state of the cell. The cell membrane loses its selective permeability and ion pumping capacity as a result of direct membrane damage. This leads, almost instantaneously, to swelling of the cell and its organelles, including the mitochondria, and leaking of the cellular contents into the extracellular space. Activation of enzymes such as hydrolases, phospholipases, proteases, RNases and DNases results in further degradation of membranes, proteins, DNA and RNA which accelerates the cellular and nuclear disintegration. This process occurs in whole fields of damaged cells where the leaked debris elicits an inflammatory reaction in the adjacent viable tissues (Vermes *et al.*, 1997).

Apoptosis, however, is the form of cell death responsible for the maintenance of the cellular balance between proliferation and death and therefore has a central role in the pathogenesis of human disease when the genes controlling the apoptotic process are suppressed, overexpressed or altered by mutation. Progressive inhibition of this process appears to be involved in the pathogenesis of gastrointestinal neoplasia, in particular colorectal cancer (Kam and Ferch, 2000).

2.4.2 COLORECTAL CANCER DEVELOPMENT

The orderly process of cell turnover is dysregulated in the adenoma. Hyperproliferation with upward expansion of proliferative compartment, a characteristic feature at all stages of malignant progression in colorectal carcinogenesis, occurs. The proliferative compartment moves up to the surface of the crypt and there is continued mitosis, retarded cell maturation and differentiation and lack of apoptosis suggesting that malfunction of the mechanisms controlling cell kinetics underlies the first steps of colorectal carcinogenesis (Roncucci *et al.*, 2000; Sheik and Yasmeen, 2002; Milovich and Turchanowa, 2003). Consequently, the cells are retained in the mucosa and develop into various types of adenomatous lesion.

At the histopathological level the earliest recognisable entity may be an "aberrant crypt focus (ACF)" (Wargovich, 2001). Two types of ACFs have been observed in humans. The common one is a hypercellular crypt that has normal individual cells and is called the hyperplastic or non-dysplastic crypt because it is unlikely to lead to clinically significant lesions. Less common but more important are dysplastic ACFs which are believed to be the precursors of the adenomas and carcinomas and are referred to as unicyptal polyps (Sheik and Yasmeen, 2002).

The evolution of a carcinoma from an adenoma, whether sporadic or hereditary, is generally believed to be a multi-step process of tumourigenesis called the "adenoma-carcinoma sequence". At the molecular level the initiating events in the tumourigenesis are a series of genetic alterations that confer a growth advantage to some cells over their progenitors leading to clonal expansion of these abnormal cells. These alterations may be mutational activation of oncogenes like the K-ras (retrovirus-associated DNA sequence) gene coupled with inactivation of tumour suppressor genes like the APC (Adenomatous Polyposis Coli), p53 (Phosphoprotein 53) and DCC (Deleted in Colorectal Cancer) genes (Wargovich, 2001; Sheik and Yasmeen, 2002) where the latter changes predominate (Milovich and Turchanowa, 2003).

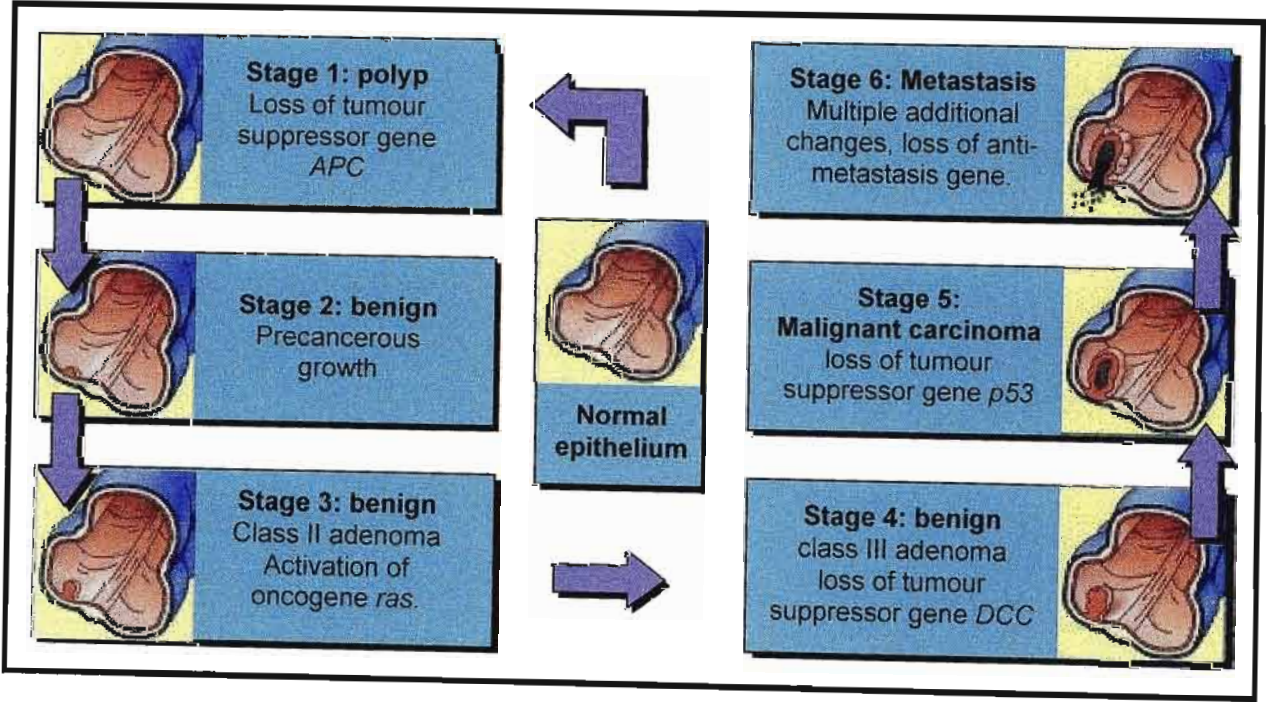


Figure 2.9: A stepwise model of colorectal carcinogenesis (Progression of colon cancer, 2001).

The accumulation of approximately five mutations is required to cause malignant transformation and fewer changes result in benign tumourigenesis (Figure 2.9) (Milovich and Turchanowa, 2003). The initial mutations in most of the cases occur at the APC tumour-suppressor gene locus and the resulting polyp may be present and proliferate for 10-15 years before undergoing malignant transformation (Sheik and Yasmeen, 2002). The p53 tumour suppressor gene appears to be the most important determinant of malignancy in colorectal neoplasia (mutations are found in more than 75% of colorectal adenocarcinomas) and is frequently lost in colorectal malignancy. It is considered to be a transcription factor because it activates other genes and promotes their expression. These genes are involved in growth inhibition and loss of the p53 gene may therefore lead to unregulated cellular growth. The varied functions of p53 including control of the cell cycle, DNA repair and programmed cell death have earned it the name "guardian of the genome" (Sheik and Yasmeen, 2002).

Colorectal carcinogenesis is therefore a stepwise process (Figure 2.9) which leads from the normal mucosa to the development of invasive carcinoma through a series of genetic alterations. These genetic alterations can be the result of the effects of the environment or genetic injuries and of the adaptive responses of the host and is a very long process usually taking many years, if not decades, to reach the invasive stage. There is therefore time to take adequate measures to prevent the onset of cancer. Unfortunately, however, at the present time colorectal cancer remains a major cause of death in most developed countries (Roncucci *et al.*, 2000).

2.5 CHEMOPREVENTION

Cancer chemoprevention is a discipline of cancer research emerging from its infancy 20 years ago to now gain centre stage in the armamentarium against cancer. It is recognised as the pharmacologic intervention with synthetic or naturally occurring chemicals to prevent, inhibit or reverse carcinogenesis or prevent the development of invasive cancer (Singletary, 2000).

The use of plants or their crude extracts in the prevention and/or treatment of several chronic diseases has been traditionally practiced in various different ethnic societies worldwide and there has been considerable scientific evidence to suggest that nutritive and non nutritive plant based dietary constituents or phytochemicals can inhibit the process of carcinogenesis effectively (Singletary, 2000). This cancer inhibitory action has been confirmed in different animal tumour models and has led to an increased emphasis on cancer prevention strategies (Singletary, 2000; Wargovich, 2001).

Chemoprevention of colorectal cancer is one of the most promising options for those who are at increased risk of this disease which is one of the leading causes of cancer death (Bus *et al.*, 2000). In fact colorectal cancer is the fourth commonest cancer in men with 678 000 estimated new cases per year worldwide, representing 8.9% of all new cancers (Langman and Boyle, 1998). Since the development of colon cancer results not from any single genetic event but from the accumulation of a number of genetic alterations, interfering with these molecular events by chemoprevention could inhibit or reverse the development of adenomas or the progression from adenoma to cancer (Janne and Mayer, 2000). In this way chemoprevention has the potential to be a major component of colorectal cancer control.

2.5.1 MECHANISMS OF COLORECTAL CANCER CHEMOPREVENTION

2.5.1.1 Induction of Phase 2 Enzymes

An association between reduced risk of colorectal cancer and diets high in fruit, fiber or vegetables has been well established in epidemiological studies. While there are several mechanisms that could contribute to this association, a well characterised defense mechanism involves the induction of detoxification enzymes, including members of the glutathione S-transferase family and NAD(P)H:quinone reductase (Kirlin *et al.*, 1999).

These enzymes are generally referred to as phase 2 enzymes because they catalyse conversion of mutagenic metabolites or their precursors to compounds that are less reactive and/or more readily excreted. This detoxification function is in contrast to phase 1 enzymes such as cytochrome P450 which bioactivate foreign compounds to DNA-reactive metabolites and contribute to carcinogenesis (Kirlin *et al.*, 1999).

Therefore it can be said that specific chemicals in the human diet protect against cancer by increasing the activities of detoxification enzymes and decreasing the concentrations of genotoxic compounds that could give rise to carcinogenic mutations (Kirlin *et al.*, 1999).

2.5.1.2 Suppression of Cyclooxygenases

Over the past decade, several lines of investigation have shown that the intake of non-steroidal anti-inflammatory drugs (NSAIDs) inhibits the occurrence and/or growth of colorectal cancer. The antiproliferative effects of NSAIDs have been demonstrated in various studies with human colorectal cancer cell lines and the ability of these compounds to prevent the chemical induction of this cancer has been shown in experimental animal studies. The mode of action of NSAIDs is mediated by their ability to interfere in the metabolism of arachidonic acid (AA) by cyclooxygenases (Bus *et al.*, 2000).

The cyclooxygenase pathway involves two enzymes cyclooxygenase-1 (COX-1) and cyclooxygenase-2 (COX-2) which converts AA into prostoglandins (PGs) and thromboxanes. The constitutive COX-1 is expressed in most tissues and appears to be responsible for housekeeping functions. It plays a role in the maintenance of intestinal homeostasis and its expression during colorectal carcinogenesis is unaffected (Bus *et al.*, 2000).

In contrast, COX-2 is not detectable in most normal tissues but is induced by oncogenes, growth factor carcinogens and tumour promoters during colorectal carcinogenesis (Bus *et al.*, 2000). Cyclooxygenase-2 has also been shown to be elevated in up to 90 percent of sporadic colon carcinomas and 40 percent of colonic adenomas but is not elevated in the normal colonic epithelium (Janne and Mayer, 2000).

Several different mechanisms could account for the link between the activity of COX-2 and carcinogenesis. One such mechanism is the enhanced synthesis of PGs which occurs in a variety of tumours. Prostaglandins can promote angiogenesis, inhibit immune surveillance and increase cell proliferation. Another is the overexpression of COX-2 which inhibits apoptosis and increases the invasiveness of malignant cells (Zhang *et al.*, 1999).

The inhibition of COX-2 leads to an increase in AA, which in turn, stimulates the conversion of sphingomyelin to ceramide, a mediator of apoptosis. This inhibition may also lead to apoptosis by altering prostaglandin production and by decreasing angiogenic factors (Janne and Mayer, 2000).

Several other studies have demonstrated that inhibitors of PG synthesis such as aspirin and sulindac suppress colon carcinogenesis in animal model assays and the inhibition of colon carcinogenesis was consistently associated with a decrease in the activity of COX in colon tumours (Kawamori *et al.*, 1999).

A wealth of evidence links elements of the Asian diet to reduced risk for certain cancers, hence the recent interest in herbals and botanicals of Asian origin as potential sources of cancer inhibitors (Wargovich, 2001). One such compound is curcumin.

2.5.2 CURCUMIN

2.5.2.1 Physical and Chemical Properties

Curcumin (Figure 2.10), also known as diferuloylmethane, is a low molecular weight plant phenolic antioxidant present in large quantities in the rhizome of the perennial herb *Curcuma longa* Linn (Zingiberaceae) (Zhang *et al.*, 1999; Sharma *et al.*, 2001a).

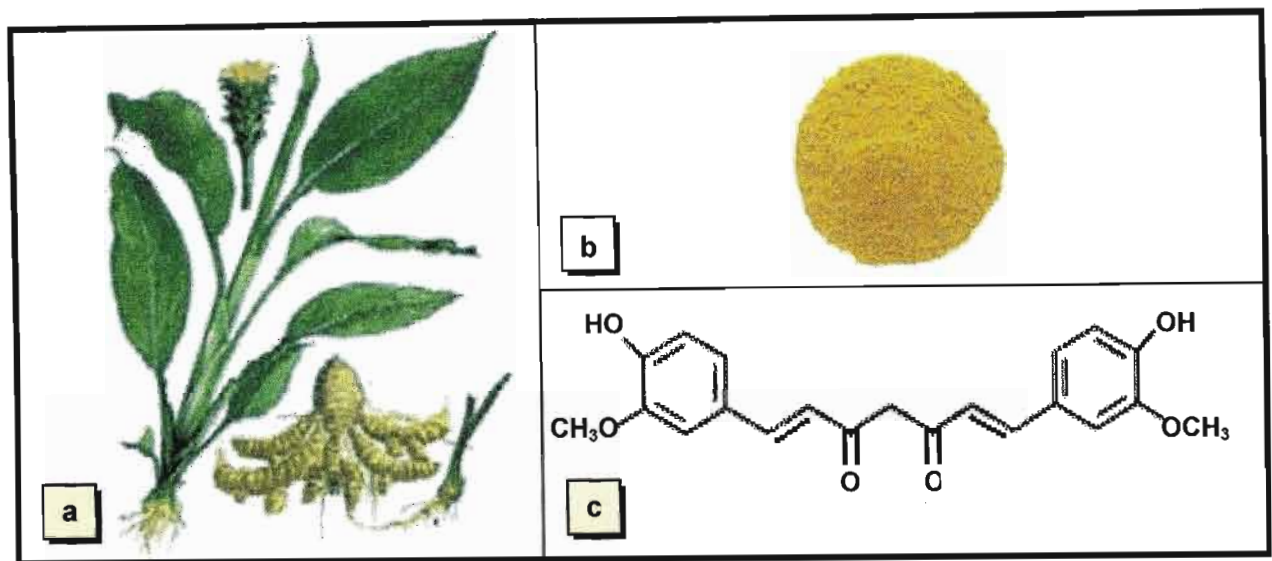


Figure 2.10: An illustration of (a) *Curcuma longa* (Campana, 2004), (b) turmeric powder (Turmeric powder, 2000) and (c) the chemical structure of curcumin (Zhu *et al.*, 2004).

It is responsible for the yellow colour of turmeric, a dried ground preparation of the plant rhizomes that is widely used as a spice and colouring agent in food (Chuang *et al.*, 2000) and consumed in the diet of many countries which also appear to have low incidence rates of colorectal cancer. Although the rhizomes contain other curcuminoids as well as essential oils, curcumin is regarded as the constituent with the highest biological activity (Sharma *et al.*, 2001a).

The particular compound is known to exhibit free radical scavenger and anti-inflammatory activities (Zhang *et al.*, 1999; Limtrakul *et al.*, 2001) as well as to prevent tumourigenesis and mutagenesis, block carcinogen–DNA adduct formation and to inhibit angiogenesis (Dinkova-Kostova and Talalay, 1999).

Many studies, both in epidemiology and animal model studies have demonstrated that compounds that possess antioxidant or anti-inflammatory properties can inhibit carcinogenesis (Limtrakul *et al.*, 2001). Curcumin has been shown to inhibit the development of chemically induced tumour formation in the skin, forestomach, duodenum and colon of mice (Kawamori *et al.*, 1999; Zhang *et al.*, 1999) and in the tongue, colon, mammary glands and sebaceous glands of rats (Sharma *et al.*, 2001a) when it is administered during initiation and/or postinitiation stages (Kawamori *et al.*, 1999).

The inhibition of tumour formation has been attributed to its anti-initiation and anti promotion effects. The anti-initiation effect may result from its ability to inhibit the formation of DNA damage while the antipromotion effect may be mediated through anti-proliferation or apoptosis-promotion of the initiated cells (Kawamori *et al.*, 1999; Chuang *et al.*, 2000). As such, curcumin has been considered a potentially important chemopreventive agent against cancer (Chuang *et al.*, 2000).

2.5.2 Mechanism of Action

Several possibilities have been raised regarding the potential mechanisms of the observed antitumour effects of curcumin and among these its antioxidant and anti-inflammatory properties have received major attention.

Curcumin scavenges active oxygen species including superoxide, hydroxyl radical and nitric oxide. It decreases the 12-O-tetradecanoylphorbol-13-acetate (TPA)-induced expression of *c-jun*, *c-fos* and *c-myc* protooncogenes (Limtrakul *et al.*, 2001) and suppresses activation of nuclear factor kB. It also causes inhibition of kinases and lipid peroxidation (Dinkova-Kostova and Talalay, 1999).

Curcumin has been shown to inhibit colon carcinogenesis during the postinitiation or promotion stage through the elevation of the activities of phase 2 detoxification enzymes of xenobiotic metabolism such as glutathione transferases and quinone reductase and the inhibition of procarcinogen activating phase 1 enzymes such as cytochrome P4501A1. It has also been reported to suppress COX-2 activity in the tumour tissue (Sharma *et al.*, 2001a). Evidence suggests that the induction of phase 2 enzymes as well as the suppression of COX are critical and sufficient conditions for protection against toxicity and carcinogenicity (Dinkova-Kostova and Talalay, 1999) therefore curcumin presents a promising candidate for a natural chemoprotective agent. In addition the non-toxic nature of curcumin as well as its multiple beneficial clinical effects has made it one of the most attractive compounds to be explored for the chemoprevention of cancers (Chuang *et al.*, 2000).

CHAPTER 3

CELL CULTURE

3.1 INTRODUCTION

The field of carcinogenesis research has been much advanced by experimental animal studies. However, there is a need to develop and validate efficient *in vitro* assays in order to reduce the use of laboratory animals and to extrapolate data from these animal studies to the human situation. To this end, the culturing of human and animal cells has proven to be most useful.

Cell culture is the cultivation of populations of isolated cells artificially in the laboratory and is useful for studying mechanisms of carcinogenesis on a cellular level (Gabrielson and Harris, 1985). This technique may be performed with a variety of cells provided they are maintained *in vitro* in similar conditions to that experienced *in vivo* and may be used for the study of the biochemistry, physiology and behaviour of cells in defined conditions. Changes in these cytological parameters allows for the potential toxicity of various compounds to be evaluated (Terse *et al.*, 1993).

Cancerous cell lines are widely used in experimental studies as they are able to accomplish a practically infinite number of cell divisions and double in population size in a short time in contrast to normal cell lines which grow senescent after a limited number of passages. In addition cancerous cells tolerate a greater cell density and are less sensitive to the composition of the culture medium making them easier and less expensive to maintain (Luccioni, 2000). In this study, the cytotoxicity of the selected mycotoxins, namely deoxynivalenol and fumonisin B₁, was evaluated using the HT-29 human colonic adenocarcinoma cell line.

This continuous cell line was established by Jorgen Fogh in 1964 from the primary tumour of a 44-year-old Caucasian woman with colon adenocarcinoma and consists of adherent, epithelial cells growing as monolayers and in large colonies (HT-29, 2001). It is described as heterotransplantable, forming well-differentiated adenocarcinomas consistent with colonic primary (grade I) tumours in nude mice and steroid treated hamsters (Cell Lines, 2003) and is able to express differentiation features characteristic of mature intestinal cells (HT-29 Cell, 2004). Ultrastructural features include microvilli, microfilaments, large vacuolated mitochondria with dark granules, smooth and rough endoplasmic reticulum with free ribosomes, lipid droplets, a few primary and many secondary lysosomes (Cell Lines, 2003).

This chapter describes the cell culture techniques used for the maintenance and storage of HT-29 cells.

3.2 MATERIALS AND METHODS

Ethical approval for this study was granted by the Research Ethics Committee and the Higher Degrees Committee on 13 May 2003 (Ref. No.:H051/03).

3.2.1 MATERIALS

Eagle's Minimum Essential Medium (EMEM) containing HEPES (25mM), Hank's Balanced Salt Solution (HBSS) containing phenol red, foetal calf serum (FCS), PenStrep-Fungizone, trypsin versene, L-glutamine and Corning plastic tissue culture flasks (25cm² and 75cm²) were purchased presterilised from Adcock Ingram [KwaZulu-Natal, South Africa (SA)]. Trypan blue was purchased from Sigma Aldrich Chemical Company (Johannesburg, SA). Ethanol (EtOH), methanol (MeOH) and dimethylsulphoxide (DMSO) were purchased from Merck (Johannesburg, SA).

3.2.2 METHODS

All cell culture procedures were performed in a LabAire microbiological safety cabinet (Class II) equipped with a vertical laminar flow hood and a short wave ultraviolet (UV) light. This vertical hood causes a continuous displacement of air which then passes through a HEPA (high efficiency particulate) filter thus removing particulates from the air. The filtered air is then blown down from the top of the cabinet to maintain a contaminant free working area. In addition to the hood running continuously, a UV light source was used to maintain sterility. The UV light was switched off before working in the cabinet and the unit was swabbed with a mixture of ethanol:methanol (70%:30%). This swabbing procedure was repeated on completion of cell culture work prior to switching the UV light back on.

3.2.2.1 Growth and Maintenance

The cells were maintained using complete culture medium (CCM; Appendix 1.3). This medium consisted of EMEM supplemented with FCS (10%), L-Glutamine (1%) and PenStrep-Fungizone (1%).

Eagle's minimum essential medium is a defined basal cell culture medium comprising of balanced salt solution, glucose, essential amino acids and vitamins. The HEPES (free acid) present, is an organic buffer that maintains the physiological pH level of the media between 7.2 and 7.6 which is critical for cell viability (Mediatech, Inc. cell culture reference guide, 2001).

Foetal calf serum is a very complex supplement containing proteins, growth factors, hormones, amino acids, sugars, trypsin inhibitors, and lipids that is often used as a standard supplement due to its rich growth factor and low gamma globulin content. As serum is a blood product, it must be heat inactivated prior to its use in order to inactivate any complement present which can lead to complement-mediated cell lysis

Heat inactivation is accomplished by incubation of the FCS at 56°C for duration of 30 minutes. These limits must be adhered to as overheating may compromise the integrity of growth factors, amino acids, and vitamins in the serum and thereby adversely affect the growth of cells in culture (Mediatech, Inc. cell culture reference guide, 2001).

L-glutamine (Appendix 1.2) is an essential amino acid that is required to sustain high rates of cellular proliferation in cell culture. It stimulates antibody production and cell growth and is a major source of energy as well carbon and nitrogen (Elwood, 2004). Although L-glutamine is synthesised by normal cells, neoplastic cells are dependent on external sources as the enzymes involved in specialised function such as L-glutamine synthesis are frequently lost (Mellors, 1999). PenStrep-Fungizone is a formulation of three antibiotics namely, Penicillin, Streptomycin and Fungizone which are effective against Gram positive, Gram negative and fungal organisms respectively.

The media (CCM) in each flask was changed every 3 to 4 days (10ml media in 75cm² flasks and 5ml in 25cm² flasks) and the cells were grown to 75% confluency before being subcultured (Figure 3.1). All cell cultures were incubated in a SAF-A-LERT incubator (Labcon) preset at a temperature of 37°C. The incubator was also routinely swabbed with the ethanol:methanol mixture to maintain sterility.

3.2.2.2 Subculturing

Most cell cultures grow as a single thickness layer or sheet (monolayer) attached to a substrate (Figure 3.1a) and there is a frequent need to subculture cells so that they may be propagated for the purpose of increasing cell numbers or providing cells in a suitable culture vessel.

Methods utilised in the subculturing procedure include mechanical means (scrapping) as well as the use of chelating agents (ethylenediaminetetraacetic acid [EDTA]) and enzymes (trypsin, pronase, collagenase). The most commonly used method utilises the proteolytic enzyme trypsin derived from porcine pancreas and the procedure is termed trypsinisation. Trypsin breaks down the intercellular matrix binding cells to each other or to a substrate surface and facilitates the detachment of cells (Figure 3.1b).

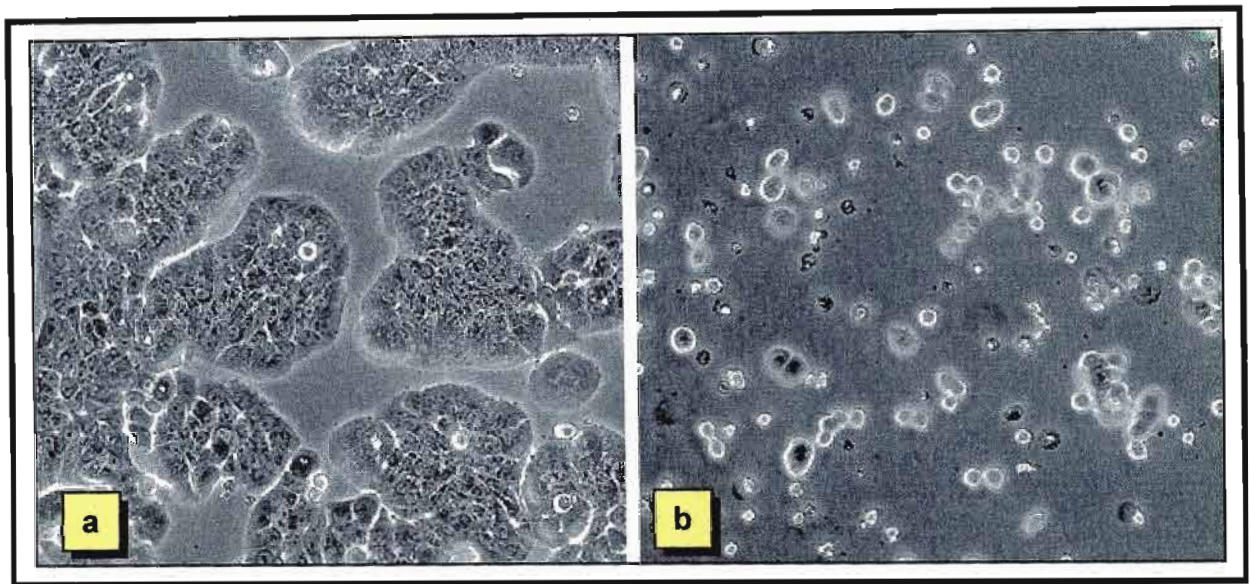


Figure 3.1: Cultured HT-29 colorectal adenocarcinoma cells: (a) approaching confluency and (b) following subculturing (Cell Lines, 2003).

The CCM in the flasks was poured off into a waste container and HBSS (Appendix 1.1) was used to wash the cell monolayer and remove cellular debris prior to trypsinisation. This calcium (Ca^{2+}) and magnesium (Mg^{2+}) free salt solution provides the cells with the correct pH and salt balance as well as glucose and essential inorganic ions. The flasks were thoroughly shaken and the HBSS discarded into a waste container. This rinsing procedure was repeated until bubble formation ceased indicating that all FCS was removed. This is important as FCS affects the activity of trypsin due to its high protein content. Trypsin-Versene (Appendix 1.2) was then added to the flasks (2ml in the 25cm² flask and 4ml in the 75cm² flask) which were then gently swirled to facilitate coverage of the cells.

The presence of the chelating agent Versene (EDTA) serves to facilitate the rapid detachment of cells by chelating or sequestering the Ca^{2+} and Mg^{2+} ions present between the cells that would otherwise increase the stability of the intercellular matrix and slow down the digestive action of the trypsin (Biowhittaker cell biology products catalogue, 2002).

The flasks were placed in the incubator and periodically viewed using an inverted microscope. The cells, which were initially spread out, start to round up and detach (Figure 3.2).

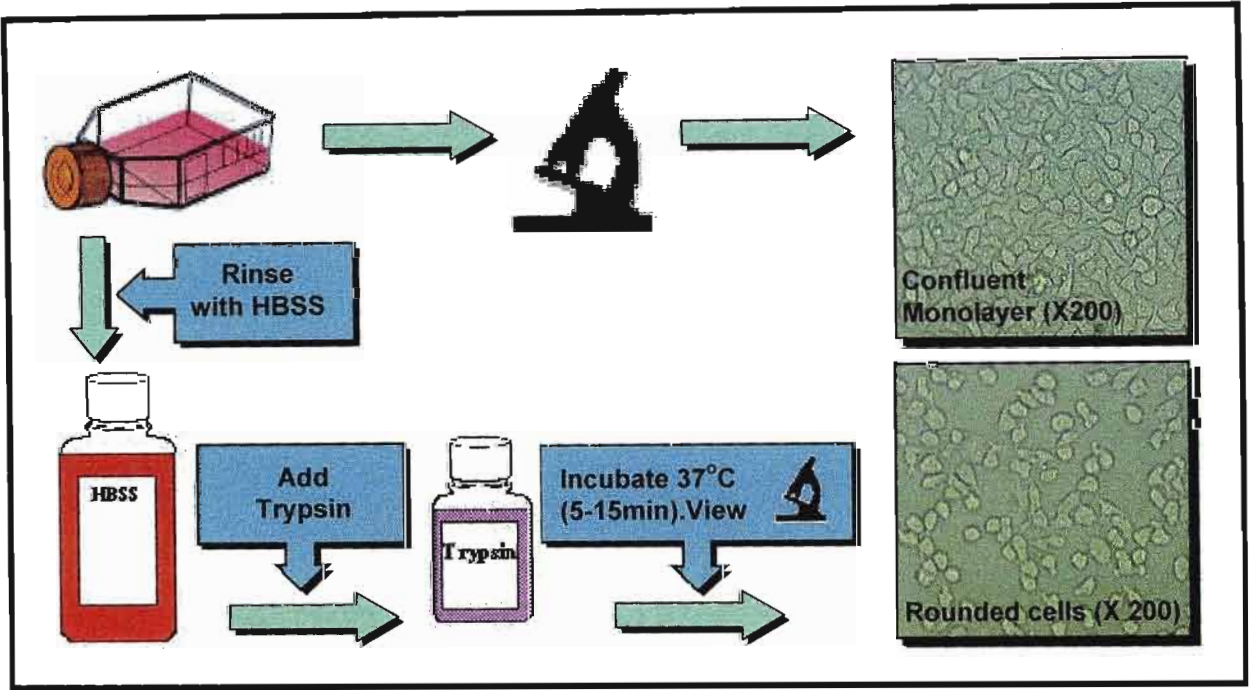


Figure 3.2: An illustration depicting the process of trypsinisation.

The cells were not left in trypsin for longer than about 15 minutes. The flasks were then shaken gently to dislodge the cells and the resulting cell suspension was aliquoted as needed into culture vessels required for different procedures. Once the cells were rounded the trypsin was discarded and CCM was added so that that the FCS present neutralised the action of the trypsin and prevented further protein breakdown.

3.2.2.3 Cryopreservation

Cryopreservation is an integral part of cell culture involving the successful preservation of cell lines with the primary objective of maximum recovery with minimal damage to the cells. This technique involves the freezing of cells to very low temperatures at which the biological material remains genetically stable and metabolically inert, while minimising the formation of ice crystals which puncture organelles and cell membranes. This is achieved by replacing some of the water present in the cells with a cryopreservative agent such as DMSO that does not form large crystals when frozen thereby protecting the cells from mechanical and physical stress during the cryopreservation process (Mediatech, Inc. cell culture reference guide, 2001).

The cryopreservation media (Appendix 1.4) consisted of CCM and the cryopreservative DMSO. The confluent flasks were trypsinised and resuspended in approximately 2ml of this media. The cell suspension to be cryopreserved had to be strong to ensure maximal recovery. This suspension was then aliquoted into cryovials and frozen in three stages (4°C, -8°C and -70°C).

As the media begins to freeze, the salt concentration outside the cells becomes greater than that in the cells and water leaves the cells to be replaced by DMSO. High concentrations of FCS (10%) were also used because it also does not crystallise and surrounds the cells preventing water from entering and crystallising within the cells.

3.2.2.4 Thawing Cryopreserved Cells

During the recovery process, the cryopreserved cells are fragile and require gentle handling. The cells were thawed in the incubator and the suspension was inoculated into a 25cm² flask containing warm CCM. Plating the thawed cells into a small culture flask (25cm²) promotes faster adjustment to the medium and increased growth as many types of cells prefer an environment that allows close contact between cells.

The flask was placed in the incubator overnight to allow sufficient time for the cells to recover from the thawing process and to reduce cell loss. The medium was then replaced with fresh CCM without the cryopreservative. Replacement of the medium with cryopreservative-free media is critical as the cells may be sensitive to the cryopreservative used during the freezing process (Mediatech, Inc. cell culture reference guide, 2001).

3.2.2.5 Cell Counting and Cell Viability Staining

Counting cells by the use of the haemocytometer is a convenient and practical method for determining cell numbers in a suspension culture or from dispersed monolayer cultures. The haemocytometer, originally designed for counting haemocytes in blood samples, is a thick glass slide with two counting platforms positioned in its centre (Figure 3.3). Each of these consists of nine accurately ruled 1.0 mm squares. A coverglass is supported 0.1mm over these squares so that the total volume over each square is 1.0 mm X 0.1 mm or 0.1 mm³ or 10⁻⁴cm³. Since 1cm³ is approximately equivalent to 1ml, the cell concentration per ml is the average count per square X 10⁴ (Biowhittaker cell biology products catalogue, 2002). In this way, by counting the cells in a square, the number of cells in a certain volume can be calculated. It is assumed that the total volume in the chamber represents a random sample.

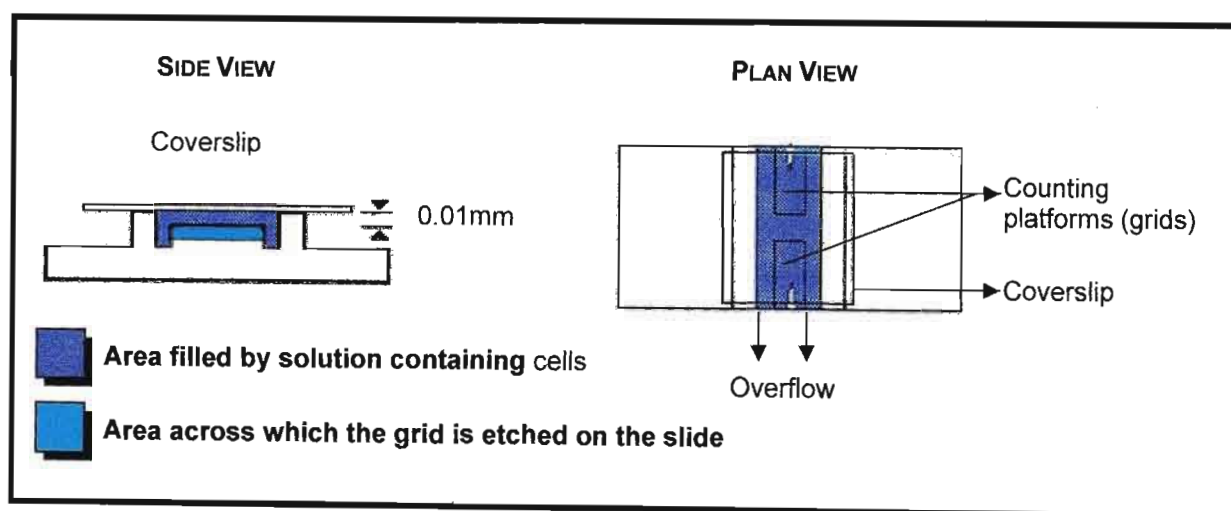


Figure 3.3: A schematic diagram of a haemocytometer (adapted from Caprette, 2003).

Haemocytometer counts alone do not distinguish between living and dead cells. This distinction can only be made with the use of certain stains. One such stain is trypan blue. This vital stain allows the differentiation between live viable cells and dead cells on the premise that it is excluded by the membrane of the viable cells and taken up by the nuclei of the damaged or dead cells such that dead cells appear blue while live viable cells appear clear.

Trypan blue (0.4%) is a particulate dye that exists in colloidal form in aqueous salt solutions and is commonly used to distinguish viable cells from nonviable ones. Its particulate properties caused it to be excluded from viable cells with preserved plasma membrane integrity and absorbed by nonviable cells with a compromised cell membrane. Consequently viable cells appear refractile and round while the nonviable cells absorb appear blue and may also be asymmetrical. The use of this stain is, however, time sensitive as viable cells can absorb trypan blue over time and affect results.

The cells were trypsinised and suspended in complete culture medium (CCM). Trypan blue solution (0.5 ml; Appendix 1.5) was aliquoted into an eppendorf tube and incubated for a few minutes to warm up. The cell suspension (0.5 ml) was then added and the resulting solution was mixed thoroughly to obtain an even distribution of cells. This mixture was then allowed to stand for 5-15 minutes to allow uptake of the stain.

The haemocytometer slide and coverglass were cleaned with distilled water (1X) and ethanol (1X) and dried to facilitate proper capillary action. The sides of the coverglass were then moistened, placed over the counting platforms on the slide and gently pressed down to hold the coverglass in position and to create a vacuum. A micropipette was used to transfer a small volume of the trypan blue/cell suspension mixture (50µl) to the edge of the coverglass where capillary action caused both counting platforms to be completely filled. The haemocytometer slide was then placed under the microscope and each counting chamber was viewed.

All the cells in the 1mm centre square and the four corner squares were counted. If a cell lay across a North or West line a line of a small square, it was counted but if it lay on a South or East line, it was ignored. This was performed for both chambers. If more than 10% of the cells appeared to be clumped, the procedure was repeated. If less than 200 cells (20 cells/square) or greater than 500 cells (50 cells/square) were observed in the 10 squares, the procedure was repeated following an adjustment to the dilution. A second sample was withdrawn to ensure accuracy.

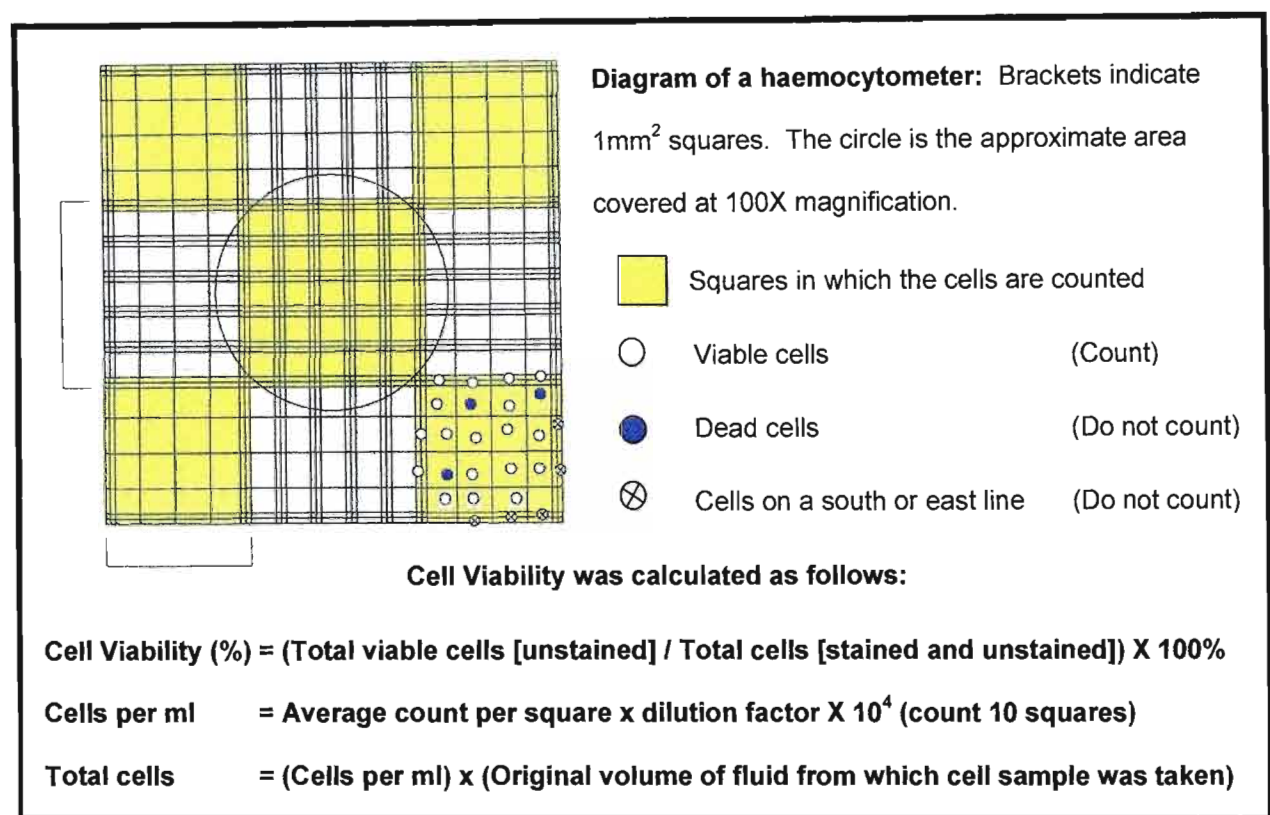


Figure 3.4: Calculating cell viability using the haemocytometer (adapted from Biowhittaker cell biology products catalogue, 2002).

3.3 CONCLUSION

The HT-29 colonic adenocarcinoma cell line demonstrated optimal growth, rapid detachment and excellent viability using the described cell culture techniques and was established to be a cell culture system suitable for the needs of this study.

CHAPTER 4

CYTOTOXICITY OF DEOXYNIVALENOL AND FUMONISIN B₁ ON THE HT-29 CELL LINE

4.1 INTRODUCTION

4.1.1 CYTOTOXICITY

Cell death occurs via two distinguishable mechanisms, namely necrosis and apoptosis. Necrosis is an “accidental” cell death that occurs when cells are subjected to a severe physical or chemical insult while apoptosis is a “normal” cell death that removes unwanted or useless cells. Cytotoxicity, however, has no specific death mechanism and is basically the cell-killing property of a chemical compound or a mediator cell independent of the mechanism of death (Rode *et al.*, 2004). It is an important factor in understanding the mechanisms of action of chemicals on cells and tissues and is thought to play an important role in a number of pathological processes including carcinogenesis and inflammation (Putnam *et al.*, 2002). As a result, cytotoxicity assays have become essential in the toxicological assessment of chemicals.

Various biological methods based on the biological properties and modes of action of mycotoxins have been developed to characterise the toxicity of fungal metabolites. These bioassays ranged from functional *in vivo* experiments using chicken embryos and laboratory animals to *in vitro* morphological and/or functional tests using plants, microorganism and cell culture systems (Robb and Norval, 1983; Reubel *et al.*, 1987). Cell culture systems have since become the *in vitro* model of choice for the evaluation of cytotoxicity and characterisation of mycotoxins (Yike *et al.*, 1999).

Cell culture based cytotoxic evaluation was initially based mostly on morphological criteria, e.g. simple macroscopical examination of cell damage or microscopical evaluation following fixation and staining. The disadvantage of such morphological evaluation, however, is the subjective judgement of cytotoxicity (Reubel *et al.*, 1987). Other assays used involved altered cellular functions such as inhibition of protein or DNA synthesis. These assays, while very sensitive, are limiting as they are time consuming and require specialised laboratory equipment and radioactive isotopes for cell labeling which pose a significant health hazard (Twentyman and Luscombe, 1987; Riss and Moravec, 1996). Overall, these assays do not allow for large numbers of samples to be processed and this need has led to attempts to introduce rapid efficient assays which can be automated.

Recently, Mosmann (1983) described an extremely rapid colorimetric assay based on a study published by Slater *et al.* (1963) investigating the staining reactions of four tetrazolium salts caused by the intact respiratory chain of rat liver mitochondria. The main point of interest was the applicability of these observations for measuring the mitochondrial activity of living cells and resulted in the development of the Methylthiazol tetrazolium (MTT) Bioassay.

4.1.2 THE METHYLTHIAZOL TETRAZOLIUM (MTT) BIOASSAY

The MTT assay is a quantitative colorimetric method based on the reductive cleavage of the water soluble monotetrazolium salt MTT (3-[4,5-dimethylthiazol-2-yl]-2,5-diphenyltetrazolium bromide), a pale yellow substrate, to a purple formazan (Mosmann, 1983) in metabolically active cells. The MTT salt is actively transported into viable cells where the tetrazolium ring is cleaved (Figure 4.1a) resulting in the formation of ultraviolet-absorbing purple formazan crystals (Figure 4.1b) which are insoluble in aqueous solutions (Putnam *et al.*, 2002). Once solubilised with the appropriate solvent, the absorbance of the solution can be determined using a spectrophotometer.

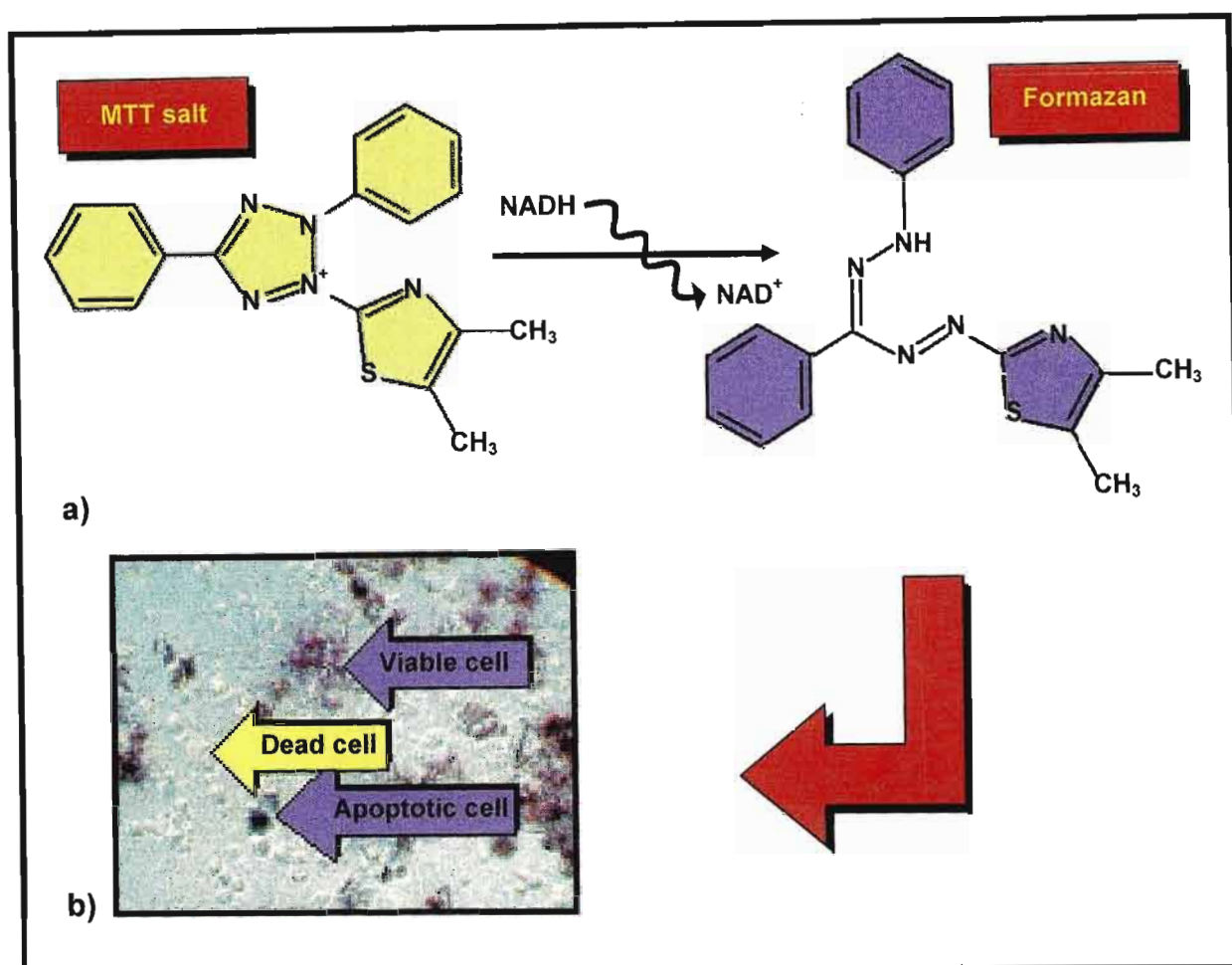


Figure 4.1: An illustration of: (a) the cellular reduction of MTT salt (Rode *et al.*, 2004) and (b) formazan formation (Klipski *et al.*, 2003).

Despite the widespread use of this assay as a measure of cell viability and proliferation, the mechanism of cell mediated reduction has not been fully elucidated. It was initially established, in a study using rat liver homogenates, that mitochondrial reduction by the succinate reductase system (Slater *et al.*, 1963) was the major contributor to MTT reduction. However, recent studies have demonstrated that contrary to the generally excepted view, most reduction of MTT occurs extramitochondrially with MTT salt crossing the intact plasma membranes to be reduced intracellularly.

There are however, conflicting reports on the interaction of MTT with the plasma membrane as it appears to vary with different types of cells. A study conducted by Liu *et al.* (1997), using the B12 rat brain tumour cell line, concluded that MTT is not permeable to the plasma membrane and is taken into the cell via endocytosis and reduced by a flavin oxidase. The resulting formazan is then thought to be deposited in granular form predominantly in the endosomal/lysosomal compartments and transported to the cell surface via exocytosis to form the needle like formazan crystals. However, in another investigation using HepG2 human hepatoma cells, Bernas and Dobrucki (2000) showed the MTT salt to readily cross the intact plasma membranes to be reduced in the endoplasmic reticulum and cytosol as well as the in the mitochondria. A subsequent study demonstrated that only a fraction of MTT formazan was observed to be deposited in or at the surface of mitochondria whereas most MTT was seen to be reduced in other cellular compartments, in the cytoplasm and in regions of the plasma membranes (Bernas and Dobrucki, 2002). This is supported by the fact that tetrazolium salts are widely utilised in immunohistochemistry for demonstration of specific non-mitochondrial enzymes (Vistica *et al.*, 1991).

Other investigations have demonstrated that most of the cellular reduction of MTT is dependent on microsomal enzymes and not only on succinate dehydrogenase (Berridge and Tan, 1993; Berridge *et al.*, 1996; Riss and Moravec, 1996). The reduction by microsomal enzymes requires the reduced pyridine nucleotide cofactors NADH and NADPH and is not affected by respiratory inhibitors (Berridge and Tan, 1993). This indicates that cellular reduction of MTT is related more to the glycolytic rate and thus to NADH production than to respiration and is therefore primarily a measure of the rate of glycolytic NADH production (Berridge *et al.*, 1996; Riss and Moravec, 1996). This view is supported by the fact that cellular MTT reduction is affected by glucose in the culture media (Vistica *et al.*, 1991; Berridge *et al.*, 1996).

Overall, it can be said that the reduction of MTT is an intracellular process that is brought about by the action of NADH, NADPH and succinate. It predominantly involves NAD(P)H-dependent enzymes of the endoplasmic reticulum, although succinate dehydrogenase may also contribute to reduction through succinate. However, this reduction is slow and contributes little to total cellular MTT reduction (Berridge *et al.*, 1996).

In principle, an increase in the number of viable cells results in an increase in the overall enzyme activity in a sample which in turn results in increased formazan dye formation. This cellular conversion has been demonstrated to show good correlation between spectrophotometric absorbance and viable cell number for most commonly used assay procedures (Gerlier and Thomasset, 1986; Carmichael *et al.*, 1987; Riss and Moravec, 1996; Wang and Cynader, 2001). It must be noted however that this assay does not differentiate between viable cells and apoptotic cells since apoptosis is an active mode of cell death that requires the metabolism of cells.

This experiment investigated the cytotoxic effects of DON and FB₁ individually and in combination on the HT-29 cell line. Four concentrations (5µM, 10µM, 25µM and 50µM) were tested over exposure periods from 24 to 96 hours. This range of concentrations was selected as it has been demonstrated to exert significant *in vitro* effects on epithelial intestinal cells (Schmelz *et al.*, 1998; Maresca *et al.*, 2002; Bouhet *et al.*, 2004). In addition concentrations of FB₁ between 5 to 50µM corresponds to feed contaminated at 4 to 40 ppm, concentrations that are in the range observed in contaminated feed, throughout the world (Shephard *et al.*, 1996). The cytotoxicity of curcumin was also determined using these cells. A concentration reported to induce apoptosis (50µM) was selected for this purpose (Goel *et al.*, 2001).

4.2 MATERIALS AND METHODS

4.2.1 MATERIALS

The mycotoxins (DON and FB₁), curcumin and MTT salt were purchased from Sigma Aldrich Chemical Company (Johannesburg, SA). Ethanol (EtOH) and DMSO were purchased from Merck (Johannesburg, SA).

4.2.2 METHODS

4.2.2.1 Preparation of Mycotoxin Stock Solutions

Fumonisin B₁ (1mg) was dissolved in CCM (6ml) to give a 200µM FB₁ solution. Deoxynivalenol (0.5mg) was solubilised in EtOH (10µl) and topped up to 6ml with CCM to provide a 200µM DON solution. A 100µM combination of DON and FB₁ (DFB₁) was then prepared by combining equal volumes (3ml) of both toxins. The remaining individual toxin solutions (3ml) were then diluted with CCM (1:1) to make 100µM toxin stocks. An EtOH control stock containing the equivalent amount of EtOH present in the DON and DFB₁ (approximately 0.08%) was then prepared. These four solutions were sterile filtered through 0.45µm filters and then diluted to prepare 50µM, 20µM and 10µM toxin concentrations and corresponding EtOH equivalents (3ml each).

4.2.2.2 Preparation of Curcumin Stock Solution

A curcumin stock solution (100µM) was prepared and used to assess the effect of the mycotoxins in the presence of this chemopreventive agent. The earliest exposure period at which the toxins demonstrated activity was selected for this purpose.

Curcumin (1.18mg) was solubilised in ethanol (38 μ l) and topped up with CCM to make 32ml of 100 μ M solution. An EtOH control containing the equivalent amount of EtOH present in the curcumin solution (approximately 0.08%) was then prepared. This was also sterile filtered through a 0.45 μ m filter.

4.2.2.3 Preparation of MTT Salt Solution

The MTT salt (5mg) was dissolved in HBSS (1ml) to give a final concentration of 5mg/ml. This suspension was agitated to dissolve clumps and filtered through a 0.45 μ m filter to remove insoluble residues. This solution was freshly prepared prior to use and stored in the dark.

4.2.2.4 The MTT Bioassay

Four culture flasks (75cm²) of confluent HT-29 cells were trypsinised and resuspended in CCM (20ml) to give a cell number of 3.5×10^4 cells/ml. Aliquots of the cell suspension (100 μ l) were then dispensed into each of the 96 wells on four microtitre plates to give a final cell count of 3500 cells per well. The plates were incubated overnight at 37°C for approximately 18 hours to allow the cells to attach to the wells. Each well was then aspirated.

Each toxin dilution was thoroughly mixed and aliquoted (100 μ l) into four wells on each microtitre plate (Figure 4.2). Complete culture medium (100 μ l) was added to each of these wells resulting in the concentrations being halved. The final concentrations of each toxin tested were therefore 50 μ M, 25 μ M, 10 μ M and 5 μ M. The wells containing the EtOH equivalents were similarly prepared. An untreated control was also performed. In this instance CCM (200 μ l) was added to four wells containing cells only. The four plates were then incubated for 24, 48, 72 and 96 hours respectively at 37°C in the culture environment.

To assess the effect of the toxins in the presence of curcumin (50µM) at a selected exposure time the cells were plated out and treated as above. In the wells containing toxin, curcumin (100µM; 100µl) was added instead of CCM to halve the concentrations. In the case of the toxin EtOH control the curcumin EtOH control (100µl) was added in place of CCM. In addition, curcumin (100µl) was added to four wells and topped up with CCM (100µl) as a curcumin (50µM) control.

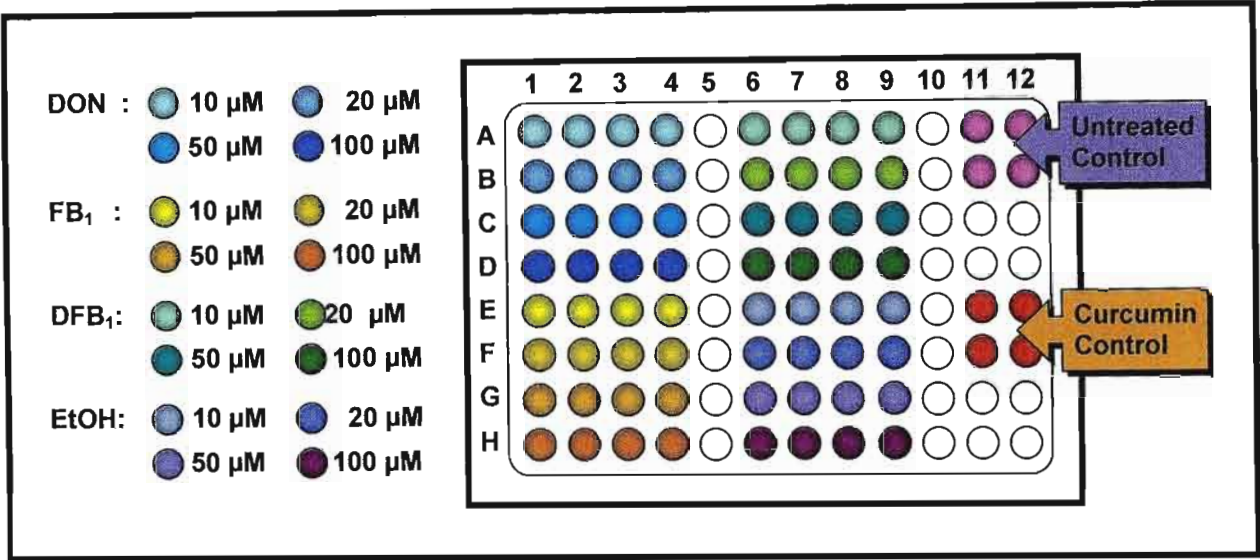


Figure 4.2: An illustration depicting the treatment procedure for the MTT assay.

Following each incubation period, the plates were aspirated and the cells were incubated with 90µl CCM and 10µl of MTT salt solution for 4 hours at 37°C (Figure 4.3). The plates were then aspirated and DMSO (100µl) was added to each well. The plates were incubated for an hour (37°C) to allow for the solubilisation of the formazan crystals. The optical density of the wells was then measured spectrophotometrically at a wavelength of 595nm with a reference wavelength of 655nm using a Bio-Rad (Johannesburg, SA) microplate reader. This assay was performed in triplicate and cell viabilities of treated cells were calculated by comparison against the relevant control cells. Dose response graphs for each exposure period were generated using the cell viabilities obtained in relation to increasing toxin concentration.

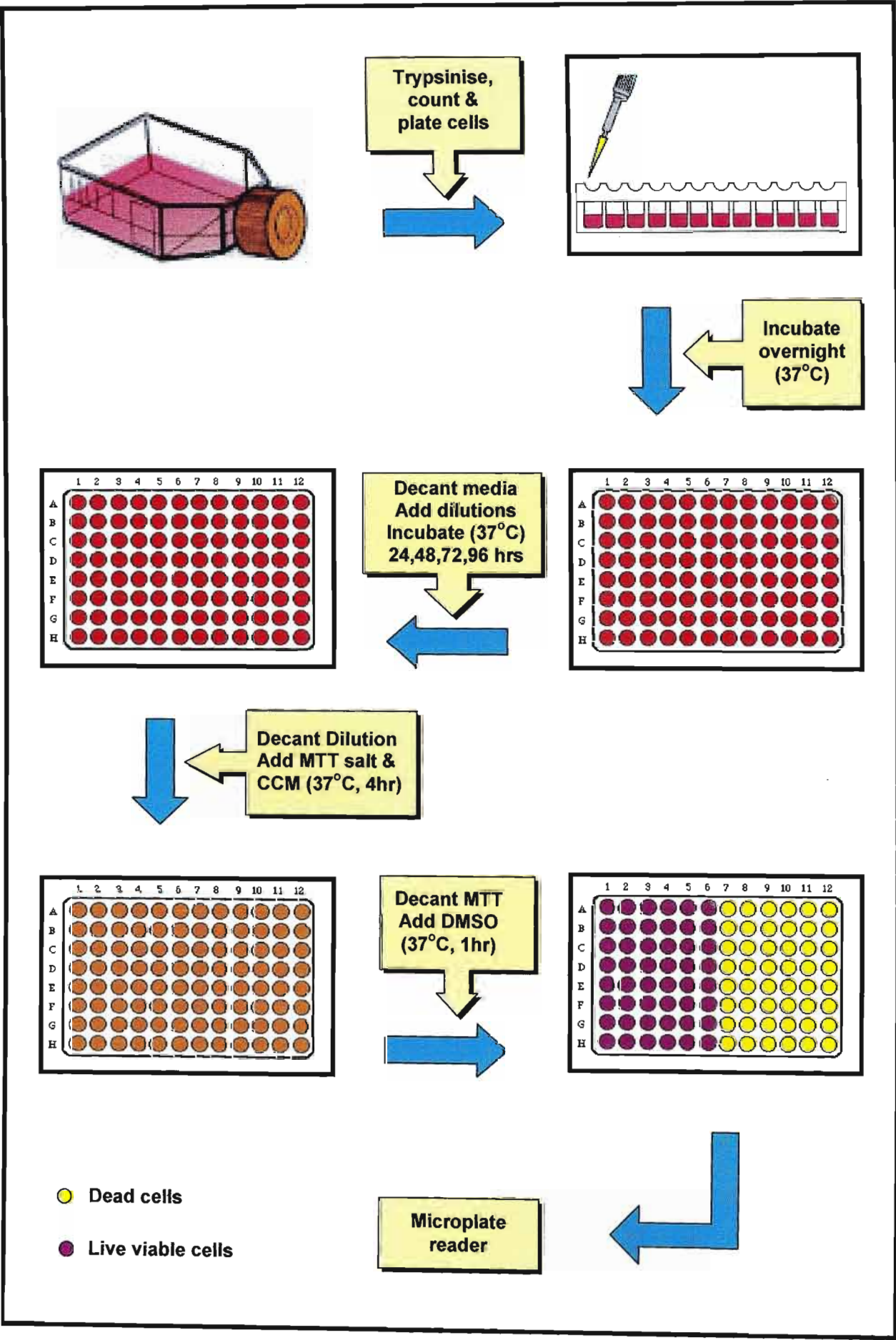


Figure 4.3: An illustration of the MTT bioassay.

The CCM was replenished during the MTT incubation step to ensure the absence of substances, such as test agents, which may interfere with enzymatic regulation, consequently affecting the capacity of cells to reduce MTT to formazan. In addition, the presence of sufficient amounts of NAD(P)H or glucose in the culture medium allows for effective MTT reduction. Fresh culture medium also contains HEPES, which is important during incubation with MTT salt. This buffer controls pH preventing the presence of acidic residues in the formazan/DMSO solution, which may result in decreased absorbance values (Sieuwerts *et al.*, 1995). There was no need for a washing step following the removal of the MTT containing medium as the MTT salt and its formazan product absorb light at different wavelengths (Plumb *et al.*, 1989). Prolonged exposure of formazan crystals to air in the absence of DMSO affects absorbance readings, therefore the DMSO was added as quickly as possible to each well (Sieuwerts *et al.*, 1995).

4.2.2.5 Statistical Analyses

The percentage cell viability for each test was calculated by comparison of the absorbance of each toxin test to the absorbance of the control test.

Cell Viability (%)	=	$\frac{\text{Mean absorbance of test cells}}{\text{Mean absorbance of control cells}}$	X	100
---------------------------	----------	--	----------	------------

Standard deviations were then determined. The data was analysed on Microsoft Excel using either the Students t-test to determine significant differences between the treated and control cells or a one-way analysis of variance (ANOVA) to determine significant differences between the various concentrations of each toxin as well as between different toxins at similar concentrations. After the application of ANOVA, the significance of differences in the cell viabilities between control and treatment groups at specific culture periods was evaluated by multiple comparisons using the Bonferroni method. Differences were considered statistically significant at $p < 0.05$ and highly significant at $p < 0.01$.

4.3. RESULTS AND DISCUSSION

The results of the cytotoxicity assays are illustrated in Figures 4.4 to 4.8. Statistical analysis indicated that there were overall significant differences between the effects of the toxins and their respective controls ($p < 0.001$) as well as between various concentrations of each toxin at all four incubation periods (Figures 4.5-4.7). At the exposure period selected to assess the toxin effects in the presence of curcumin (Figures 4.8), significant differences were observed between the effects of the different toxins at similar concentrations ($p < 0.007$) as well as between those of the toxin only and toxin and curcumin.

4.3.1. THE EFFECT OF THE ETHANOL EQUIVALENTS

The effect of the EtOH present in the toxin treatments is shown in Figure 4.4. Following the 24 hour incubation period the cell viabilities for the 5 μ M (114.78%) and 10 μ M (116.21%) EtOH controls were not significantly different from each other but were significantly greater than that of the 25 μ M (102.93%) and 50 μ M (106.64%) ethanol controls as well as the untreated control. The cell viabilities for the 25 μ M and 50 μ M EtOH controls and the untreated control were not significantly different from each other.

The cell viabilities for the 5 μ M (136.83%), 10 μ M (145.50%), 25 μ M (150.72%) and 50 μ M (146.72%) EtOH controls were increased following the 48 hour incubation period and although not significantly different from each other, were significantly greater than that of the untreated control. Following 72 hours exposure, the cell viabilities were significantly greater than the untreated control. The cell viabilities of the 5 μ M (120.40%) and 10 μ M (123.19%) EtOH controls were not significantly different from each other. The cell viability for the 25 μ M (132.22%) EtOH control was significantly greater than the 5 μ M ($p = 0.042$) as well as the 50 μ M (113.89%; $p = 0.02$).

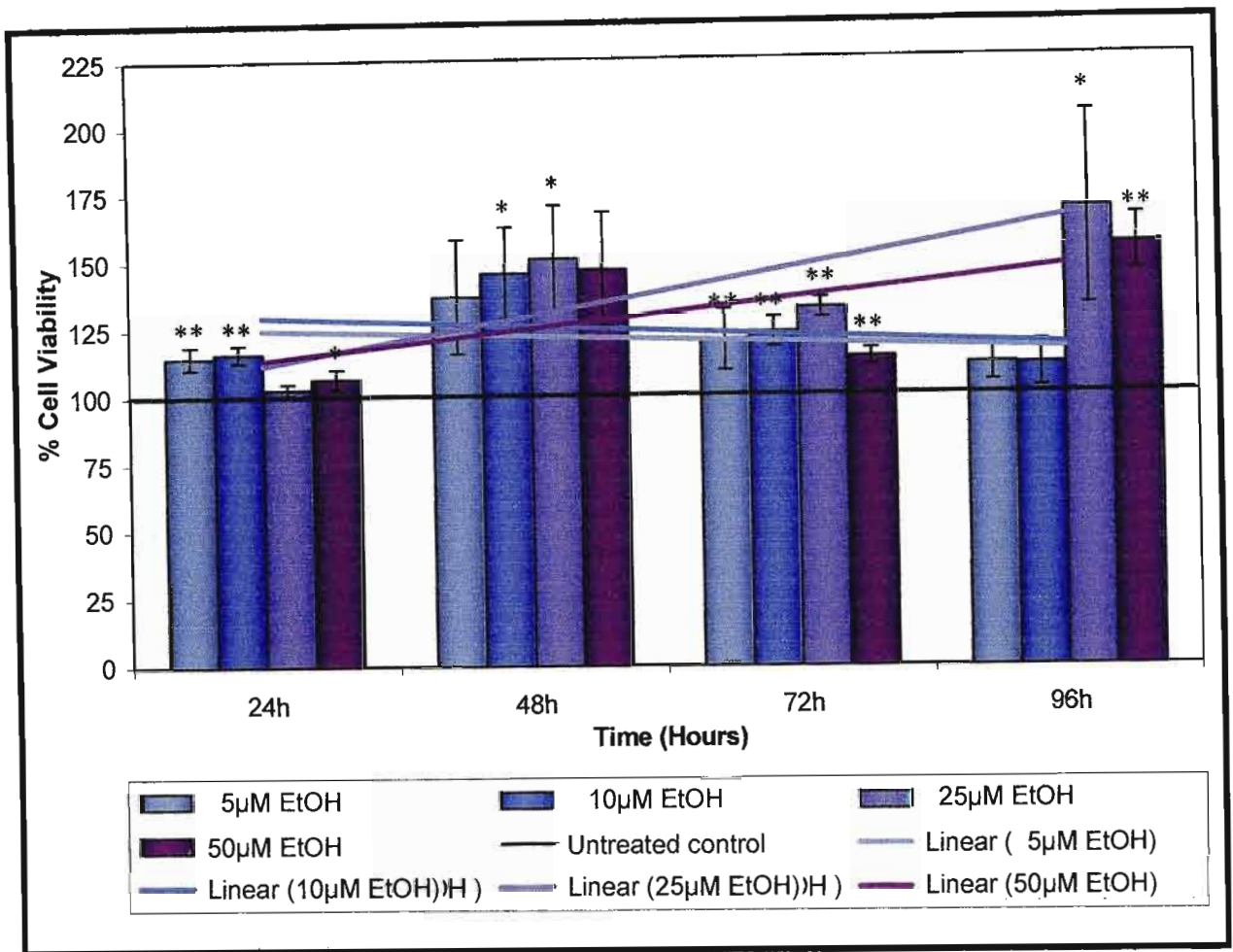


Figure 4.4: The dose response graph of the equivalent EtOH controls on the HT-29 cell line over exposure periods 24 to 96 hours: [Significant difference from the untreated control: * ($p<0.05$) and ** ($p<0.01$)].

Following the 96 hour incubation period, the cell viabilities for the 5μM (111.24%) and 10μM (110.81%) were not significant different from each other or that of the untreated control (110.47%). The cell viabilities for the 25μM (168.40%) and 50μM (155.20%) EtOH controls were also not significantly different from each other but were significantly greater than that of the 5μM and 10μM ethanol controls as well as the untreated control ($p<0.043$).

Ethanol appeared to exert a proliferative effect at all concentrations tested however, the trend lines indicated that at the low EtOH concentrations (5μM and 10μM), the proliferative effect decreased slightly with time whilst at the higher concentrations (25μM and 50μM), the proliferative effect increased with time.

This proliferative effect of EtOH has been previously demonstrated in a study conducted by Etique *et al.* (2004) using MCF-7 cells grown in the presence of 0.1% ethanol and may be a consequence of increased energy produced from ethanol metabolism. During EtOH metabolism ethanol is oxidised to acetaldehyde by alcohol dehydrogenases in the cytosol. The acetaldehyde is then further oxidised to acetate, principally in the mitochondria, by acetaldehyde dehydrogenases. The NADH produced from these reactions is then used for ATP generation through oxidative phosphorylation (Smith *et al.*, 2004).

The difference in proliferative effects between the low and high EtOH controls is a possible consequence of the ethanol concentration as well as the manner in which it enters the cell. Ethanol crosses biological membranes by passive diffusion down its concentration gradient, therefore the higher the concentration of ethanol the greater is the resulting concentration gradient and the more rapid is its absorption (Cederbaum, 2001). Accordingly, the high concentrations of EtOH will cross the cell membrane rapidly and have a greater effect on cell proliferation while the lower concentrations are absorbed slower and have a less marked effect. The decrease in proliferation with time observed for the low concentrations is a possible result of the complete utilisation of the ethanol present while the increase with the high concentrations may be due to the additional ethanol present.

These results demonstrate that EtOH exhibits no cytotoxic effect on the HT-29 cell line, as at no point during the four exposure periods was the cell viability of the EtOH control cells below 100%. Therefore, any cytotoxic effect observed in the toxin treated cells would be due to the action of the toxin and not its carrier solvent. Consequently, hereafter the cell viabilities of the toxin treated cells are compared to that of the CCM control (100% cell viability).

4.3.2 THE EFFECT OF DEOXYNIVALENOL

The cytotoxic effect of DON is illustrated in Figure 4.5. Following the 24 hour incubation period, DON appeared to decrease cell viability slightly when compared to the untreated control. No significant difference was noted between the cell viabilities for the 5µM (90.94%), 10µM (88.31%) and 50µM (83.20%) DON treated cells. A significant difference was only observed between the cell viabilities for the 25µM (100.48%) and 50µM (83.20%) DON-treated cells with a resulting 17.28% decrease in viability.

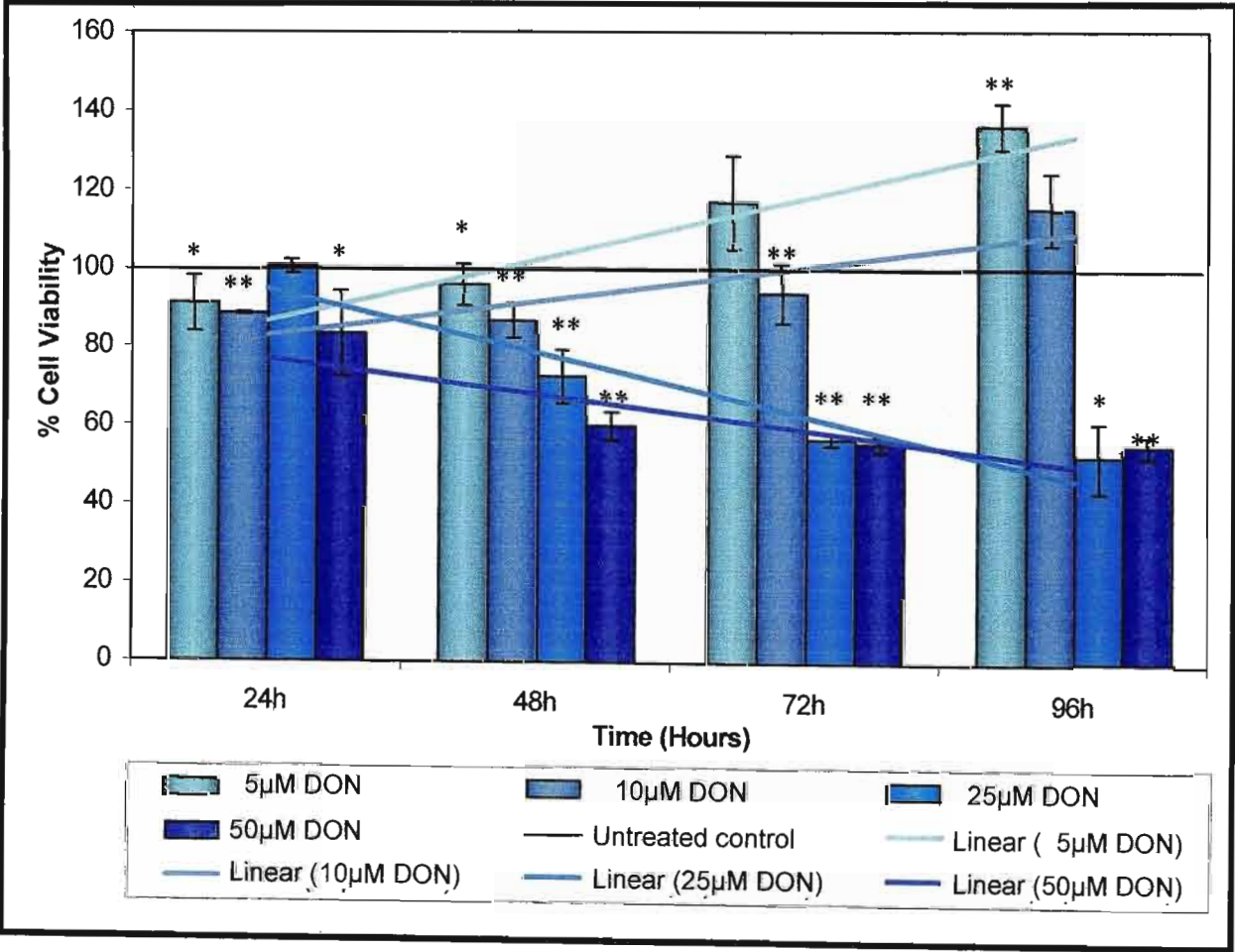


Figure 4.5: The dose response graph of varying concentrations of DON on the HT-29 cell line over exposure periods 24 to 96 hours: [Significant difference from the untreated control: * (p<0.05) and ** (p<0.01)].

After the 48 hour incubation with DON, the cell viabilities for all concentrations tested were less than that of the untreated control. No significant differences were observed between the cell viabilities of the 5 μ M (95.78%) and 10 μ M (86.25%) DON treated cells. Significant differences were observed between the cell viabilities for the 10 μ M, 25 μ M (72.34%) and 50 μ M (59.84%) DON treated cells ($p<0.031$) with cell viability decreasing with increasing toxin concentration indicating that DON exerted a dose dependent cytotoxic effect on HT-29 cells.

At the next incubation period of 72 hours, all cell viabilities were less than that of the untreated control with the exception of that of the 5 μ M (116.72%) DON treated cells. The cell viabilities for the 5 μ M, 10 μ M (93.59%), 25 μ M (56.55%) and 50 μ M (55.38%) DON treated cells decreased dose dependently and were all significantly different from each other ($p<0.002$) with the exception of that of the 25 μ M and 50 μ M DON treated cells.

A similar effect was observed following the 96 hour incubation period. All cell viabilities were less than that of the untreated control with the exception of that of the 5 μ M (136.13%) and 10 μ M (115.03%) DON treated cells. The cell viabilities for the 5 μ M, 10 μ M, 25 μ M (51.99%) and 50 μ M (54.75%) DON-treated cells again decreased dose dependently and were all significantly different from each other ($p<0.002$) with the exception of the 25 μ M and 50 μ M DON treated cells.

These results indicate that DON exhibits a dose dependent effect on HT-29 cells, decreasing cell viability with increasing toxin concentration. This effect was achieved following 48 hours of incubation with this toxin and was maintained over the 72 and 96 hour incubation periods. At the higher concentrations, no significant differences were observed in the cell viabilities over the 72 and 96 hour time intervals indicating that the cells were unable to recover from the toxin effect.

In addition, trend lines indicate that at the low concentrations of DON (5 μ M and 10 μ M) the HT-29 cells suffered slight cytotoxic effect and proliferated exponentially over the four exposure periods while the high concentrations (25 μ M and 50 μ M) caused time dependent decreases in cell viability in this cell line. It may be that at high concentrations DON induces long term changes that the cell is unable to recover from while at low concentrations, the effect is transitory and is decreased as compensatory or adaption mechanisms are established resulting in cellular proliferation. It is also possible that the lack of toxicity observed at the low DON concentrations is due to the toxin being fully utilised by the cells. The toxicity noted at the high concentrations may thus be due to the cells being unable to cope with and utilise the high toxin dose.

The cytotoxic effect of DON has been reported previously in a number of cell lines. These include human and rat granulomonocytic progenitors (Lautraite *et al.*, 1997), the K562 human erythroleukemia and MIN-GL1 lymphoid B cell lines (Viseonti *et al.*, 1991; Minervini *et al.*, 2004) as well as the Caec-2 human colon, A549 lung and U937 monocytic cell lines (Instanes and Hetland, 2004). This cytotoxicity may be attributed to the involvement of DON in lipid peroxidation (Garaleviciene, 2003; Marciniak *et al.*, 2003), a process that may yield products that react with DNA and proteins to cause oxidative modifications or the ability of this mycotoxin to bind to ribosomes and inhibit protein synthesis (Rotter *et al.*, 1996).

Proteins encompass an enormous range of biopolymers that are synthesised in ribosomes which may be attached to the endoplasmic reticulum or free in the cytoplasm. These molecules are responsible for numerous roles within the cell including transport and storage of smaller molecules, structural support, hormone regulation, receptor functions, movement, defence and enzymatic reactions (Mathews *et al.*, 1995). The most varied and highly specialised are enzymatic proteins which catalyse a tremendous variety of reactions that channel metabolism into essential pathways. As such, inhibition of protein synthesis by DON may have widespread consequences for the cell.

It should be noted that DON may also inhibit the synthesis of the NAD(P)H-dependent enzymes of the endoplasmic reticulum involved in the cleavage of MTT salt to formazan.

4.3.3 THE EFFECT OF FUMONISIN B₁

The effect of FB₁ over the four incubation periods is illustrated in Figure 4.6. Following the 24 hour exposure period, no significant difference was noted between the cell viabilities of the 5µM (91.63%) and the 50µM (94.94%) and between those of the 10µM (104.22%) and the 25µM (103.33%) FB₁ treated cells. Although the cell viabilities of the 5µM and 50µM FB₁ treated cells were significantly less than that of the 10µM and 25µM FB₁ treated cells ($p < 0.003$), the cytotoxic effect was minimal when compared to the untreated control.

Following 48 hours of incubation with FB₁, the cell viabilities for all concentrations tested were greater than that of the untreated control and were thus indicative of the proliferative effects of this toxin. No significant differences were observed between the cell viabilities for 10µM (188.03%), 25µM (211.80) and 50µM (171.30%) FB₁ treated cells as well as between those of the 5µM (131.89%) and the 50µM FB₁ treated cells. The cell viability for the 5µM FB₁ treated cells was significantly less than that of the 10µM and 25µM FB₁ treated cells ($p < 0.026$).

At 72 hours, the cell viabilities for the 5µM (114.46%), 10µM (112.42%), 25µM (133.61%) and 50µM (104.74%) FB₁ treated cells were not significantly different from each other but were again greater than that of the untreated control although not to the extent observed following the 48 hour incubation period.

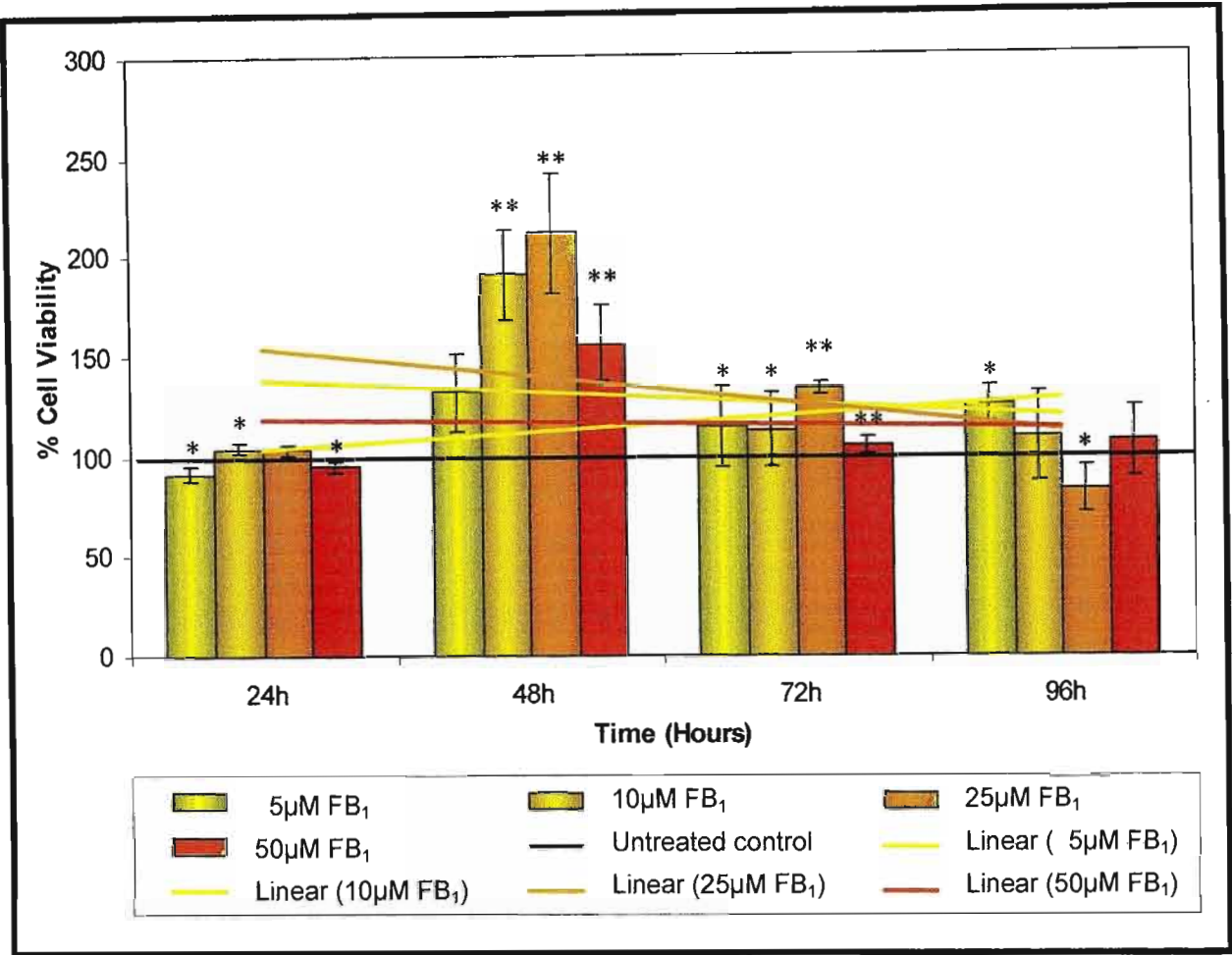


Figure 4.6: The dose response graph of varying concentrations of FB₁ on the HT-29 cell line over exposure periods 24 to 96 hours: [Significant difference from the untreated control: * (p<0.05) and ** (p<0.01)].

At 96 hours, the cell viabilities for all concentrations tested were greater than that of the untreated control with the exception of the 25μM (82.84%) FB₁ treated cells. No significant differences in cell viability were observed between the 5μM (125.06%); 10μM (108.89%), 25μM and 50μM (106.52%) FB₁ treated cells with the exception of that of the 5μM and 25μM FB₁ treated cells (p<0.015).

These results suggest that FB₁ exerts little cytotoxicity following the 24 and 48 hour exposure periods having instead a dose dependent proliferative effect at concentrations ranging from 5μM to 25μM that is maximal following 48 hours exposure and reduced over the 72 and 96 hour exposure periods.

This reduction in proliferation is a possible consequence of nutrient depletion and reduction in growth area resulting from the high rate of proliferation observed at 48 hours. The proliferation of cells observed following 48 hours of incubation with FB₁ (5μM, 10μM and 25μM) persisted at the 50μM concentration but was lower than that noted at 25μM signifying a decrease in proliferation ability.

In addition, the trend lines indicate that the proliferative effect exerted by the 5μM, 10μM and 25μM FB₁ concentrations were also time dependent. It can also be seen that the proliferative effect of 5μM, although not as potent as that of the 10μM and 25μM, was maintained over all four exposure periods and not just the 24 and 48 hour periods. The 50μM concentration appears to exhibit no marked proliferative ability over the various incubation periods.

The proliferative effect of FB₁ observed on the HT-29 cell line following 48 hours of incubation may be a consequence of the ability of this mycotoxin to cause perturbations in the metabolism of sphingolipids, a class of lipids that occurs primarily in cellular membranes, lipoproteins and other lipid-rich structures of all eukaryotic cells. Briefly, as discussed in Chapter 2, FB₁ binds to the catalytic site of ceramide synthase and inhibits the condensation of sphinganine and fatty acyl CoA and the reacylation of sphingosine formed from the breakdown of complex sphingolipids (Dragan *et al.*, 2001). This results in a decrease in the formation of the pro-apoptotic sphingolipid ceramide (Ahn and Schroeder, 2002) accompanied by an accumulation of the sphingoid bases sphinganine and sphingosine (Riley *et al.*, 2001). These sphingoid bases are broken down by the respective sphingoid kinases to form mitogenic and anti-apoptotic 1-phosphates (Spiegel and Merrill, 1996; Malagarie-Cazenave *et al.*, 2002) that are subsequently cleaved by sphingoid lyases to form fatty aldehydes and ethanolamine phosphates, which can lead to imbalances in phosphoglycerolipids and fatty acids. However, once the reducing capacity of the sphingoid kinases is exceeded, the sphingoid bases accumulate to toxic concentrations and result in cell death (Riley *et al.*, 2001).

It may therefore be postulated that the concentrations of FB₁ used in this experiment were insufficient to induce cell death as a consequence of toxic sphingoid base concentrations, but decreased ceramide formation, resulting in the accumulation of sphingoid bases that were reduced by the sphingoid kinases to the mitogenic 1-phosphates.

A slow decrease in the reducing capacity of the sphingoid kinases may account for the decreased proliferation exerted by the 50µM concentration and it is therefore probable that higher concentrations of FB₁ would be necessary to exert a cytotoxic effect.

Fumonisin B₁ has been established to be cytotoxic in several animal cell lines including the Vero monkey kidney (Abado-Becognee *et al.*, 1998), LLC-PK1 pig kidney (He *et al.*, 2002a) and RK13 rabbit kidney (Rumora *et al.*, 2002) cell lines. It has been demonstrated to be poorly cytotoxic toward several human cell lines namely the K-562 erythroleukemia (Minervini *et al.*, 2004), the SNO oesophageal (Myburg *et al.*, 2002) and the CaCo-2 colon carcinoma cell lines (Caloni *et al.*, 2002). In addition, it has been shown to be mitogenic in Swiss 3T3 fibroblasts (Schroeder *et al.*, 1994). This indicates that cell type is a critical determinant of FB₁ toxicity.

The proliferative effect observed in this experiment is in keeping with that of Schroeder *et al.* (1994) who described the possible mitogenic effect of FB₁ and suggested that the potential carcinogenicity of FB₁ may be related to its ability to stimulate cell division (Riley *et al.*, 2001). Cell division is necessary for conversion of adducts or other single stranded DNA damage to gaps or mutation and allows for mitotic recombinations that result in changes that are more profound than those from a single mutation. Consequently the stimulation of cell proliferation will increase the risk of various types of genetic errors and cell transformation and may provide a plausible molecular mechanism to explain the role of FB₁ in initiation and promotion during tumour formation.

4.3.4 THE EFFECT OF A DEOXYNIVALENOL AND FUMONISIN B₁ MIXTURE

The combined effect of DON and FB₁ (DFB₁) is demonstrated in Figure 4.7. Following the 24 hour incubation period, DFB₁ appeared to decrease cell viability when compared to the untreated control. No significant difference was noted between the cell viabilities for the 5µM (88.09%), 10µM (74.35%), 25µM (93.55%) and 50µM (78.39%) DFB₁ treated cells with the exception that the cell viability of 10µM DFB₁ treated cells was significantly less than that of the 25µM ($p<0.001$) DFB₁ treated cells.

After 48 hours of incubation with this DFB₁, the cell viabilities for all concentrations tested were less than that of the untreated control. No significant differences were observed between the cell viabilities of the 5µM (92.61%), 10µM (90.34%) and 25µM (85, 13%) DFB₁ treated cells. The cell viability for the 50µM treated cells (61.17%) was significantly less than that of all the other concentrations tested ($p<0.001$). A slight dose dependent effect was observed. This effect was not as potent as that following DON treatment at the 48 hour exposure period (Figure 4.5) and may be a consequence of the increase in proliferative activity induced by FB₁ at this same exposure period (Figure 4.6).

At the next incubation period of 72 hours, all cell viabilities were less than that of the untreated control. No significant differences were observed between the 5µM (94.98%), 10µM (92.17%) and 25µM (82.69%) DFB₁ treated cells. The cell viability for 50µM DFB₁ treated cells (69.54%) was significantly less than that of all the concentrations tested with the exception of that of the 25µM ($P<0.003$) DFB₁ treated cells. A similar dose dependent effect to that observed following the 48 hour exposure period was apparent.

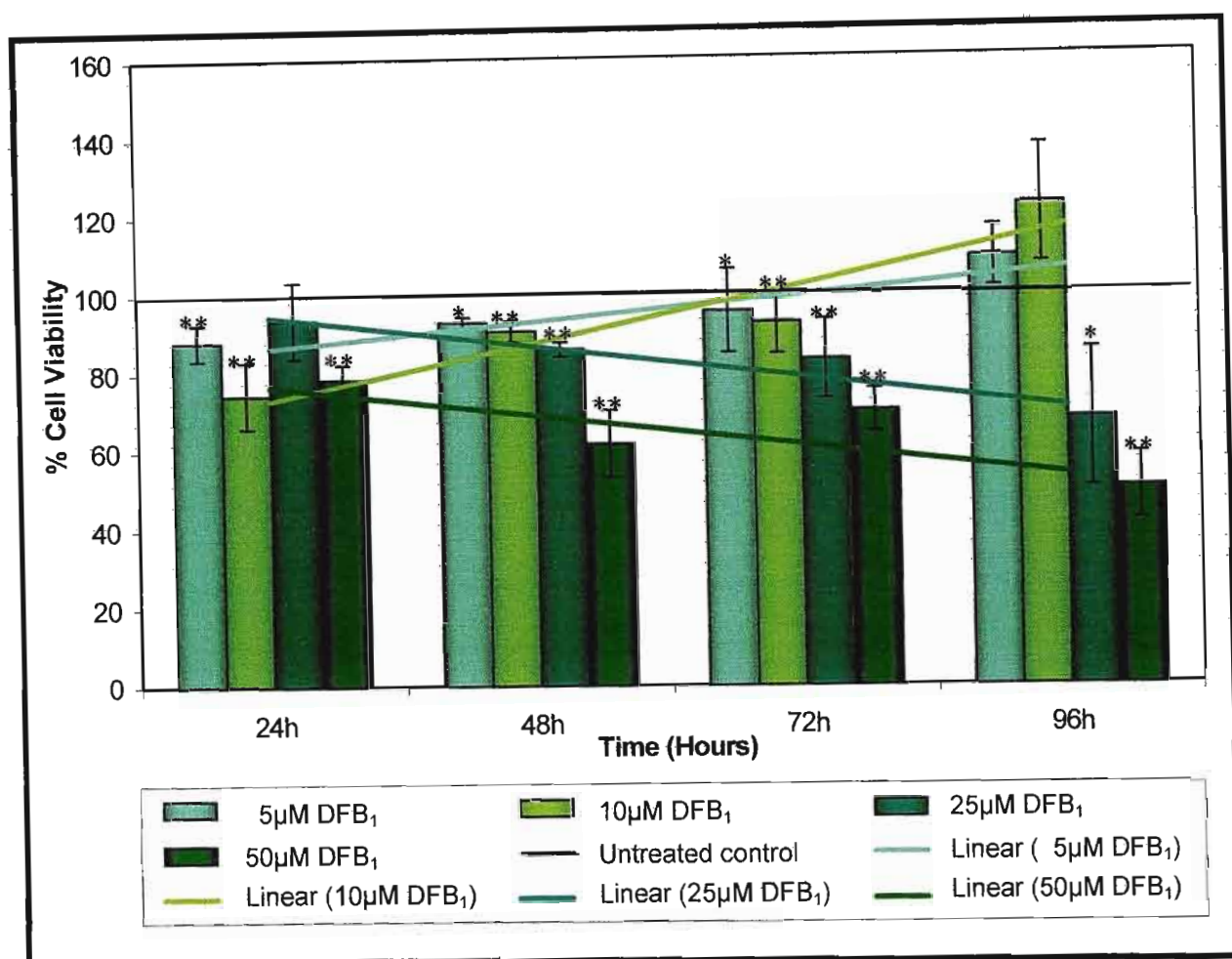


Figure 4.7: A dose response graph of varying concentrations of DFB₁ on the HT-29 cell line over exposure periods 24 to 96 hours: [Significant difference from the untreated control: * (p<0.05) and ** (p<0.01)].

At the 96 hour incubation period, all cell viabilities were less than that of the untreated control with the exception of that of the 5μM (108.84%) and 10μM (122.08%) DFB₁ treated cells. No significant differences were observed between the cell viabilities of the 5μM and 10μM DFB₁ treated cells although both these viabilities were significantly greater from those expressed by 25 μM (67.40%) (p<0.004) and 50μM (49.90%) (p<0.001) DFB₁ treated cells. No significant differences in cell viability were noted between the 25 and 50μM DFB₁-treated cells. The dose dependent effect previously observed appeared augmented and this may be a result of the reduced proliferative activity induced by FB₁ at the 96 hour incubation period (Figure 4.6).

These results indicate that DFB₁ exhibits a dose dependent effect on HT-29 cells. This effect was achieved following 48 hours of exposure to this toxin mixture and was maintained over the 72 and 96 hour incubation periods. In addition, the trend lines indicate that at the low concentrations of DFB₁ (5 μ M and 10 μ M) the HT-29 cells suffered slight cytotoxic effect and proliferated exponentially over the four exposure periods while the high concentrations (25 μ M and 50 μ M) caused time dependent decreases in cell viability in this cell line.

The effect of this toxin mixture appeared to follow a similar trend to that exhibited by DON individually but was agonistic with DON counteracting the mitogenic effect of FB₁ and FB₁ reducing the cytotoxic effect of DON to some extent. The ability of DON to inhibit mitogen induced cell proliferation has been previously documented (Rotter *et al.*, 1996; Charoenpornsook *et al.*, 1998).

Structure-activity studies on trichothecenes in a variety of lymphocyte models indicate that the inhibition of proliferation *in vitro* decreases upon substitution of acyl groups at the C8 position with keto or hydroxyl moieties and is also dependent on the nature of substitutions at the C3, C4 and C15 positions. This structure-activity response is reported to pattern that observed for protein synthesis inhibition and suggests that translational arrest may be an underlying mechanism for impaired proliferation (Rotter *et al.*, 1996).

4.3.5 THE CYTOPROTECTIVE EFFECT OF CURCUMIN IN THE PRESENCE OF THE SELECTED MYCOTOXINS

The earliest incubation period at which both toxins demonstrated significant activity was 48 hours. It was therefore the exposure period selected in which to compare the effects of the toxins and to assay their effects in the presence of curcumin to determine any cytoprotective effect afforded by this chemopreventive agent.

4.3.5.1 Comparison of the Effects of Deoxynivalenol, Fumonisin B₁ and the Mycotoxin Mixture

Comparison of the cell viabilities for each toxin treatment at the same concentration (Figure 4.8a) demonstrated significant differences between the effects of DON and FB₁ ($p < 0.026$) and between the effects of FB₁ and DFB₁ ($p < 0.015$) at 5, 10, 25 and 50 μ M concentrations. No significant differences were observed between the effects of DON and DFB₁. In addition, as indicated by the trend lines (Figure 4.8a) and discussed earlier, both DON and DFB₁ demonstrated a dose dependent cytotoxic effect while FB₁ displayed a dose dependent proliferative effect.

Cytotoxicity depends on the ability of a molecule to bind cellular receptors and/or penetrate the cell membrane and may be dependent on size, structural conformation and polarity of the compound. Of these, polarity appears to be an important determinant in the cytotoxic behaviour of mycotoxins with less polar molecules generally exhibiting higher cytotoxicity (Myburg *et al.*, 2002). The differences in cytotoxicity exhibited by DON and FB₁ may thus be explained by the polarity of these mycotoxins as FB₁ is highly polar in comparison to DON which is non polar.

4.3.5.2 Comparison of the Effects of Deoxynivalenol, Fumonisin B₁ and the Mycotoxin Mixture Following Co-treatment With Curcumin

The cell viabilities of the toxin and curcumin EtOH controls was significantly greater than the toxin EtOH controls ($p < 0.001$). This proliferative effect may be a consequence of the ability of this solvent to serve as a source of energy and therefore attributed to the presence of increased amounts of EtOH in the toxin and curcumin EtOH controls.

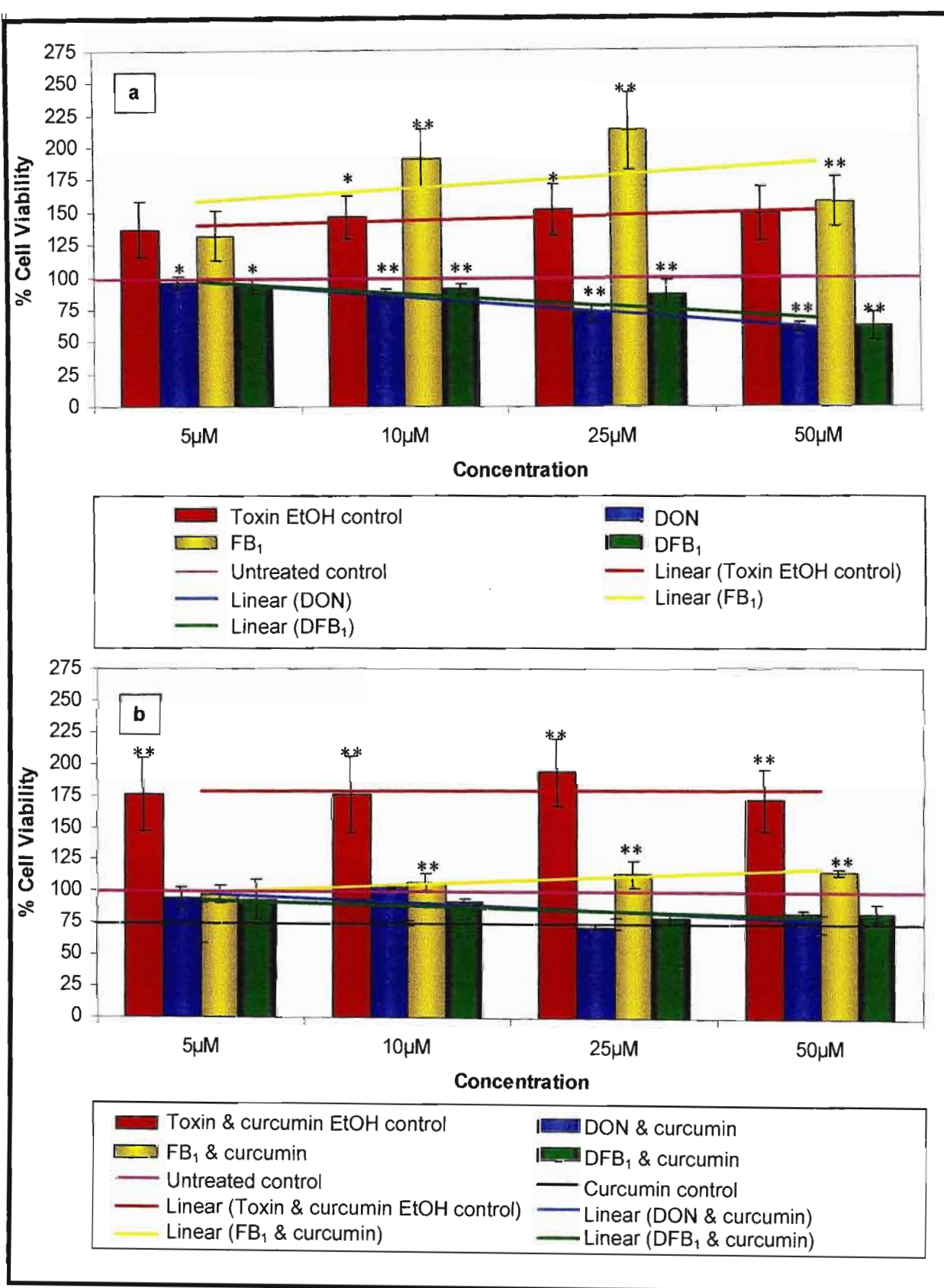


Figure 4.8: The dose response graph of the effects of DON, FB₁ and DFB₁ following: (a) individual treatment and (b) co-treatment with curcumin at the 48 hour exposure period: [Significant difference from untreated control: * ($p < 0.05$) and ** ($p < 0.01$)].

Comparison of the cell viabilities for each toxin treatment co-administered with curcumin at the same concentration (Figure 4.8b) demonstrated significant differences between the cell viabilities of FB₁ and curcumin and DON and curcumin treated cells at the 25µM and 50µM concentrations ($p<0.001$) and between the cell viabilities of FB₁ and curcumin and DFB₁ and curcumin treated cells at the 10µM, 25µM and 50µM concentrations ($p<0.001$). Significant differences between the cell viabilities of DFB₁ and curcumin and DON and curcumin treated cells were only noted at the 10µM concentration ($p<0.001$).

Curcumin (50µM) itself exerted a cytotoxic effect on HT-29 cells decreasing the cell viability to 74.56% (Figure 4.8b). The cytotoxicity of curcumin has been previously demonstrated in transformed human cells in culture (Jee *et al.*, 1998; Radhakrishna Pillai *et al.*, 2004) and may a consequence of its capacity to induce apoptosis. Curcumin has been demonstrated to induce phase 2 enzymes (Dinkova-Kostova and Talalay, 1999; Lin and Lin-Shiau, 2001) and specifically inhibit COX-2 expression in HT-29 cells (Goel *et al.*, 2001) both of which have been implicated in the induction of apoptosis. The role of phase 2 enzymes in the induction of apoptosis is thought to be distinct from that associated with enhanced detoxification of carcinogenic compounds (Kirlin *et al.*, 1999) but is yet to be elucidated. The inhibition of COX-2 however, alters prostaglandin production and leads to an increase in arachidonic acid which stimulates the conversion of sphingomyelin to pro-apoptotic ceramide (Janne and Mayer, 2000; Taraphdar *et al.*, 2001).

Comparison of the trend lines (Figure 4.8a & b) as well as cell viabilities of toxin treated cells and toxin and curcumin co-treated cells (Table 4.1) shows that the cytotoxic effects of DON and DFB₁ as well as the proliferative activity of FB₁, although still dose dependent, appeared significantly reduced in the presence of curcumin.

Curcumin has been demonstrated to possess potent antioxidant properties (Sharma *et al.*, 2001a) and DON has been implicated in lipid peroxidation (Garaleviciene, 2003; Marciniak *et al.*, 2003) in addition to protein synthesis inhibition (Rotter *et al.*, 1996). Consequently, this may account for the reduced cytotoxic effect of this mycotoxin in the presence of this compound. In addition, curcumin inhibits COX-2 expression and stimulates the conversion of sphingomyelin to pro-apoptotic ceramide. This may be responsible for the reduced proliferation of FB₁ as FB₁'s proliferative activity has been reported to be a possible consequence of its ability to inhibit ceramide synthase and cause decreased ceramide formation and accumulation of sphingoid bases (Schroeder *et al.*, 1994).

Table 4.1: Comparison of cell viabilities following treatment with the toxins individually and in combination with curcumin: [Significant difference from individual toxin treatment: * (p<0.05) and ** (p<0.01)].

Toxin	Concentration	Cell Viabilities	
		Individually Treated	Co-treated with Curcumin
DON	5µM	95.78%	94.43%
	10µM	86.25%	103.11%**
	25µM	72.34%	72.18%
	50µM	59.84%	82.46%**
FB ₁	5µM	131.89%	97.17%*
	10µM	188.03%	107.34%**
	25µM	211.80%	113.70%**
	50µM	171.30%	115.56%**
DFB ₁	5µM	92.61%	93.17%
	10µM	90.34%	92.18%
	25µM	85.13%	78.80%*
	50µM	61.17%	83.50%*

The cytoprotective effect of curcumin appeared to be effective for all concentrations of FB₁, the 50µM concentration of DON and the 25µM and 50µM concentrations of DFB₁. Its protective effect at a lower concentration of DFB₁ and not DON may be a consequence of the reduced cytotoxicity of the DON mycotoxin in the presence of FB₁.

4.4 CONCLUSION

In conclusion, DON appears to exhibit a time and dose dependent cytotoxic effect in contrast to FB₁ which elicits a dose dependent mitogenic response on the HT-29 cell line. Combination treatment of DON and FB₁ (DFB₁) exhibited a time and dose dependent effect that was similar to that of DON but was reduced and this may be a result of the proliferative effect of FB₁. Curcumin (50µM) appeared to reduce the cytotoxicity of DON and DFB₁ as well as the proliferative activity of FB₁.

The MTT assay is a fast and efficient colorimetric assay well suited for the screening of mycotoxin cytotoxicity as it allows the examination of a large number of variables such as mycotoxins, concentrations, cells and exposure times. In addition, the rapid and objective data analysis obtained by measuring the optical density of formazan with multiwell scanning plate readers is a point of particular interest as it provides a simple, automated and highly efficient method for the characterisation of cytotoxicity.

CHAPTER 5

AN ASSESSMENT OF THE GENOTOXIC EFFECTS OF FUMONISIN B₁ AND DEOXYNIVALENOL ON THE HT-29 CELL LINE

5.1 INTRODUCTION

5.1.1 GENOTOXICITY

Increased incidence of DNA damage is a contributing feature in many pathological conditions. The most common example of this is the initiation of carcinogenesis as a consequence of mutations in the DNA. In addition, increases in cellular DNA damage have been demonstrated to precede or correspond with higher order cellular effects such as cell cycle arrest, or the induction of apoptosis, and in whole test organisms, reduced growth, abnormal development, and reduced survival (DNA Damage Monitoring, 2002).

Mycotoxins have been shown to be involved in DNA damage manifesting in the form of base alterations, adduct formation, strand breaks, and cross linkages (Wang and Groopman, 1999). The most prevalent type of genetic damage is the DNA single strand break which may be introduced directly by genotoxic compounds, through the induction of apoptosis or necrosis, secondarily through the interaction with oxygen radicals or other reactive intermediates, or as a consequence of excision repair enzymes (Lee and Steinert, 2003). A number of techniques for detecting DNA damage have been developed to identify substances with genotoxic activity.

The most frequently reported methods involve the detection of DNA repair synthesis (so-called unscheduled DNA synthesis (UDS) in individual cells, a technique based on the replication of DNA during the excision repair of certain types of DNA lesions as demonstrated by the incorporation of tritiated thymidine into the DNA repair sites or the alkaline elution assay which allows detection of DNA SSB (DNA single-strand breaks) and ALS (alkali labile sites) in pooled cell populations. The UDS technique provides information at the level of the individual cell but is technically cumbersome, requires the use of radioactivity and is limited in sensitivity while the alkaline elution assay ignores the critical importance of intracellular differences in DNA damage and requires relatively large numbers of cells (Tice *et al.*, 2000). A more useful approach for assessing genotoxicity, as evidenced by breaks in nuclear DNA, is the single cell gel electrophoresis (SCGE) or comet assay.

5.1.2 THE SINGLE CELL GEL ELECTROPHORESIS (SCGE) ASSAY

The single cell gel electrophoresis (SCGE) or comet assay is a simple, sensitive, and versatile method for the detection of DNA damage in individual cells. This assay can be applied to cells collected from virtually any eukaryotic organism, and can be used to detect DNA damage resulting from exposure to a broad spectrum of genotoxic and cytotoxic compounds *in vitro*, *in vivo*, as well as *in situ*.

Eukaryotic DNA molecules are several centimeters in length and are tightly condensed for accommodation within the confines of the 5-10 μ m wide nucleus. The SCGE assay is based on the principle that breaks in the negatively charged DNA strands damage this tightly-packed structure of DNA creating fragments or supercoiled DNA-loops that will migrate outside the region of the nucleus towards the anode in an electric field when embedded in an agarose gel. The result is a characteristic comet formation which can be then be visualised with a fluorescent DNA stain (Nelms *et al.*, 1997).

Two versions of the SCGE assay exist which are based on variation of the pH conditions (Bauch *et al.*, 1999). The original version developed by Ostling and Johansson (1984) involved the electrophoresis of cells under neutral conditions which does not induce denaturation and consequently only allows for the detection of double-strand damage. In contrast, the modified version developed by Singh *et al.* (1988), involved the electrophoresis of cells under alkaline conditions ($\text{pH} > 13$) which facilitates the unwinding and denaturation of the DNA molecules thus allowing for the sensitive detection of single-strand damage. The alkaline technique is capable of detecting DNA SSB, ALS, DNA-DNA/DNA-protein cross-linking as well as the SSB associated with incomplete excision repair sites and offers more sensitivity for identifying genotoxic agents as almost all genotoxic agents induce more SSB and/or ALS than double strand breaks (DSB) (Tice *et al.*, 2000).

Under both neutral and alkaline conditions, DNA damage is visualised by the characteristic comet shape formed as a result of the migration of genetic material from the nucleus towards the anode (Hellman *et al.*, 1997). Each comet consists of a "head" region, which represents DNA that does not migrate outside the region of the nucleus, and the "tail", which represents DNA migrating out of the nucleus due to fragmentation and loss of structure (Nelms *et al.*, 1997).

The length of the migration is generally believed to be directly related to fragment size and would be expected to be proportional to the level of SSB and ALS and inversely proportional to the extent of DNA cross-linking and can be quantified either manually or by computerised image analysis allowing indirect measurement of the number of DNA breaks at the single-cell level (Tice *et al.*, 2000; Giovannelli *et al.*, 2002). The latter technique offers considerable advantages as it is less subjective and allows rapid analysis of a large number of cells (Hellman *et al.*, 1997).

5.1.3 DETECTION OF APOPTOSIS USING THE SCGE ASSAY

Increased DNA migration has been established to accompany the DNA fragmentation associated with cytotoxicity arising through apoptosis as well as necrosis as both modes of death result in the excessive formation of double strand breaks. Cell undergoing apoptosis and necrosis can however be distinguished from each other based on the characteristic appearance of the comets produced under alkaline electrophoretic conditions.

Massive fragmentation of cellular DNA makes apoptotic cells easy to distinguish, as almost the entire volume of DNA migrates outside the nucleus resulting in the comet exhibiting a small head and a large fan-like tail (Figure 5.1c) in contrast to healthy cells in which most of the DNA remains in the nucleus with very little migration in the electric field outside of the cell (Figure 5.1a). Necrotic cells have been demonstrated to form comets with relatively large heads and narrow tails of varying lengths (Figure 5.1b) (Tice *et al.*, 2000).

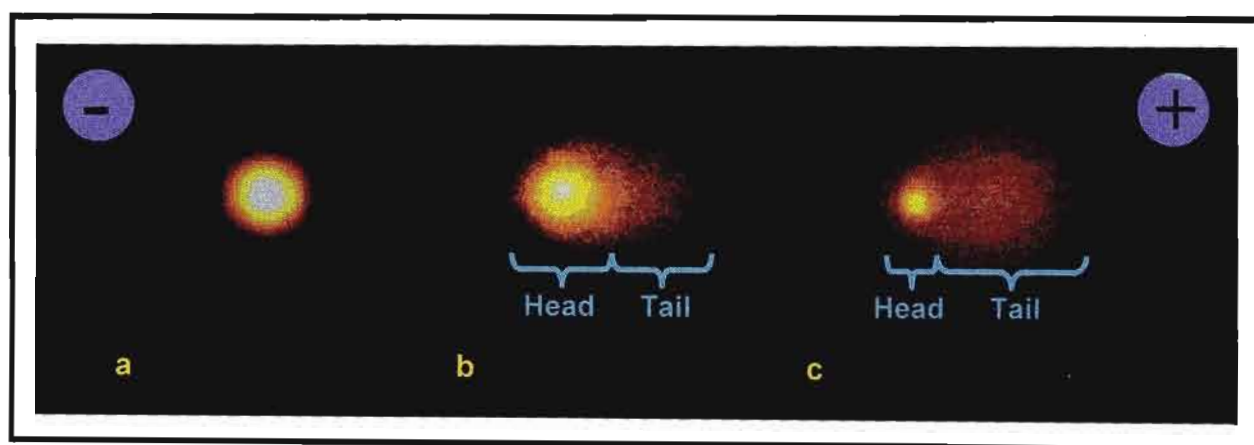


Figure 5.1: An illustration of typical comets produced by (a) healthy, (b) necrotic and (c) apoptotic cells following electrophoresis (Krebsfaenger, 2001).

The SCGE assay provides a simple method to measure the fragmentation of cellular DNA in individual cells and allows analyses of the biological changes induced by apoptosis as well as necrosis (Nelms *et al.*, 1997; Tice *et al.*, 2000).

The aim of this study was to investigate the genotoxic or DNA damaging effects of the mycotoxins DON and FB₁, as well as the mixture DFB₁, individually as well as in combination with curcumin (50µM), on the HT-29 cell line.

5.2 METHODS AND MATERIALS

5.2.1 MATERIALS

Low melting point agar, ethidium bromide (EtBr), ethylenediaminetetracetic acid (EDTA), sodium chloride (NaCl), sodium hydroxide (NaOH), disodium EDTA, Tris and Triton X were purchased from Sigma Aldrich (Johannesburg, SA). Dimethylsulfoxide (DMSO) was purchased from Merck (Johannesburg, SA) and microscope slides and coverslips (22mm X 50mm) were purchased from Lasec Laboratory Services (KwaZulu Natal, SA).

5.2.2 METHODS

5.2.2.1 Dilutions and Treatments

Stock solutions of DON and FB₁ were made up at concentrations of 20µM (18ml) and 200µM (18ml) for both toxins. A stock solution of 100µM curcumin (27ml) was also prepared. As per the solutions made up for the MTT assay, both DON and curcumin were solubilised in EtOH. The final concentration of EtOH in these dilutions was approximately 0.08%. To negate the effects of EtOH in this experiment, a 0.08% EtOH control was also prepared

An aliquot of the 20µM DON solution (9ml) was then combined with an equal quantity of the 20µM FB₁ solution to formulate a 10µM DFB₁ stock solution (18ml). The same was done with the 200µM stock solutions so as to produce a 100µM DFB₁ stock solution (18ml). The remaining 20µM and 200µM stock solutions of DON and FB₁ were then further diluted with CCM to halve the concentrations. The EtOH control was also similarly diluted.

The HT-29 cells (3ml suspension) were aliquoted into each well of three 6 well plates and incubated until the cells formed a confluent monolayer. The media was then aspirated and the cells treated as indicated below.

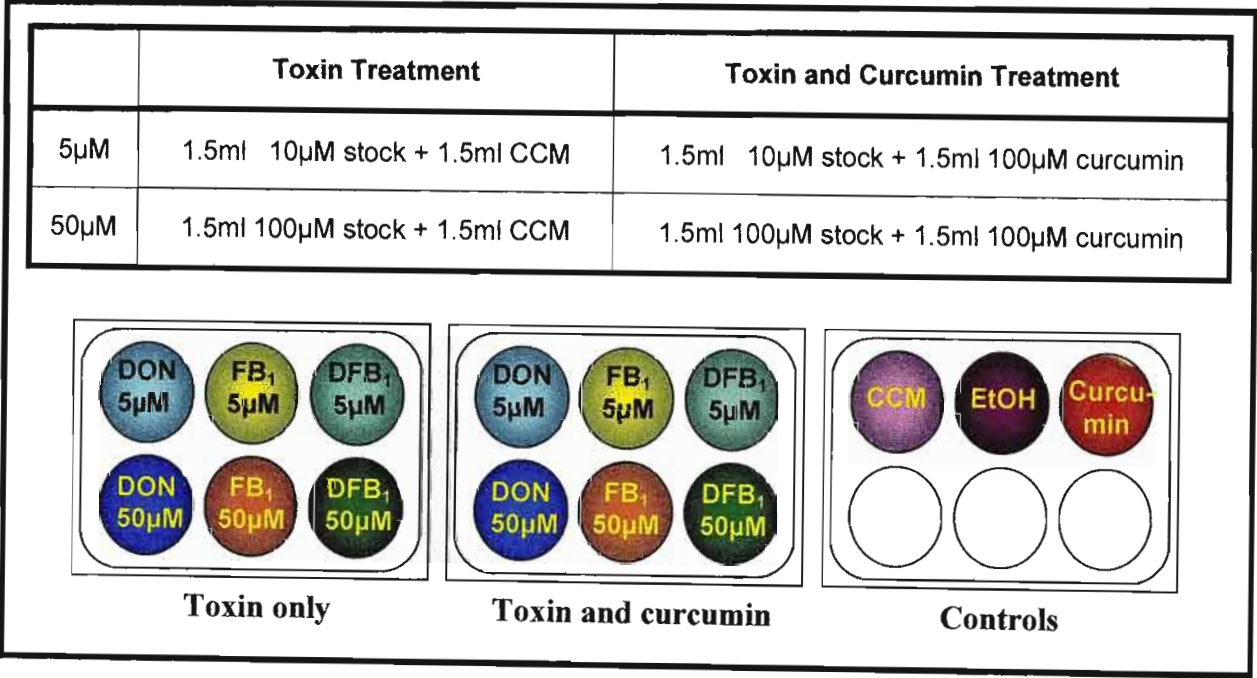


Figure 5.2: An illustration elucidating the treatment procedure for the SCGE assay.

The ethanol control consisted of 1.5ml EtOH (0.08%) and 1.5ml CCM. This ethanol content in this solution was approximately 0.04% which was the highest concentration of ethanol the cells were exposed to. The curcumin control consisted of 1.5ml curcumin (100µM) and 1.5ml CCM and the CCM or untreated control was made up of 3ml of CCM only. The plates were then incubated at 37°C for 48 hours. This assay was performed in triplicate.

5.2.2.2 Slide Preparation

Microscope slides were labelled and precoated with 1% low melting point agarose (LMPA) (Appendix 2.2) to increase gel stability. Coating was achieved by placing each slide in a vertical staining jar containing melted agarose, draining off the excess and wiping the back clean prior to drying in a warm oven (60°C for 4 hours). These were prepared a day in advance and stored at room temperature.

Following 48 hours incubation in cell culture environment, the treated cells in each well were trypsinised and resuspended in 1ml CCM. Cell suspensions (50µl) were aliquoted into labelled eppendorfs and molten 0.5% LMPA (Appendix 2.2; 500µl) at 37°C was added. This agarose-cell suspension mixture (250µl) was then pipetted onto a corresponding labeled precoated microscope slide, covered with a coverslip and stored at 4°C for 30 minutes to solidify.

This technique of slide preparation (Figure 5.3) facilitated the formation of uniform gels sufficiently stable to remain anchored during the lysis, electrophoresis and neutralizing stages and ensured easily visualised comets.

5.2.2.3 Cell Lysis

The coverslips were carefully removed from the slides and the slides were placed in a trough into which freshly prepared ice cold lysing solution (Appendix 2.2) was carefully decanted until all slides were completely immersed (Figure 5.3). They were then stored at 4°C for 1 hour. This lysing solution is chilled to maintain the stability of the agarose (Tice *et al.*, 2000) and contains high concentrations of NaCl and the detergent Triton X-100. This facilitates cell lysis and DNA liberation by removing cytoplasm and most nuclear proteins and leaving the DNA in a supercoiled form as nucleoids (Collins *et al.*, 2001). At the conclusion of the 1 hour period the lysing solution was carefully aspirated from the trough so as not to dislodge the agarose gel.

5.2.2.4 Alkali Unwinding and Electrophoresis

The procedure described by Singh *et al.* (1988) was followed. After the lysis step the slides were removed from the trough and placed in the electrophoresis tank with the ends of the gels facing the anode. The tank was then carefully filled with freshly prepared alkaline buffer (pH 13) (Appendix 2.2) to a level of approximately 0.5 cm above the slides. The slides were allowed to rest in the electrophoresis buffer for approximately 20 minutes prior to electrophoresis (Figure 5.3).

The purpose of this was to disrupt the hydrogen bonds between double stranded DNA thereby facilitating the unwinding and denaturation of the DNA molecules to produce single-stranded DNA. In addition this pH maximises the expression of alkali-labile sites as single strand breaks thus allowing for the sensitive detection of single strand damage (Nelms *et al.*, 1997; Tice *et al.*, 2000). Electrophoresis was then conducted using a BioRad compact power supplier for 20 minutes at 25V and 300mA to allow the migration to occur in a controlled manner. These steps were performed in dim light to prevent additional DNA damage.

5.2.2.5 Neutralisation and Staining

Following electrophoresis, the slides were carefully removed from the tank and placed in a clean trough into which 0.4M Tris (Appendix 2.2) was then carefully decanted. The slides were allowed to rest in this buffer for 5 minutes before the solution was removed from the trough with a syringe so as not to disturb the agarose gels. This rinsing procedure was performed in triplicate and served to neutralise the alkali in the gels as well as remove detergents which would interfere with the EtBr staining. Each slide was then removed from the trough and the excess buffer drained off onto laboratory tissue paper. They were then stained by the addition of 50µl of EtBr solution (20µg/ml) prior to being coverslipped (Nelms *et al.*, 1997).

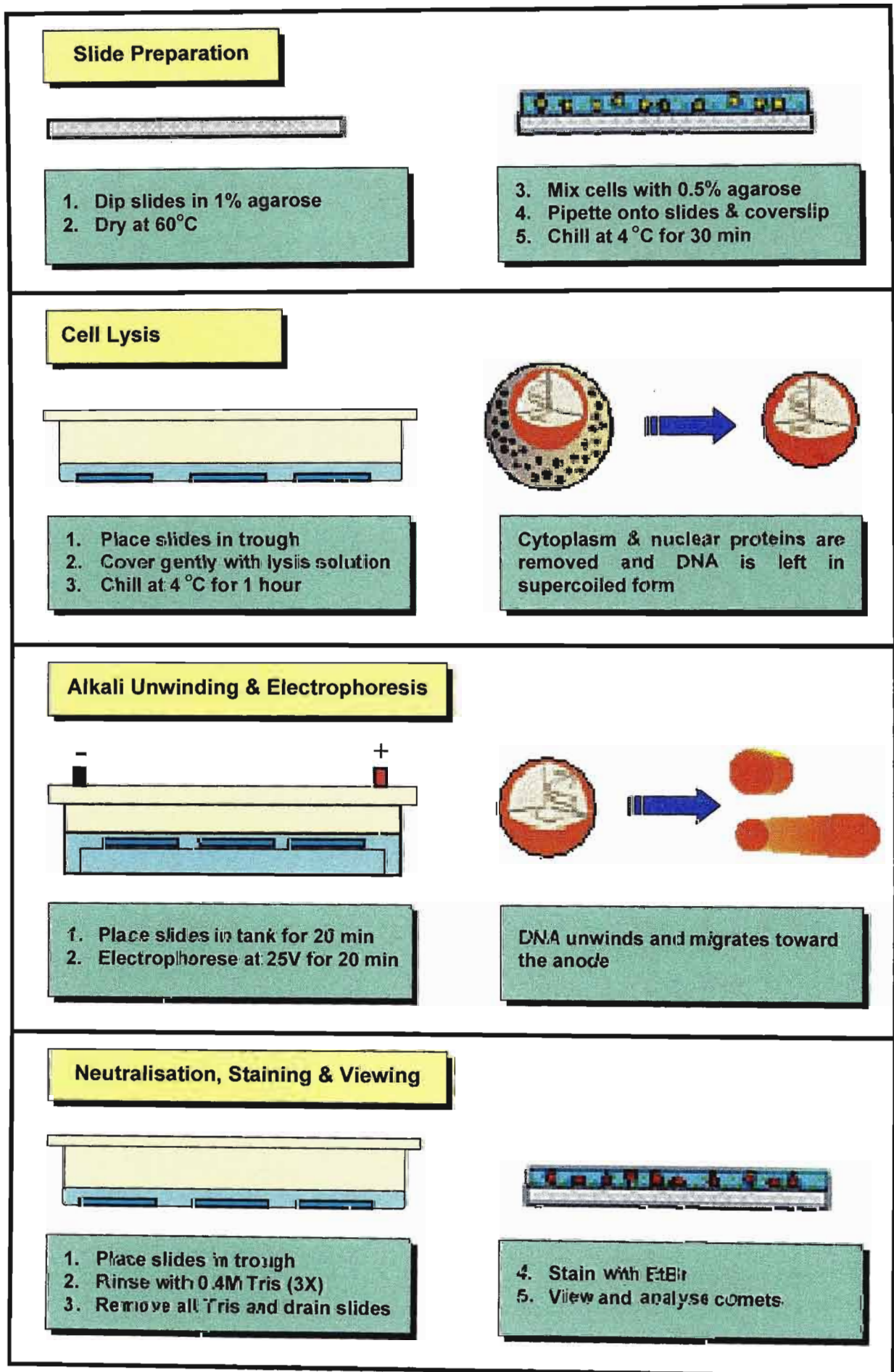


Figure 5.3: The principal steps of the alkaline comet assay (Krause *et al.*, 2001).

5.2.2.6 Image Analysis

Observation of slides was conducted using the Olympus X130 inverted tissue culture microscope using an excitation filter of 450-490nm and a barrier filter of 520nm. Images of single cells were captured at 100x magnification and analysed using Scion image software. DNA migration lengths were determined by measuring the nuclear DNA and the migrating DNA in 25 randomly selected cells (5 cells per 5 random fields).

The data was analysed on Microsoft Excel using either the Students t-test to determine significant differences between the tail lengths of treated and control cells or a one-way analysis of variance (ANOVA) to determine significant differences between the tail lengths at each toxin concentrations as well as between different toxins at similar concentrations. After application of ANOVA, the significance of differences in the tail lengths between the treatment groups was evaluated by multiple comparisons using the Bonferroni method. Differences were considered statistically significant at $p < 0.05$ and highly significant at $p < 0.01$.

5.3 RESULTS AND DISCUSSION

The results of the SCGE assay are illustrated in Figures 5.4 to 5.8. Statistical analysis indicated that there were overall significant differences between the effects of the toxin treated cells and their respective controls ($p < 0.001$) as well as between various concentrations of each toxin individually ($p < 0.001$) and in the presence of curcumin ($p < 0.001$).

5.3.1 THE EFFECT OF ETHANOL

The results of the SCGE assay showed that the untreated and ethanol (0.08%) treated cells (Figure 5.4a & b) retained their spherical shape and size, indicating that the DNA was still tightly packed within the nucleus.

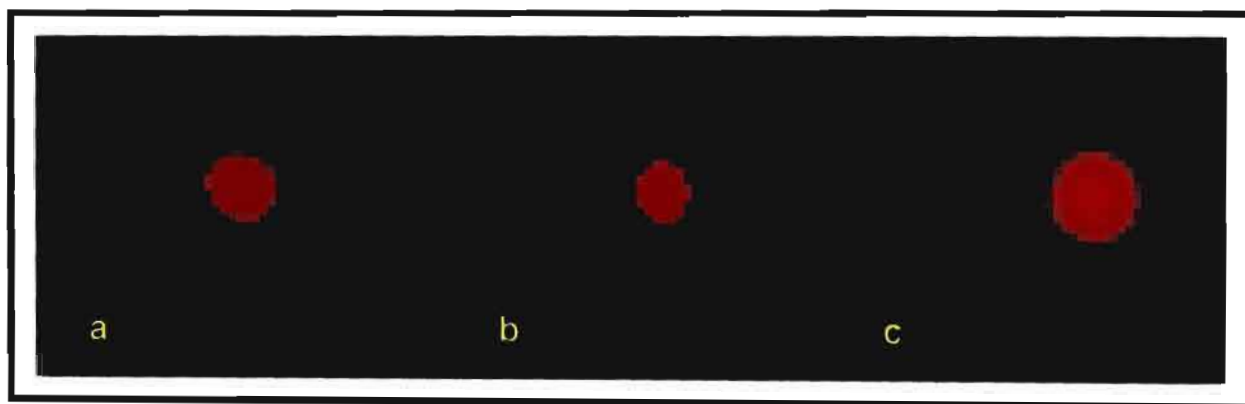


Figure 5.4: Photomicrographs illustrating tail lengths observed for: (a) untreated, (b) ethanol (0.08%) treated and (c) curcumin treated cells (X100).

This result demonstrates that ethanol (0.08%) exhibited little effect on DNA damage at the concentration used and advocates that the DNA damage noted hereafter is due to the action of the test agents and not the carrier solvent.

5.3.2 THE EFFECT OF CURCUMIN

Curcumin (50 μ M) treated HT-29 cells (Figure 5.4c) displayed relatively large nuclei and short tails indicating that this chemopreventive agent induces DNA fragmentation. The analysis of DNA migration showed that tail length was approximately 0.122 μ m. This result is in keeping with a study conducted by Blasiak *et al.* (1999) who established that curcumin damages DNA of gastric mucosal cells at concentrations ranging from 10 μ M to 50 μ M in a dose-dependent manner.

The determination that curcumin is capable of binding to DNA and causing DNA degradation in the presence of copper (Cu) was made by Ahsan *et al.* (1999). This is an essential trace element present in chromatin that exists in the oxidation states Cu(I) and Cu(II) under physiological conditions (O'Connor, 2001).

Ahsan *et al.* (1999) established that DNA cleavage occurred through the generation of reactive oxygen species (ROS), such as the hydroxyl radical (OH^\cdot) and hydrogen peroxide (H_2O_2) by means of the curcumin-Cu(II) system. In this system curcumin generates superoxide anion (O_2^\cdot) that reacts with Cu(II) to form Cu(I) and leads to the formation of H_2O_2 . The Cu(I) subsequently reacts with H_2O_2 that is available exogenously or formed by endogenous metabolism and results in the generation of the more reactive and toxic OH^\cdot radical.

Although the precise mode of action of curcumin remains elusive, studies have shown that its chemopreventive action might be due to its ability to induce apoptosis in cancer cells as this polyphenolic, hydrophobic compound, can diffuse easily into the cytosol, triggering specific apoptotic events (Bhaumik *et al.*, 1999). Curcumin has been demonstrated to inhibit COX-2 expression (Goel *et al.*, 2001) resulting in the alteration of prostaglandin production and leading to an increase in arachidonic acid which stimulates the conversion of sphingomyelin to ceramide, a pro-apoptotic sphingolipid (Taraphdar *et al.*, 2001) and has been shown to induce DNA damage in a concentration and time-dependent manner resulting in the appearance of cellular features characteristic of apoptosis (Scott and Loo, 2004). The possibility of ceramide acting as a mediator in the genotoxic response has been suggested (Yang and Duerksen-Hughes, 2001).

The involvement of ROS in curcumin-mediated apoptosis has been reported previously and may be attributed to the ability of ROS to cause damage in most biomolecules including DNA, protein and lipid membrane. In addition, superoxide may react with nitric oxide to yield peroxynitrite, a more powerful and damaging oxidant than either of the two.

Thus ROS could also play an important role in the antitumour events leading to apoptotic tumour cell death (Bhaumik *et al.*, 1999). This contradicts previous reports of the antioxidant properties of curcumin which also accounts for the chemopreventive action of this compound since ROS have been implicated in the development of various pathological conditions (Chattopadhyay *et al.*, 2004). The contrasting properties of curcumin appear to be cell type specific.

The fragmentation of DNA observed may thus be related to the apoptosis inducing ability of curcumin as a result of its pro-oxidant activity as well as its ability to inhibit COX-2 expression.

5.3.3 THE EFFECT OF DEOXYNIVALENOL

5.3.3.1 The Effect of Deoxynivalenol Only

Exposure to DON also appeared to result in DNA damage in HT-29 cells at both the 5 μ M and 50 μ M concentrations (Figure 5.5a & b).

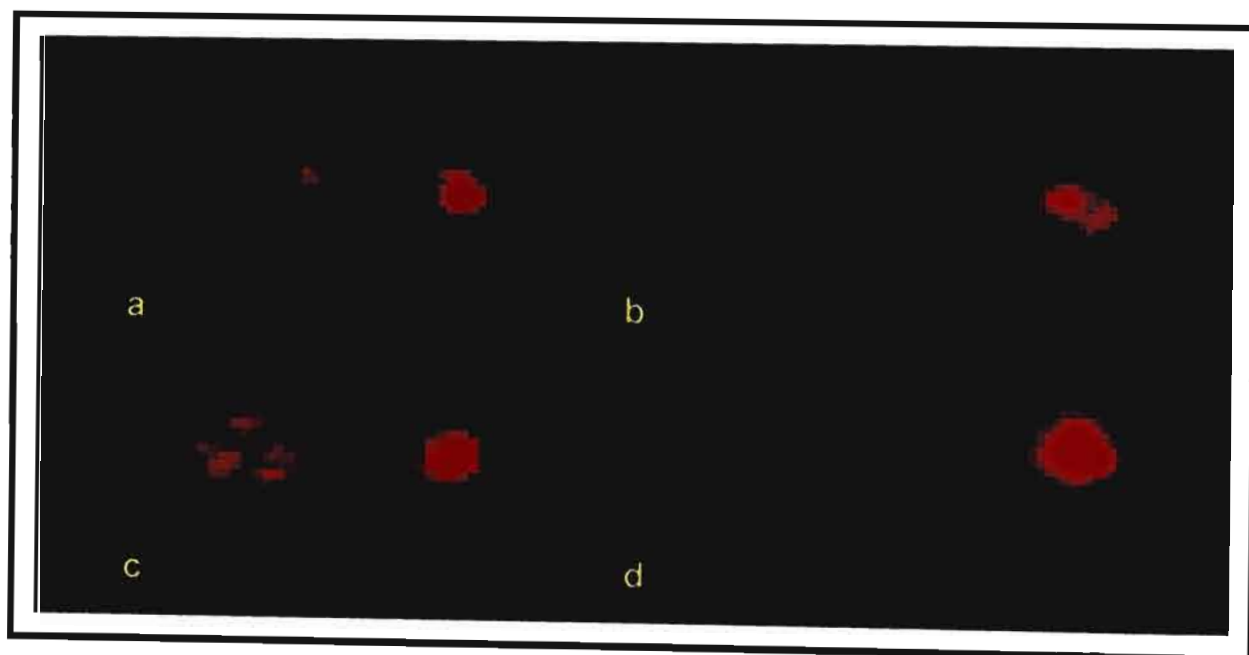


Figure 5.5: Photomicrographs illustrating tail lengths observed for cells treated with: (a) DON (5 μ M), (b) DON (50 μ M), (c) DON (5 μ M) and curcumin and (d) DON (50 μ M) and curcumin (X100).

Analysis of comets indicated a significant increase in tail length from 0.163 to 0.223 μm (Figure 5.8; $p < 0.001$) with increasing concentration. The comets exhibited a shape characteristic of apoptosis with a large fanlike tail and a small head, although at the 50 μM concentration, the head appeared fragmented. The ability of DON to induce apoptosis has been previously reported in human T-cells (Pestka *et al.*, 1999) as well as the K562 erythroleukaemia cell line (Minervini *et al.*, 2004) and has been reported to be a consequence of its ability to inhibit translation at the cellular level (Rotter *et al.*, 1996).

In addition DON has been demonstrated to be an inducer of COX-2 (Moon and Pestka, 2002) and COX-2 activity has been demonstrated to be associated with the formation of malondialdehyde (MDA), a by-product of lipid peroxidation (Sharma *et al.*, 2001b) in colon cells. Lipid peroxidation is a manifestation of cell damage that facilitates the transformation and degradation of membrane polyunsaturated fatty acids to hydroperoxides and low molecular species respectively (Garaleviciene, 2003; Marciniak *et al.*, 2003). Malondialdehyde is an indicator of free radical activity that is known to be mutagenic and carcinogenic, reacting with DNA to form adducts to deoxyguanosine and deoxyadenosine (Marnett, 1999). Consequently, the DNA fragmentation observed may be due to the release of free radicals and reaction products related to this process (Knasmüller *et al.*, 1997). It can be said therefore that this result indicates a significant DNA damaging effect that increased at the higher concentration and may be correlated to the severity of apoptosis induced by this compound.

5.3.3.2 The Effect of Deoxynivalenol Following Co-treatment With Curcumin

Co-treatment with curcumin appeared to increase the genotoxic effect of DON. Tail length for the DON and curcumin treatments (Figure 5.5c & d) significantly increased to 0.3 and 0.531 μm from 0.163 to 0.223 μm (Figure 5.8; $p < 0.001$) when compared to the DON only (5 μM and 50 μM) treated cells (Figure 5.5a & b).

The 5 μ M DON and curcumin treated cells retained their apoptotic appearance while the 50 μ M toxin and curcumin treated cells appeared necrotic with a large head and long tail. This occurrence may be a result of secondary necrosis, an event involving the breakdown of plasma membrane and intracellular organelles that is incited if apoptotic bodies are not quickly removed by phagocytes or neighbouring cells (Toescu, 2003). As discussed previously, curcumin is able to inhibit COX-2 expression which can stimulate the conversion of sphingomyelin to ceramide thus mediating the genotoxic response. The DNA damage observed may thus be a result of a synergism between DON and curcumin as a result of DON's involvement in COX-2 expression and lipid peroxidation and curcumin's involvement in the inhibition of COX-2 expression and its pro-oxidant activity.

5.3.4 THE EFFECT OF FUMONISIN B₁

5.3.4.1 The Effect of Fumonisin B₁ Only

The HT-29 cells displayed DNA damage following exposure to both toxin concentrations. Considerable DNA fragmentation was observed following exposure to the 5 μ M FB₁ concentration (Figure 5.6a) with the cells forming comets with a small head and long fan-shaped tail (0.207 μ m) characteristic of apoptosis. Cells exposed to 50 μ M FB₁ concentration (Figure 5.6b) appeared to exhibit significantly less fragmentation (Figure 5.8; $p < 0.001$) with a shorter tail (0.146 μ m) and large head. This is in agreement with the results achieved by Schmelz *et al.* (1998) who demonstrated significant DNA fragmentation in HT-29 cells following exposure to 10 μ M FB₁ which decreased following exposure to 50 μ M FB₁. Mobio *et al.* (2000) also demonstrated major DNA fragmentation in C6 glioma cells with concentrations between 9 μ M and 18 μ M which was reduced at higher concentrations. This phenomenon has been suggested to be indicative of further DNA cleavage after cell death (Mobio *et al.*, 2000).

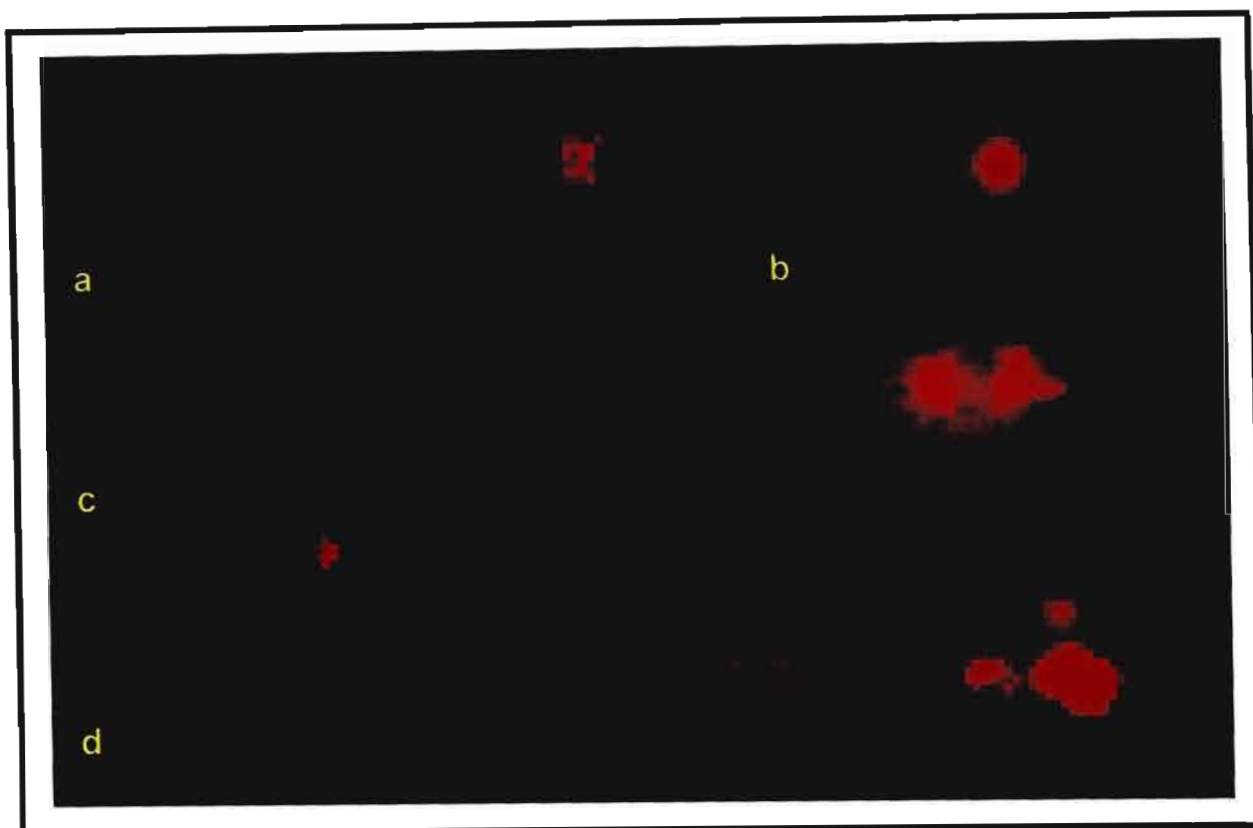


Figure 5.6: Photomicrographs illustrating tail lengths observed for cells treated with: (a) FB₁ (5μM), (b) FB₁ (50μM), (c) FB₁ (5μM) and curcumin and (d) FB₁ (50μM) and curcumin (X100).

The DNA damaging effect of FB₁ has been reported in a number of cell lines (Schmelz *et al.*, 1998; Galvano *et al.*, 2002a; Galvano *et al.*, 2002b) and has been attributed to its ability to inhibit ceramide synthase and disrupt sphingolipid metabolism. The inhibition of this enzyme induces a subsequent intracellular accumulation of biologically active sphingoid bases and the depletion of more complex sphingolipids such as ceramide which are believed to impair cellular signal transduction, cell proliferation and cell differentiation and induce DNA fragmentation and apoptosis (Merrill *et al.*, 1997; Schmelz *et al.*, 1998). This result is contradictory to the proliferative effect of this toxin noted in Chapter 4 but may be explained by the fact that, in contrast to necrotic cell death, cell membrane integrity and mitochondrial function are maintained until the apoptotic process is well advanced and although apoptosis is observed, the cells are very viable as measured by the MTT assay.

Fumonisin B₁ has also been implicated in lipid peroxidation, via the induction of increased malondialdehyde (MDA) production in culture (Abado-Becognee *et al.*, 1998; Mobio *et al.*, 2003) and as discussed previously, malondialdehyde is mutagenic and carcinogenic (Marnett, 1999). The DNA damage observed may thus also be a possible consequence of the release of damaging free radicals and reaction products of lipid peroxidation (Knasmuller *et al.*, 1997).

5.3.4.2 The Effect of Fumonisin B₁ Only Following Co-treatment With Curcumin

Co-treatment with curcumin appeared to enhance the genotoxic effect of FB₁ (Figure 5.6c & d). Tail length for the FB₁ and curcumin treatments significantly increased to 0.401 and 0.395 μm from 0.207 and 0.146 μm ($p < 0.001$) when compared to the FB₁ only (5 μM and 50 μM) treated cells (Figure 5.8).

This result indicated that the modest DNA fragmentation observed following treatment with 50 μM FB₁ increased considerably in the presence of curcumin. No significant differences were noted between the 5 μM and 50 μM concentrations of FB₁ following co-treatment with curcumin (Figure 5.8). The fragmented appearance of the comet heads may be indicative of an enhanced apoptotic effect due to the curcumin which stimulates the conversion of sphingomyelin to ceramide (Taraphdar *et al.*, 2001). In addition, as with DON, FB₁ has been implicated in lipid peroxidation and as such these results may also be an effect of a similar synergism between FB₁ and curcumin.

5.3.5 THE EFFECT OF A DEOXYNIVALENOL AND FUMONISIN B₁ MIXTURE

5.3.5.1 The Effect of a Deoxynivalenol and Fumonisin B₁ Mixture Only

Exposure to a mixture of the DON and FB₁ toxins appeared to exert a synergistic effect. The comets exhibited the small heads and fan-like tails characteristic of apoptosis (Figure 5.7a & b).

A significant increase ($p < 0.001$) in tail length was observed following treatment with $5\mu\text{M}$ ($0.289\mu\text{m}$) and $50\mu\text{M}$ ($0.386\mu\text{m}$) toxin mixture as compared to those observed following individual toxin treatment (Figure 5.8).

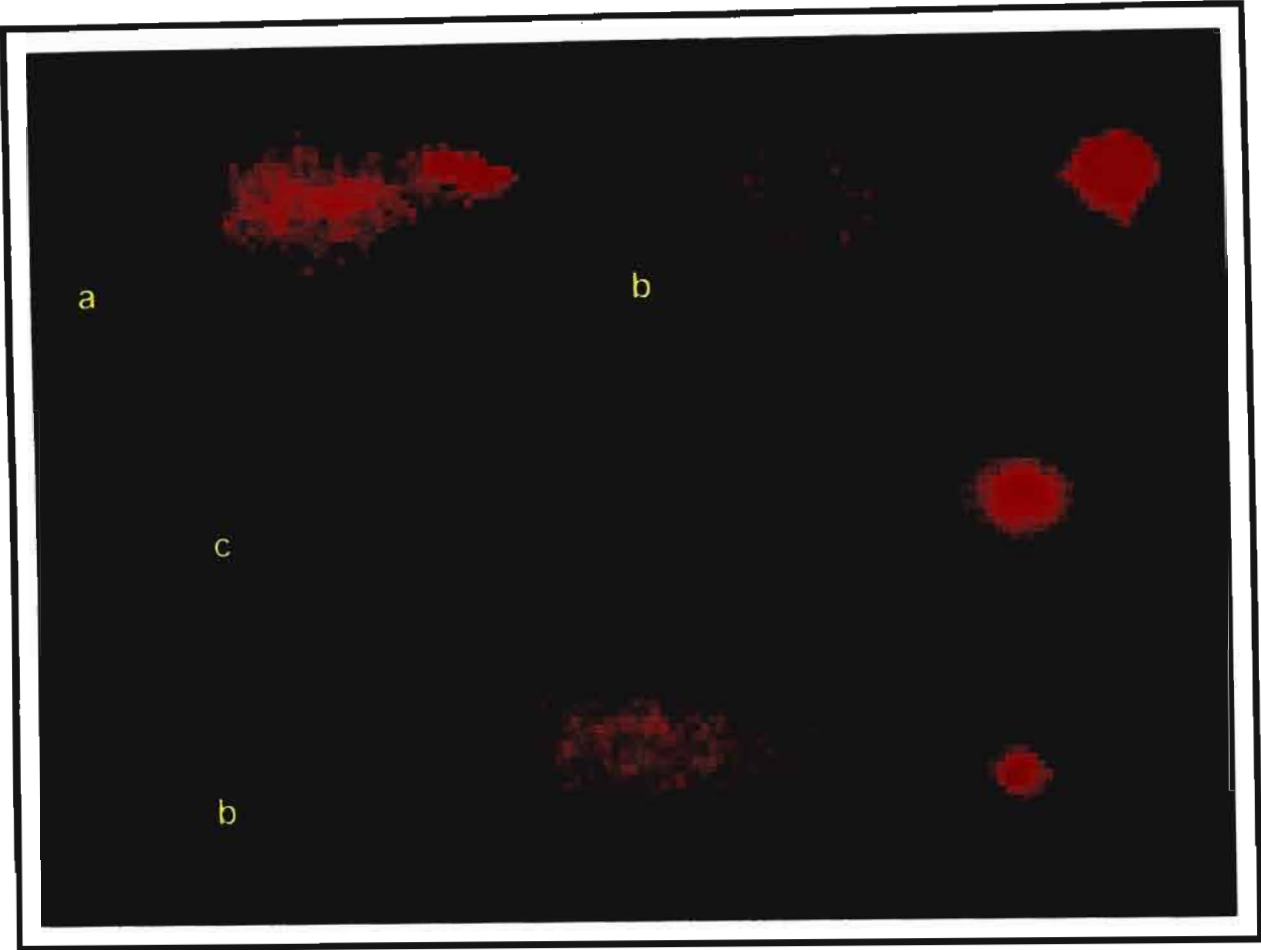


Figure 5.7: Photomicrographs illustrating tail lengths observed for cells following treatment with: (a) DFB₁ ($5\mu\text{M}$), (b) DFB₁ ($50\mu\text{M}$) (c) DFB₁ ($5\mu\text{M}$) and curcumin and (d) DFB₁ ($50\mu\text{M}$) and curcumin (X100).

The presence of DON appeared to increase the DNA fragmentation observed following treatment with $5\mu\text{M}$ FB₁. The increased DNA damage observed is a possible result of a synergism between these toxins as both have been implicated in lipid peroxidation resulting in the release of DNA damaging free radicals and reaction products. In addition FB₁, as discussed earlier, plays a role in sphingolipid metabolism resulting in the generation of the pro-apoptotic sphingolipid ceramide.

5.3.5.2 The Effect of a Deoxynivalenol and Fumonisin B₁ Mixture Following Co-treatment With Curcumin

As with the individual toxin treatments, following co-treatment with curcumin, the comet shape characteristic of apoptosis was maintained (Figure 5.7c & d). Genotoxicity appeared increased with tail length increasing to 0.528 and 0.607µm from 0.289 and 0.386 µm (Figure 5.8; p<0.001) for the 5µM and 50µM concentrations. The increased fragmentation observed following treatment with the toxin mixture and curcumin is a possible result of the accumulation of free radicals and other reaction products of lipid peroxidation in combination the reaction products formed as a result of curcumin’s pro-oxidant activity.

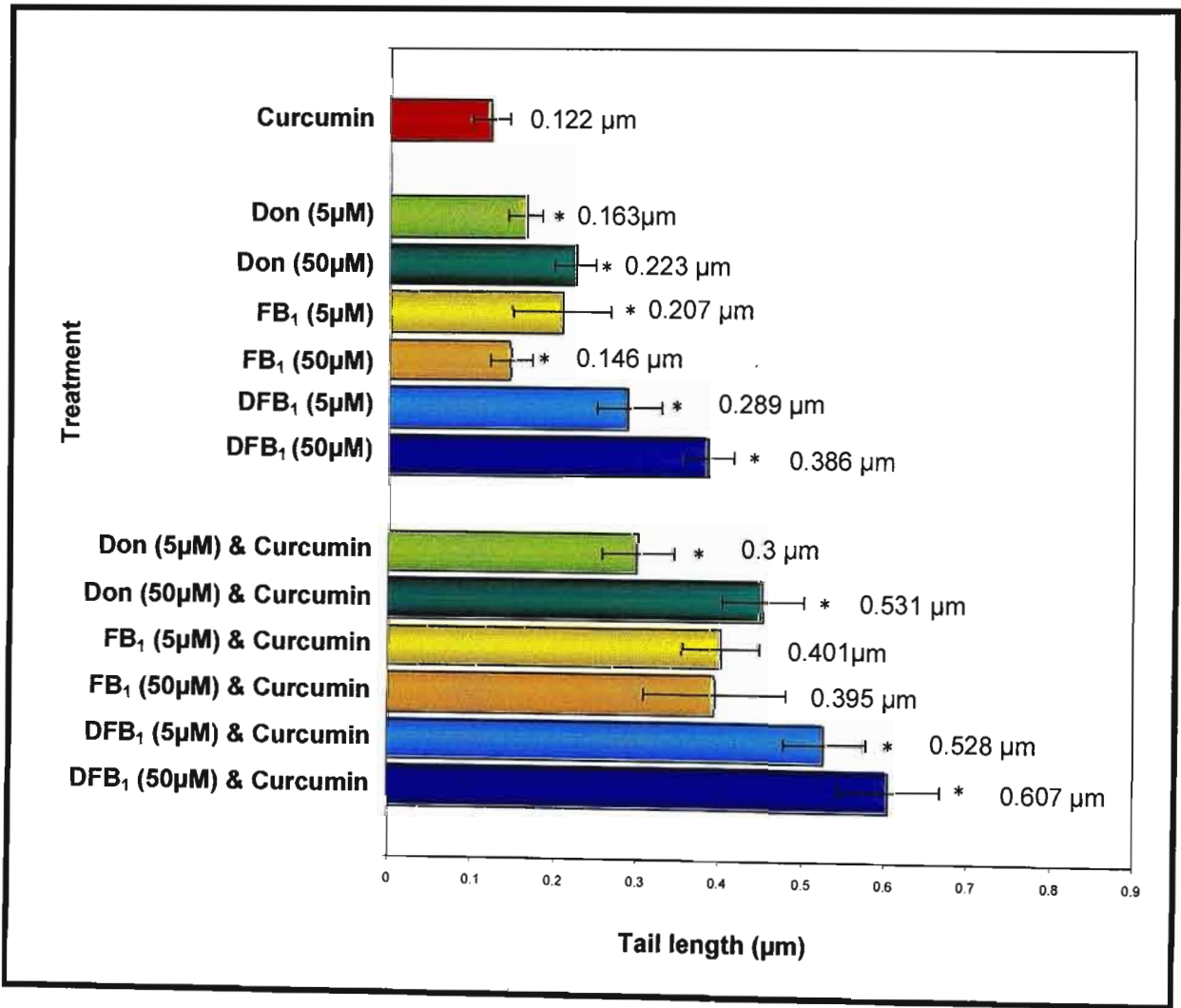


Figure 5.8: Graphical representation of tail lengths observed following electrophoresis:
[Significant difference between concentrations: * (p<0.01)].

5.4 CONCLUSION

The SCGE assay demonstrates sensitivity for detecting low levels of DNA damage and is an excellent method for the detection of DNA damage due to its flexibility, low cost and ease of application. It requires small numbers of cells per sample, relatively small amounts of test substance and a short time to complete a study. In addition, the SCGE assay is capable of detecting cell death by apoptosis due to its ability to detect double-stranded DNA breaks characteristic of apoptotic DNA fragmentation as well as single-stranded breaks and alkali-labile sites.

The results of this study demonstrated that both DON and FB₁ (5 μ M and 50 μ M) are able to cause DNA fragmentation in the HT-29 cell line. Deoxynivalenol increased DNA fragmentation at 50 μ M while FB₁ exhibited the opposite effect. Mixtures of both toxins exhibited greater fragmentation than the individual toxins and may be indicative of a potential synergism between these compounds. Curcumin was shown to also damage the DNA of these cells and the total effect of the toxins following individual (DON and FB₁) and combination (DFB₁) treatment, with curcumin proved to be additive.

CHAPTER 6

A STRUCTURAL INVESTIGATION INTO THE EFFECTS OF DEOXYNIVALENOL AND FUMONISIN B₁ ON THE HT-29 CELL LINE

6.1 INTRODUCTION

6.1.1 CELL MORPHOLOGY

The morphology of cells is a defining characteristic of apoptosis, a component of the development and health of multicellular organisms where cells die in response to a variety of stimuli in a controlled, regulated fashion. Upon receiving specific signals instructing the cells to undergo apoptosis, a number of distinctive biochemical and morphological changes occur in the cell. In the early stages, a family of proteins known as caspases are typically activated. These proteins cleave the key cellular substrates required for normal cellular function including structural proteins in the cytoskeleton and nuclear proteins such as DNA repair enzymes. The caspases can also activate other degradative enzymes such as DNases, which begin to cleave the DNA in the nucleus (Gewies, 2003).

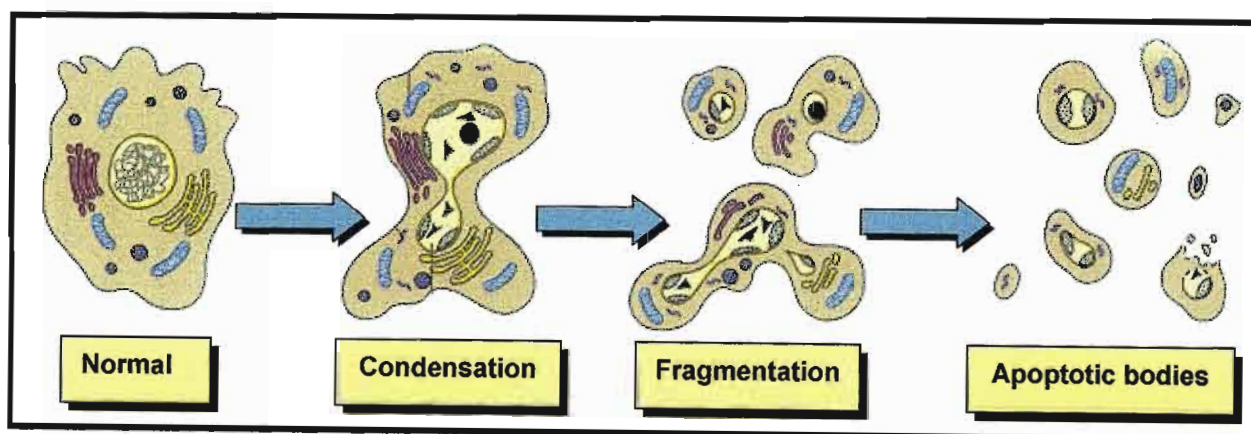


Figure 6.1: Morphological changes of apoptosis (Rode *et al.*, 2004).

The result of these biochemical changes is the appearance of morphological changes in the cell (Figure 6.1). These changes include cell shrinkage, chromatin margination, membrane blebbing, nuclear condensation, segmentation and division into apoptotic bodies (Gewies, 2003), all of which may be observed using light microscopy.

6.1.2 LIGHT MICROSCOPY

Microscopy has become increasingly important for analysis of cells and cell function in recent years due in large part to advances in light microscopy that facilitate quantitative studies and improve imaging of living cells. This microscopy technique is a powerful tool and a significant complement to other analysis techniques.

The light microscope is one of the most useful and often used types of microscopes available and although the limit of resolution and magnification capabilities are much less when compared to an electron microscope, its affordability, ease of use, and ability to perform several modes of microscopy principles make it a popular tool in most research laboratories. One mode of light microscopy that has gained increasing popularity is fluorescence microscopy.

6.1.3 FLUORESCENCE MICROSCOPY

Fluorescence microscopy exploits the ability of a specimen to selectively absorb radiation of short wavelength and re-emit it as characteristic longer wavelength radiation. It requires a powerful illumination source, usually a mercury lamp, and is used to detect fluorescent structures, molecules or proteins within cells (Kline, 1999). This fluorescence may be due to natural compounds such as botanical cell constituents like chlorophyll, pollen and cell walls (autofluorescence), certain DNA-binding dyes such as ethidium bromide and DAPI or highly specific, highly sensitive tags generated from fluorescent stains conjugated to the constant region of antibodies (immuno-fluorescence).

Radiation is generated by means of the mercury light source and the wavelength is adjusted to narrow bands by means of excitation or primary filters which eliminate those wavelengths above or below the required range. After this light has interacted with the specimen, a barrier or secondary filter is used to select the longer wavelengths that will participate in the image forming process (also blocking harmful UV radiation from reaching the eye). A longer wavelength is required because the electron in a given orbital rises to a higher energy level (the excited state) when fluorescent molecules absorb a specific absorption wavelength. Electrons in this state are unstable and will return to the ground state, releasing energy in the form of light and heat (fluorescence). This loss of energy results in radiation of a longer wavelength being emitted (Kline, 1999).

The barrier filter allows only the emitted wavelength to reach the eyepieces or camera port of the microscope resulting in the dyes glowing brightly against a dark background. Differences in the emission characteristics of the specimen features give rise to wavelength/colour differences in the image, thus generating contrast in the image.

The usefulness of this microscopy mode is illustrated by its routine use in a number of techniques, including imaging of fluorescent labelled proteins in living cells, single cell physiological experiments using fluorescent indicator probes and immuno-fluorescence localization of specific targets in tissues (Robinson *et al.*, 2001).

6.1.3.1 ACRIDINE ORANGE AND ETHIDIUM BROMIDE DIFFERENTIAL STAINING

Acridine orange is a membrane permeable vital stain that intercalates into the DNA of all cells causing the nuclei to exhibit green fluorescence at excitation and emission wavelengths 502nm and 526nm respectively. It also binds to RNA, but cannot intercalate so that the RNA fluoresces red-orange.

Ethidium bromide is membrane impermeable and intercalates into the DNA of cells with damaged cell membranes causing them to fluoresce orange at excitation and emission wavelengths of 510 and 595nm respectively. It is also able to bind weakly to RNA (Lauricella *et al.*, 2001). The similar excitation and emission wavelengths of these two stains permits the concomitant viewing of both and allows for the identification of viable, early apoptotic, late apoptotic and non-viable or necrotic cells based on morphology of the nuclei and uptake of stain.

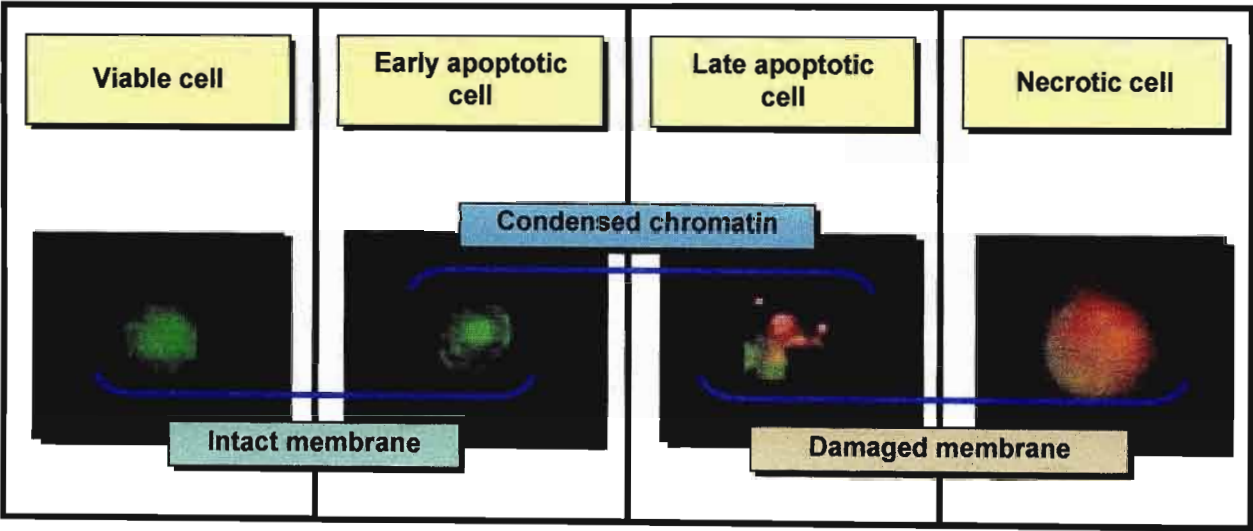


Figure 6.2: An illustration depicting the principle of acridine orange and ethidium bromide differential staining.

Viable cells (with an intact cell membrane) display normal nuclei with a homogeneous chromatin staining pattern and bright green fluorescence as opposed to the non-viable cells (damaged cell membrane) which display a diffuse orange staining pattern with a regular sized or increased nucleus as a result of EtBr infiltrating the cells and overwhelming the fluorescence of the acridine orange (Lauricella *et al.*, 2001). Cells in the early phase of the apoptotic death process generally demonstrate chromatin condensation and intact cell membranes and therefore retain their green fluorescence and exhibit condensed or shrunken nuclei. Those in the late phase display nuclear fragmentation and leaky cell membranes (Boersma *et al.*, 1996) and consequently present with fragmented nuclei and orange florescence (Lauricella *et al.*, 2001).

6.1.3.2 Hoechst 33258 Staining

Hoechst 33258 is a bisbenzimidazole DNA intercalator. This membrane permeant, crescent shaped molecule binds specifically to the Adenine–Thymine (A-T) base pairs in double stranded DNA with a minimum binding size of four consecutive A-T base pairs causing widening of the minor grooves (Teng *et al.*, 1988; Chen *et al.*, 1993). It is used with living, unfixed cells as a fluorescent cytological stain for DNA that fluoresces blue when excited by UV light. Its excitation and emission wavelengths are approximately 352 and 461nm respectively.

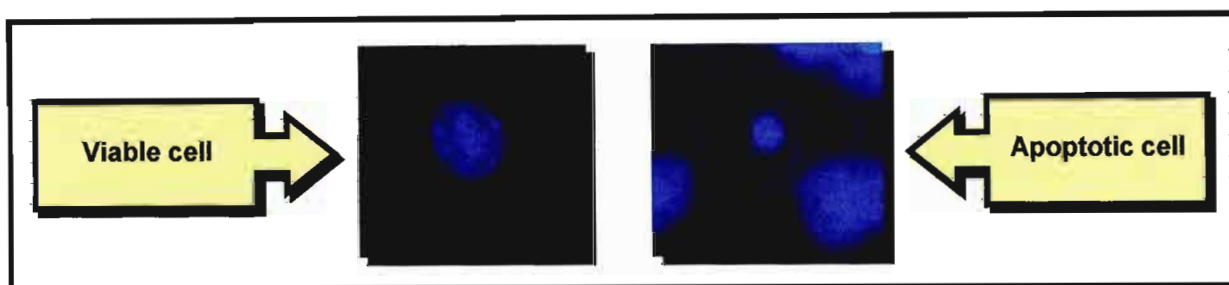


Figure 6.3: An illustration depicting the principle of Hoechst 33258 staining.

Exposure to Hoechst 33258 causes apoptotic cells to exhibit stronger blue fluorescence when compared to non-apoptotic cells as the nuclei of apoptotic cells have highly condensed chromatin that is uniformly stained by Hoechst 33342 in contrast to normal cells. This staining can take the form of crescents around the periphery of the nucleus, or the entire nucleus can appear to be one or a group of featureless, bright spherical beads.

The aim of this experiment was to identify the morphological characteristics of apoptosis that are usually accompanied by DNA fragmentation. This was to confirm the apoptotic inducing effects of DON, FB₁ and the toxin mixture DFB₁ on the HT-29 cell line individually and in combination with the chemopreventive agent curcumin (50μM).

6.2 METHODS AND MATERIALS

6.2.1 MATERIALS

Acridine orange (AcOr), ethidium bromide (EtBr), Hoechst 33258, paraformaldehyde (PFA), potassium chloride (KCl), potassium dihydrogen phosphate (KH_2PO_4) sodium chloride (NaCl) and sodium dihydrogen phosphate ($\text{NaH}_2\text{PO}_4 \cdot \text{H}_2\text{O}$) were purchased from Sigma Aldrich (Johannesburg, SA). Coverslips (20mm X 20mm), and 6 well plates were purchased from Adcock Ingram (Johannesburg, SA).

6.2.2 METHODS

6.2.2.1 Dilutions and Treatments

Stock solutions of DON, FB_1 , DFB_1 (10 μM and 100 μM), curcumin (100 μM) and EtOH (0.04%) were prepared as described in Chapter 5.

The HT-29 cells (3ml suspension) were seeded onto coverslips in each well of three 6 well plates and incubated until the cells formed a confluent monolayer. The media was then aspirated and the cells were treated in the same manner as in Chapter 5. Briefly, for each toxin treatment, 1.5ml of toxin dilution was added to a well with an equal volume of CCM to halve the concentration. A similar pattern was formed for toxin and curcumin treatments with 1.5ml of curcumin (100 μM) being added instead of CCM. The EtOH control consisted of 1.5ml EtOH (0.08%) and 1.5ml CCM. The curcumin control consisted of 1.5ml curcumin (100 μM) and 1.5ml CCM and the untreated CCM control was made up of 3ml of CCM only. The plates were then incubated at 37°C for 48 hours prior to staining.

This plating and treatment procedure was performed in duplicate to accommodate the two staining techniques used in this experiment.

6.2.2.2 Acridine Orange and Ethidium Bromide Differential Staining

The wells containing the cell laden coverlips were washed 3 times with PBS (Appendix 1.1) to remove all traces of CCM. This was achieved by flooding and aspiration of the wells with PBS. Acridine orange (Appendix 3.1; 100µg/ml) and ethidium bromide (Appendix 3.2; 100µg/ml) were then added in equal volumes (50µl) to each well to make final concentrations of 50 µg/ml. The plates were then incubated for 10 minutes at 37°C to allow the cells to interact with the stains. The wells were then again rinsed with PBS to remove excess stain. The coverslips containing the treated cells were then carefully removed from the wells with forceps and mounted onto clean labelled microscope slides using glycerol jelly.

6.2.2.3 Hoechst 33258 Staining

The cell laden coverslips were washed with PBS as described for AcOr and EtBr staining prior to the addition of equal volumes (50µl) of Hoechst working stock (Appendix 3.3) and PBS in each well. The plates were then incubated for 15 minutes at 37°C to allow for interaction with the dye. The cells were rinsed with PBS to remove excess stain and fixed in 10% PFA (Appendix 3.4) for 5 minutes at 37°C to preserve the structure of the cells. They were finally rinsed with PBS. The coverslips were then removed from the wells and mounted onto clean labelled microscope slides.

The cellular morphology and uptake of stain was then evaluated by using the Olympus IX51 inverted research microscope equipped with the Olympus DP12 microscope digital camera system (Wirsam Scientific). Acridine orange and ethidium bromide stained slides were viewed using filter 3 which encompassed excitation and barrier wavelengths of 450-480nm and 515nm while Hoechst stained slides were viewed using filter 2 which encompassed excitation and barrier wavelengths of 330-385nm and 420nm.

6.3 RESULTS AND DISCUSSION

6.3.1 THE EFFECT OF ETHANOL

The AcOr and EtBr stained slides of the untreated (Figure 6.4a) and ethanol (0.08%) treated (Figure 6.4b) cells displayed the normal nuclei with a homogeneous chromatin staining pattern and bright green fluorescence characteristic of live viable cells. The respective Hoechst stained slides demonstrated similar cellular morphology.

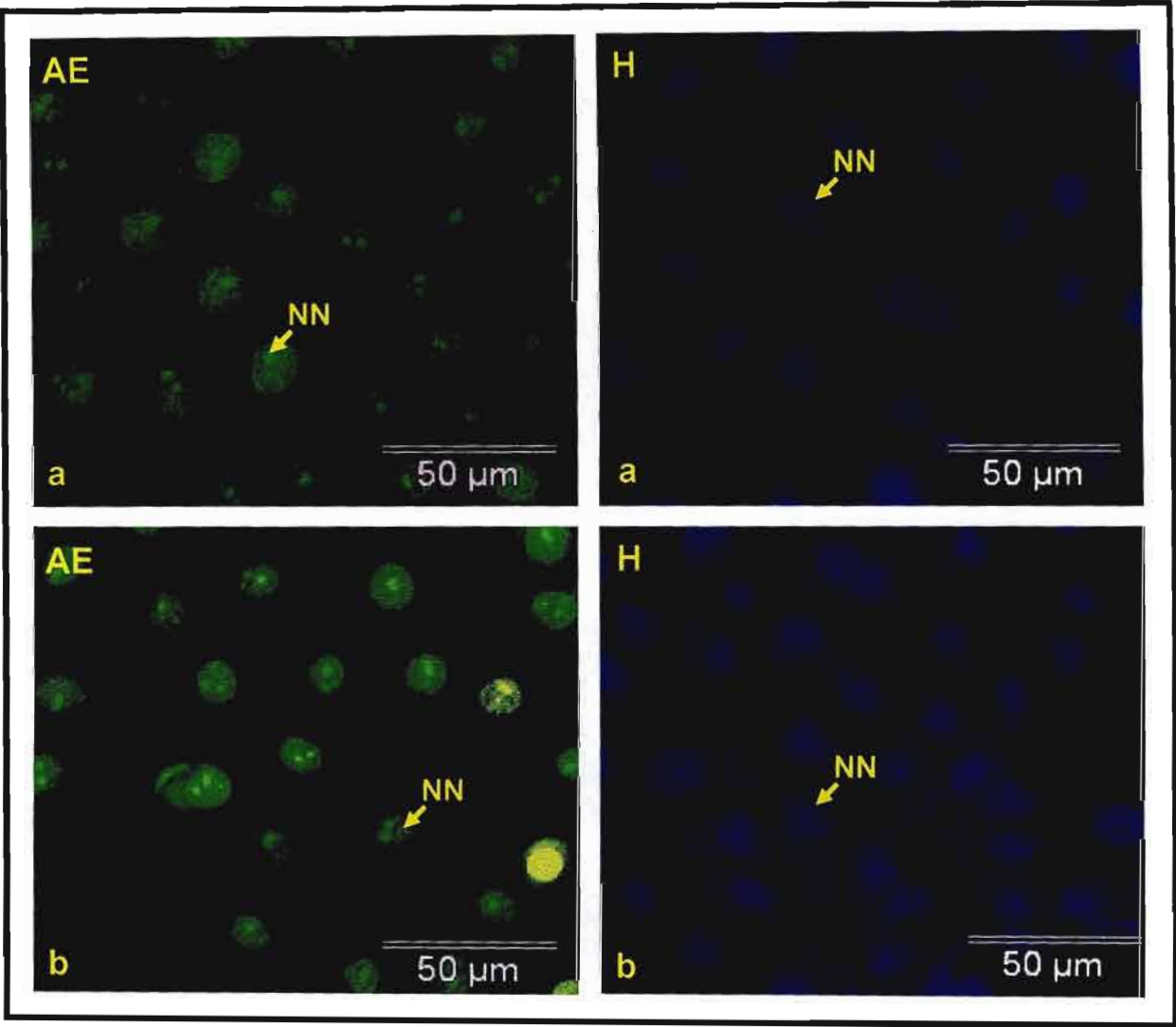


Figure 6.4: Photomicrographs illustrating AcOr/EtBr (AE) and Hoechst (H) stained (a) untreated and (b) ethanol (0.08%) treated cells showing intact cell membranes and normal nuclei (NN) (X400).

These results showed minimal or no ethanol toxicity on the HT-29 cell line at the concentration used. This signifies that any effect on the cells noted hereafter is due to the action of the test compounds and not the carrier solvent.

6.3.2 THE EFFECT OF CURCUMIN

The AcOr/EtBr stained cells treated with curcumin (50 μ M) (Figure 6.5) showed green fluorescence with normal nuclei as observed in the untreated cells. In addition, some cells from this treatment also showed features characteristic of early and late apoptosis (condensed and fragmented nuclei respectively).

The cells stained with Hoechst 33258 (Figure 6.5) displayed similar features as well as blebbing a typical feature of late apoptosis.

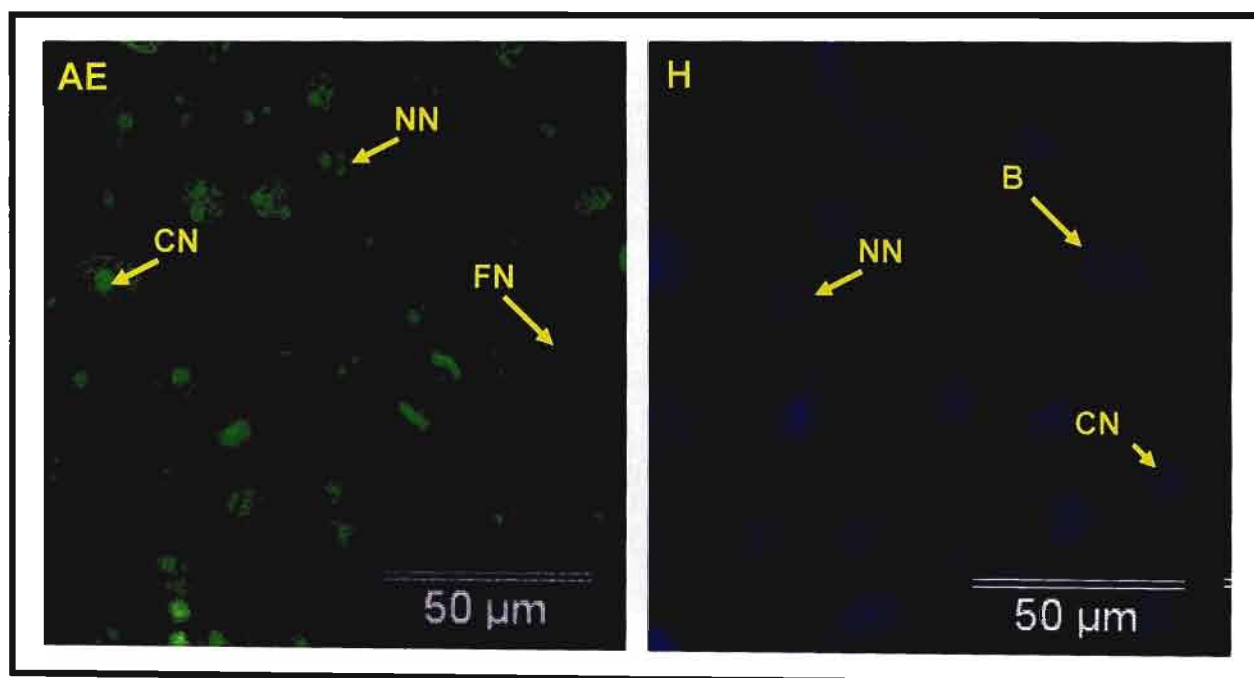


Figure 6.5: Photomicrographs illustrating AE and H stained curcumin (50 μ M) treated cells displaying normal (NN), condensed (CN) and fragmented (FN) nuclei as well as blebbing (B) (X400).

These apoptotic features have been demonstrated in various transformed cell lines following exposure to curcumin (Jee *et al.*, 1998; Radhakrishna Pillai *et al.*, 2004) and may be attributed to the ability of this compound to induce phase 2 detoxification enzymes (Dinkova-Kostova and Talalay, 1999; Lin and Lin-Shiau, 2001) and specifically inhibit cyclooxygenase-2 (COX-2) expression (Goel *et al.*, 2001).

The inhibition of COX-2 may account for the induction of apoptosis as inhibition of this enzyme alters prostaglandin production and leads to an increase in arachidonic acid which stimulates the conversion of sphingomyelin to the pro-apoptotic sphingolipid ceramide (Janne and Mayer, 2000; Taraphdar *et al.*, 2001). The role of phase 2 enzymes in the induction of apoptosis is thought to be distinct from that associated with enhanced detoxification of carcinogenic compounds but is yet to be elucidated however studies indicate that compounds that induce phase 2 enzymes activate apoptosis in HT-29 cells (Kirlin *et al.*, 1999).

6.3.3 THE EFFECT OF DEOXYNIVALENOL

6.3.3.1 The Effect of Deoxynivalenol Only

The AcOr/EtBr stained slides of DON (5 μ M; Figure 6.6a and 50 μ M; Figure 6.6b) treated cells both exhibited a decrease in cell proliferation when compared to the controls. In addition alterations in cellular morphology were observed with the cells appearing shrunken and fibroblast-like. The 5 μ M treated cells displayed features of early apoptosis with typical condensed nuclei and green fluorescence while the 50 μ M treated cells exhibited features of early as well as late apoptosis with fragmented nuclei and blebbing accompanied by bright orange fluorescence. The Hoechst stained slides of DON treated cells (5 μ M and 50 μ M) exhibited similar characteristics as those stained with AcOr/EtBr in terms of cell number and morphology.

The 5μM treated cells however, exhibited homogenous distribution of stain while the 50μM treated cells displayed condensed nuclei exhibiting brighter staining typical of apoptosis.

These results indicated that DON induced alterations in cell morphology indicative of apoptosis in the HT-29 colorectal cell line at both concentrations tested and that the morphological changes were more severe at the higher concentration. This may be correlated to an increase in the induction of apoptosis by this compound at the higher concentration.

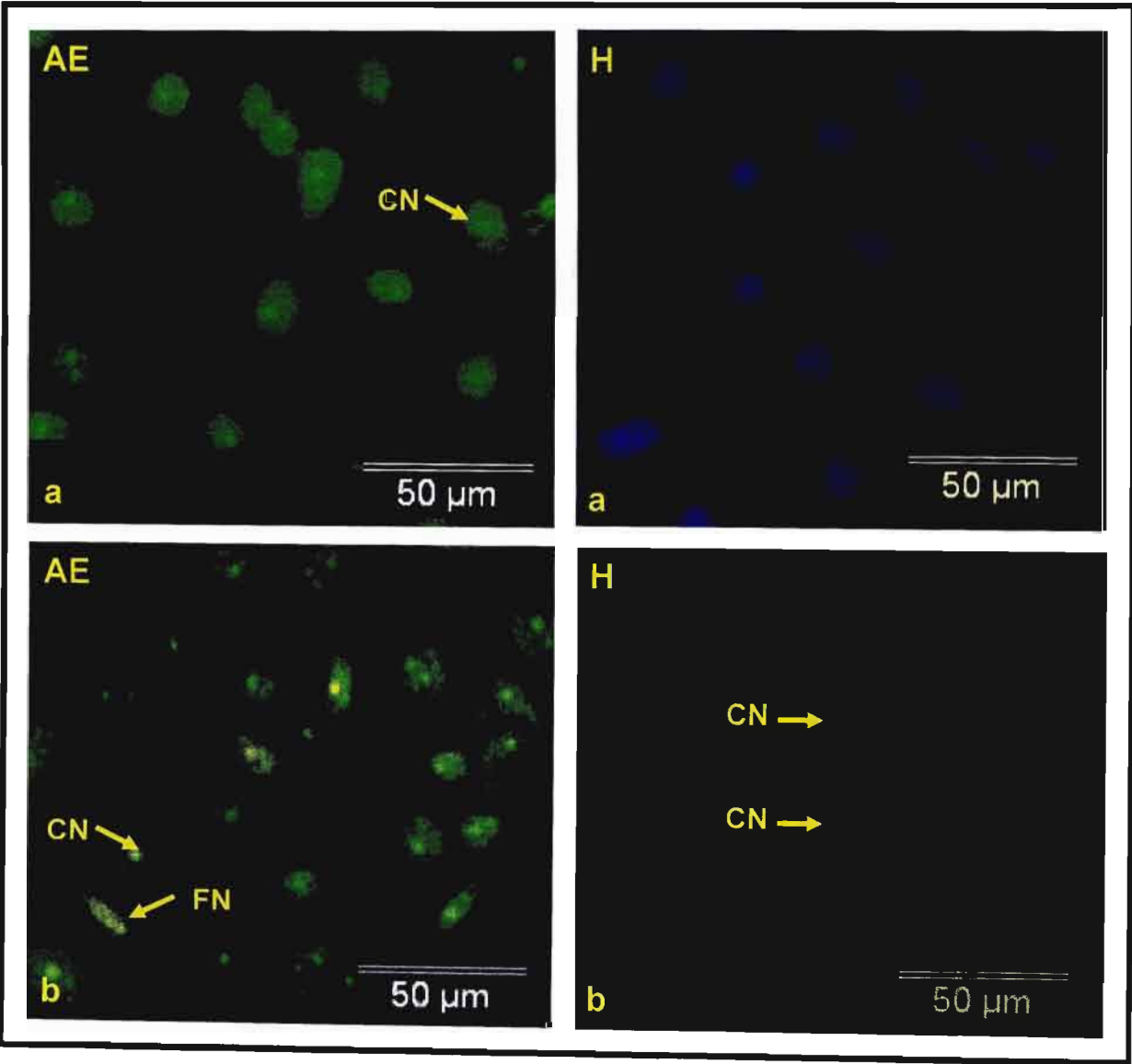


Figure 6.6: Photomicrographs illustrating AE and H stained (a) DON (5μM) and (b) DON (50μM) treated cells depicting condensed (CN) and fragmented (FN) nuclei (X400).

The apoptotic alterations in cellular morphology observed may be attributed to DON's involvement in protein synthesis inhibition and lipid peroxidation as a result of the high protein and lipid content in membrane structures (Arms and Camp, 1995). A major consequence of lipid peroxidation is the transformation and degradation of membrane polyunsaturated fatty acids to ROS (Garaleviciene, 2003; Marciniak *et al.*, 2003).

The ability of ROS to cause damage in most biomolecules including DNA, protein and lipid membrane has been previously reported and is thought to play an important role in the events leading to apoptotic cell death (Bhaumik *et al.*, 1999).

The ability of DON to inhibit cell proliferation and induce apoptosis has been previously reported in human T-cells (Pestka *et al.*, 1999) as well as the K562 erythroleukaemia cell line (Minervini *et al.*, 2004) and has been reported to be a consequence of its capability to inhibit protein translation (Rotter *et al.*, 1996).

6.3.3.2 The Effect of Deoxynivalenol Following Co-treatment With Curcumin

Acridine orange/EtBr and Hoechst stained slides of the DON (5 μ M) and curcumin and the DON (50 μ M) and curcumin treated cells (Figure 6.7a & b) displayed similar morphology and features compared to that exhibited following individual treatment with the toxin (Figure 6.6a & b) although the fibroblast-like morphology appeared to be alleviated in the DON (50 μ M) and curcumin treated cells.

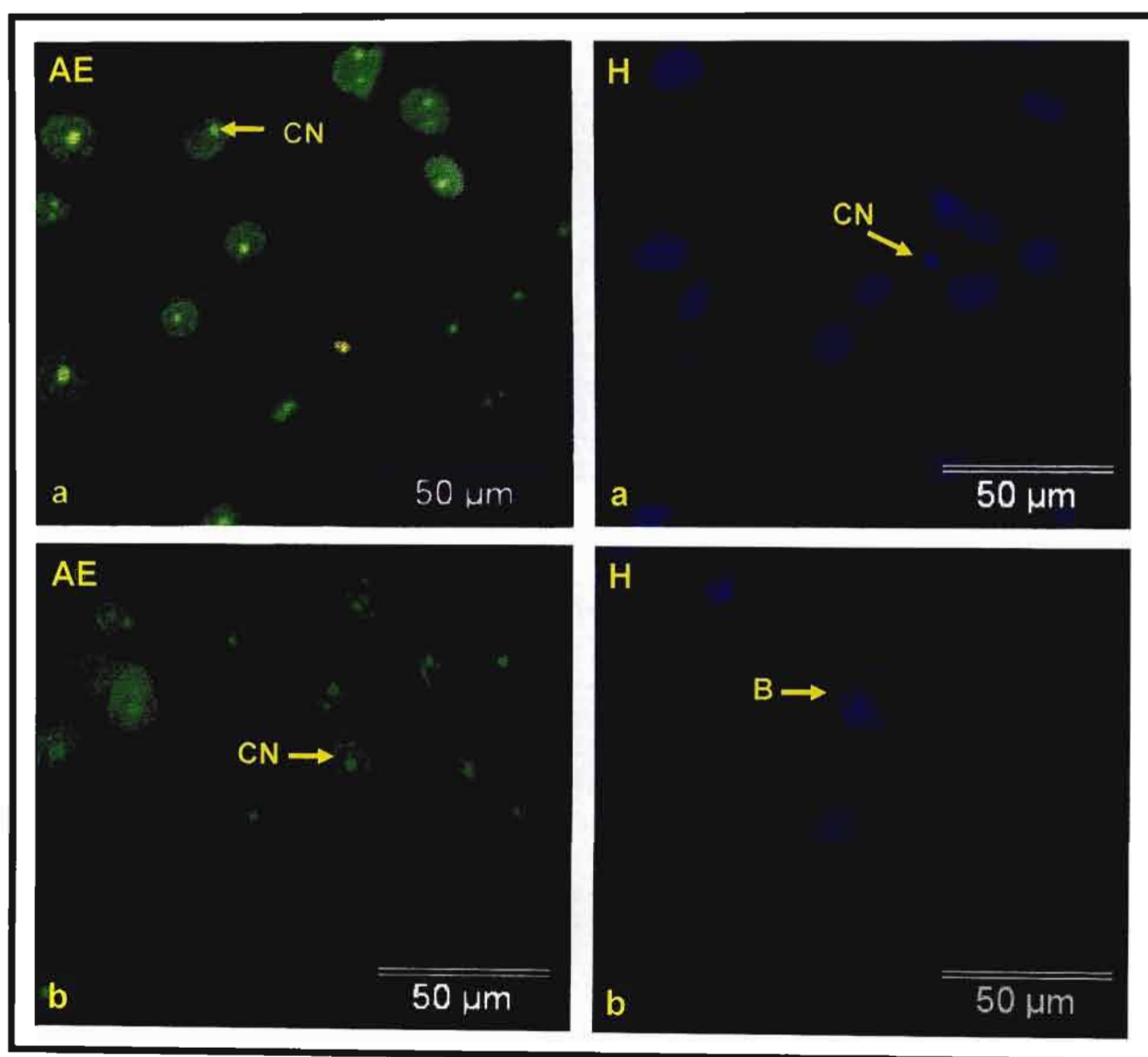


Figure 6.7: Photomicrographs illustrating AE and H stained (a) DON (5 μ M) and curcumin and (b) DON (50 μ M) and curcumin treated cells depicting condensed nuclei (CN) and blebbing (B) (X400).

No significant differences were noted between DON treated and DON and curcumin treated cells at the concentrations tested although a protective effect was expected as a consequence of curcumin's properties as an antioxidant and inhibitor of COX-2 expression (Goel *et al.*, 2001) in contrast to DON's properties as an inducer of COX-2 expression (Moon and Pestka, 2002) and its involvement in lipid peroxidation (Garaleviciene, 2003). It is possible that the interaction between these two compounds in terms of their opposing activities may, to some extent, be responsible for the insignificant effect noted.

6.3.4 THE EFFECT OF FUMONISIN B₁

6.3.4.1 The Effect of Fumonisin B₁ only

Following AcOr/EtBr staining, cells treated with FB₁ (5μM and 50μM; Figure 6.8a & b respectively) both exhibited an increase in proliferation when compared to the untreated cells (Figure 6.4a). The 5μM treated cells displayed green fluorescence with normal, condensed and fragmented nuclei associated with early apoptosis. The presence of mitotic cells was also noted. In contrast the 50μM treated cells exhibited condensed and fragmented nuclei and the orange fluorescence associated with cell membrane damaged typical of late apoptotic cells. Hoechst staining confirmed these results with the presence of condensed nuclei in the 5μM (Figure 6.8a) and apoptotic bodies in the 50μM (Figure 6.8b) treatments.

Fumonisin B₁ is known to block complex sphingolipid biosynthesis resulting in the accumulation of free sphingoid bases and their 1-phosphates (Wang *et al.*, 1999). Merrill (2002) reported that partial inhibition of ceramide synthase can result in elevations in sphingoid base 1-phosphate levels without a great increase in the free sphingoid base concentration resulting in cell proliferation. This could account for the increased cell number observed in FB₁ treated cells.

The induction and increase in severity of apoptosis induction in the FB₁ treated cells may be due to the variations in increased sphinganine production as described by Schmelz *et al.* (1998) who demonstrated that in the HT-29 cell line sphinganine levels were elevated 5-, 20- and 500-fold in the presence of 1μM, 10μM and 50μM FB₁ respectively following 24 hours incubation while sphingosine levels only increased moderately. These results indicated that although FB₁ increased proliferation at both concentrations tested it also induced apoptosis which increased in severity with increasing concentration.

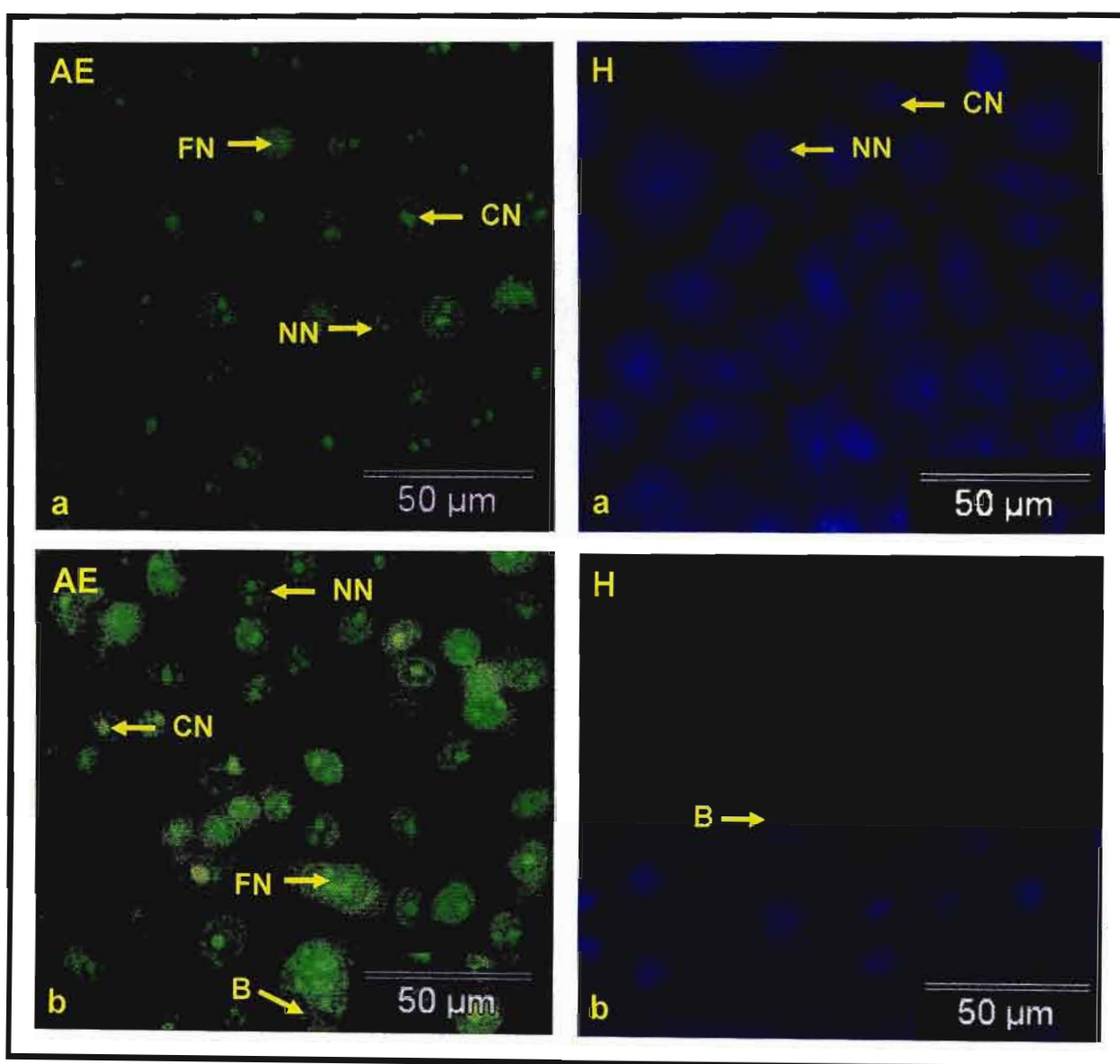


Figure 6.8: Photomicrographs illustrating AE and H stained (a) FB_1 ($5\mu M$) and (b) FB_1 ($50\mu M$) treated cells depicting normal (NN), condensed (CN) and fragmented (FN) nuclei as well as blebbing (B) (X 400).

In addition FB_1 has been implicated in lipid peroxidation, via the induction of increased MDA production (Abado-Becognee *et al.*, 1998; Mobio *et al.*, 2003). Malonyldialdehyde generation may contribute to the toxic effects of FB_1 as a consequence of its mutagenic and carcinogenic properties (Marnett, 1999).

6.3.4.2 The Effect of Fumonisin B₁ Following Co-treatment With Curcumin

Co-treatment with curcumin (50µM) and FB₁ (5µM and 50µM; Figure 6.9a & b) appeared to negate the cell proliferation observed at both FB₁ concentrations when stained with AcOr/EtBr, although condensed and fragmented nuclei were still observed. The FB₁ (5µM) treatment also exhibited blebbing, a feature associated with late apoptosis. The Hoechst stained cells displayed similar results with blebbing and other morphological features characteristic of apoptosis.

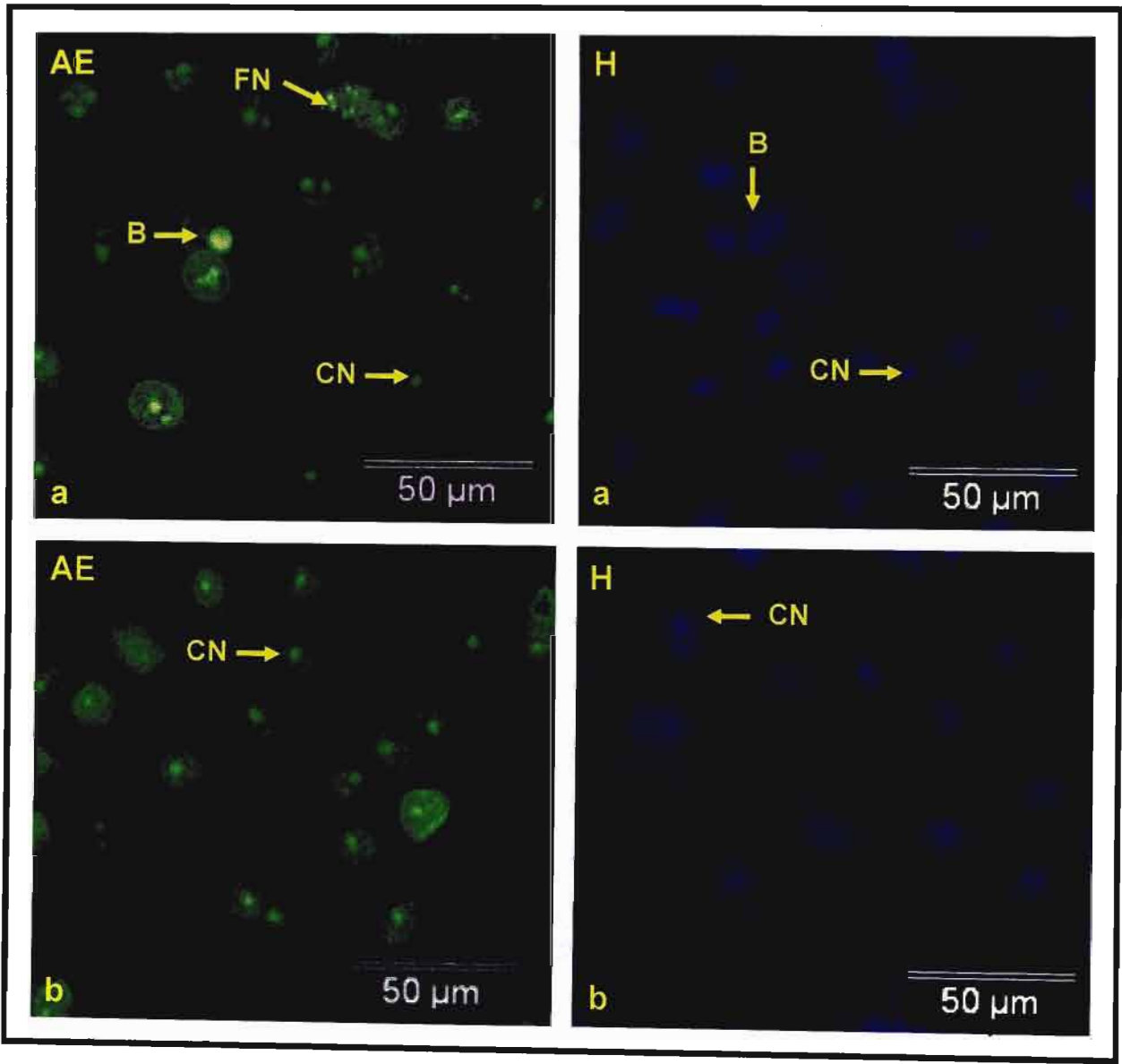


Figure 6.9: Photomicrographs illustrating AE and H stained (a) FB₁ (5µM) and curcumin and (b) FB₁ (50µM) and curcumin treated cells depicting condensed (CN) and fragmented (FN) nuclei as well as blebbing (B) (X400).

These results indicate that curcumin alleviates the proliferation exerted by FB₁ at both concentrations used; a result which is consistent with studies which report that curcumin inhibits proliferation and enhances apoptosis (Kawamori *et al.*, 1999). As discussed earlier, FB₁ stimulates proliferation by inhibiting ceramide synthase resulting in the accumulation of the mitogenic 1-phosphates with depletion of the pro-apoptotic complex sphingolipid, ceramide. As curcumin stimulates the conversion of sphingomyelin to ceramide by inhibiting COX-2 expression, this may account for the effect observed.

In addition, curcumin has been demonstrated to exhibit both pro- and anti-oxidant effects. The decreased proliferation observed may thus be attributed to the collective ROS generated by lipid peroxidation via both curcumin and FB₁. It may also be postulated that the decreased proliferation may be due to the anti-oxidant properties of curcumin (Lin and Lin-Shiau, 2001). As previously detailed, FB₁'s toxic effect may be attributed to its involvement in lipid peroxidation via the induction of MDA and antioxidant agents have previously been demonstrated to prevent increases in MDA production in two cell types (Mobio *et al.*, 2003). Bearing in mind that curcumin is a potent antioxidant agent it is possible that these activities have decreased the cell proliferation induced by FB₁.

6.3.5 THE EFFECT OF A DEOXYNIVALENOL AND FUMONISIN B₁ MIXTURE

6.3.5.1 The Effect of a Deoxynivalenol and Fumonisin B₁ Mixture Only

Acridine orange/EtBr and Hoechst staining demonstrated that cells treated with a DON and FB₁ (DFB₁) mixture (5μM and 50μM; Figure 6.10a & b) exhibited the decreased proliferation, fibroblast-like morphology and apoptotic features exhibited in the DON treated cells (Figure 6.6a & b), thereby indicating that the DON overcomes the proliferative effects of FB₁ at the concentrations tested.

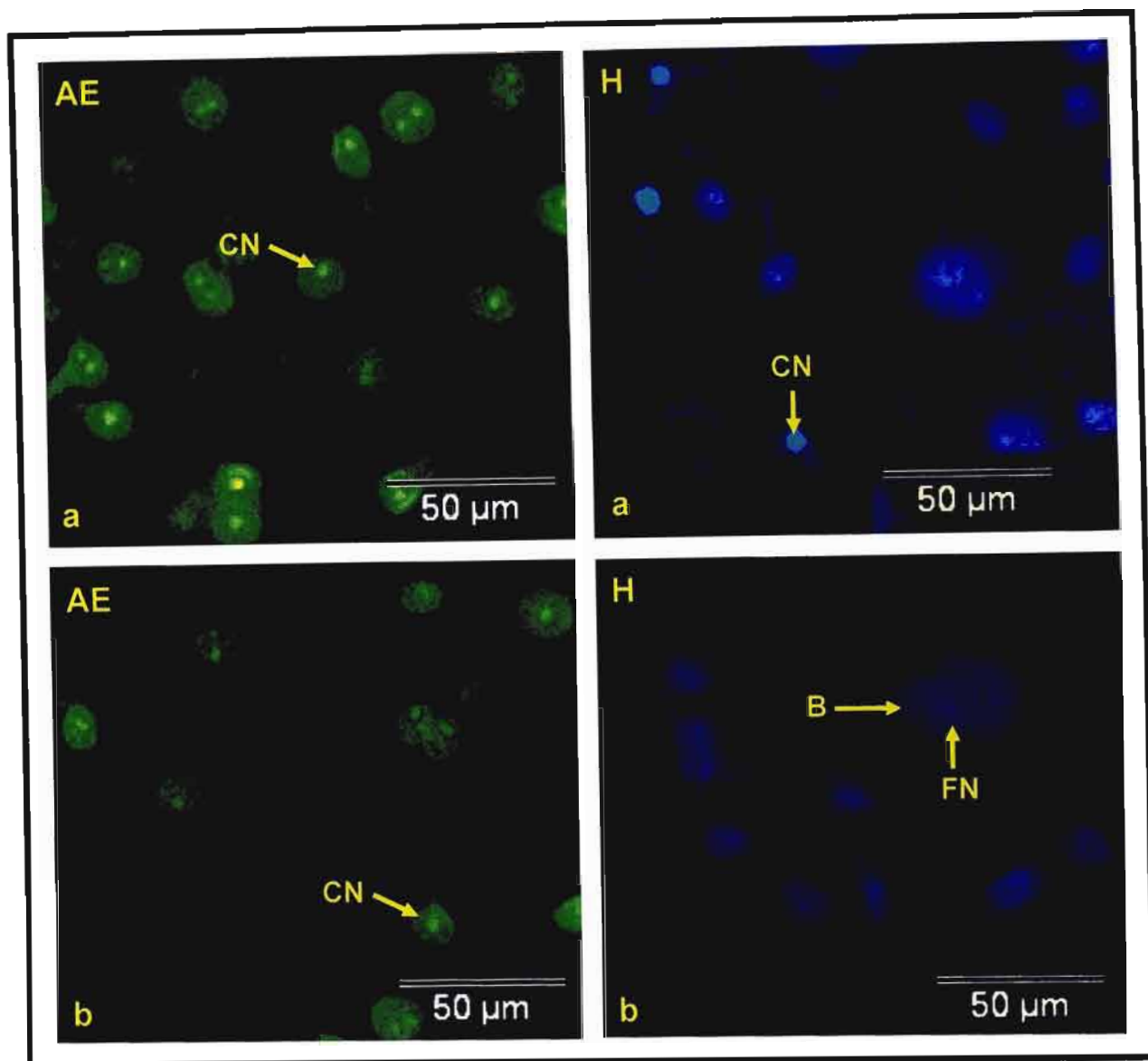


Figure 6.10: Photomicrographs illustrating AE and H stained (a) DFB₁ (5μM) and (b) DFB₁ (50μM) treated cells depicting condensed (CN) and fragmented (FN) nuclei as well as blebbing (B) (X400).

This may be as a result of DON's ability to induce COX-2 expression and affect arachidonic acid metabolism and prostaglandin production (Subbaramaiah *et al.*, 1998) or its ability to decrease mitogen induced proliferation (Rotter *et al.*, 1996). As discussed in Chapter 4, the inhibition of proliferation by trichothecenes *in vitro* decreases upon substitution of acyl groups at the C8 position with keto or hydroxyl moieties and is dependent on the nature of substitutions at the C3, C4 and C15 positions. These structure-activity responses mimic those observed for protein synthesis inhibition and suggest that translational arrest may be an underlying mechanism for impaired proliferation (Rotter *et al.*, 1996).

6.3.5.2 The Effect of a Deoxynivalenol and Fumonisin B₁ Mixture Following Co-treatment with Curcumin

Cells co-treated with curcumin (50µM) and DFB₁ (5µM and 50µM; Figure 6.11a & b) displayed similar morphology and features as compared to that exhibited following individual treatment with the toxin mixture (Figures 6.10a & b) indicating that the presence of curcumin had no significant effect.

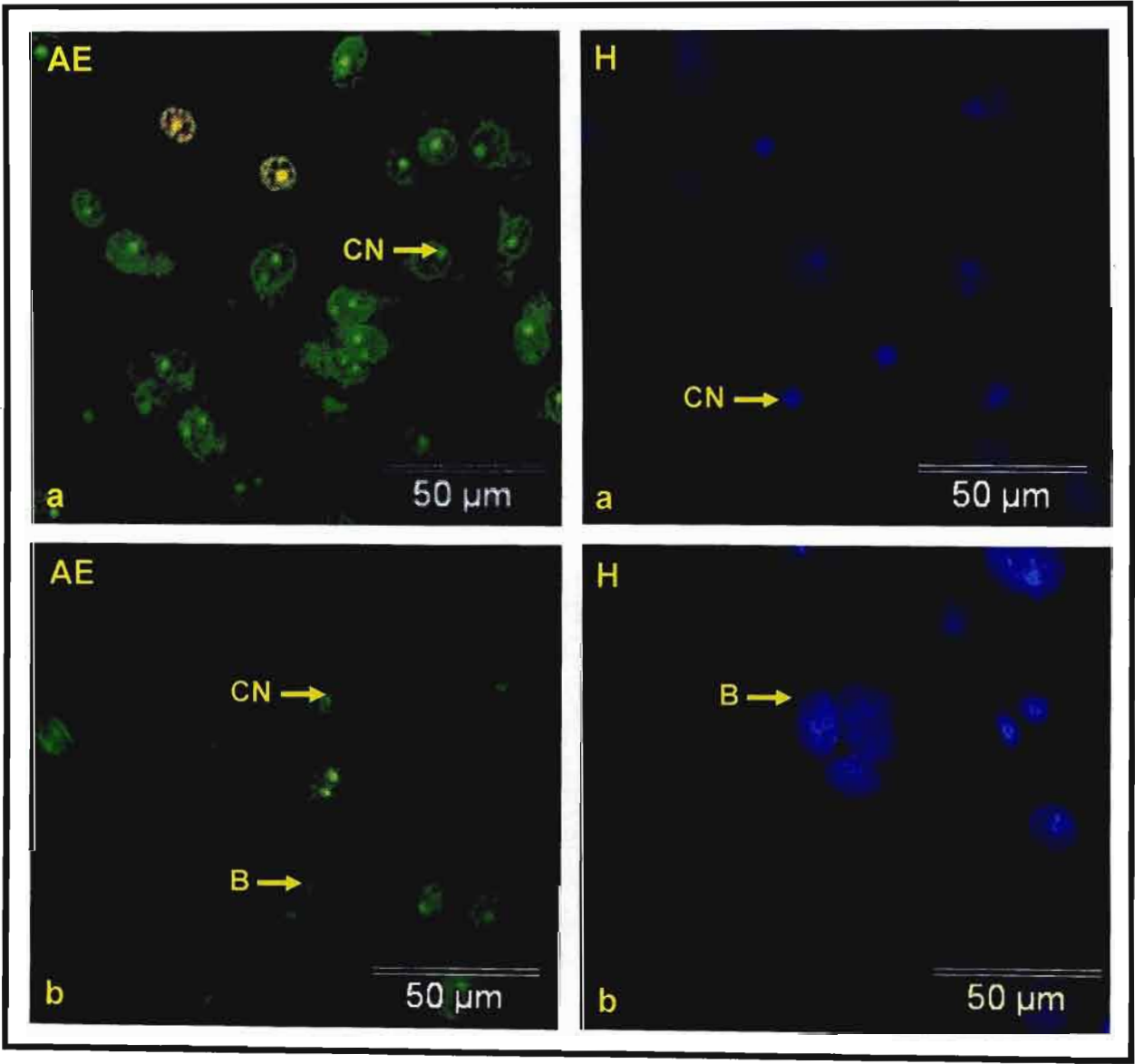


Figure 6.11: Photomicrographs illustrating AE and H stained (a) DFB₁ (5µM) and curcumin and (b) DFB₁ (50µM) and curcumin treated cells condensed nuclei (CN) and blebbing (B) (X400).

Curcumin exhibited no significant effect in the presence of DON (Figure 6.7) and reduced the proliferation induced by FB₁ (Figure 6.9) when compared to the respective toxin controls (Figures 6.6 & 6.8). The insignificant effect of curcumin observed in the presence of DFB₁ therefore suggests that DON is able to overcome the effects of FB₁ as discussed earlier.

This effect is therefore a probable result of the interaction between DON and curcumin in terms of their opposing activities in terms of their roles in COX-2 expression and ROS generation as discussed previously.

6.4 CONCLUSION

The results of this investigation indicated that both toxins are able to induce apoptosis in the HT-29 cell line. Deoxynivalenol decreased cell number and induced apoptosis at both the 5µM and 50µM concentration with the severity increasing with increasing concentration. Fumonisin B₁ demonstrated a mitogenic effect at the 5µM concentration and appeared to decrease proliferation and induce apoptosis at the 50µM concentration. A combination of the two toxins indicated that DON overcomes the effect of FB₁ with both concentrations showing results similar to those observed following DON treatment. Co-treatment with curcumin appeared to alleviate the effects of FB₁ in terms of its ability to inhibit proliferation and induce apoptosis but appeared to exert no effect in the presence of DON.

The AcOr and EtBr differential staining technique provided better visualisation of the toxin effects in comparison to the Hoechst 33258 staining technique as greater detail could be observed in terms of cell structure and features and demonstrates that light microscopy coupled with the use of fluorescent stains provides a rapid and simple method for the observation of cellular morphology and detection of apoptosis in adherent cell lines.

CHAPTER 7

AN ASSESSMENT OF HT-29 CELL SURFACE MORPHOLOGY FOLLOWING EXPOSURE TO FUMONISIN B₁ AND DEOXYNIVALENOL

7.1 INTRODUCTION

7.1.1 THE CELL SURFACE

The exterior morphology of intestinal epithelial cells (Figure 7.1a) includes tight junctions between adjacent cells which form the apical and basolateral domains of the cell membrane. The apical cell surface is covered by the brush border which increases the surface area of the plasma membrane (Cohen *et al.*, 1999).

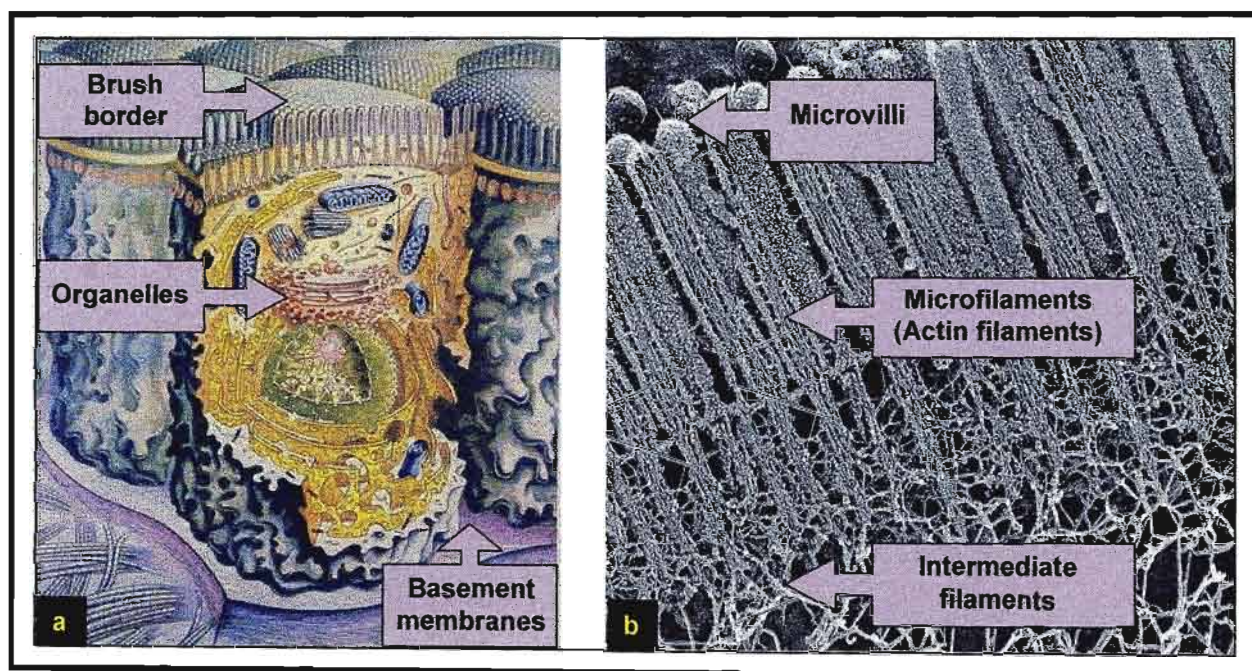


Figure 7.1: Illustration depicting: (a) absorptive cell exterior and interior (Med Note, 1998), (b) microvillus structure (Mallery, 2004).

The plasma membrane is a very fragile structure consisting of a lipid bilayer containing phospholipids composed of either saturated or unsaturated fatty acids. It is covered by the glycocalyx (a layer of carbohydrate comprised of oligosaccharides attached to the membrane's glycoproteins) as well as glycolipids. The plasma membrane is strengthened by the cell cortex, a supporting framework of proteins rich in actin filaments that is attached to transmembrane proteins on the cytoplasmic face. Actin-containing filaments control cell shape, adhesion, and contraction and the actin-based cytoskeleton plays a central role in cell motility and cortical morphogenesis (Shen *et al.*, 2003).

The plasma membrane is relatively impermeable to essential non lipid-soluble molecules such as ions, sugars and amino acids but contain proteins such as receptors and transport proteins that bind to and transport molecules into and out of the cell thereby acting as a selective barrier that separates the contents of the cell from its environment and regulates the passage of molecules into and out of the cell (Arms and Camp, 1996).

The brush border consists of tightly packed, uniform, apical microvilli rooted in the filamentous meshwork of the subjacent terminal web domain from which organelles are restricted. The polarised actin cores of the microvilli are bundled by villin, a brush border specific protein, and the more generally distributed fimbrin (Cohen *et al.*, 1999). The actin bundles are linked to the overlying membrane by spirally arranged crossbridges that are comprised, in part, of brush border myosin I. The actin cores extend into the inter-rootlet domain of the terminal web and are crosslinked by a network of myosin II and non-erythroid spectrin (Peterson *et al.*, 1993). These villous structures have numerous purposes as they may be used to trap nutrients, adhere to substances needed for uptake and protect from toxic assault (Childs, 1995).

The membrane and actin cytoskeletons play crucial roles in morphological changes of the cell surface. Cytoskeletal proteins are known to be substrates for caspases and calpains whose action may cause collapse of the congruous cytoskeletal structure in apoptotic cells and it has been suggested that a degradation of the cortical cytoskeleton impairs microfilament organisation, which leads to plasma membrane blebbing (Veselská *et al.*, 2003).

Veselská *et al.* (2003) suggested that the actin skeleton plays an important role in the execution phase of apoptosis as it undergoes specific structural changes and is responsible for the blebbing of the plasma membrane and cell disintegration into apoptotic bodies, two main morphological features of apoptosis. This study demonstrated three different structural changes in the actin pattern that were specific for apoptosis, namely type AI (granules under the plasma membrane), type AII (3D-network) and type AIII (complete disintegration of the actin filaments) and demonstrated that type AI and/or AII were indicators of apoptosis.

This study by Veselská *et al.* (2003) proposed a general scheme for the development of changes in actin structures during apoptosis (Figure 7.2). In the execution phase of apoptosis, a fine meshwork of microfilaments, present both in interphase (stage 1A) and mitotic (stage 1B) cells, disappears and actin is accumulated in the form of large granules (stages 2A-D) localised close to the plasma membrane of the cell with a fragmented nucleus. In most of the apoptotic cells, these granules are distributed under the whole cell surface (stage 2A). Less frequently, the granules are localised only to a certain part of the cell (stage 2B), or only a few single granules are found (stage 2C). Blebbing of the plasma membrane was related to actin reorganisation into granules because blebs on the cell surface appeared to occur together with actin granules (stage 2D). The accumulation of large numbers of actin granules under the plasma membrane was considered a primary change, whereas the other situations represented a step leading to the formation of a 3D actin filament network (stage 3A). A low number of actin granules was rarely associated with a 3D-network (stage 3B) (Veselská *et al.*, 2003).

The 3D-network was never found in cells with morphologically intact nuclei, i.e., in the initial phase of apoptosis and it was assumed that the actin molecules, previously present as numerous granules under the plasma membrane, were subsequently utilised for the formation of the 3D-network that serves as a contractile apparatus accomplishing the final disintegration of a cell into apoptotic bodies (stage 5).

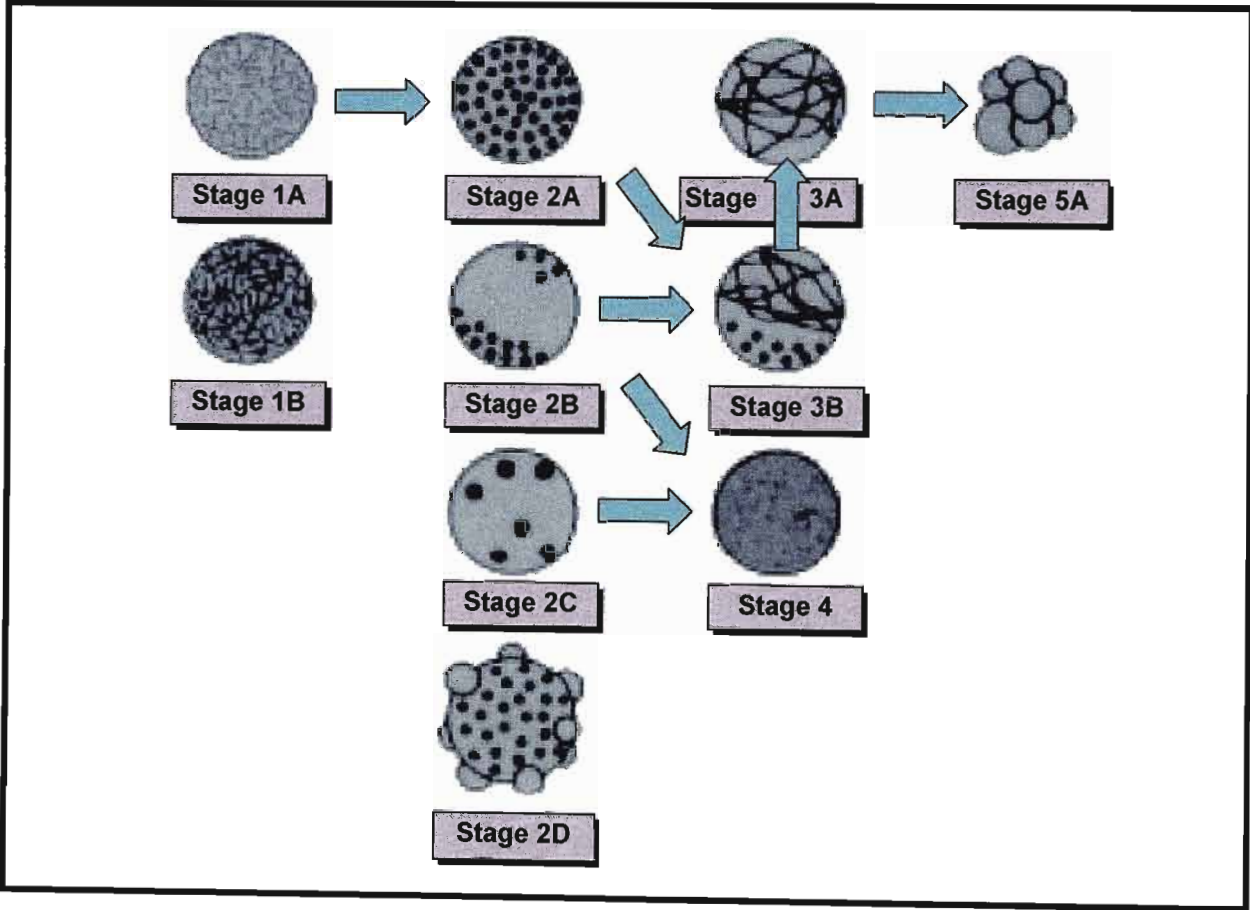


Figure 7.2: Depiction of the development of changes in the actin cytoskeleton during apoptotic cell death (stages 1-5) (Veselská *et al.*, 2003).

As a result of the actin content in the cell cortex as well as in the numerous microvilli of HT-29 cells, it can be hypothesised that changes in the actin structures during apoptosis may result in cell surface alteration in terms of microvillus structure, blebbing and formation of apoptotic bodies, all of which may be observed using scanning electron microscopy.

7.1.2 SCANNING ELECTRON MICROSCOPY

Scanning electron microscopy (SEM) is a technique that creates an image using electrons emitted from a specimen instead of light energy. Briefly, a finely focused beam of electrons is scanned across a specimen, and the electron intensity variations are used to construct a three-dimensional greyscale image of the specimen at high magnification, the resolution of which is far beyond the capabilities of a light microscope. The path of the beam is kept under vacuum so that electrons do not interact with air molecules and the specimen is usually coated with a thin electrically conductive layer of gold to withstand the electron irradiation. Accordingly, microscopy performed using this instrument allows high-resolution visualisation of the surface topography of solid and inanimate materials and is useful technique to characterise surface structure.

The aim of this study was to investigate cell membrane alterations of the HT-29 cells after exposure to DON, FB₁ and DFB₁ individually and in combination with curcumin using SEM.

7.2 METHODS AND MATERIALS

7.2.1 MATERIALS

Potassium chloride (KCl), potassium dihydrogen phosphate (KH₂PO₄) sodium chloride (NaCl), sodium dihydrogen phosphate (NaH₂PO₄·H₂O) and glutaraldehyde (25%) were purchased from Sigma Aldrich (Johannesburg, SA). Ethanol and osmium tetroxide was purchased from Merck and Capital Laboratory Supplies (Johannesburg, SA) respectively. Coverslips (22mm X 50mm) were procured from Lasec Laboratory Services (KwaZulu-Natal, SA) and carbon tape and gold were purchased from Wirsam Scientific (Johannesburg, SA).

7.2.2 METHODS

7.2.2.1 Dilutions and Treatments

Stock solutions of DON, FB₁, DFB₁ (10µM and 100µM), curcumin (100µM) and EtOH (0.04%) were prepared as described in Chapter 5.

The HT-29 cells (3ml suspension) were seeded onto coverslips in each well of three 6 well plates and incubated until the cells formed a confluent monolayer. The media was then aspirated and the cells treated. Briefly, for each toxin treatment, 1.5ml of toxin dilution was added to a well with an equal volume of CCM to halve the concentration. A similar pattern was formed for toxin and curcumin treatments with 1.5ml of curcumin (100µM) being added instead of CCM. The EtOH control consisted of 1.5ml EtOH (0.08%) and 1.5ml CCM. The curcumin control consisted of 1.5ml curcumin (100µM) and 1.5ml CCM and the untreated CCM control was made up of 3ml of CCM only. The plates were then incubated at 37°C for 48 hours.

7.2.2.2 Preparation for Scanning Electron Microscopy

The treated cells on coverslips were thrice rinsed with PBS and chemically fixed in 1% glutaraldehyde (Appendix 4.1) for 45 minutes to cross-link proteins. The cells were then further rinsed with PBS to remove all traces of the fixative before being osmicated by adding 1% osmium tetroxide (cross-link lipids) (Appendix 4.2; 100µl) to each coverslip. The cells were then incubated at 4°C in the dark. The osmium was then removed from the wells by thoroughly rinsing with PBS. The cells were dehydrated by immersing in ethanol solutions of increasing strength (70%, 90% and 100%) (Appendix 4.3) for half an hour per immersion. The cells were finally re-immersed in 100% EtOH (Figure 7.3).

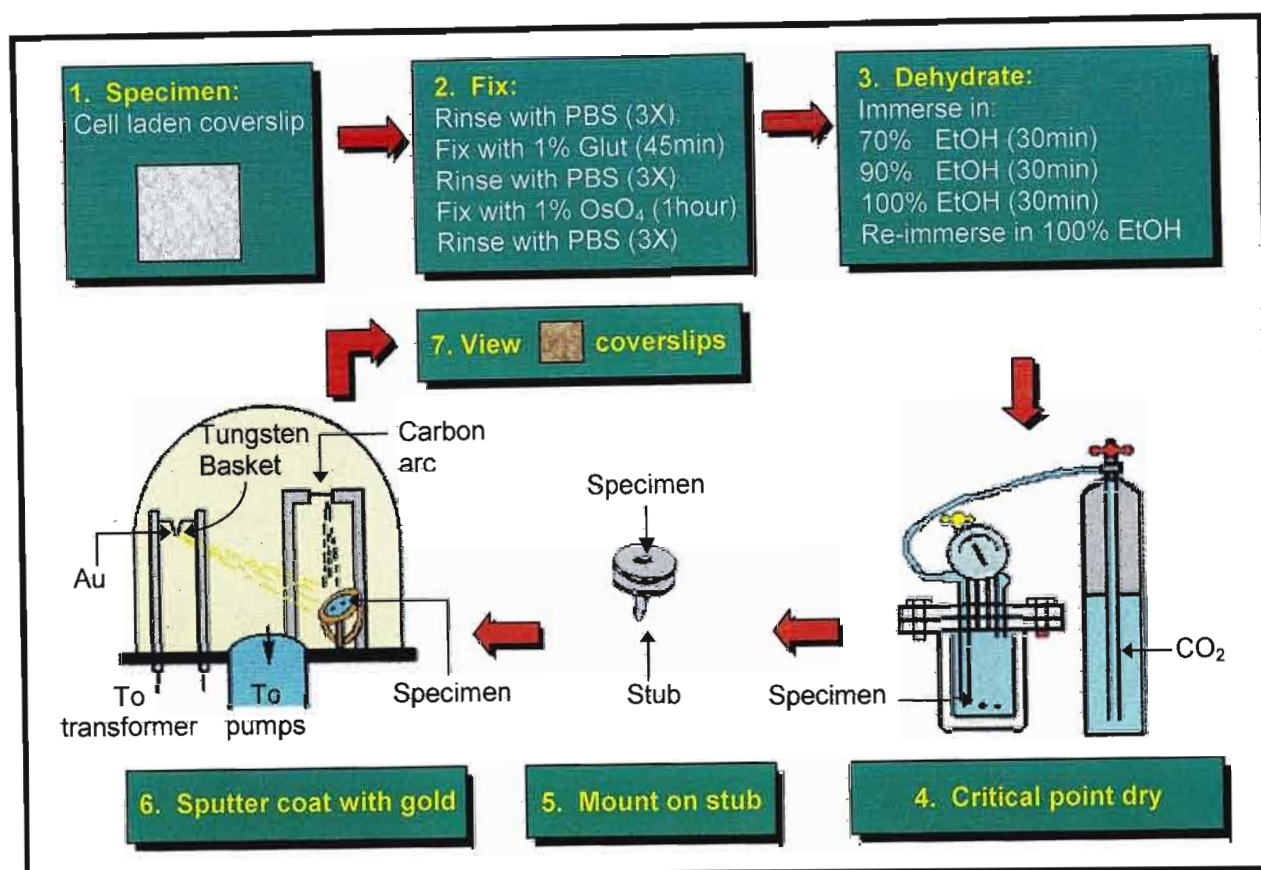


Figure 7.3: Schematic diagram illustrating specimen preparation for SEM (adapted from: Allan, 2003).

The cells were critical point dried using the Hitachi HCP-I Critical Point Dryer. This procedure involved immersing the cells in liquid carbon dioxide which was then brought to its critical point, a combination of pressure and temperature at which the fluid and gaseous phases exist together without an interface or meniscus (Electron Microscopy Services, 1999). This process eliminates surface tension which is disruptive and may cause visible distortion to the cells.

The coverslips were mounted onto aluminium specimen stubs with double sided carbon tape and sputter coated in a vacuum with a thin layer of electrically conductive gold using the Polaron E5100 SEM coating unit to enhance surface detail as well as signal emission and to reduce the effects of charging (Electron Microscopy Services, 1999). The stubs were stored in a desiccator until ready for observation. Observation and image capturing of the cells was performed using the LEO 1450 scanning electron microscope system (Carl Zeiss SMT) with LEO software.

7.3 RESULTS AND DISCUSSION

7.3.1 THE EFFECT OF ETHANOL

Scanning electron micrographs of the apical surfaces of both untreated (Figure 7.4a) and EtOH (0.08%) treated (Figure 7.4b) HT-29 cells displayed uniform brush border formation with short microcrovilli and extended pseudopodial (temporary cytoplasmic projections that are involved in locomotion and phagocytosis) basal like material. In addition minimal cell shrinkage was observed as well as occasional apoptotic blebs. These results confirmed that ethanol exerted no or minimal detrimental effects on the cell surface of the HT-29 cells.

7.3.2 THE EFFECT OF CURCUMIN

Curcumin treated cells (Figure 7.4c) however, appeared shrunken and slightly elongated displaying increased numbers of apoptotic bodies blebbing off the surface. As opposed to the control cells, these bodies often occurred in aggregates and varied in size. Additional morphological changes included the abnormal formation of the brush border, shrinkage of microvilli structures to form a fine network on the surface and the reduction of the pseudopodial basal like material. The basal-like material appeared electron dense and did not display protrusions as observed in the controls. The network of microvilli is a possible result of 3D network formation of actin filaments (stage 3A).

This result suggests that curcumin is able to cause alterations in microvilli structure. Holy (2004) demonstrated alterations in microfilament organisation and cell motility resulting in arrested cell movement and altered cell shape in the PC-3 human prostate bone adenocarcinoma cell line.

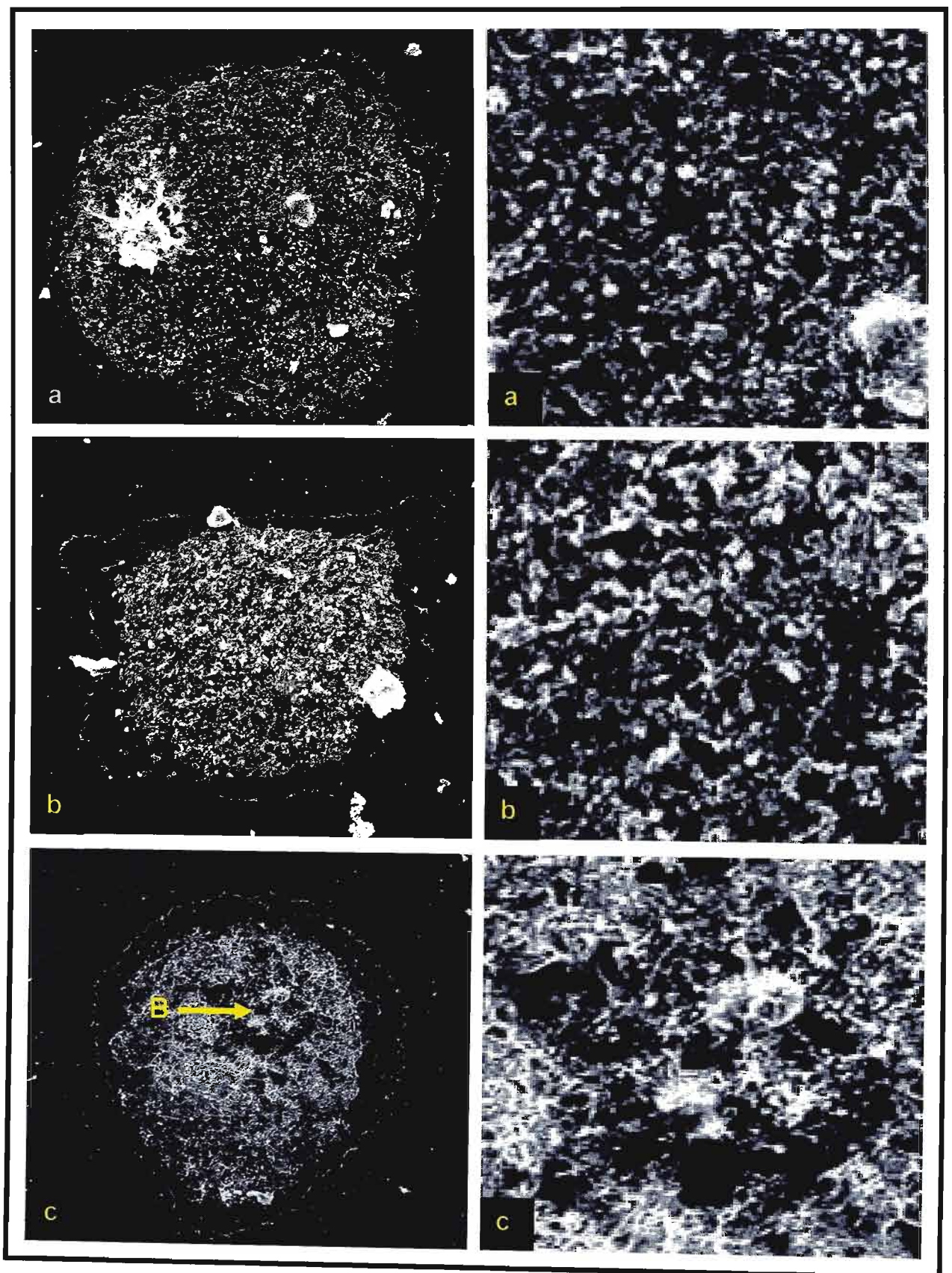


Figure 7.4: Scanning electron micrographs of (a) untreated control, (b) EtOH control and (c) curcumin control cells exhibiting blebbing (B) (X1000) and enlarged X4 to observe microvilli.

These changes may be a result of the hydrophobic properties of this compound that enable it to spread easily through the lipid phase of membranous structures such as plasma membrane, endoplasmic reticulum and nuclear envelope (Jaruga *et al.*, 1998). The apoptotic inducing ability of curcumin has been confirmed by several studies (Radhakrishna Pillai *et al.*, 2004; Jee *et al.*, 1998) and is attributed to its ability to induce Phase 2 enzymes (Dinkova-Kostova and Talalay, 1999; Kirlin *et al.*, 1999) and inhibit COX-2 expression (Goel *et al.*, 2001).

7.3.3 THE EFFECT OF DEOXYNIVALENOL

7.3.3.1 The Effect of Deoxynivalenol Only

Scanning electron microscopic analysis of HT-29 cells treated with 5 μ M DON (Figure 7.5a) revealed abnormal brush border formation with the cellular material and microvilli beginning to clump toward the centre of the cell. In addition, the underlying plasmalemma appeared perforated indicating a loss of membrane integrity and the pseudopodia exhibited inconspicuous protrusional activity when compared to that of the solvent control (Figure 7.4b). Cells treated with 50 μ M DON (Figure 7.5b) also displayed irregular brush border formation with the microvilli clumping together to form a network. The pseudopodial protrusions were greatly reduced as well as electron dense and apoptotic bodies were observed blebbing off the membrane surface. Perforation of the plasmalemma was also observed. The abnormal formation of brush borders in the presence of DON has been confirmed using the Caco-2 colon cell line (Kasuga *et al.*, 1998).

The clumping of microvilli observed in the 5 μ M and 50 μ M treated cells may be a possible result of the formation of a 3D-network of actin filaments. At the low concentration, the actin granules may be changing into the network (stage 3B) and at the high concentration the 3D network may already be present and beginning buds to form apoptotic buds (stage 5).

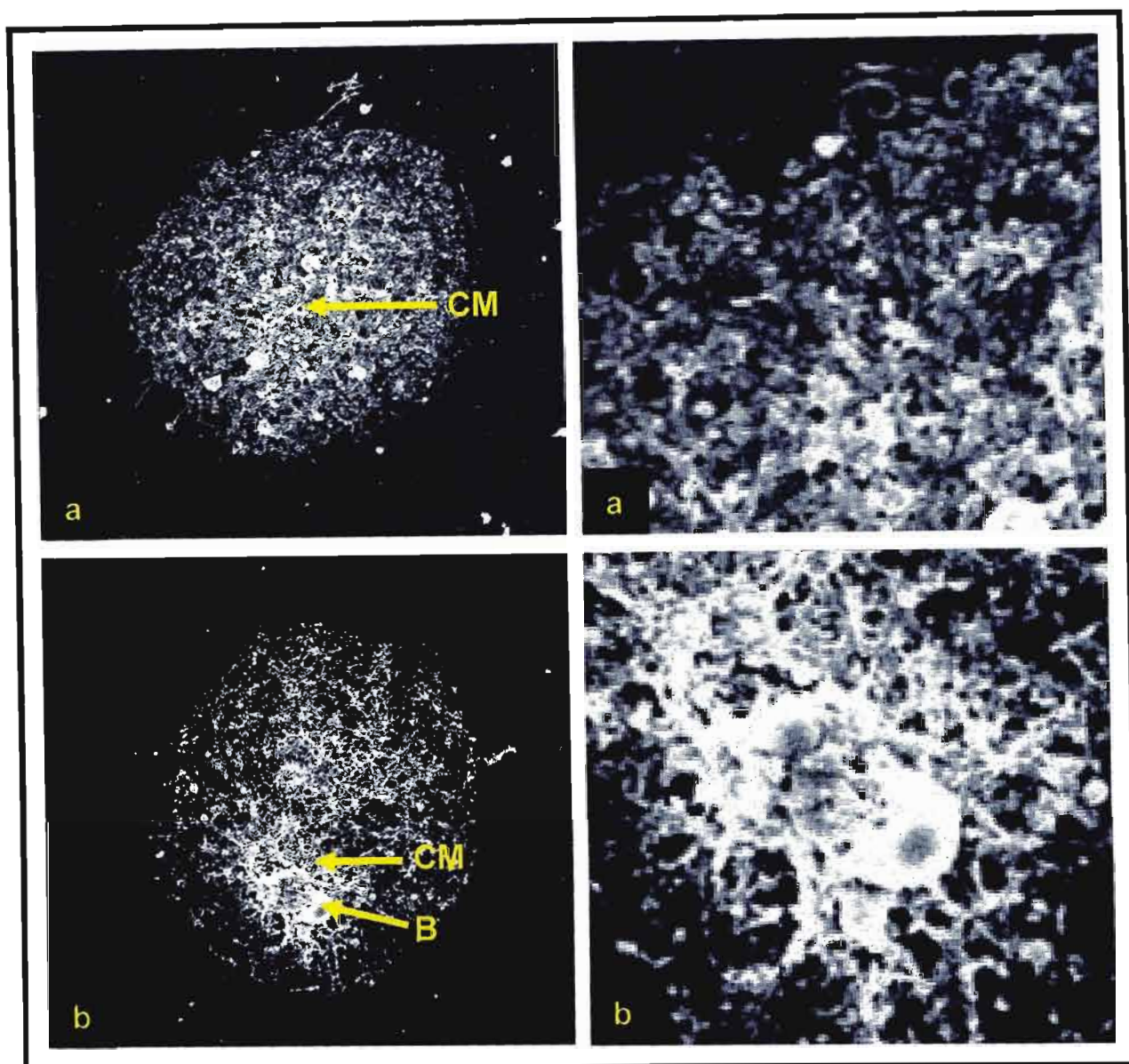


Figure 7.5: Scanning electron micrographs of the (a) 5 μ M and (b) 50 μ M DON treated cells (X1000) displaying blebbing (B) and clumping of microvilli (CM) and enlarged X4 to observe microvilli.

The alterations in the cell membrane may be attributed to the ability of DON to induce the rate-limiting enzyme COX-2 (Moon and Pestka, 2002) as this enzyme catalyses the oxygenation of arachidonic acid to prostaglandin endoperoxides. The resulting metabolites are converted enzymatically into prostaglandins and thromboxane A₂, which play both physiologic and pathologic roles in a diverse range of inflammatory sequelae.

In addition, the alterations may be due to DON's involvement in lipid peroxidation (Garaleviciene, 2003; Marciniak *et al.*, 2003) or its ability to selectively modulate the activities of intestinal transporters as described by Maresca *et al.* (2002) using the HT-29-D4 human epithelial intestinal cell line. Concentrations below 10 μ M were demonstrated to inhibit the D-glucose/D-galactose sodium-dependent transporter (SGLT1), the D-fructose transporter GLUT5 as well as the active and passive L-serine transporters by 50%, 42%, 30% and 38% respectively and increase the transport of palmitate by 35%. The activity of SGLTI was further decreased to 76% while all the activities of all other transporters were increased at a higher concentration of 100 μ M. This decrease in carbohydrate and L-serine transport and increase in palmitate transport may play a significant role in membrane alteration.

Individual sugars have been demonstrated to exert a selective effect on the cell morphology and pattern of growth of certain mammalian cell lines (Cox and Gesner, 1965) and glucose depletion has been found to result in cellular stress and the production of reactive oxygen species (Chang *et al.*, 2003) while the condensation of L-serine and palmitoyl-CoA generated from palmitate is a principal step in a cascade of reactions that result in the synthesis of sphingolipids, a class of lipids that occur primarily in cell membranes.

Consequently, it can be hypothesised that, at both concentrations of DON tested (Figure 7.5a & b), the decreased transport of L-serine and increased transport of palmitate may have resulted in altered sphingolipid synthesis and the accumulation of palmitate, conditions that may possibly have manifested as perforations in the plasma membrane. These results indicate that the high concentration of DON displays a greater effect in terms of alterations in cell surface structure and induction of apoptosis in the HT-29 colorectal cell line. This apoptotic inducing ability of DON has been previously reported (Pestka *et al.*, 1999; Minervini *et al.*, 2004) and is reported to be a consequence of its ability to inhibit protein synthesis at the cellular level (Rotter *et al.*, 1996; Maresca, 2002).

7.3.3.2 The Effect of Deoxynivalenol Following Co-treatment With Curcumin

Scanning electron micrographs of DON and curcumin co-treated cells revealed that in the presence of curcumin (50 μ M), the effects of 5 μ M DON (Figure 7.6a) appeared to be enhanced with the cells displaying a combination of the morphological alterations observed following DON and curcumin treatment. These included increased shrinkage and formation of a microvilli network as well as some clumping of microvilli as observed in curcumin treated and DON treated cells (Figure 7.4c & 7.5a) respectively. It is possible that the curcumin enhanced the 3D-network formation observed in 5 μ M DON treated cells from stage 3B to stage 3A.

The detrimental effect of 50 μ M DON (Figure 7.6b), however, appeared to be overcome in the HT-29 cells with the microvilli although clustered, retaining a semblance of normal morphology. It has been reported that cytoskeletal filaments are the targets of some anticancer drugs (Shen *et al.*, 2003) and it therefore is possible that the curcumin diminished the 3D-network formation with the 50 μ M treated cells from stage 5 to stage 2A. In addition, a loss of membrane integrity was observed and the basal pseudopodia like material also appeared to be affected with the combination treatment appearing less prominent in areas. The results suggest that curcumin (50 μ M) exerts a synergistic effect with DON at the low 5 μ M concentration and a protective effect against DON at the high 50 μ M concentration.

Current literature indicates that DON and curcumin have a number of contrasting properties. Deoxynivalenol has been demonstrated to be an inducer of the ROS-generating enzyme COX-2 (Moon and Pestka, 2002) and has been implicated in lipid peroxidation (Garaleviciene, 2003) while curcumin is a known antioxidant and an inhibitor of COX-2 (Goel *et al.*, 2001).

In addition, DON has been implicated in increased palmitate transport (Maresca *et al.*, 2002) while curcumin has been found to decrease the concentrations of palmitic acid (Akrishnan and Menon, 2001) and increase the levels of arachidonic acid, a compound that stimulates the conversion of sphingomyelin to pro-apoptotic ceramide (Janne and Mayer, 2000; Taraphdar *et al.*, 2001). As a result the effects noted could be due to the interaction of these two compounds.

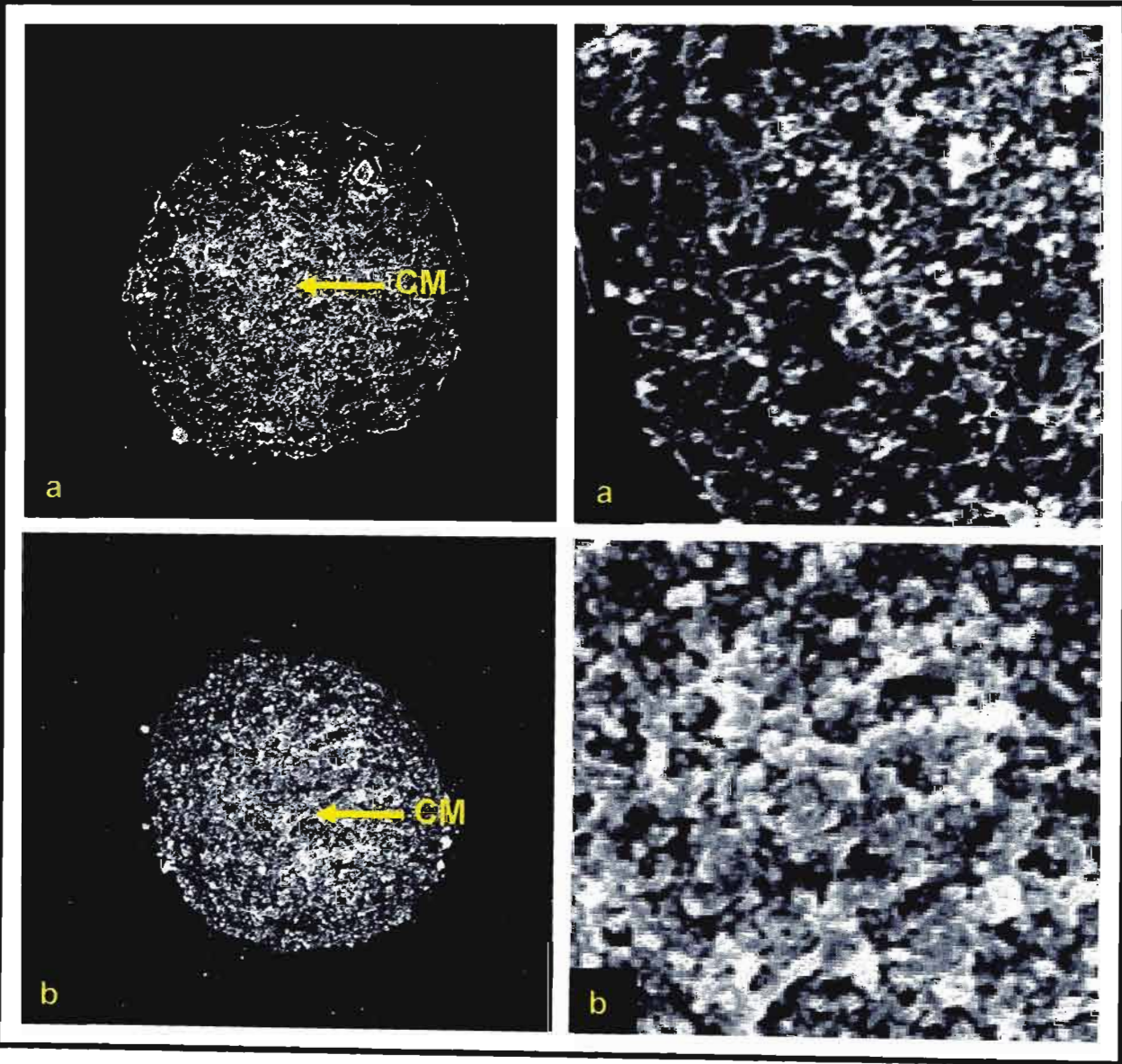


Figure 7.6: Scanning electron micrographs of (a) 5μM and (b) 50μM DON and curcumin co-treated cells displaying clumping of microvilli (CM) (X1000) and enlarged X4 to observe microvilli.

Deoxynivalenol may differ in its ability to induce its effects with varying concentration. As a result, its effect following interaction with curcumin may differ. This may account for the different effects observed following treatment with 5 μ M DON and 50 μ M DON in combination with curcumin.

7.3.4 THE EFFECT OF FUMONISIN B₁

7.3.4.1 The Effect of Fumonisin B₁ Only

Scanning electron micrographs of FB₁ treated cells revealed membrane and pseudopodial damage when compared to the untreated control (Figure 7.4a). This may be a result of excessive degeneration of membrane structure at both concentrations tested. In addition the brush border appeared irregular exhibiting a reduction in microvilli. The microvilli displayed a loss of structural elements and appeared shrunken, collapsed and glutinous. This may be correlated to the formation of a 3D-network of actin filaments (stage 3A/5). This effect was noted at both concentrations tested (Figure 7.7a & b) however it appeared to be advanced at the lower 5 μ M FB₁ concentration.

The degeneration effects noted is a possible consequence of FB₁'s involvement in lipid peroxidation (Abado-Becognee *et al.*, 1998; Mobio *et al.*, 2003) or its interaction with the sphingolipid pathway, more specifically, its ability to inhibit complex sphingolipid synthesis as described by Meivar-Levy (1997) using Swiss 3T3 fibroblasts. In this study, it was established that incubation with FB₁ (20 μ M) causes profound changes in a number of morphological processes associated with the actin cytoskeleton including reduced pseudopodial activity, fewer microvilli and fewer actin-rich "stress fibers", and loss of actin-rich lamellipodia.

These effects on cell morphology were observed to be reversed by the addition of low concentrations of the ganglioside GM₃ suggesting that sphingolipids may be involved in the assembly of both new membrane and the underlying cytoskeleton. The effects described are presumed to be due to alterations in a plasma membrane function since gangliosides are highly enriched in this structure. It is not known whether the effects depend on alterations in a physical property of the membrane or the assembly of new membrane, but these morphological processes require membrane synthesis and assembly (Meivar-Levy *et al.*, 1997).

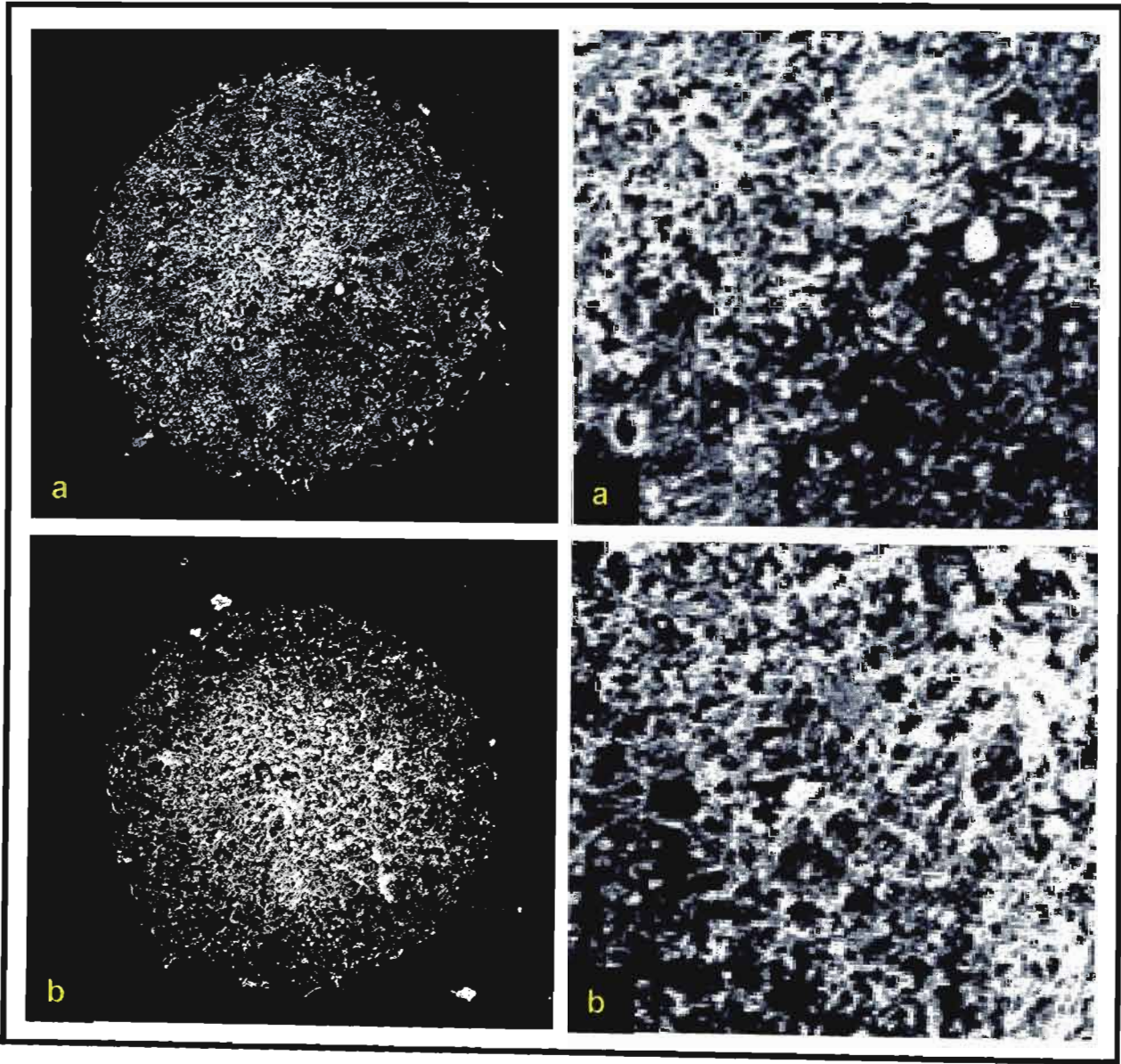


Figure 7.7: Scanning electron micrographs of (a) 5μM and (b) 50μM FB₁ treated cells (X1000) and enlarged X4 to observe microvilli.

These results suggest that FB₁ exhibited an inverse dose dependent effect with the low concentration displaying a greater effect in terms of alterations in cell surface structure in the HT-29 colorectal cell line.

7.3.4.2 The Effect of Fumonisin B₁ Following Co-treatment With Curcumin

Cells treated with 5μM FB₁ in conjunction with curcumin (Figure 7.8a) appeared shrunken in comparison to those treated with 5μM FB₁ only (Figure 7.7a) and exhibited improved cytoskeletal structural support with decreased perforation and increased microvilli formation. The microvilli still appeared stressed indicating that the 3D-network of actin filaments was still present (stage 3A). Pseudopodial activity was observed to diminish further.

Cells treated with the 50μM FB₁ concentration in combination with curcumin (Figure 7.8b) exhibited increased pseudopodial activity and brush border formation similar to the untreated control (Figure 7.4a) although some membrane damage, cytoplasmic leakage and blebbing was noted. As stated earlier, cytoskeletal filaments are the targets of some anticancer drugs (Shen *et al.*, 2003) and it is therefore possible that the curcumin diminished the 3D-network formation (stage 2A).

Fumonisin B₁ has been implicated in lipid peroxidation via the inducement of malondialdehyde production in culture (Abado-Becognee *et al.*, 1998; Mobio *et al.*, 2003), an effect that has been demonstrated to be prevented by antioxidant agents (Mobio *et al.*, 2003). The antioxidant properties of curcumin may therefore provide a explanation for the protective effect observed in terms of membrane alteration.

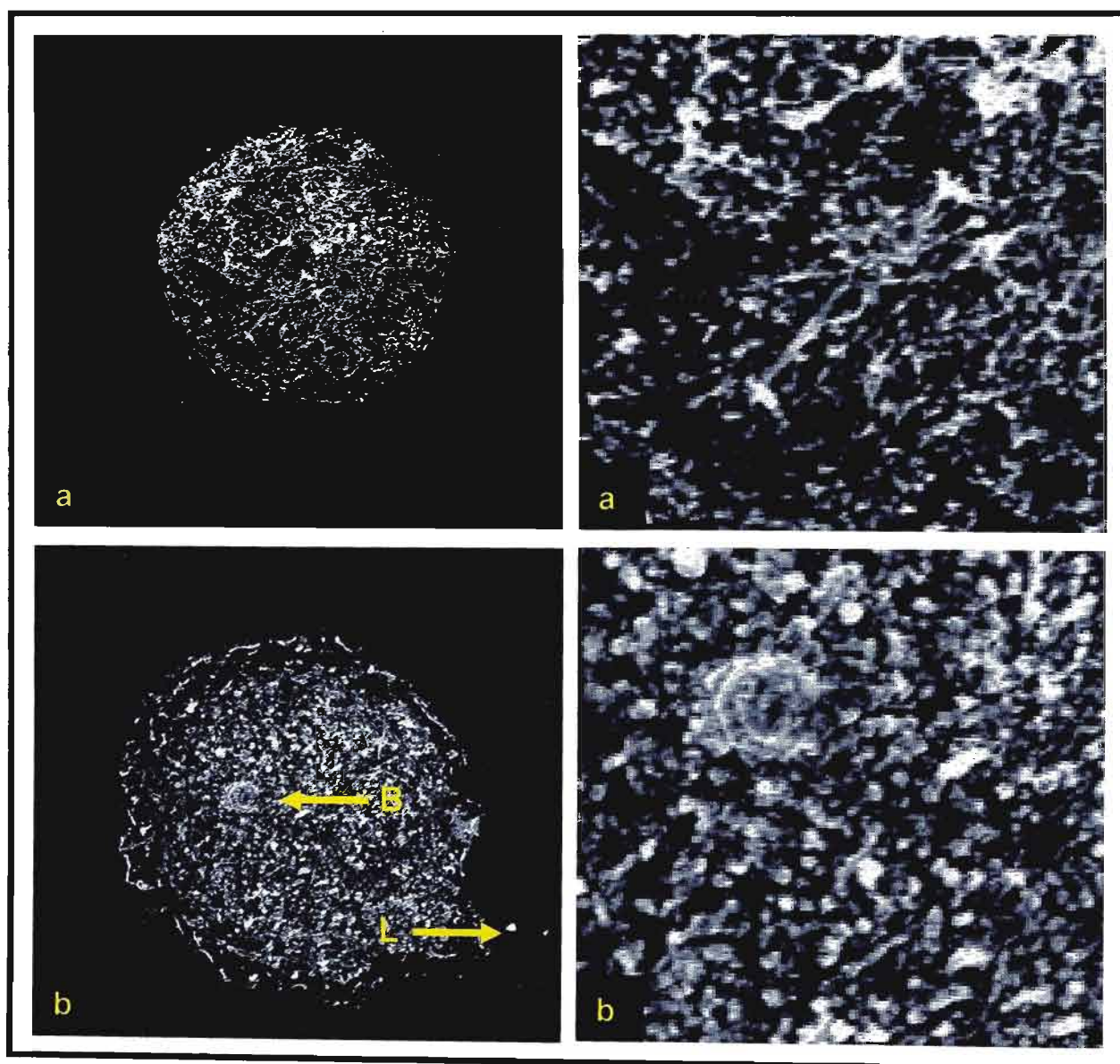


Figure 7.8: Scanning electron micrographs of (a) 5 μ M and (b) 50 μ M FB₁ and curcumin co-treated cells displaying blebbing (B) and cytoplasmic leakage (L) (X1000) and enlarged X4 to observe microvilli.

These results are consistent with the finding that the lower toxin concentration exerts a greater deleterious effect and indicate that curcumin exerts a protective effect with the damaging effect of FB₁ appearing less marked. This was more evident at the higher toxin concentration and may be attributed to the ability of curcumin to reverse the weakened toxin effect.

7.3.5 THE EFFECT OF A DEOXYNIVALENOL AND FUMONISIN B₁ MIXTURE

7.3.5.1 The Effect of a Deoxynivalenol and Fumonisin B₁ Mixture Only

Scanning electron micrographs of cells treated with a DON and FB₁ (DFB₁) mixture (5μM; (Figure 7.9a) displayed brush border formation resembling that of the solvent control (Figure 7.4b) although the microvilli appeared slightly swollen and clumped towards the centre. This may be attributed to the formation of actin granules (stage 2A). The pseudopodial activity appeared reduced and the membrane perforations noted when treated individually with DON (Figure 7.5a) and FB₁ (Figure 7.7a) were not observed. Cells treated with 50μM DFB₁ displayed similar membrane perforation, abnormal brush border formation with stressed microvilli and possible blebbing as seen in the FB₁ (50μM) treated cells (Figure 7.7b) but appeared shrunken. This may be attributed to the formation of 3D-network of actin filaments resulting in the disintegration into apoptotic bodies (stage 3A/5).

At the low 5μM concentration, the combined effect of the toxins appeared antagonistic. Deoxynivalenol has been reported to decrease L-serine transport and increase palmitate transport in HT-29-D4 cells at concentrations below 10μM (Maresca *et al.*, 2002) while FB₁, in addition to its ability to inhibit sphingolipid synthesis, has been demonstrated to block the deleterious effects of palmitic acid on B-cell turnover at a concentration of 15μM (Maedler *et al.*, 2003). There is therefore a possibility that the antagonistic effect observed at this particular concentration is a consequence of their combined interaction. At the high 50μM concentration of DFB₁, the combined effect of the toxins appeared less than additive. This may be due to the inability of the higher FB₁ concentration to cope with the increased palmitic acid transport at higher DON concentration as reported by Maresca *et al.* (2002).

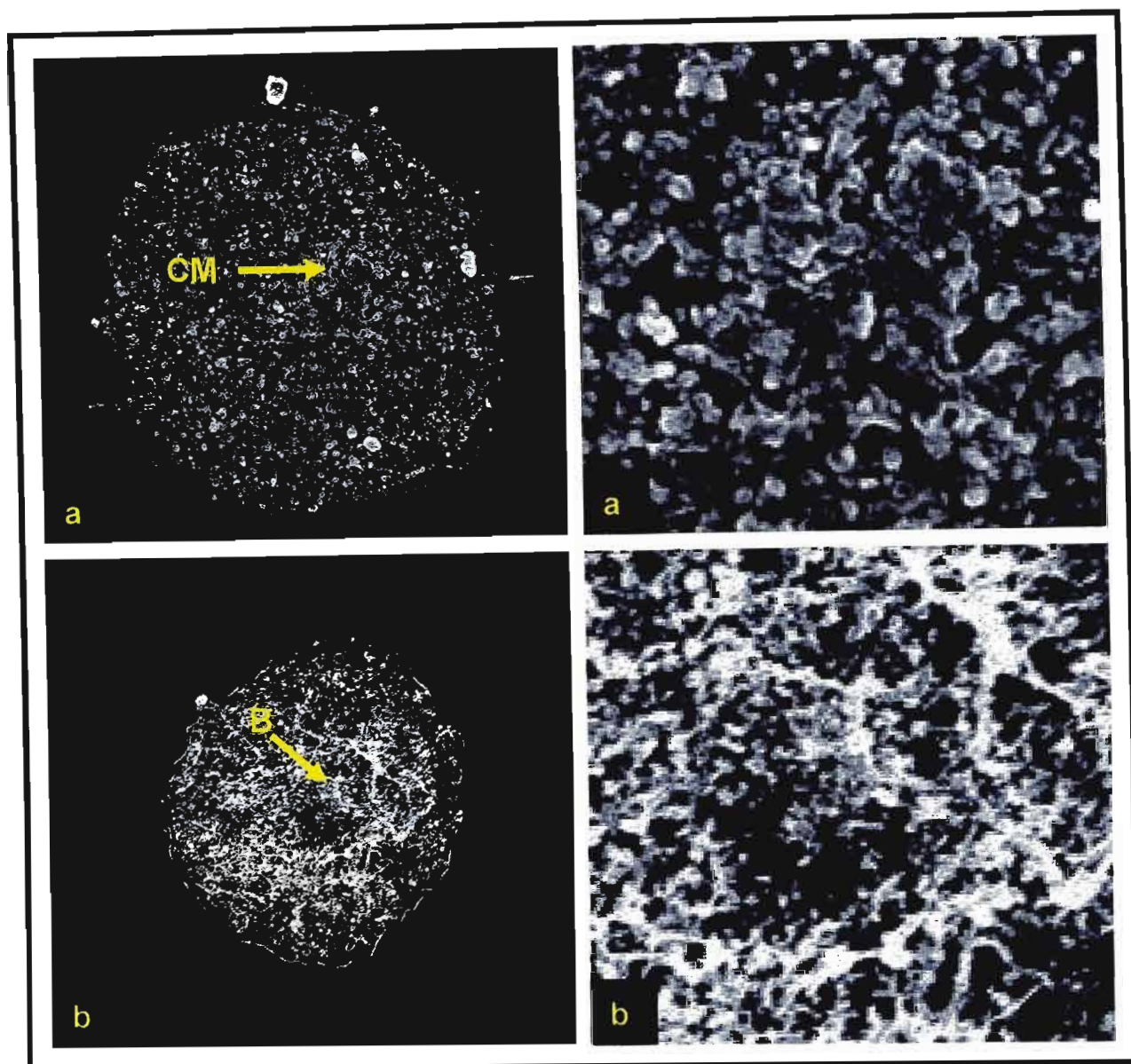


Figure 7.9: Scanning electron micrographs of the (a) 5μM and (b) 50μM DFB₁ treated cells displaying blebbing (B) and clumping (CM) (X1000) and enlarged X4 to observe microvilli.

These results indicate that, in combination, the toxins exert an antagonistic effect at the 5μM concentration, reducing the individual toxins effects in terms of membrane damage and a less than additive effect at the 50μM concentration. The less than additive toxicity of these two mycotoxins in combination has been previously reported by Kubena *et al.* (1997) in a study using broiler chicks.

7.3.5.2 The Effect of a Deoxynivalenol and Fumonisin B₁ Mixture Following Co-treatment With Curcumin

The 5 μ M DFB₁ and curcumin treated cells (Figure 7.10a) displayed external morphology similar to that exhibited by 5 μ M DFB₁ only treated cells (Figure 7.9a). The cells treated with the 50 μ M DFB₁ concentration (Figure 7.10b) displayed similar brush border formation as observed in the 5 μ M DFB₁ treated cells but displayed an increased number of apoptotic bodies blebbing off the surface (stage 2D). These results indicated that the presence of curcumin did not appear to exert any protective effect in the presence of the low 5 μ M DFB₁ concentration of both mycotoxins (DFB₁) (Figure 7.10a) when compared to the DFB₁ only treated cells (Figure 7.9a). This result is consistent with the effects of curcumin observed following the co-administration of curcumin and each individual toxin at the same low concentration (Figure 7.6a & 7.8a) when compared to the individual toxin treated cells (Figure 7.5a & 7.7a). This may be attributed to the inability of curcumin to ameliorate the adverse individual effects of both toxins at this concentration.

In the presence of the high 50 μ M DFB₁ concentration (Figure 7.10b), however, curcumin appeared to exhibit a protective effect improving the brush border formation when compared to the DFB₁ only treated cells (Figure 7.9b) however, it also appeared to promote the induction of apoptosis. The addition of curcumin appears to cancel out the effects of the toxins and to induce the appearance of normal morphological features. This apparent cytoprotective effect is in agreement with that observed following co-administration with curcumin and each individual toxin at the same high concentration (Figure 7.6b & 7.8b) when compared to the individual toxin treated cells (Figure 7.5b & 7.7b). The ability of curcumin to exert a cytoprotective effect, has been previously observed in rat hepatocytes and NGI08-15 cells following treatment with paracetamol and H₂O₂ respectively and has been attributed to its ability to its potent antioxidant properties (Donatus *et al.*, 1990; Mahakunakom *et al.*, 2003).

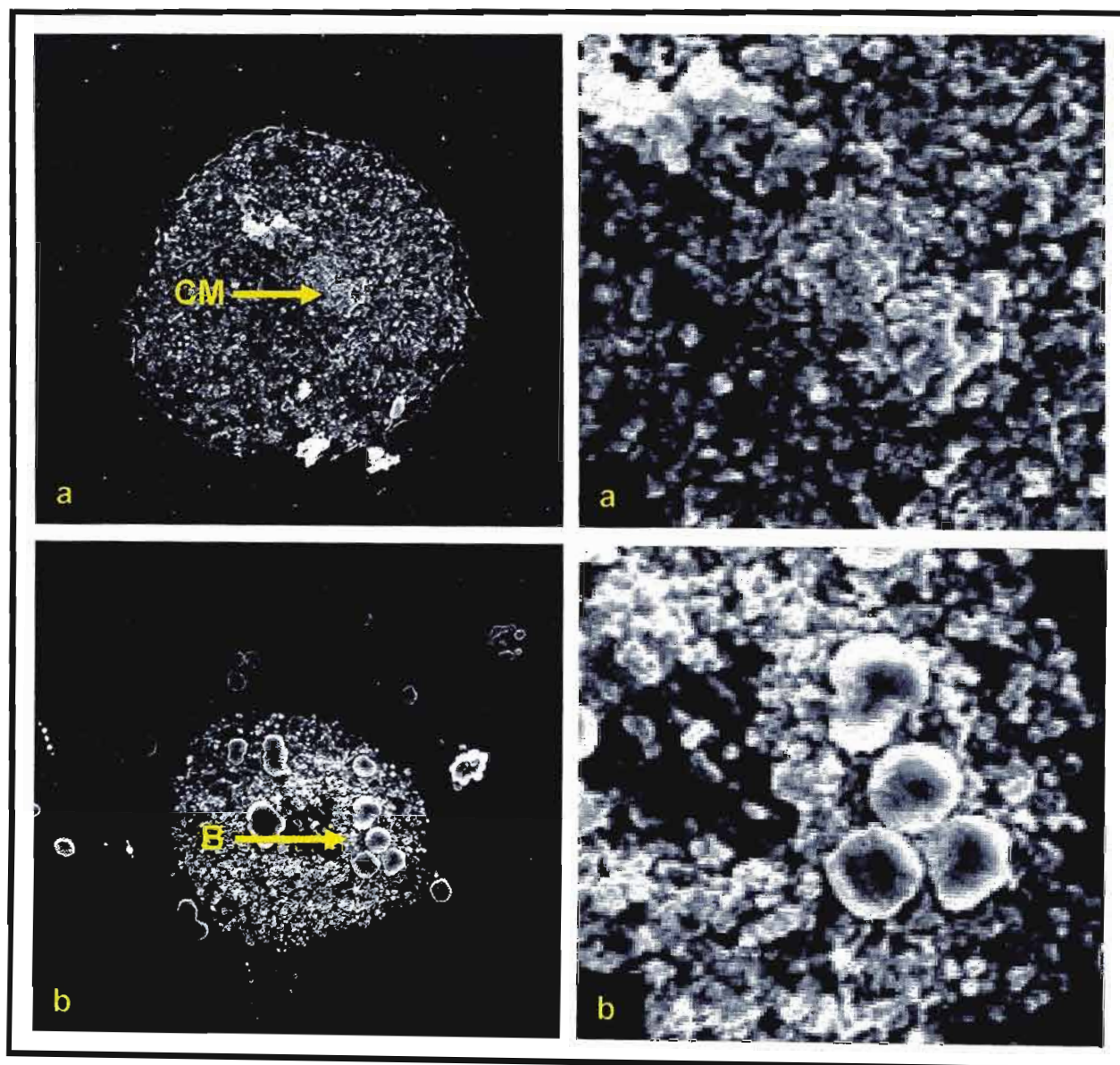


Figure 7.10: Scanning electron micrographs of (a) 5 μ M and (b) 50 μ M DFB₁ and curcumin treated cells displaying blebbing (B) and clumping (CM) (X1000) and enlarged X4 to observe microvilli.

It may be hypothesised that the induction of apoptosis occurs as a consequence of curcumin being unable to cope with the injurious effects inflicted on the cell by the toxins at this concentration.

7.4 CONCLUSION

This investigation demonstrated that DON exhibited a deleterious effect on the cell membrane that increased with increasing concentration while FB₁ exhibited the opposite effect, with the low 5µM concentration displaying greater damage than the high 50µM in terms of microvilli morphology and cell surface alterations in the HT-29 colorectal cell line. A combination of the two toxins (DFB₁) appeared to exhibit an antagonistic effect at the 5µM concentration reducing the individual effect of each toxin and a less than additive effect at the 50µM concentration.

Curcumin itself exhibited an adverse effect on the HT-29 cells and co-treatment with curcumin appeared to enhance the deleterious effect of 5µM DON and antagonise the effects of 50µM DON on this cell line. The antagonistic effect of curcumin was also noted in the 5µM and 50µM FB₁ treated cells although the effect was prominent in the 50µM FB₁ treated cells. No significant effect was noted following co-treatment with curcumin and 5µM DFB₁ although curcumin appeared to antagonise the effect of 50µM DFB₁ and to promote apoptosis.

The scanning electron microscope has a large depth of field, allowing a large amount of the sample to be in focus at one time and produces images of high resolution, permitting closely spaced features to be examined at a high magnification. In addition, preparation of the samples is relatively easy as the sample need only be conductive and topographic detail can be readily interpreted using optical analogy. This combination of high magnification, large depth of focus, superior resolution and ease of observation makes the SEM one of the most useful research instruments.

CHAPTER 8

CONCLUSION

A substantial amount of evidence indicates that chemicals present in the environment pose a significant toxic and potentially carcinogenic hazard and consequently affects almost every sphere of human activity in industrialised society. Diet represents a major source of these compounds and the colon faces a high potential of exposure as a result of its normal functioning, an occurrence that may play a role in colon carcinogenesis. In this study, the HT-29 cell culture system was used to assess the effects of the mycotoxins deoxynivalenol and fumonisin B₁ as well as the possible cytoprotective effects of curcumin on colonic cells.

The results of this study indicate that deoxynivalenol displays a dose dependent effect on HT-29 colon adenocarcinoma cells by exerting a cytotoxic effect at the high concentration that may be a consequence of its ability to induce apoptosis as demonstrated by its ability to induce DNA fragmentation and morphological features characteristic of apoptosis as evidenced by the SCGE assay, fluorescence and scanning electron microscopy respectively. Fumonisin B₁ was demonstrated to exert a dose dependent proliferative effect on this particular cell line. The fragmentation of DNA and morphological features of apoptosis were also observed. These effects were more pronounced at the lower concentration indicating that low concentrations of FB₁ may induce apoptosis and are possibly indicative of FB₁ exerting a stronger toxic effect at the low concentration. A combination of DON and FB₁ displayed similar effects to those exhibited by DON in terms of cytotoxicity and DNA fragmentation. Analysis of the cell surface (SEM) demonstrated an antagonistic effect at the 5µM concentration reducing the individual effect of each toxin and a less than additive effect at the 50µM concentration. These results indicate that DON is able to antagonise the effects of FB₁ at the concentrations tested.

Curcumin (50 μ M) itself, was found to decrease cellular viability (25.44%), cause DNA fragmentation, induce apoptosis and alter microvilli structure. In combination with the toxins, curcumin appeared to alleviate the cytotoxic effect imposed by both DON and DFB₁ while inhibiting the proliferative effect exerted by FB₁. It increased the severity of DNA damage in all instances. Fluorescent microscopy indicated that the presence of curcumin demonstrated no observable effect on DON and DFB₁ treated cells in terms of cellular morphology and proliferation but decreased the proliferation exerted by FB₁ as noted using the MTT assay. Scanning electron microscopy demonstrated that curcumin appeared to enhance the membrane alteration exerted by the low DON concentration and antagonise the effects of the high concentration. This antagonistic effect of curcumin was also noted in the FB₁ treated cells although the effect was prominent in the high concentration. No significant effect was noted following co-treatment with curcumin and 5 μ M DFB₁ although curcumin appeared to antagonise the effect of 50 μ M DFB₁ and to promote apoptosis

Deoxynivalenol and FB₁ are frequently found in maize, a major component of the diet of rural populations in South Africa and the fact that low concentrations of DON and FB₁ (5 μ M) were sufficient to induce apoptosis in this cell line suggests a danger from natural contamination by these toxins. Curcumin appeared to exhibit some protective effect when co-administered with the 50 μ M toxin concentration and warrants further investigation with regards to its cytoprotective activities in the presence of these mycotoxins as it could present a promising candidate for a natural chemoprotective agent in the armamentarium against mycotoxin induced cancers.

REFERENCES

- Abado-Becognee, K., Mobio, T. A., Ennamany, R., Fleurat-Lessard, F., Shier, W. T., Badria, F., and Creppy, E. E. (1998). Cytotoxicity of fumonisin B₁: implication of lipid peroxidation and inhibition of protein and DNA syntheses. *Arch Toxicol* **72**, 233-236.
- A.D.A.M. Medical Illustration Team (2002). The Structure of the Colon. University of Maryland Medical Center [online]. Available from: <http://www.umm.edu/imagepages/19218.htm>. Accessed: 27 March 2004.
- Ahn, E. H., and Schroeder, J. J. (2002). Sphingoid bases and ceramide induce apoptosis in HT-29 and HCT-116 human colon cancer cells. *Exp Biol Med (Maywood)* **227**, 345-353.
- Ahsan, H., Parveen, N., Khan, N. U., and Hadi, S. M. (1999). Pro-oxidant, anti-oxidant and cleavage activities on DNA of curcumin and its derivatives demethoxycurcumin and bisdemethoxycurcumin. *Chem Biol Interact* **121**, 161-175.
- Akrishnan, V. R., and Menon, V. P. (2001). Potential role of antioxidants during ethanol-induced changes in the fatty acid composition and arachidonic acid metabolites in male Wistar rats. *Cell Biol Toxicol* **17**, 11-22.
- Allan, B. (2003). SEM specimen preparation. Humboldt State University: Department of Biology [online]. Available from: http://sorrel.humboldt.edu/~wval1/images%20spec%20prep%20SEM_spec_prep_summary.g f. Accessed: 13 August 2004
- Arms, K., and Camp, P. S. (1995). Biology, pp. 89-90. Harcourt Brace College Publishers, New York.

- Bauch, T., Bocker, W., Mallek, U., Muller, W. U., and Streffer, C. (1999). Optimization and standardization of the "comet assay" for analyzing the repair of DNA damage in cells. *Strahlenther Onkol* **175**, 333-340.
- Beasley, V. (1999). Trichothecenes. In *Veterinary Toxicology*. International Veterinary Information Service [online]. Available from:
http://www.ivis.org/advances/Beasley/Cpt12c/chapter_frm.asp?LA=1 Accessed: 23 March 2002.
- Bernas, T., and Dobrucki, J. W. (2000). The role of plasma membrane in bio-reduction of two tetrazolium salts, MTT, and CTC. *Arch Biochem Biophys* **380**, 108-116.
- Bernas, T., and Dobrucki, J. (2002). Mitochondrial and nonmitochondrial reduction of MTT: interaction of MTT with TMRE, JC-1, and NAO mitochondrial fluorescent probes. *Cytometry* **47**, 236-242.
- Berridge, M. V., and Tan, A. S. (1993). Characterization of the cellular reduction of 3-(4,5-dimethylthiazol-2-yl)-2,5-diphenyltetrazolium bromide (MTT): subcellular localization, substrate dependence, and involvement of mitochondrial electron transport in MTT reduction. *Arch Biochem Biophys* **303**, 474-482.
- Berridge, M. V., Tan, A. S., McCoy, K. D., and Wang, R. (1996). The Biochemical and Cellular Basis of Cell proliferation Assays That Use Tetrazolium salts. *Biochemica* **4**, 14-19.
- Bhat, R. V., Beedu, S. R., Ramakrishna, Y., and Munshi, K. L. (1989). Outbreak of trichothecene mycotoxicosis associated with consumption of mould-damaged wheat production in Kashmir Valley, India. *Lancet* **1**, 35-37.

- Bhaumik, S., Anjum, R., Rangaraj, N., Pardhasaradhi, B. V., and Khar, A. (1999). Curcumin mediated apoptosis in AK-5 tumor cells involves the production of reactive oxygen intermediates. *FEBS Lett* **456**, 311-314.
- Bigwood, J. (2000). The Drug War's Fungal "Solution" in Latin America [online]. Available from: <http://jeremybigwood.net/Lectures/GWU-WOLA-JB/GWUNov2000.htm>. Accessed: 14 April 2003.
- Biowhittaker cell biology products catalogue (2002). Biowhittaker. 149-156.
- Blasiak, J., Trzeciak, A., Malecka-Panas, E., Drzewoski, J., Iwanienko, T., Szumiel, I., and Wojewodzka, M. (1999). DNA damage and repair in human lymphocytes and gastric mucosa cells exposed to chromium and curcumin. *Teratog Carcinog Mutagen* **19**, 19-31.
- Blunden, G., Roch, O. G., Rogers, D. J., Coker, R. D., Bradburn, N., and John, A. E. (1991). Mycotoxins in food. *Med Lab Sci* **48**, 271-282.
- Boeira, L. S., Bryce, J. H., Stewart, G. G., and Flannigan, B. (2000). The effect of combinations of Fusarium mycotoxins (deoxynivalenol, zearalenone and fumonisin B₁) on growth of brewing yeasts. *J Appl Microbiol* **88**, 388-403.
- Boersma, A. W., Nooter, K., Oostrum, R. G., and Stoter, G. (1996). Quantification of apoptotic cells with fluorescein isothiocyanate-labeled annexin V in chinese hamster ovary cell cultures treated with cisplatin. *Cytometry* **24**, 123-130.
- Bouhet, S., Hourcade, E., Loiseau, N., Fikry, A., Martinez, S., Roselli, M., Galtier, P., Mengheri, E., and Oswald, I. P. (2004). The mycotoxin fumonisin B₁ alters the proliferation and the barrier function of porcine intestinal epithelial cells. *Toxicol Sci* **77**, 165-171.

- Bus, P. J., Verspaget, H. W., Lamers, C. B., and Griffioen, G. (2000). Chemoprevention of colorectal cancer by non-steroidal anti-inflammatory drugs. *Scand J Gastroenterol Suppl*, 101-104.
- Caloni, F., Spotti, M., Pompa, G., Zucco, F., Stamatì, A., and De Angelis, I. (2002). Evaluation of Fumonisin B₁ and its metabolites absorption and toxicity on intestinal cells line Caco-2. *Toxicon* **40**, 1181-1188.
- Campana, A. (2004). *Curcuma longa* (Zingiberaceae). Geneva Foundation for Medical Education and Research [online]. Available from: http://www.gfmer.ch/TMCM/Atlas_medicinal_plants/Curcuma_longa.htm. Accessed: 27 March 2004
- Canady, R. A., Coker, R. D., Egan, S.K., Krska, R., Kuiper-Goodman, T., Olsen, M., Pestka, J., Resnik, S., and Schlatter, J. (2001). Deoxynivalenol. Inchem Home [online]. Available from: <http://www.inchem.org/documents/jecfa/jecmono/v47je05.htm>. Accessed: 23 June 2003.
- Caprette, D.R. (2003). Using a Counting Chamber. Rice University: Department of Biochemistry and Cell Biology [online]. Available from: <http://www.ruf.rice.edu/~bioslabs/methods/microscopy/cellcounting.html>. Accessed 23 September 2004.
- Carmichael, J., DeGraff, W. G., Gazdar, A. F., Minna, J. D., and Mitchell, J. B. (1987). Evaluation of a tetrazolium-based semiautomated colorimetric assay: assessment of chemosensitivity testing. *Cancer Res* **47**, 936-942.

- Cederbaum, A. I. (2001). Introduction-serial review: alcohol, oxidative stress and cell injury. *Free Radic Biol Med* **31**, 1524-1526.
- Cell Lines (2003). American Type Culture Collection [online]. Available from: <http://www.atcc.org/SearchCatalogs/longview.cfm?view=ce,6003585,HTB-38&text=ht29&max=20>. Accessed: 11 May 2003.
- Chambers, R. W. (1985). Chemical carcinogenesis: a biochemical overview. *Clin Biochem* **18**, 158-168.
- Chang, S. H., Garcia, J., Melendez, J. A., Kilberg, M. S., and Agarwal, A. (2003). Haem oxygenase 1 gene induction by glucose deprivation is mediated by reactive oxygen species via the mitochondrial electron-transport chain. *Biochem J* **371**, 877-885.
- Charoenpornsook, K., Fitzpatrick, J. L., and Smith, J. E. (1998). The effects of four mycotoxins on the mitogen stimulated proliferation of bovine peripheral blood mononuclear cells in vitro. *Mycopathologia* **143**, 105-111.
- Chattopadhyay, I., Biswas, K., Bandyopadhyay, U., and Banerjee, R. K. (2004). Turmeric and curcumin: Biological actions and medicinal applications. *Current Science* **87**, 44-53.
- Chauhan, D. P. (2002). Chemotherapeutic potential of curcumin for colorectal cancer. *Curr Pharm Des* **8**, 1695-1706.
- Chen, A. Y., Yu, C., Gatto, B., and Liu, L. F. (1993). DNA minor groove-binding ligands: a different class of mammalian DNA topoisomerase I inhibitors. *Proc Natl Acad Sci U S A* **90**, 8131-8135.

- Childs, G. V. (1995). An Electron microscope view of membranes: Surface specializations. University of Texas Medical Branch: Cell Biology Graduate Program [online]. Available from: <http://www.cytochemistry.net/Cell-biology/membrane3.htm>. Accessed: 27 March 2004.
- Chu, F. S., and Li, G. Y. (1994). Simultaneous occurrence of fumonisin B₁ and other mycotoxins in moldy corn collected from the People's Republic of China in regions with high incidences of esophageal cancer. *Appl Environ Microbiol* **60**, 847-852.
- Chuang, S. E., Kuo, M. L., Hsu, C. H., Chen, C. R., Lin, J. K., Lai, G. M., Hsieh, C. Y., and Cheng, A. L. (2000). Curcumin-containing diet inhibits diethylnitrosamine-induced murine hepatocarcinogenesis. *Carcinogenesis* **21**, 331-335.
- Cohen, E., Ophir, I., and Shaul, Y. B. (1999). Induced differentiation in HT29, a human colon adenocarcinoma cell line. *J Cell Sci* **112 (Pt 16)**, 2657-2666.
- Collins, A. R., Dusinska, M., and Horska, A. (2001). Detection of alkylation damage in human lymphocyte DNA with the comet assay. *Acta Biochim Pol* **48**, 611-614.
- Coulombe, R. A., Jr. (1993). Biological action of mycotoxins. *J Dairy Sci* **76**, 880-891.
- Cox, R. P., and Gesner, B. M. (1965). Effect of simple sugars on the morphology and growth pattern of mammalian cell cultures. *Proc Natl Acad Sci U S A* **54**, 1571-1579.
- Cunningham, G. (2004). Clinical Description of the Effects of Fusarium Mycotoxin-Vomitoxin in a Breeding Company Farrow to Finish Operation. Alberta Government: Agriculture, Food and Rural Development [online]. Available from: [http://www1.agric.gov.ab.ca/\\$department/deptdocs.nsf/all/pig8371](http://www1.agric.gov.ab.ca/$department/deptdocs.nsf/all/pig8371). Accessed: 27 August 2004.

Desjardins, A. E., Hohn, T. M., and McCormick, S. P. (1993). Trichothecene biosynthesis in *Fusarium* species: chemistry, genetics, and significance. *Microbiol Rev* **57**, 595-604.

Dinkova-Kostova, A. T., and Talalay, P. (1999). Relation of structure of curcumin analogs to their potencies as inducers of Phase 2 detoxification enzymes. *Carcinogenesis* **20**, 911-914.

DNA Damage Monitoring: Genotoxicity & Cytotoxicity Testing Using the Comet Assay (Comet method slide) (2002) [online]. SPAWAR Systems Center: Biomarker Laboratory. Available from: <http://environ.nosc.mil/randd/BiomarkerLab/DNA damage.htm>. Accessed: 14 June 2003.

Donatus, I. A., Sardjoko, and Vermeulen, N. P. (1990). Cytotoxic and cytoprotective activities of curcumin. Effects on paracetamol-induced cytotoxicity, lipid peroxidation and glutathione depletion in rat hepatocytes. *Biochem Pharmacol* **39**, 1869-1875.

Dragan, Y. P., Bidlack, W. R., Cohen, S. M., Goldsworthy, T. L., Hard, G. C., Howard, P. C., Riley, R. T., and Voss, K. A. (2001). Implications of apoptosis for toxicity, carcinogenicity, and risk assessment: fumonisin B(1) as an example. *Toxicol Sci* **61**, 6-17.

Dugyala, R. R., Sharma, R. P., Tsunoda, M., and Riley, R. T. (1998). Tumor necrosis factor- α as a contributor in fumonisin B₁ toxicity. *J Pharmacol Exp Ther* **285**, 317-324.

Electron Microscopy Services (1999). MACS Lab Incorporated [online]. Available from: <http://www.macslab.com/electron.html>. Accessed: 17 August 2003.

Elwood, A. (2004). Glutamine stability in cell culture. *Art to Science. A publication on advancements in tissue and cell culture technology* **23**, 6-10.

- Etique, N., Chardard, D., Chesnel, A., Merlin, J. L., Flament, S., and Grillier-Vuissoz, I. (2004). Ethanol stimulates proliferation, ERalpha and aromatase expression in MCF-7 human breast cancer cells. *Int J Mol Med* **13**, 149-155.
- Etzel, R. A. (2002). Mycotoxins. *Jama* **287**, 425-427.
- Events in Apoptosis (2002). University of Florida: College of Veterinary Medicine [online]. Available from: <http://www.vetmed.ufl.edu/path/pbteach/wlc/vem5161/apopl.jpg>. Accessed: 19 April 2004.
- Fazekas, B., Kis, M., and Hajdu, E. T. (1996). Data on the contamination of maize with fumonisin B₁ and other fusariotoxins in Hungary. *Acta Vet Hung* **44**, 25-37.
- Gabrielson, E. W., and Harris, C. C. (1985). Use of cultured human tissues and cells in carcinogenesis research. *J Cancer Res Clin Oncol* **110**, 1-10.
- Galvano, F., Campisi, A., Russo, A., Galvano, G., Palumbo, M., Renis, M., Barcellona, M. L., Perez-Polo, J. R., and Vanella, A. (2002a). DNA damage in astrocytes exposed to fumonisin B₁. *Neurochem Res* **27**, 345-351.
- Galvano, F., Russo, A., Cardile, V., Galvano, G., Vanella, A., and Renis, M. (2002b). DNA damage in human fibroblasts exposed to fumonisin B(1). *Food Chem Toxicol* **40**, 25-31.
- Garaleviciene, D. (2003). Effect of Antioxidant Preparation "Oxynil" on Health Status and Productivity of Laying Hens Fed Naturally Moulded Feed. *Veterinarija Ir Zootechnika* **24**, 22-29.
- Garcea, G., Dennison, A. R., Steward, W. P., and Berry, D. P. (2003). Chemoprevention of gastrointestinal malignancies. *ANZ J Surg* **73**, 680-686.

- Gelderblom, W. C., Kriek, N. P., Marasas, W. F., and Thiel, P. G. (1991). Toxicity and carcinogenicity of the *Fusarium moniliforme* metabolite, fumonisin B₁, in rats. *Carcinogenesis* **12**, 1247-1251.
- Gelderblom, W. C., Semple, E., Marasas, W. F., and Farber, E. (1992). The cancer-initiating potential of the fumonisin B mycotoxins. *Carcinogenesis* **13**, 433-437.
- Gerlier, D., and Thomasset, N. (1986). Use of MTT colorimetric assay to measure cell activation. *J Immunol Methods* **94**, 57-63.
- Gewies, A. (2003). ApoReview. In *Introduction to Apoptosis*, pp. 1-26.
- Gimeno, A. (2000). Mycotoxins - Deoxynivalenol, a Risk Mycotoxin for Children. Analytical Methods. Deoxynivalenol Levels in Wheat-Based Food Products. Egormix.com [online]. Available from: http://www.engormix.com/e_articles_mycotoxins.asp?ID=58. Accessed 23 July 2004.
- Giovannelli, L., Cozzi, A., Guarnieri, I., Dolara, P., and Moroni, F. (2002). Comet Assay as a Novel Approach for Studying DNA Damage in Focal Cerebral Ischemia: Differential Effects of NMDA Receptor Antagonists and Poly(ADP-Ribose) Polymerase Inhibitors. *Journal of Cerebral Blood Flow & Metabolism* **22**, 697-704.
- Goel, A., Boland, C. R., and Chauhan, D. P. (2001). Specific inhibition of cyclooxygenase-2 (COX-2) expression by dietary curcumin in HT-29 human colon cancer cells. *Cancer Lett* **172**, 111-118.
- Gorst-Allman, C. P., Steyn, P. S., Vleggaar, R., and Rabie, C. J. (1985). Structure Elucidation of a Novel Trichothecene Glycoside using ¹H and ¹³C Nuclear Magnetic Resonance Spectroscopy. *Journal of the Chemical Society-Perkin Transactions* **4**, 1553-1555.

- Hannun, Y. A., and Obeid, L. M. (2002). The Ceramide-centric universe of lipid-mediated cell regulation: stress encounters of the lipid kind. *J Biol Chem* **277**, 25847-25850.
- He, Q., Riley, R. T., and Sharma, R. P. (2002). Pharmacological antagonism of fumonisin B₁ cytotoxicity in porcine renal epithelial cells (LLC-PK1): a model for reducing fumonisin-induced nephrotoxicity in vivo. *Pharmacol Toxicol* **90**, 268-277.
- Hellman, B., Vaghef, H., Friis, L., and Edling, C. (1997). Alkaline single cell gel electrophoresis of DNA fragments in biomonitoring for genotoxicity: an introductory study on healthy human volunteers. *Int Arch Occup Environ Health* **69**, 185-192.
- Hernández, F., and Cannon, M. (1981). Inhibition of Protein synthesis in *Saccharomyces cerevisiae* by the 12,13-epoxytrichothecenes Trichodermol, Diacetoxyscirpenol and Verrucarín A: Reversibility of the Effects. *The Journal of Antibiotics* **35**, 875-881.
- Holy, J. (2004). Curcumin inhibits cell motility and alters microfilament organization and function in prostate cancer cells. *Cell Motil Cytoskeleton* **58**, 253-268.
- HT-29 (2001). DSMZ-Deutsche Sammlung von Mikroorganismen und Zellkulturen GmbH [online]. Available from: <http://www.dsmz.de/mutz/mutz299.htm>. Accessed: 12 April 2002.
- HT-29 Cell (2004). Medical Dictionary Online [online]. Available from: <http://www.online-medical-dictionary.org/HT%2D29+Cell.asp?q=HT%2D29+Cell>. Accessed: 17 February 2004.
- Instanes, C., and Hetland, G. (2004). Deoxynivalenol (DON) is toxic to human colonic, lung and monocytic cell lines, but does not increase the IgE response in a mouse model for allergy. *Toxicology* **204**, 13-21.

- Jacobson, E., and Sernka, T. (Eds.) (1983). *Gastrointestinal Physiology - the essentials (2nd ed.)*, pp. 100-120. Williams and Wilkins, Baltimore:USA.
- Janne, P. A., and Mayer, R. J. (2000). Chemoprevention of colorectal cancer. *N Engl J Med* **342**, 1960-1968.
- Jaruga, E., Sokal, A., Chrul, S., and Bartosz, G. (1998). Apoptosis-independent alterations in membrane dynamics induced by curcumin. *Exp Cell Res* **245**, 303-312.
- Jee, S. H., Shen, S. C., Tseng, C. R., Chiu, H. C., and Kuo, M. L. (1998). Curcumin induces a p53-dependent apoptosis in human basal cell carcinoma cells. *J Invest Dermatol* **111**, 656-661.
- Kam, P. C., and Ferch, N. I. (2000). Apoptosis: mechanisms and clinical implications. *Anaesthesia* **55**, 1081-1093.
- Kasuga, F., Hara-Kudo, Y., Saito, N., Kumagai, S., and Sugita-Konishi, Y. (1998). In vitro effect of deoxynivalenol on the differentiation of human colonic cell lines Caco-2 and T84. *Mycopathologia* **142**, 161-167.
- Kawamori, T., Lubet, R., Steele, V. E., Kelloff, G. J., Kaskey, R. B., Rao, C. V., and Reddy, B. S. (1999). Chemopreventive effect of curcumin, a naturally occurring anti-inflammatory agent, during the promotion/progression stages of colon cancer. *Cancer Res* **59**, 597-601.
- Kimura, M., Tokai, T., O'Donnell, K., Ward, T. J., Fujimura, M., Hamamoto, H., Shibata, T., and Yamaguchi, I. (2003). The trichothecene biosynthesis gene cluster of *Fusarium graminearum* F15 contains a limited number of essential pathway genes and expressed non-essential genes. *FEBS Lett* **539**, 105-110.

- Kirlin, W. G., Cai, J., DeLong, M. J., Patten, E. J., and Jones, D. P. (1999). Dietary compounds that induce cancer preventive phase 2 enzymes activate apoptosis at comparable doses in HT29 colon carcinoma cells. *J Nutr* **129**, 1827-1835.
- Kline, D. (1999). Introduction to Fluorescence Microscopy. Cell Biology: Microscopy Labs [online]. Available from: <http://dept.kent.edu/projects/cell/FLUORO.HTM>. Accessed: 15 April 2003.
- Klipski, K., Majewski, S., Kinsner, A., and Sladowski, D. (2003). Principle of the MTT test. Invitox Life [online]. Available from: <http://www.ib.amwaw.edu.pl/home/dslado/video/mtt.html>. Accessed: 14 June 2003.
- Knasmüller, S., Bresgen, N., Kassie, F., Mersch-Sundermann, V., Gelderblom, W., Zohrer, E., and Eckl, P. M. (1997). Genotoxic effects of three *Fusarium* mycotoxins, fumonisin B₁, moniliformin and vomitoxin in bacteria and in primary cultures of rat hepatocytes. *Mutat Res* **391**, 39-48.
- Kovvali, G., Shiff, S., Telang, N., Das, K., Kohgo, Y., Narayan, S., and Li, H. (2003). Carcinogenesis: The more we seek to know the more we need to know - Challenges in the post Genomic Era. *J Carcinog* **2**, 1.
- Krause, G., Wolz, L., and Scherer, G. (2001). Performing the "comet assay" for genetic toxicology applications. In *Life Science News*, pp. 1-3.
- Krebsfaenger, N. (2001) The Comet Assay. GenPharmTox [online]. Available from: <http://www.genpharmtox.com/downloads/AssaySheetsCometAssay.pdf>. Accessed: 14 June 2003.

- Kubena, L. F., Edrington, T. S., Harvey, R. B., Buckley, S. A., Phillips, T. D., Rottinghaus, G. E., and Casper, H. H. (1997). Individual and combined effects of fumonisin B₁ present in *Fusarium moniliforme* culture material and T-2 toxin or deoxynivalenol in broiler chicks. *Poult Sci* **76**, 1239-1247.
- Lake, B. G., Phillips, J. C., Walters, D. G., Bayley, D. L., Cook, M. W., Thomas, L. V., Gilbert, J., Startin, J. R., Baldwin, N. C., Bycroft, B. W., and et al. (1987). Studies on the metabolism of deoxynivalenol in the rat. *Food Chem Toxicol* **25**, 589-592.
- Langman, M., and Boyle, P. (1998). Chemoprevention of colorectal cancer. *Gut* **43**, 578-585.
- Lauricella, M., Calvaruso, G., Carabillo, M., D'Anneo, A., Giuliano, M., Emanuele, S., Vento, R., and Tesoriere, G. (2001). pRb suppresses camptothecin-induced apoptosis in human osteosarcoma Saos-2 cells by inhibiting c-Jun N-terminal kinase. *FEBS Lett* **499**, 191-197.
- Lautraite, S., Parent-Massin, D., Rio, B., and Hoellinger, H. (1997). In vitro toxicity induced by deoxynivalenol (DON) on human and rat granulomonocytic progenitors. *Cell Biol Toxicol* **13**, 175-183.
- Lee, R. F., and Steinert, S. (2003). Use of the single cell gel electrophoresis/comet assay for detecting DNA damage in aquatic (marine and freshwater) animals. *Mutat Res* **544**, 43-64.
- Li, F. Q., Luo, X. Y., and Yoshizawa, T. (1999). Mycotoxins (trichothecenes, zearalenone and fumonisins) in cereals associated with human red-mold intoxications stored since 1989 and 1991 in China. *Nat Toxins* **7**, 93-97.

- Limtrakul, P., Anuchapreeda, S., Lipigorngoson, S., and Dunn, F. W. (2001). Inhibition of carcinogen induced c-Ha-ras and c-fos proto-oncogenes expression by dietary curcumin. *BMC Cancer* **1**, 1.
- Lin, J. K., and Lin-Shiau, S. Y. (2001). Mechanisms of cancer chemoprevention by curcumin. *Proc Natl Sci Counc Repub China B* **25**, 59-66.
- Liu, Y., Peterson, D. A., Kimura, H., and Schubert, D. (1997). Mechanism of cellular 3-(4,5-dimethylthiazol-2-yl)-2,5-diphenyltetrazolium bromide (MTT) reduction. *J Neurochem* **69**, 581-593.
- Luccioni, C. (2000) Radio-Induced Cancers: Study on Cell Cultures. CLEFS CEA [online]. Available from: [http://www.clefscea.com/luccioni/radio-induced cancers](http://www.clefscea.com/luccioni/radio-induced%20cancers). Accessed: 17 July 2004.
- Maedler, K., Oberholzer, J., Bucher, P., Spinas, G. A., and Donath, M. Y. (2003). Monounsaturated fatty acids prevent the deleterious effects of palmitate and high glucose on human pancreatic beta-cell turnover and function. *Diabetes* **52**, 726-733.
- Mahakunakorn, P., Tohda, M., Murakami, Y., Matsumoto, K., Watanabe, H., and Vajragupta, O. (2003). Cytoprotective and cytotoxic effects of curcumin: dual action on H₂O₂-induced oxidative cell damage in NG108-15 cells. *Biol Pharm Bull* **26**, 725-728.
- Malagarie-Cazenave, S., Andrieu-Abadie, N., Sgui, B., Gouaz, V., Tardy, C., Cuvillier, O., and Levade, T. (2002). Sphingolipid signalling: molecular basis and role in TNF--induced cell death. *Expert Rev Mol Med* **2002**, 1-15.

- Mallery, C. (2004). Microvilli of epithelia. University of Miami: Department of Biology [online]. Available from: <http://fig.cox.miami.edu/~cmallery/150/cells/c7x26microfilaments.jpg>. Accessed: 14 November 2004.
- Marciniak, A., Szpringer, E., Lutnicki, K., and Beltowski, J. (2003). Influence of Thymus Extract (TFX) on Lipid Peroxidation in the Plasma of Rats following Thermal Injury. *Bulletin of the Veterinary Institute in Pulawy* **47**, 231-238.
- Maresca, M., Mahfoud, R., Garmy, N., and Fantini, J. (2002). The mycotoxin deoxynivalenol affects nutrient absorption in human intestinal epithelial cells. *J Nutr* **132**, 2723-2731.
- Marnett, L. J. (1999). Lipid peroxidation-DNA damage by malondialdehyde. *Mutat Res* **424**, 83-95.
- Mathews, C. K., van Holde, K. E., and Ahern, K. G. (1995). Biochemistry, pp. 45. Benjamin Cummings, San Francisco.
- Mediatech, Inc. cell culture reference guide (2001). Mediatech Incorporated. 11-22.
- Med Note (1998). Figure 2. Three-dimensional representation of simple columnar cells showing organelles, microvillous borders (also known as brush or striate borders), and basement membranes. Cytology & Histology Handout [online]. Available from: <http://www.mednote.co.kr/images/columcel.jpg>. Accessed: 3 July 2003.
- Meivar-Levy, I., Sabanay, H., Bershadsky, A. D., and Futerman, A. H. (1997). The role of sphingolipids in the maintenance of fibroblast morphology. The inhibition of protrusional activity, cell spreading, and cytokinesis induced by fumonisin B₁ can be reversed by ganglioside GM3. *J Biol Chem* **272**, 1558-1564.

- Mellors, R. C. (1999). Neoplasia: Biological Properties of Neoplastic Cells. Cornell University: Medical College [online]. Available from:
http://edcenter.med.cornell.edu/CUMC_PathNotes/Neoplasia/Neoplasia_05.html.
Accessed 13 June 2003.
- Merrill, A. H., Jr. (2002). De novo sphingolipid biosynthesis: a necessary, but dangerous, pathway. *J Biol Chem* **277**, 25843-25846.
- Merrill, A. H., Jr., Schmelz, E. M., Wang, E., Dillehay, D. L., Rice, L. G., Meredith, F., and Riley, R. T. (1997). Importance of sphingolipids and inhibitors of sphingolipid metabolism as components of animal diets. *J Nutr* **127**, 830S-833S.
- Merrill, A. H., Jr., Sullards, M. C., Wang, E., Voss, K. A., and Riley, R. T. (2001). Sphingolipid metabolism: roles in signal transduction and disruption by fumonisins. *Environ Health Perspect* **109 Suppl 2**, 283-289.
- Michel, C., van Echten-Deckert, G., Rother, J., Sandhoff, K., Wang, E., and Merrill, A. H., Jr. (1997). Characterization of ceramide synthesis. A dihydroceramide desaturase introduces the 4,5-trans-double bond of sphingosine at the level of dihydroceramide. *J Biol Chem* **272**, 22432-22437.
- Milovich, V., and Turchanowa, L. (2003). Polyamines and colon cancer. *Biochemical Society Transactions* **31**, 381-383.
- Minervini, F., Fornelli, F., and Flynn, K. M. (2004). Toxicity and apoptosis induced by the mycotoxins nivalenol, deoxynivalenol and fumonisin B₁ in a human erythroleukemia cell line. *Toxicol In Vitro* **18**, 21-28.

- Mobio, T. A., Baudrimont, I., Sanni, A., Shier, T. W., Saboureau, D., Dano, S. D., Ueno, Y., Steyn, P. S., and Creppy, E. E. (2000). Prevention by vitamin E of DNA fragmentation and apoptosis induced by fumonisin B₁ in C6 glioma cells. *Arch Toxicol* **74**, 112-119.
- Mobio, T. A., Tavan, E., Baudrimont, I., Anane, R., Carratu, M. R., Sanni, A., Gbeassor, M. F., Shier, T. W., Narbonne, J. F., and Creppy, E. E. (2003). Comparative study of the toxic effects of fumonisin B₁ in rat C6 glioma cells and p53-null mouse embryo fibroblasts. *Toxicology* **183**, 65-75.
- Moon, Y., and Pestka, J. J. (2002). Vomitoxin-induced cyclooxygenase-2 gene expression in macrophages mediated by activation of ERK and p38 but not JNK mitogen-activated protein kinases. *Toxicol Sci* **69**, 373-382.
- Moore, P. B., and Steitz, T. A. (2003). After the ribosome structures: how does peptidyl transferase work? *Rna* **9**, 155-159.
- Morin, P.J., Vogelstein, B., and Kinzler, K.W. (1996). Apoptosis and APC in colorectal tumorigenesis. *Proc. Natl. Acad. Sci. USA* **93**, 7950-7954.
- Mosmann, T. (1983). Rapid colorimetric assay for cellular growth and survival: application to proliferation and cytotoxicity assays. *J Immunol Methods* **65**, 55-63.
- Myburg, R. B., Dutton, M. F., and Chuturgoon, A. A. (2002). Cytotoxicity of fumonisin B₁, diethylnitrosamine, and catechol on the SNO esophageal cancer cell line. *Environ Health Perspect* **110**, 813-815.
- Nelms, B. E., Moravec, R., and Riss, T. (1997). Measuring Apoptosis in Individual Cells with the Comet Assay. In *Promega Notes*, pp. 13-17.

- Norred, W. P., Plattner, R. D., and Chamberlain, W. J. (1993). Distribution and excretion of [¹⁴C]fumonisin B₁ in male Sprague-Dawley rats. *Nat Toxins* **1**, 341-346.
- O'Connor, J. M. (2001). Trace elements and DNA damage. *Biochemical Society Transactions* **29**, 354-357.
- Olsson, J. (2000). Modern Methods in Cereal Grain Mycology. In *Department of Microbiology*, pp. 37. Swedish University of Agricultural Sciences, Uppsala, Sweden.
- Ostling, O., and Johanson, K. J. (1984). Microelectrophoretic study of radiation-induced DNA damages in individual mammalian cells. *Biochem Biophys Res Commun* **123**, 291-298.
- Pestka, J. J., Uzarski, R., Ross, S., Randell, A., and Yang, G.-H. (1999). Vomitoxin (Deoxynivalenol) Induces Cytokines and Apoptosis in Human T Cells. 1999 National Fusarium Head Blight Forum, pp. 115-117.
- Peterson, M. D., Bement, W. M., and Mooseker, M. S. (1993). An in vitro model for the analysis of intestinal brush border assembly. II. Changes in expression and localization of brush border proteins during cell contact-induced brush border assembly in Caco-2BBE cells. *J Cell Sci* **105 (Pt 2)**, 461-472.
- Plumb, J. A., Milroy, R., and Kaye, S. B. (1989). Effects of pH Dependence on 3-(4,5-Dimethylthiazol-2-yl)-2,5-diphenyl-tetrazolium Bromide-Formazan Absorption on Chemosensitivity Determined by a Novel Tetrazolium-based Assay. *Cancer Research* **49**, 4435-4440.
- Progression of colon cancer (2001). Kenyon College: Department of Biology [online]. Available from: <http://biology.kenyon.edu/courses/biol114/Chap07/Figure18-18.html>. Accessed 7 April 2004.

- Putnam, K. P., Bombick, D. W., and Doolittle, D. J. (2002). Evaluation of eight in vitro assays for assessing the cytotoxicity of cigarette smoke condensate. *Toxicol In Vitro* **16**, 599-607.
- Radhakrishna Pillai, G., Srivastava, A. S., Hassanein, T. I., Chauhan, D. P., and Carrier, E. (2004). Induction of apoptosis in human lung cancer cells by curcumin. *Cancer Lett* **208**, 163-170.
- Ramachandran, A., Madesh, M., and Balasubramanian, K. A. (2000). Apoptosis in the intestinal epithelium: its relevance in normal and pathophysiological conditions. *J Gastroenterol Hepatol* **15**, 109-120.
- Raskin, J.B. (2004). Anatomy of Digestive System. University of Miami: Miller School of Medicine [online]. Available from:
<http://www.med.miami.edu/med/gastroenterology/anatomy.asp>. Accessed: 12 June 2003.
- Renehan, A. G., Booth, C., and Potten, C. S. (2001). What is apoptosis, and why is it important? *Bmj* **322**, 1536-1538.
- Reubel, G. H., Gareis, M., and Amselgruber, W. M. (1987). Cytotoxicity Evaluation of Mycotoxins by an MTT Bioassay. *Mycotoxin Research* **3**, 85-96.
- Rheeder, J. P., Marasas, W. F. O., Thiel, P. G., Sydenham, E. W., Shephard, G. S., and van Schalkwyk, D. J. (1992). Fusarium moniliforme and fumonisins in corn in relation to human esophageal cancer in Transkei. *Phytopathology* **82**, 353-357.

- Riley, R. T., Enongene, E., Voss, K. A., Norred, W. P., Meredith, F. I., Sharma, R. P., Spitsbergen, J., Williams, D. E., Carlson, D. B., and Merrill, A. H., Jr. (2001). Sphingolipid perturbations as mechanisms for fumonisin carcinogenesis. *Environ Health Perspect* **109 Suppl 2**, 301-308.
- Riss, T., and Moravec, R. (1996). Improved Non-Radioactive Assay to Measure Cellular Proliferation or Toxicity: The CellTiter 96® AQueousOne Solution Cell Proliferation Assay. In *Promega Notes Magazine*, pp. 19-23.
- Robb, J., and Norval, M. (1983). Comparison of cytotoxicity and thin-layer chromatography methods for detection of mycotoxins. *Appl Environ Microbiol* **46**, 948-950.
- Robinson, J. M., Takizawa, T., Pombo, A., and Cook, P. R. (2001). Correlative fluorescence and electron microscopy on ultrathin cryosections: bridging the resolution gap. *J Histochem Cytochem* **49**, 803-808.
- Rode, H-J., Eisel, D., and Frost, I. (2004). Apoptosis and Cell Proliferation. Roche Diagnostics Corporation [online]. Available from: http://www.roche-applied-science.com/sis/apoptosis/docs/manual_apoptosis.pdf. Accessed: 31 June 2004
- Roncucci, L., Pedroni, M., Vaccina, F., Benatti, P., Marzona, L., and De Pol, A. (2000). Aberrant crypt foci in colorectal carcinogenesis. Cell and crypt dynamics. *Cell Prolif* **33**, 1-18.
- Rotter, B. A., Prelusky, D. B., and Pestka, J. J. (1996). Toxicology of deoxynivalenol (vomitoxin). *J Toxicol Environ Health* **48**, 1-34.
- Rumora, L., Kovacic, S., Rozgaj, R., Cepelak, I., Pepeljnjak, S., and Zanic Grubisic, T. (2002). Cytotoxic and genotoxic effects of fumonisin B₁ on rabbit kidney RK13 cell line. *Arch Toxicol* **76**, 55-61.

Schmelz, E. M., Dombrink-Kurtzman, M. A., Roberts, P. C., Kozutsumi, Y., Kawasaki, T., and Merrill, A. H., Jr. (1998). Induction of apoptosis by fumonisin B₁ in HT29 cells is mediated by the accumulation of endogenous free sphingoid bases. *Toxicol Appl Pharmacol* **148**, 252-260.

Schematic diagram of the colon, crypts of Lieberkuhn and associated cells (2003). University of Toronto: Faculty of Health and Sciences [online]. Available from: <http://hmb.utoronto.ca/HMB302H/Lectures/Lecture6%20Digestive%20System/Digestive%20System3frame.pdf> Accessed: 29 March 2004.

Schroeder, J. J., Crane, H. M., Xia, J., Liotta, D. C., and Merrill, A. H., Jr. (1994). Disruption of sphingolipid metabolism and stimulation of DNA synthesis by fumonisin B₁. A molecular mechanism for carcinogenesis associated with *Fusarium moniliforme*. *J Biol Chem* **269**, 3475-3481.

Scientific Committee on Food (1999). Opinion on *Fusarium* Toxins - Part 1: Deoxynivalenol (DON). European Commission: Health & Consumer Protection Directorate-General [online]. Available from: http://europa.eu.int/comm/food/fs/sc/scf/out44_en.pdf. Accessed: 12 June 2003.

Scientific Committee on Food (2002). Opinion of the Scientific Committee on Food on *Fusarium* toxins-Part 6: Group evaluation of T-2 toxin, HT-2 toxin, nivalenol and deoxynivalenol. European Commission: Health & Consumer Protection Directorate-General [online]. Available from: http://europa.eu.int/comm/food/fs/sc/scf/out123_en.pdf. Accessed: 12 June 2003

Scott, D. W., and Loo, G. (2004). Curcumin-induced GADD153 gene up-regulation in human colon cancer cells. *Carcinogenesis* **25**, 2155-2164.

- Sharma, R. A., Gescher, A., Plataras, J. P., Leuratti, C., Singh, R., Gallacher-Horley, B., Offord, E., Marnett, L. J., Steward, W. P., and Plummer, S. M. (2001a). Cyclooxygenase-2, malondialdehyde and pyrimidopurinone adducts of deoxyguanosine in human colon cells. *Carcinogenesis* **22**, 1557-1560.
- Sharma, R. A., Ireson, C. R., Verschoye, R. D., Hill, K. A., Williams, M. L., Leuratti, C., Manson, M. M., Marnett, L. J., Steward, W. P., and Gescher, A. (2001b). Effects of dietary curcumin on glutathione S-transferase and malondialdehyde-DNA adducts in rat liver and colon mucosa: relationship with drug levels. *Clin Cancer Res* **7**, 1452-1458.
- Sheik, R. A., and Yasmeen, S. (2002). Biological Markers and Colorectal Cancer. *JK-Practitioner* **9**, 215-218.
- Shen, Z. Y., Xu, L. Y., Li, E. M., Li, J. T., Chen, M. H., Shen, J., and Zeng, Y. (2003). Ezrin, actin and cytoskeleton in apoptosis of esophageal epithelial cells induced by arsenic trioxide. *Int J Mol Med* **12**, 341-347.
- Shephard, G. S., Thiel, P. G., Sydenham, E. W., Alberts, J. F., and Cawood, M. E. (1994). Distribution and excretion of a single dose of the mycotoxin fumonisin B₁ in a non-human primate. *Toxicon* **32**, 735-741.
- Shephard, G. S., Thiel, P. G., Stockenstrom, S., and Sydenham, E. W., Alberts, J. F. (1996). Worldwide survey of fumonisin contamination of corn and corn-based products. *J. A. O. A. C. Int.* **79**, 671-687.

- Sieuwert, A. M., Klijn, J. G., Peters, H. A., and Foekens, J. A. (1995). The MTT tetrazolium salt assay scrutinized: how to use this assay reliably to measure metabolic activity of cell cultures in vitro for the assessment of growth characteristics, IC50-values and cell survival. *Eur J Clin Chem Clin Biochem* **33**, 813-823.
- Singh, N. P., McCoy, M. T., Tice, R. R., and Schneider, E. L. (1988). A simple technique for quantitation of low levels of DNA damage in individual cells. *Exp Cell Res* **175**, 184-191.
- Singletary, K. (2000). Diet, natural products and cancer chemoprevention. *J Nutr* **130**, 465S-466S.
- Slater, T. F., Sawyer, B., and Straeuli, U. (1963). Studies on Succinate-Tetrazolium Reductase Systems. Iii. Points of Coupling of Four Different Tetrazolium Salts. *Biochim Biophys Acta* **77**, 383-393.
- Smith, C. M., Marks, A. D., and Lieberman, M. A. (2004). *Marks's Basic Medical Biochemistry: A Clinical Approach*, pp. 12-50. Lippincott Williams & Wilkins, Philadelphia.
- Spiegel, S., and Merrill, A. H., Jr. (1996). Sphingolipid metabolism and cell growth regulation. *Faseb J* **10**, 1388-1397.
- Sreedharan, R., and Mehta, D. I. (2004). Gastrointestinal tract. *Pediatrics* **113**, 1044-1050.
- Subbaramaiah, K., Chung, W. J., Michaluart, P., Telang, N., Tanabe, T., Inoue, H., Jang, M., Pezzuto, J. M., and Dannenberg, A. J. (1998). Resveratrol inhibits cyclooxygenase-2 transcription and activity in phorbol ester-treated human mammary epithelial cells. *J Biol Chem* **273**, 21875-21882.
- Sugimura, T. (2000). Nutrition and dietary carcinogens. *Carcinogenesis* **21**, 387-395.

- Sun, D. Y., Jiang, S., Zheng, L. M., Ojcius, D. M., and Young, J. D. (1994). Separate metabolic pathways leading to DNA fragmentation and apoptotic chromatin condensation. *J Exp Med* **179**, 559-568.
- Szkudelska, K., Szkudelski, T., and Nogowski, L. (2002). Short-time deoxynivalenol treatment induces metabolic disturbances in the rat. *Toxicol Lett* **136**, 25-31.
- Tamm, C. (1977). Chemistry and Biosynthesis of Trichothecenes. *Mycotoxins in Human and Animal Health*, 209-228.
- Taraphdar, A. K., Roy, M., and Bhattacharya, R. K. (2001). Natural products as inducers of apoptosis : Implication for cancer therapy and prevention. *Current Science* **80**, 1387-1396.
- Teng, M. K., Usman, N., Frederick, C. A., and Wang, A. H. (1988). The molecular structure of the complex of Hoechst 33258 and the DNA dodecamer d(CGCGAATTCGCG). *Nucleic Acids Res* **16**, 2671-2690.
- Terse, P. S., Madhyastha, M. S., Zurovac, O., Stringfellow, D., Marquardt, R. R., and Kemppainen, B. W. (1993). Comparison of in vitro and in vivo biological activity of mycotoxins. *Toxicon* **31**, 913-919.
- Thrasher, J. D. (2001). Poison Of The Month: An Introduction to Trichothecenes [online]. Available from: <http://www.drthrasher.org/Introduction%20to%20Trichothecenes.html>. Accessed: 23 July 2003.
- Tice, R. R., Agurell, E., Anderson, D., Burlinson, B., Hartmann, A., Kobayashi, H., Miyamae, Y., Rojas, E., Ryu, J. C., and Sasaki, Y. F. (2000). Single cell gel/comet assay: guidelines for in vitro and in vivo genetic toxicology testing. *Environ Mol Mutagen* **35**, 206-221.

- Toescu, E.C. (2003). Apoptosis and Necrosis. University of Birmingham: School of Medicine [online]. Available from:
<http://medweb.bham.ac.uk/research/calcium/Functions/ApopNec.html>. Accessed 5 July 2004.
- Turmeric powder (2000). Herbs and Spices International: Turmeric [online]. Available from:
http://www.hnspice.com/Our_Products/body_our_products.html. Accessed: 27 March 2004.
- Turnbull, G. K., Vanner, S. J., and Burnstein, M. (1997). The Colon. In *First principles of gastroenterology : the basis of disease and an approach to management* (A. B. R. Thomson, and E. A. Shaffer, Eds.), pp. 347-348. Canadian Association of Gastroenterology, Toronto.
- Twentyman, P. R., and Luscombe, M. (1987). A study of some variables in a tetrazolium dye (MTT) based assay for cell growth and chemosensitivity. *Br J Cancer* **56**, 279-285.
- Ueno, Y. (1977). Mode of action of trichothecenes. *Ann Nutr Aliment* **31**, 885-900.
- Ueno, Y., Iijima, K., Wang, S. D., Sugiura, Y., Sekijima, M., Tanaka, T., Chen, C., and Yu, S. Z. (1997). Fumonisin as a possible contributory risk factor for primary liver cancer: a 3-year study of corn harvested in Haimen, China, by HPLC and ELISA. *Food Chem Toxicol* **35**, 1143-1150.
- Vermes, I., Haanen, C., and Reutelingsperger, C. P. M. (1997). Apoptosis - the genetically controlled physiological cell death: biochemistry and measurement. *Ned Tijdschr Klin Chem* **22**, 43-50.

- Veselska, R., Zitterbart, K., Jelinkova, S., Neradil, J., and Svoboda, A. (2003). Specific cytoskeleton changes during apoptosis accompanying induced differentiation of HL-60 myeloid leukemia cells. *Oncol Rep* **10**, 1049-1058.
- Visconti, A., Minervini, F., Lucivero, G., and Gambatesa, V. (1991). Cytotoxic and immunotoxic effects of Fusarium mycotoxins using a rapid colorimetric bioassay. *Mycopathologia* **113**, 181-186.
- Vistica, D. T., Skehan, P., Scudiero, D., Monks, A., Pittman, A., and Boyd, M. R. (1991). Tetrazolium-based assays for cellular viability: a critical examination of selected parameters affecting formazan production. *Cancer Res* **51**, 2515-2520.
- Wang, E., Norred, W. P., Bacon, C. W., Riley, R. T., and Merrill, A. H., Jr. (1991). Inhibition of sphingolipid biosynthesis by fumonisins. Implications for diseases associated with Fusarium moniliforme. *J Biol Chem* **266**, 14486-14490.
- Wang, E., Riley, R. T., Meredith, F. I., and Merrill, A. H., Jr. (1999). Fumonisin B₁ consumption by rats causes reversible, dose-dependent increases in urinary sphinganine and sphingosine. *J Nutr* **129**, 214-220.
- Wang, H., Wei, H., Ma, J., and Luo, X. (2000). The fumonisin B₁ content in corn from North China, a high-risk area of esophageal cancer. *J Environ Pathol Toxicol Oncol* **19**, 139-141.
- Wang, J. S., and Groopman, J. D. (1999). DNA damage by mycotoxins. *Mutat Res* **424**, 167-181.
- Wang, X. F., and Cynader, M. S. (2001). Pyruvate released by astrocytes protects neurons from copper-catalyzed cysteine neurotoxicity. *J Neurosci* **21**, 3322-3331.

- Wannemacher, R. W., and Wiener, S. L. (2002). Textbook of Military Medicine: Medical Aspects of Chemical and Biological Warfare: Chapter 34. Virtual Naval Hospital [online]. Available from:
http://www.vnh.org/MedAspChemBioWar/chapters/chapter_34.htm. Accessed: 15 February 2002.
- Wargovich, M. J. (2001). Colon cancer chemoprevention with ginseng and other botanicals. *J Korean Med Sci* **16 Suppl**, S81-86.
- Wheater, P. R., Burkitt, H. G., and Daniels, V. G. (1987). Functional Histology A Text and Colour Atlas (2nd ed.), pp. 222-223. Churchill Livingstone, London.
- Wijnands, L. M., and van Leusden, F. M. (2000). An overview of adverse health effects caused by mycotoxins and bioassays for their detection, pp. 1-99. National Institute of Public Health and the Environment.
- Yang, J., and Duerksen-Hughes, P. J. (2001). Activation of a p53-independent, sphingolipid-mediated cytolytic pathway in p53-negative mouse fibroblast cells treated with N-methyl-N-nitro-N-nitrosoguanidine. *J Biol Chem* **276**, 27129-27135.
- Yike, I., Allan, T., Sorenson, W. G., and Dearborn, D. G. (1999). Highly sensitive protein translation assay for trichothecene toxicity in airborne particulates: comparison with cytotoxicity assays. *Appl Environ Microbiol* **65**, 88-94.
- Yoshizawa, T., Yamashita, A., and Luo, Y. (1994). Fumonisin occurrence in corn from high- and low-risk areas for human esophageal cancer in China. *Appl Environ Microbiol* **60**, 1626-1629.

Zhang, M. Z., Harris, R. C., and McKanna, J. A. (1999). Regulation of cyclooxygenase-2 (COX-2) in rat renal cortex by adrenal glucocorticoids and mineralocorticoids. *Proc Natl Acad Sci USA* **96**, 15280-15285.

Zhu, Y. G., Chen, X. C., Chen, Z. Z., Zeng, Y. Q., Shi, G. B., Su, Y. H., and Peng, X. (2004). Curcumin protects mitochondria from oxidative damage and attenuates apoptosis in cortical neurons. *Acta Pharmacol Sin* **25**, 1606-1612.

APPENDICES

APPENDIX 1: REAGENTS FOR CELL CULTURE

1.1 COMPOSITION OF EMEM, HBSS AND PBS

Components	EMEM (mg/l)	HBSS (mg/l)	PBS (g/l)
Inorganic Salts			
Calcium chloride dihydrate ($\text{CaCl}_2 \cdot 2\text{H}_2\text{O}$)	265.00		
Potassium chloride (KCl)	400.00	400.00	0.2g/l
Potassium dihydrogen phosphate (KH_2PO_4)		60.00	0.2g/l
Magnesium Sulphate Septahydrate ($\text{MgSO}_4 \cdot 7\text{H}_2\text{O}$)	200.00		
Sodium chloride (NaCl)	5,800.00	8,000.00	8.0g/l
Sodium Bicarbonate (NaHCO_3)	2,200.00	350.00	
Sodium Hydrogen Phosphate ($\text{NaH}_2\text{PO}_4 \cdot \text{H}_2\text{O}$)	140.00	90.00	1.15g/l
Vitamins			
D-Ca Pantothenate	1.00		
Choline Chloride	1.00		
Folic Acid	1.00		
I-Inositol	2.00		
Nicotinamide	1.00		
Pyridoxine.HCl	1.00		
Thiamine.HCl	1.00		
Riboflavin	0.10		

Components	EMEM (mg/l)	HBSS (mg/l)	PBS (g/l)
Amino acids			
L-Arginine.HCl	126.40		
L-Cystine	24.00		
L-Histidine.HCl.H ₂ O	42.00		
L-Isoleucine	52.40		
L-Leucine	52.40		
L-Lysine.HCl	73.00		
L-Methionine	15.00		
L-Phenylalanine	33.00		
L-Threonine	47.60		
L-Tryptophan	10.20		
L-Tyrosine	36.20		
L-Valine	46.80		
Other Components			
Glucose	1,000.00	1,000.00	
HEPES	5,957.40		
Phenol Red.Na	10.00	20.00	

The EMEM and HBSS were prepared in water for injection (WFI) quality water. This is water that has been ultrafiltered, deionised, distilled and sterile filtered. The PBS was prepared in sterile distilled water and autoclaved at 121°C for 15 minutes. All were stored at 15°C to 30°C.

1.2 COMPONENTS OF L-GLUTAMINE (200mM), PENICILLIN STREPTOMYCIN FUNGIZONE (PENSTREP) AND TRYPSIN VERSENE

Components	L-Glutamine (200mM)	PenStrep Fungizone	Trypsin Versene
L-Glutamine	29.3mg/ml		
Sodium chloride (NaCl)	8.5mg/ml	8.5mg/ml	8,000.00mg/l
Potassium penicillin		10,000 units/ml	
Streptomycin sulfate		10,000 µg/ml	
Fungizone		25 µg/ml	
Glucose			1,000.00mg/l
Potassium chloride (KCl)			400.00mg/l
Sodium Bicarbonate (NaHCO ₃)			580.00mg/l
Phenol Red.Na			2.00mg/l
Trypsin			500.00mg/l
Versene (EDTA)			200.00mg/l

Each of these was prepared in WFI quality water. The L-Glutamine and PenStrep Fungizone were stored at −10°C to −20°C while the Trypsin Versene was stored at 2°C to 8°C.

1.3 PREPARATION OF COMPLETE CULTURE MEDIUM

Eagles Minimal Essential Medium (EMEM) was supplemented with 10% foetal calf serum (FCS), 1% L - Glutamine and 1% PenStrep-Fungizone (anti-biotic). Heat inactivated foetal calf serum was filtered into the media using a 0.45µm millipore filter.

1.4 PREPARATION OF CRYOPRESERVATION MEDIUM

Cryopreservation medium was prepared by supplementing CCM with 10% DMSO.

1.5 PREPARATION OF TRYPAN BLUE (0.4%)

Trypan Blue stain was prepared by dissolving 0.4g trypan blue dye in 0.85% NaCl and stored at -10°C to -20°C.

APPENDIX 2: REAGENTS FOR SINGLE CELL GEL ELECTROPHORESIS

2.1 PREPARATION OF 1M TRIS (pH 10)

Tris (1M) was prepared by dissolving 121.12g of Tris in 800ml sterile distilled H₂O. The pH was adjusted with concentrated HCl and distilled H₂O was added to make a final volume of 1000ml.

2.2 PREPARATION OF TANK BUFFER, LYSING SOLUTION, TRIS (0.4M) AND LMPA (1% AND 0.5%)

Components	Tank Buffer (pH 13)	Lysing Solution	Tris (0.4 M)	LMPA (1%)	LMPA (0.5%)
NaOH	12g				
EDTA(Na ₂)	0.372g				
NaCl		146g			
EDTA		29.2g			
Tris (1M) (Appendix 2.1)		10ml	40ml		
DMSO		100ml			
Distilled H ₂ O	1L	880ml	60ml		
PBS				100ml	100ml
Triton X-100 (Add last)		10ml			
Low Melting Point Agar (LMPA)				1g	0.5g

The tank buffer, lysing solution and 0.4M Tris were made up fresh as indicated above and thoroughly mixed. The lysing solution was chilled at 2°C to 8°C until ready for use. The 1% and 0.5% solutions of LMPA were heated until all solid had dissolved and the solutions appeared clear. These were stored at room temperature.

APPENDIX 3: REAGENTS FOR FLUORESCENT MICROSCOPY

3.1 ACRIDINE ORANGE

Acridine orange (1mg) was dissolved in PBS (1ml) to make a stock solution (1mg/ml). This stock solution (1ml) was then further diluted in PBS (9ml) to formulate the 100µg/ml working stock used in the experiment

3.2 ETHIDIUM BROMIDE

Ethidium bromide (1mg) was dissolved in PBS (1ml) to make a stock solution (1mg/ml). This stock solution (1ml) was then further diluted in PBS (9ml) to formulate the 100µg/ml working stock used in the experiment

3.3 HOECHST 33258

A stock solution was initially prepared by dissolving Hoechst 33258 (4mg) in DMSO (2ml). This solution was stored overnight at 4°C. This stock solution (1.4ml) was then added to PBS (1ml) to formulate the final working stock used in the experiment.

3.4 PARAFORMALDEHYDE (10%)

Paraformaldehyde (1g) was dissolved in PBS (10ml) and heated for 30 min at 60°C or until dissolved. The pH was then adjusted to 7.2.

APPENDIX 4: REAGENTS FOR SCANNING ELECTRON MICROSCOPY

4.1 GLUTARALDEHYDE (1%)

Glutaraldehyde (25%; 1ml) was dissolved in HBSS (24ml).

4.2 OSMIUM TETROXIDE (1%)

Osmium tetroxide (1 ampoule) was dissolved in EtOH (100ml)

4.3 ETHANOL (70% AND 90%)

Ethanol (70%)

Ethanol (70ml) was added to 30ml distilled H₂O.

Ethanol (90%)

Ethanol (90ml) was added to 10ml distilled H₂O.

